Proceedings for the 26th Annual Conference of the Society for Astronomical Sciences

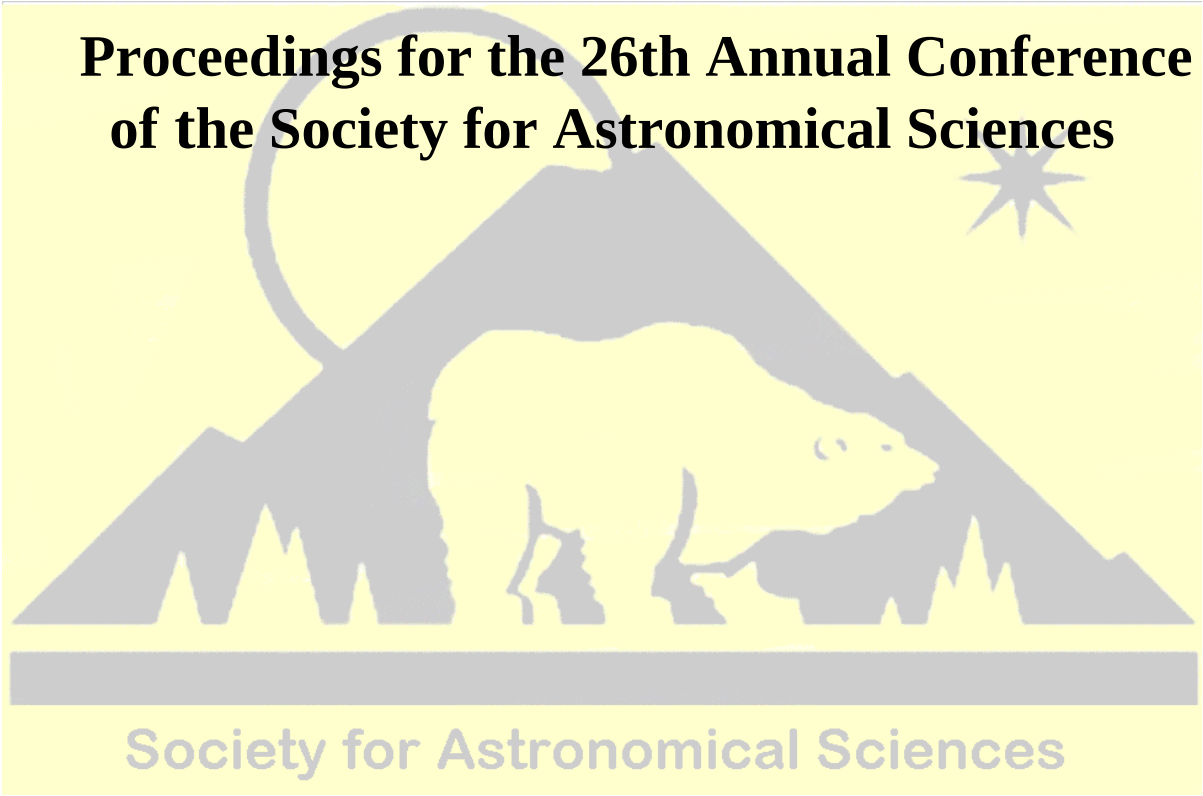

Symposium on Telescope Science

Editors:
Brian D. Warner
Jerry Foote
David A. Kenyon
Dale Mais

May 22-24, 2007
Northwoods Resort, Big Bear Lake, CA

Reprints of Papers

Distribution of reprints of papers by any author of a given paper, either before or after the publication of the proceedings is allowed under the following guidelines.

1. The copyright remains with the author(s).
2. Under no circumstances may anyone other than the author(s) of a paper distribute a reprint without the express written permission of all author(s) of the paper.
3. Limited excerpts may be used in a review of the reprint as long as the inclusion of the excerpts is NOT used to make or imply an endorsement by the Society for Astronomical Sciences of any product or service.

Notice

The preceding "Reprint of Papers" supersedes the one that appeared in the original print version

Disclaimer

The acceptance of a paper for the SAS proceedings can not be used to imply or infer an endorsement by the Society for Astronomical Sciences of any product, service, or method mentioned in the paper.

Published by the Society for Astronomical Sciences, Inc.

First printed: May 2007

ISBN: 0-9714693-6-9

Table of Contents

PREFACE 7

CONFERENCE SPONSORS 9

Submitted Papers

THE OLIN EGGEN PROJECT
ARNE HENDEN *13*

AMATEUR AND PROFESSIONAL ASTRONOMER COLLABORATION EXOPLANET RESEARCH PROGRAMS AND TECHNIQUES
RON BISSINGER *17*

EXOPLANET OBSERVING TIPS
BRUCE L. GARY *23*

STUDY OF CEPHEID VARIABLES AS A JOINT SPECTROSCOPY PROJECT
THOMAS C. SMITH, KENNETH E. KISSELL, *27*

LHIRES III HIGH RESOLUTION SPECTROGRAPH
OLIVIER THIZY *31*

PRECISION UBVJH SINGLE CHANNEL PHOTOMETRY OF EPSILON AURIGAE
JEFFREY L. HOPKINS, ROBERT E. STENCEL *37*

A NEW PROGRAM TO SEARCH FOR FLARE EVENTS IN LONG PERIOD VARIABLE LIGHTCURVES: ARCHIVED GNAT DATA
ERIC R. CRAINE, ROGER B. CULVER,
ADAM L. KRAUS, ROY A. TUCKER, DOUGLAS WALKER, ROBERT F. WING *45*

BVRI CCD PHOTOMETRY OF THETA-1 ORIONIS A
JEFFREY L. HOPKINS, GENE A. LUCAS *51*

THE HALLOWEEN STELLAR OUTBURST OF 2006 – A NEARBY MICROLENS?
ROBERT KOFF, JOSEPH PATTERSON, THOMAS KRAJCI *57*

PARAMETER SOLUTIONS FOR THE SYSTEM AP LEONIS
LEE F. SNYDER, JOHN LAPHAM *61*

PHOTOMETRY WITH DSLR CAMERAS
JOHN E. HOOT *67*

CCD VIDEO PHOTOGRAPHY AND ANALYSIS OF COMET SCHWASSMAN-WACHMAN 73P FRAGMENTS B & C USING THE LOW-COST MEADE DSI CAMERA
STEVE GIFFORD *73*

INITIAL EFFORTS AT ASTEROID LIGHTCURVE INVERSION
BRIAN D. WARNER ***79***

VARIABLE STAR PHOTOMETRY AT WEST CHALLOW OBSERVATORY
DAVID BOYD ***89***

SELECTIVE AVAILABILITY OF ASTRONOMICAL DATA
P. R. MCCULLOUGH ***95***

DEVELOPING AN UNDERGRADUATE ASTRONOMICAL RESEARCH PROGRAM
RUSSELL M. GENET ***99***

IMAGING AUTOMATION
JERRY D. HORNE ***103***

FAST PHOTOMETRY
JOHN MENKE ***111***

Poster Papers

DIFFERENTIAL CCD PHOTOMETRY USING MULTIPLE COMPARISON STARS
DAVID BOYD ***119***

GALILEO'S LEGACY
RUSSELL M. GENET ***127***

TIME-SERIES ASTRONOMICAL PHOTOMETRY CONFERENCE
RUSSELL M. GENET ***129***

AN AMATEUR ASTRONOMER'S INITIAL ASTEROID LIGHTCURVES
CHARLES GREEN ***131***

FOLLOW-UP OBSERVATIONS OF GNAT MG1 SURVEY STARS: A SUMMER COMMUNITY COLLEGE STUDENT RESEARCH PROJECT
NOLL ROBERTS ***135***

ECLIPSING BINARY SYSTEM CU SAGITTAE
LEE F. SNYDER, J.LAPHAM@SBCGLOBAL.NET ***137***

ECLIPSING BINARY SYSTEMS AN TAU, V506 OPH, V609 AQL, AND RV TRI
JOHN LAPHAM, LEE F. SNYDER ***141***

A PELLICLE AUTOGUIDER FOR THE DSS-7 SPECTROGRAPH
GARY M. COLE ***153***

Preface

This year, we start our second quarter century. Unlike a 25th anniversary being "silver," we couldn't find one for 26 years. So, we'll take the liberty of calling this the "Silicon Anniversary" for the Society. Why Silicon? Because so much of the work being done by amateurs and professionals relies on CCD cameras and computers, where silicon is the prime ingredient in the chips in both that make them do their magic.

We have, indeed, entered a "golden" era for astronomy. Not for many years has amateur involvement been so critical to the advancement of at least this branch of science. Amateurs have capable resources and, most important, the time and flexibility of schedule that allows them observing opportunities not always available to professionals. Of course, on the other side of the coin, professionals have access to much more sophisticated equipment that can go fainter, deeper, and finer. The two groups working together are a very powerful force in unlocking the secrets of the Universe.

The Symposium on Telescope Science, originally under the direction of the IAPPP and since 2003 by the Society for Astronomical Sciences, has been held in Southern California since 1982 but not always in its current location of Big Bear Lake, California. The timing and location of the meeting are not by chance. The Symposium is meant to be a lead-in to one of the biggest star parties and astronomical swap meets in the world, the annual RTMC Astronomy Expo, held just a few miles from Big Bear on the weekend following the Symposium.

Through the three days of the Symposium on Telescope Science, the Society hopes to foster new friendships and new collaborations among amateur and professional astronomers. Our goals are the personal scientific advancement of Society members, the development of the amateur-professional community, and promoting research that increases our understanding of the Universe.

It takes many people to have a successful conference, starting with the Conference Committee. This year the committee members are:

Lee Snyder	Robert Stephens
Robert Gill	Dave Kenyon
Dale Mais	Brian D. Warner
Jerry Foote	

There are many others involved in a successful conference. The editors take time to note the many volunteers who put in considerable time and resources. We also thank the staff and management of the Northwoods Resort in Big Bear Lake, CA, for their efforts at accommodating the Society and our activities.

Membership dues alone do not cover the costs of the Society and annual conference. We owe a great debt of gratitude to our corporate sponsors: Sky and Telescope, Software Bisque, Santa Barbara Instruments Group, and Apogee Instruments, Inc.

Finally, there would be no conference without our speakers and poster presenters. We thank them for making the time to prepare and present the results of their research.

Brian D. Warner
Jerry Foote
Dale Mais
Dave Kenyon

Conference Sponsors

The conference organizers thank the following companies for their significant contributions and financial support. Without them, this conference would not be possible.

Apogee Instruments, Inc.

Manufactures of astronomical and scientific imaging cameras
http://www.ccd.com

Santa Barbara Instruments Group

Makers of astronomical instrumentation
http://www.sbig.com

Sky Publishing Corporation

Publishers of Sky and Telescope Magazine
http://skyandtelescope.com

Software Bisque

Developers of TheSky Astronomy Software and the Paramount Telescope Mount
http://www.bisque.com

Submitted Papers

The Olin Eggen Project

Arne Henden
American Association of Variable Star Observers (AAVSO)
arne@aavso.org

Abstract

Olin Eggen was one of the most prolific professional observers in the Southern Hemisphere. Over a 50-year career, he collected hundreds of thousands of photoelectric observations. This paper describes an ambitious project started by the AAVSO to digitize his observational archive.

1. Introduction

Olin Jeuck Eggen (July 9, 1919 – October 2, 1998) received his Ph.D. in astrophysics from the University of Wisconsin (Madison) in 1948 (only the second one awarded by UW), working with Joel Stebbins and Albert Whitford on the lightcurves of Algol. His seminal paper in 1962 with Lynden-Bell and Sandage ("Evidence from the Motions of Old Stars that the Galaxy Collapsed", Eggen et al. 1962) is his most cited paper (both Lynden-Bell and Sandage later were awarded the Bruce medal by the ASP, partly based on this paper). Eggen also introduced the concept of moving (or kinematic) groups of stars. A photograph of Eggen, Lynden-Bell and Sandage is given in Figure 1 (from the PASP obituary: Eggen 2001).

Figure 1. Photograph of Olin Eggen, Donald Lynden-Bell, and Alan Sandage (left to right).

Eggen moved to the Southern Hemisphere in 1966, assuming Directorship of Mt. Stromlo Observatory and pursuing the development of the AAT large reflector. He moved to Cerro Tololo Inter-American Observatory (CTIO) in 1977 where he stayed until he passed away 20 years later.

Olin Eggen was a vice-president of the RAS, a life member of the ASP, was awarded the American Astronomical Society Henry Norris Russell Lectureship in 1985 and the Pawsey Memorial Lectureship of the Australian Institute of Physics. The Australian National University has established a scholarship program in his name; the CTIO library is named after Eggen.

He was an extremely prolific researcher, publishing some 400 research articles over his 50-year career, with articles being written up until his death in 1998 from a heart attack. He worked with many of the notable astronomers over the last half of the 20th century, including Sandage, Lynden-Bell, Greenstein, Herbig and others. He was well known as a careful researcher, never observing unless it was perfectly clear, and always substantiating any claim he made in a paper. However, Eggen was not without controversy, having a gruff personality, always willing to voice his opinion on a topic, even resigning his membership in the IAU around 1970. We will leave his most famous episode, "the Neptune file," for other historians to comment about!

2. Eggen's Legacy

Eggen was well known as a proponent of small-telescope science. However, what the AAVSO is most interested in is that Eggen published only a small part of the enormous amount of data he collected over his lifetime. He initially developed a photometric system called (P,V) (for photographic and visual), roughly comparable to B and V, and published many papers of photometry on this system.

Astronomers migrated to the Johnson U,B,V system and Eggen's P,V system fell into disuse. However, the P,V system is nearly identical to Johnson B and V (see Moro and Munari, 2000: the Asiago Database on Photometric Systems), and can be easily transformed into the Johnson system. Later in life, Eggen worked mostly in the Stromgren narrow-band system. All of these observations were handwritten onto index cards that he kept in his office. Often, when a visitor would ask a question about a star, he would look up the coordinates, go to his card file, and retrieve observations that he had made of that target.

3. The Eggen Observation Card File

In early 2007, we made contact with CTIO to find out what had happened to that card catalog, mainly because we were interested in some observations that Eggen had made but never published. CTIO had taken the cards out of Eggen's office upon his passing, and had placed them in storage at La Serena. Since they were not serving any useful purpose in storage, the Director of CTIO, Alistair Walker, gave the AAVSO permission to study these cards, sending them to us on long-term loan.

The box containing the index cards is shown in Figure 2. This large box contains an estimated 100,000 3x5 index cards, each of which refers to a single star and the observations of that star. The majority of these stars are in the southern hemisphere; all observations are photoelectric and of high quality. Our intent is to make these observations available to the astronomical community.

Figure 2. Large cardboard box containing Eggen's cards.

The first phase will be a general examination of the cards, moving them out of the miscellaneous cardboard boxes into more organized storage, and placing them into a logical sequence (Right Ascension is the obvious one, as this is how Eggen originally filed the cards). We will take some test scans of the cards, to see what resolution, file type and compression ratio can be tolerated. An example of such a scan is given in Figure 3, where 6 cards are shown to

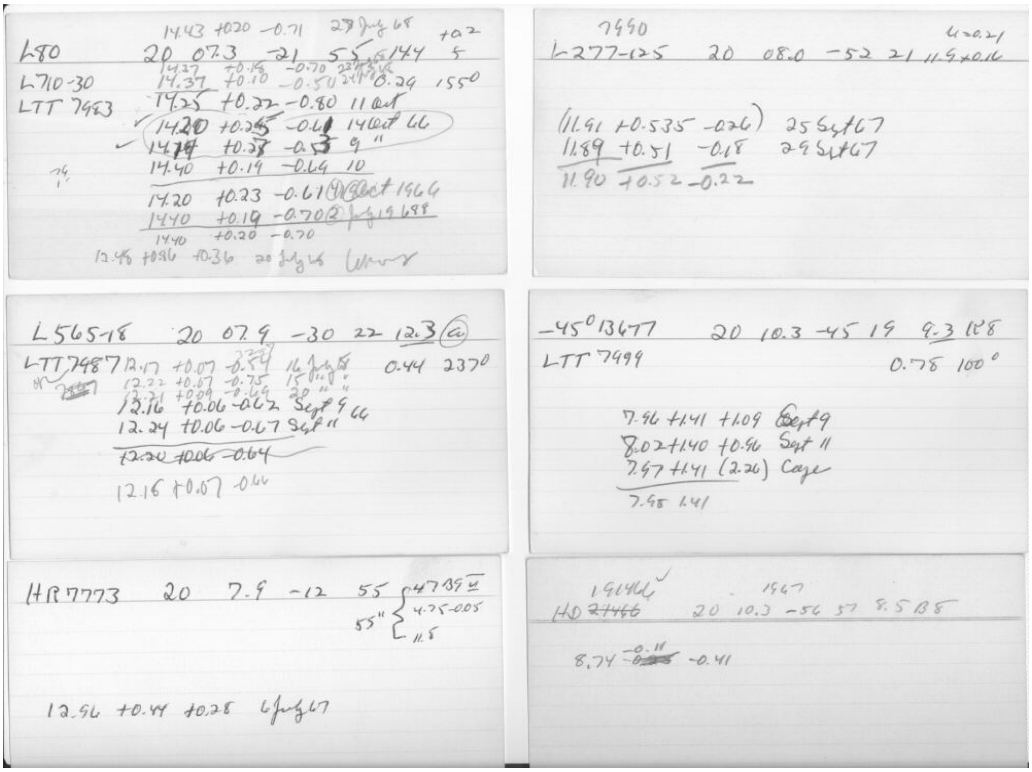

Figure 3. Scan of 6 Eggen index cards.

demonstrate the quality of a typical scan and the information content of the cards.

The next phase will be to scan all of the cards. We hope to hire a summer student to perform the mundane task of scanning, with funding from the AAS and perhaps a grant of a high-speed scanner from a commercial company. We expect the entire catalog to fit on a single DVD for off-line, permanent archival.

The third phase will be to place the scans on-line at the AAVSO website. The scans will be logically named, with a lookup table to find an appropriate star in the sequence. A Graphical User Interface (GUI) will be developed so that an outside researcher can request copies of any scan.

The final phase is where we need the most help. Our intent is to digitize the observations themselves, and place them in a separate MySQL database for ready access. Since the observations are handwritten, OCR techniques are nearly useless, and we need volunteers to "check out" scanned cards and enter the measurements from those cards into a computer file that we can read and upload into the database. Since there are 100K cards, this is the most labor-intensive part of the exercise and will require dedication by a large number of people to accomplish the task.

4. Summary

Our ultimate goal is to make the photoelectric observations that Eggen made over his career available in a convenient, machine-readable and easily queried format to researchers worldwide. They are a treasure-trove of information, both on infrequently studied southern stars, as well as measurements of variables over decades of time. The initial phases can be accomplished quite quickly, so at least individual stars can be found and measurements extracted; the final phases may take years to accomplish. Eggen was a great observer – we should make use of his efforts.

5. References

Eggen, O. J., Lynden-Bell, E., Sandage, A.R. (1962). *ApJ* **136**, 748.

Eggen, O. J. (2001) *PASP* **113**, 131.

Moro, D. and Munari, U. (2000). *A&AS* **147**, 361.

Amateur and Professional Astronomer Collaboration Exoplanet Research Programs and Techniques

Ron Bissinger
Racoon Run Observatory
1142 Mataro Court, Pleasanton, CA 94566
racrun@comcast.net

Abstract

In 1995 the breakthrough announcement was made that a planet had been discovered orbiting a star in the constellation Pegasus. Prior to that time, for decades astronomers had searched in vain to confirm that planets existed around any other star besides our own Sun. Yet it was a mere five years after the first exoplanet discovery that the first amateur astronomers observed a transit of an exoplanet using a 16-inch (40 cm) telescope in Finland. The realization that amateur astronomers could in fact detect exoplanets lead to the formation of transitsearch.org, the first amateur/professional collaboration to discover exoplanets. In the ensuing years numerous other such collaborations have been formed and dozens of amateur astronomers around the world now regularly observe stars identified by professional astronomers as possibly harboring exoplanets. This paper summarizes the more notable amateur and professional collaborations now ongoing to discover and characterize exoplanets. Tools and techniques used by amateur astronomers in such research are reviewed with an eye towards how amateur astronomers may soon help discover the first earth-sized exoplanet capable of supporting life as we know it.

1. Introduction

1. 1. Background

As humanity seeks to determine if intelligent life exists elsewhere in the universe, current efforts are focused on finding planets similar to our own Earth. While evidence was found in 1994 of planets orbiting a pulsar, it was in 1995 that the first exoplanet was found orbiting a sun-like star in Pegasus (Mayor & Queloz, 1995). Until 2000 exoplanets were found using Doppler shifts in stellar spectra as the orbiting exoplanets pulled on the parent star. One such exoplanet, HD 209458b, also in Pegasus, was determined to cross in front of, or transit, its parent star as seen from Earth (Charbonneau et al 2000).

Detection of exoplanets using spectroscopy requires large, professional observatories and expensive equipment beyond the reach of amateur astronomers. But the dip in the light of a star caused by the transit of an exoplanet is within reach of the amateur. So it was on September 16, 2000 that a group of amateur astronomers using a 16-inch (40 cm) telescope at the Nyrola Observatory in Finland observed a 1.7% decrease in the light of the parent star caused by a transit of HD 209458b. Inspired by the success of the Finnish amateurs, Transitsearch.org was formed in 2001 as the first collaboration between professional and amateur astronomers to find new transiting exoplanets. Since then, dozens of amateur astronomers worldwide have captured the signature dips in lightcurves caused by transiting exoplanets.

Professional astronomers have used two broad approaches to selecting and observing transiting exoplanet candidates. The first is a wide field search using wide angle optics and large CCDs to survey large swaths of the sky. The second is a targeted search where telescopes are used to monitor star clusters or specific stars. The wide field searches generally identify transit candidates with m_v <12 but are generally not suited for finding transits in dimmer stars.

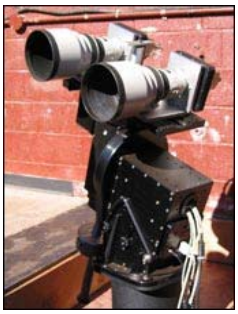

Figure 1. XO Project Wide Field System

Figure 1 shows an example of the instruments employed in wide field searches, in this case the system used by the XO Project on the 3054 meter summit of Haleakala on Maui, Hawaii. This automated

system uses two commercial 200mm f/1.8 Canon EF200 lenses coupled to two Apogee Ap8p CCD camera. Each lens covers 7.2 degrees of the sky.

1. 2. An Increasing Focus on Red Dwarfs

Most of the exoplanets discovered to date are much larger than Earth with orbits closer to their stars than Mercury is to our own Sun. Since their stars are as hot as or hotter than our own Sun, we know that these exoplanets are far too hot to harbor life similar to that on Earth.

In recent years researchers have proposed that exoplanets orbiting class M stars, particularly red dwarfs, may be capable of supporting life. Red dwarfs have surface temperatures of 3,000 deg K or even lower compared to over 6,000 deg K for our own Sun. Even if orbiting close to their stars, exoplanets of red dwarfs could have zones in their atmospheres where liquid water could persist, allowing life to flourish.

Confirmation of this possibility came in May 2007 with the announcement that an exoplanet only 1.5 times the size of Earth was found to orbit the red dwarf Gliese 581 which lies 20.5 light years from Earth. The exoplanet has an orbital period of 13 days and is at a sufficient distance from its relatively cool parent star that liquid water could persist.

As red dwarfs become subject to more scrutiny, amateur astronomers have the opportunity to participate and contribute to the newest frontier of exoplanet research.

2. Habitable Transiting Exoplanets Detectible by Amateur Astronomers

2. 1. Minimum Detectable Transit Depth by Amateur Astronomers

The measurement of changes in stellar light flux, called photometry, is limited from ground-based observatories largely by atmospheric scintillation as well as the intensity of the stellar flux relative to that of the background sky. Increasing the aperture of the telescope and increasing the time of exposure can improve the overall precision of the photometry but realistically only to certain levels.

Amateur astronomers commonly use telescopes with apertures ranging from 10 to 14 inches (25 to 35 cm) although some have access to instruments with apertures greater than 20 inches (0.5 m). For ground-based instruments with apertures of 14 inches (35 cm) or greater, it has been shown that exoplanet transits with depths of 0.2% to 0.3% (2 to 3 mmag) can be detected using multiple observations assuming stellar magnitudes m_v <12 (Bissinger 2005). In practice, a 14-inch (35 cm) telescope was used by the author to detect the 0.3% depth transit of HD149026b as shown in Figure 2.

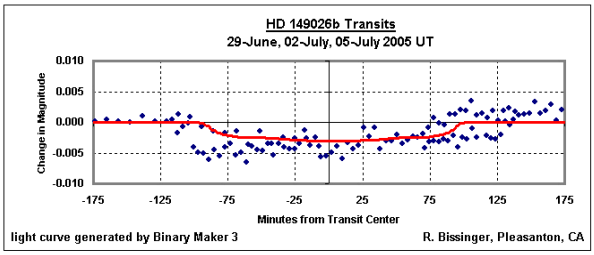

Figure 2. Exoplanet transit with 0.3% depth

2. 2. Sizes of Detectable Exoplanets

Given the typical equipment used by amateur astronomers, the possibility of whether they could detect an Earth-sized planet can be determined as well as the conditions under which it would be possible to do so.

Assuming a telescope aperture of 14 inches (35 cm) and a minimum detectable transit depth of 0.2% the relationship between exoplanet and parent star sizes can be approximated simply by using the ratio of the squares of their radii as shown in Figure 3.

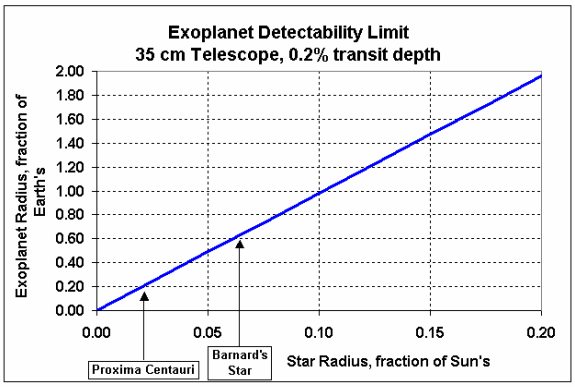

Figure 3. Minimum Detectable Exoplanet Size

Figure 3 plots the parent star radius as a fraction of that of our own Sun against the radius of the transiting exoplanet expressed as a fraction of the radius of Earth. We see that it is then possible for an amateur astronomer using a 14 inch (35 cm) telescope to detect transits of an exoplanet the size of Earth if it is orbiting a star with a radius 0.10 that of our Sun.

There are, however, certain conditions that need to be satisfied for Figure 3 to apply. The first would be that the star's magnitude would need to be m_v <12. Obtaining 0.2% (2 mmag) photometric precision on fainter stars with a 14-inch (35 cm) telescope would

be difficult if not impossible. The second would be that a single observation of a transit event by itself may not be evident, nor would it be convincing. So multiple observations of a transit need to be obtained, either by multiple observers detecting the same transit or by a single observer detecting multiple transits of the same star. Two to four such multiple observations would be required to indicate a significant probability that such a transit is indeed occurring (Bissinger 2005).

2. 3. Target Stars for Earth-sized Exoplanet Searches

Figure 3 shows that in order for amateur astronomers using typical equipment to detect transiting exoplanets approximately the same size as Earth they must observe stars that have radii less than 20% that of our own Sun.

Fortunately, our sky is filled with such targets, but they are not the stars we can see with our naked eyes. They are a class of stars called red dwarfs which are estimated to account for as many as 75% of the stars in our galaxy..

For example, Figure 3 also shows that two well known red dwarfs, Proxima Centauri and Barnard's Star, could provide transit signatures sufficient to be detected by amateur astronomers if they harbored transiting Earth-sized exoplanets.

An excellent discussion of the probability of terrestrial-sized planets forming in red dwarf systems and why such exoplanets might be capable of supporting life as we know it has been provided previously (Wolf, Laughlin 2006). In recent years a number of papers have presented strong arguments as to why such exoplanets make compelling targets for indicators of life (Tarter et al, 2007; Segura et al, 2005).

While several space-based instruments are or will be searching for exoplanets using the transit method (the European Space Agency's COROT, NASA's Kepler, and the Canadian Space Agency's MOST, for example) amateur astronomers have the equipment and time to monitor many single red dwarf targets for transiting exoplanets.

But unlike previous efforts where amateurs observed fairly bright stars with $m_v<9$, red dwarfs are considerably fainter with $m_v>11$. In order to yield usable signal to noise ratios, the red dwarfs that lend themselves to amateur observing must be relatively close to Earth. So it is indeed fortunate for the interested amateur astronomer that professional astronomers have prepared several lists of potential close-in red dwarf targets as part of their preparations for the space missions mentioned previously as well as future missions such as NASA's Terrestrial Planet Finder and Space Interferometry missions.

An ongoing project, the Research Consortium on Nearby Stars (RECONS), is in the process of identifying our closest neighbors. A list of the closest 100 stars, including many red dwarf stars brighter than m_v =12, is maintained and updated by the group at:

http://www.chara.gsu.edu/RECONS/

Another target list developed for NASA's upcoming Space Interferometry Mission (SIM) includes many red dwarfs and is maintained at:

http://tauceti.sfsu.edu/~chris/SIM/t1.html

Figure 4 shows some of our nearest neighbors in space, many of which are red dwarfs not visible to the naked eye.

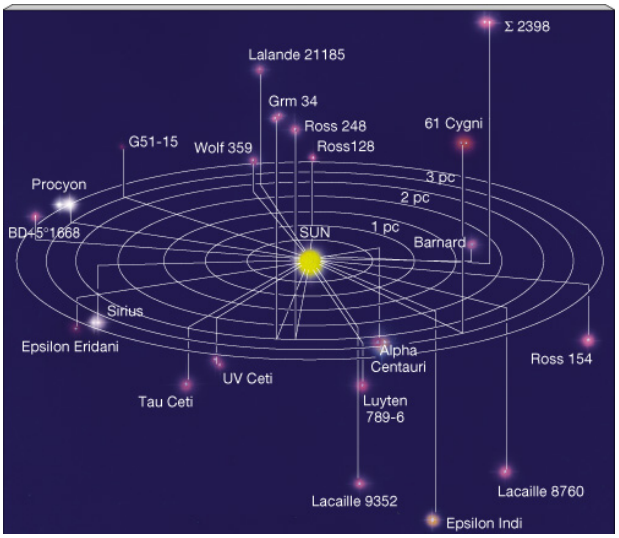

Figure 4. Our Nearest Neighbors (from Astronomy Today, Chaisson and McMillan, 2002)

As is apparent from inspecting the RECONS and other lists, however, the number of red dwarfs observable by typical amateur astronomers is quite large.

One approach for selecting a suitable target to monitor would be to pick one that is observable in the eastern sky shortly after nightfall and then make repeated observations over a month or two. Unfortunately, visual inspection alone might not be sufficient to pick out a small transit in such a large set of data.

There are some commercially available software packages that have the capability to isolate a transit signal buried within a large set of data taken over multiple observing sessions. One such package is

PERANSO, available at http://www.peranso.com. Another product that could be used is MPO, available at http://www.minorplanetobserver.com.

3. Pro-Am Exoplanet Search Collaborations

3. 1. History of Pro-Am Collaborations

Most amateur astronomers, however, will quickly find it quite daunting and challenging to sift through the gigabytes of data an individual might generate from such an observing endeavor. A better approach for the individual observer might be to participate in a professional-amateur (Pro-Am) collaboration to monitor red dwarf candidates.

The advantages of such participation are many. First, the amateur will be able to observe a list of target stars that are prioritized based on the professional astronomers' latest understandings of planetary formation. Second, the amateur will be able to pool their observations with those of others so as to maximize the coverage of a target star, increasing the likelihood that they will observe and detect a transit if one occurs.

One of the first, if not the first, such Pro-Am collaborations was Transitsearch.org which was launched in 2002 to find new transiting exoplanets. Other Pro-Am collaborations followed, including the XO Project which has yielded the discovery of the transiting exoplanet XO-1b and offers the promise of uncovering more exoplanets in the future (see http://www-int.stsci.edu/~pmcc/xo/science/).

3. 2. Systemic – A Web-based Collaboration

It was in 2006 that an innovative program called Systemic was launched that allows interested amateurs and the public to participate in a wide-scale simulation to quantify the likelihood of planetary formation. No equipment is necessary. The project is web-based, and uses a catalog of 100,000 stars to allow users to discover exoplanets using model radial velocity curves for the catalog stars. The properties of the theoretically-discovered exoplanets are then compared with those of real ones.

Systemic has the potential to provide additional guidance for follow-up radial velocity or transit observations of promising candidate stars.

3. 3. A Red Dwarf Exoplanet Pro-Am Collaboration

Interest in red dwarf systems as potential harbors of life has spurred increasing professional observations as well as a new Pro-Am collaboration. GEMSS, an acronym for Global Exoplanet M-dwarf Search Survey, is designed to provide focus for professional and amateur efforts to observe red dwarfs (http://gemss.wordpress.com). The project is in its early stages but will be reaching out to interested amateurs, the AAVSO and Transitsearch.org for additional participation.

4. Exoplanet Transit Detection Tips and Techniques

The literature and online forums are full of procedures and techniques for performing photometry. As instruments used by amateurs have increased in capability over the years, so has the number of people performing precision photometry. Five years ago amateurs aspired to achieve differential photometric precisions of 1%, or 0.01 mag. Recently, in part driven by the need for high precision photometric time series of exoplanet transit candidates, differential photometric precisions of 0.2%, or 0.003 mag, are becoming commonplace.

Much has been said and written about the quality of flat fields, dark subtraction, and signal to noise ratios, all of which is valuable to learn and to put into practice. But beyond these frequent topics, it is from the author's experience observing exoplanet transit targets for several years that two techniques stand out that have consistently helped achieve high levels of differential photometric precision.

4. 1. Sticky Pixels

It is commonly accepted that flat fielding is necessary when performing CCD photometry, and very often it is. It is also recognized that unless carefully prepared, flat fields themselves can introduce errors and artifacts into the science images.

The combination of precision telescope mounts and CCD guiders that can track to sub-pixel accuracy allows observers to keep a star image on a very small spot of their CCD chips. Doing so minimizes errors introduced by small difference in sensitivities of individual pixels and other variations on the chip itself. A slight amount of defocusing can spread the star image over a small number of pixels and the precise tracking will keep the image on the same spot throughout the observing session. The author has found this technique very useful.

Another advantage of this technique is that only carefully prepared flat fields will improve the accuracy of the photometry. For example, in the situation where a near-full moon can cause uneven illumination of the sky depending on telescope position, flat fielding will not correct all the images uniformly and

can actually degrade photometric precision when applied to a series of images taken over an entire night, especially when differential photometric precisions of ~0.5% (5 mmag) or less are required. In such cases it has been seen that raw images reduced with only darks and bias frames can provide better results, again assuming precise tracking of the star on a small area of the chip.

4. 2. Systemic De-trending

Amateur and professional photometrists will often use color transformations to account for differential atmospheric extinction of stars of different colors. By doing so they are eliminating a quantifiable factor in their data that would provide an inaccurate result.

For years professional astronomers have used a similar philosophy when working with time series differential photometry. They have recognized that there are predictable and quantifiable trends in their photometry that have been introduced because of variations in tracking, individual pixel sensitivity, artifacts on their CCD chips and other factors. They have characterized these trends as systemic errors (not to be confused with the Systemic exoplanet project mentioned previously!) and have developed methodologies for their removal from their data. Several variations of de-trending algorithms can be found in the literature (Manfroid et al, 2001; Mazeh et at, 2006).

While the application of complex de-trending algorithms can be done by amateurs, differential photometric precisions can often be improved in time series by some simple mathematics.

Amateur differential photometry time series often exhibit cyclic trends readily discernable to the eye. These cycles will often have periods considerably longer than that of an exoplanet transit. It then becomes possible to use a simple sine function to remove the long period trends from the data without compromising short term variations.

Figure 5 shows an example of differential photometry obtained with a 14-inch (35cm) telescope. The standard deviation of the raw data shown is 0.14% (1.4 mmag). The figure also shows a cyclic trend in the data which was modeled using a sine function and least squares fit to the data. The sine function was then simply subtracted from the raw data yielding a smoother time series having a standard deviation of 0.12% (1.2 mmag), a 14% reduction in scatter.

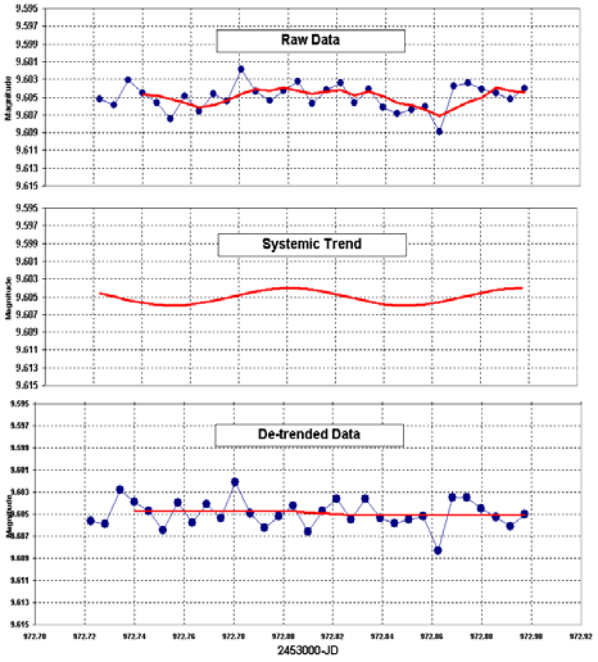

Figure 5. Simple De-trending Algorithm Effect

While 14% reduction may not appear to be that much, when several nights worth of such time series observations are combined, the de-trending algorithm makes discerning a small transit significantly easier.

As more amateurs seek smaller exoplanet transits it is likely that more de-trending approaches will be used in the data analysis.

5. Conclusions

The monitoring of red dwarfs for transiting exoplanets is a new opportunity for amateur and professional astronomer collaboration. Amateur astronomers have ready access to the equipment, tools and time with which to make a significant contribution to exoplanet research and the ultimate search for life in the universe.

6. Acknowledgements

The author would like to thank Greg Laughlin of UC Santa Cruz and Tim Castellano for their early guidance and encouragement to pursue exoplanet observing. Most recently the author has been inspired by the tireless efforts and wisdom of Peter McCullough of the Space Telescope Science Institute as well as the other participants in the XO Project.

7. References

Mayor, M., Queloz, D. (1995). "A Jupiter-Mass Companion to a Solar-Type Star," *Nature* **378**, 355.

Charbonneau, D., Brown, T.M., Latham, D.W., Mayor, M. (2000). "Detection of Planetary Transits Across a Sun-like Star," *Astrophysical Journal* **529**, pp. L45-L48.

Bissinger, R. (2005). "Using A Distributed Observer Network To Characterize Transit Lightcurves Of Exoplanet Tres-1b," *Proceedings for the 24th Annual Conference of the Society for Astronomical Science* (B.D. Warner, D. Mais, D.A. Keynon, J. Foote, eds.) pp. 75-84. Society for Astronomical Sciences.

Wolf, A. Laughlin, G. (2006). "Extrasolar Planets and the Race to Uncover the First Habitable Terrestrial Planet," *Proceedings for the 25th Annual Conference of the Society for Astronomical Science* (B.D. Warner, J. Foote, D. Mais, D.A. Kenyon, eds.) pp. 91-96. Society for Astronomical Sciences.

Tarter, J.C., Backus, P.R., Mancinelli, R.L., Aurnou, J.M., Backman, D.E., Basri, G.S., Boss, A.P., Clarke, A., Deming, D., Doyle, L.R., Feigelson, E.D., Freund, F., Grinspoon, D.H., Haberle, R.M., Hauck, S.A., Heath, M.J., Henry, T.J.; Hollingsworth, J.L., Joshi, M.M., Kilston, S., Liu, M.C., Meikle, E., Reid, I.N., Rothschild, L.J., Scalo, J., Segura, A., Tang, C.M., Tiedje, J.M., Turnbull, M.C., Walkowicz, L.M., Weber, A.L., Young, R.E. (2007). "A Reappraisal of the Habitability of Planets Around M Dwarf Stars," *Astrobiology* **7**, 30-65.

Segura, A., Kasting, J.F., Meadows, V., Cohen, M., Scalo, J., Crisp, D., Butler, R.A.H., Tinetti, G. (2005). "Biosignatures from Earth-Like Planets Around M Dwarfs," *Astrobiology* 5, 706 –725.

Manfroid, J., Royer, P., Rauw, G., Gosset, E. (2001). "Correction of Systematic Errors in Differential Photometry," *Astronomical Society of the Pacific*, ISSN: 1080-7926, p.373

Mazeh, T., Tamuz, O., Zucker, S. (2006). "The Sys-Rem Detrending Algorithm: Implementation and Testing," PASP Proceedings of "Transiting Extrasolar Planets Workshop" (C. Afonso, D. Weldrake, T. Henning, eds.), MPIA Heidelberg Germany, 25th-28th September 2006, submitted.

Exoplanet Observing Tips

Bruce L. Gary
5320 E. Calle Manzana
Hereford, AZ 85615
brucegary1@cis-broadband.com

Abstract

Exoplanet transit lightcurves with depths less than ~25 mmag require observing practices that challenge the amateur and professional alike. The gold standard of 2 mmag precision per minute during a 6-hour observing session is possible, but difficult – especially using amateur hardware. Pitfalls are present in almost every aspect of observing and image analysis, but perhaps the most important, which is too often neglected, is the use of same-color reference stars. Different-color reference stars affect transit depth, shape and timing. Transit observations are used to illustrate these effects and a simple procedure for selecting same-color reference stars is presented.

1. Introduction

Procedures commonly used for observing and processing images of variable stars may be inadequate for exoplanet transits. When variations of 10 to 25 milli-magnitude (mmag) are to be measured during a 6-hour observing session subtle effects that can be regarded as "second order" for cataclysmic variable stars, undergoing >100 mmag changes during the same period, become "first-order" effects for the exoplanet transit lightcurve (XLC).

This article describes a few "good practices" for the XLC observing phase. A more extensive treatment is given for one aspect of the image analysis phase: the need to select reference stars having the same color as the target star.

2. Observing Phase Precautions

Flat fields are sometimes taken without subtracting dark frames with the same exposure. This can lead to a master flat frame sprinkled with hot and cold pixels that would have been removed had darks been used. The magnitude of these defects can be especially large for old CCDs. During a 6-hour XLC observation the target star and reference stars will move across the CCD pixel field and any defects along these paths will produce systematic errors in the XLC. Always use dark frame calibrations when acquiring flat frames.

A master dark frame should be free of systematic defects and have a low level of stochastic noise. Systematic defects can be produced by assuming that the master dark frame can be created when the CCD is cooled to one temperature and then used for XLC observations taken at another temperature. It is a good observing practice to set the CCD cooler to a coldest possible temperature prior to XLC observations, and acquire a dozen or more dark frames before and after the XLC observations. If an insufficient number of dark frames are taken, or if they are made at a different temperature than the XLC observations, any deviations from perfect will lead to slowly changing systematic variations in the final XLC.

Auto-guiding during the entire XLC observing session will reduce movement of the star field across the CCD pixel field, and this will reduce systematic effects related to imperfect flat fields and imperfect master dark frames. However, even if the auto-guiding is perfect the star field will move. The amount of movement will be proportional to the polar axis alignment error. The auto-guider star may stay fixed to the same pixel location on the auto-guider chip but the location on the sky for the auto-guider star will be a center of rotation for the image on the main CCD chip. A polar axis alignment error of only 1/2 degree can lead to an image rotation of 30 'arc (depending on source declination), or 10 pixels for my telescope system. Therefore, it is important to achieve a polar alignment accuracy of ~0.1 degree.

Differential photometry requires the presence in the same image as the target star at least one bright and unsaturated star for use as reference. Several reference stars will reduce scintillation noise, and if they surround the target star it's reasonable to expect that the additional stars will reduce systematic effects related to an imperfect flat field. Thus, a large field-of-view (FOV) is desirable, and this means there's an incentive to use a focal reducer (or "telecompressor") lens. The farther the focal reducer lens is placed from the CCD chip, the larger the FOV. However, it is also

true that the farther the focal reducer is placed from the CCD chip (than intended in its design), the greater are the optical degradations, such as coma. The size of these degradations will increase with distance from the optical "center" on the CCD image (which hopefully is somewhere near the center of the FOV). If during a 6 or 8-hour observing session the focus changes and is not corrected the point-spread-function (PSF) will become different near the FOV corners and edges compared with near the FOV center. This will cause the percentage of the PSF that's inside a photometry aperture to vary with image location. This, in turn, will produce a systematic error related to how the focus changed. Therefore, if a focal reducer is used it is important to place it at the designed distance from the CCD chip.

Plate scale, the number of "arc per pixel, should be matched to the observing site's "atmospheric seeing" and it must also meet the spatial sampling criterion for precision photometry of at least 3 pixels per full-width half-maximum (FWHM) of the sharpest image's PSF. For example, if the best FWHM is 2.5 "arc, the plate scale should be <0.8 "arc/pixel. This requirement places a constraint on how much FOV increase can be produced using a focal reducer.

These are a few precautions that should be considered before an observing session. In my opinion, however, the most important precaution for achieving accurate XLCs occurs after the observing session, during the image analysis phase. It has to do with choosing the best star, or stars, for use as reference. This is the subject of the rest of this article.

3. Atmospheric Extinction Spectrum

Because amateurs observe exoplanet transits through an atmosphere it is not sufficient to choose a reference star that is brighter than the target star, unsaturated and non-varying. This is because each star's flux changes with air mass at a rate that depends on the star's color. Blue stars fade with increasing air mass faster than red stars. To understand why this occurs let's review what causes star light to fade with increasing air mass.

There are three sources for atmospheric extinction, listed here in the order of their importance: 1) Rayleigh scattering by molecules, 2) Mie scattering by atmospheric aerosols (dust), and 3) resonant absorption by three atmospheric molecules (oxygen, ozone and water vapor). Figure 1 is a plot of the spectrum of Rayleigh scattering for the CCD response wavelength region.

Figure 2 plots aerosol scattering for four site altitudes. Figure 3 shows the sum of these two scattering components compared with measured zenith extinction at a 4600-foot altitude site.

Notice in these figures that atmospheric extinction increases with decreasing wavelength. The effect is greatest for the B-band filter.

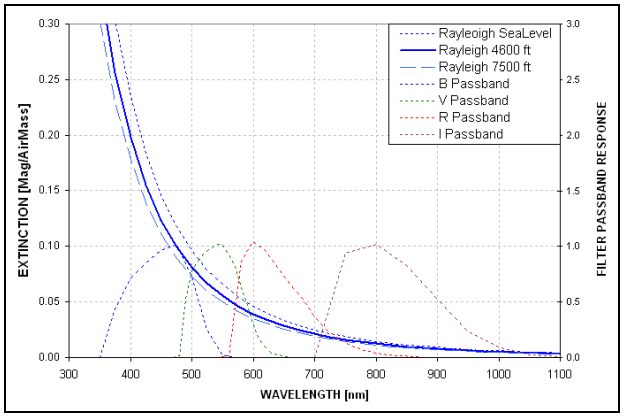

Figure 1. Rayleigh scattering spectrum for 3 observing site altitudes. Typical spectral response curves are shown for B, V, Rc and Ic filters.

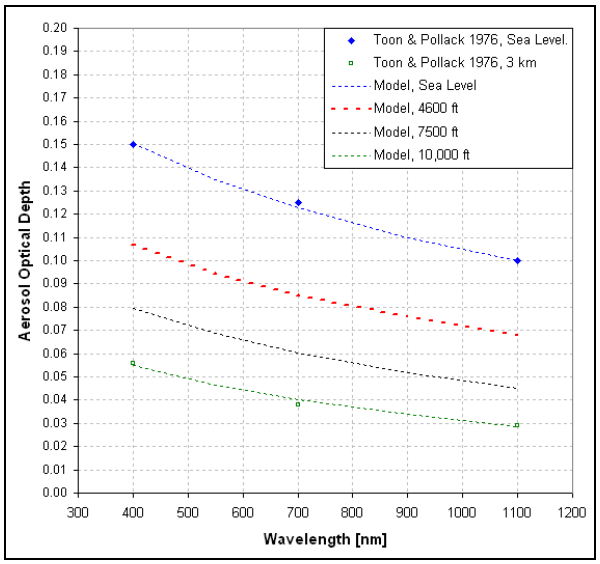

Figure 2. Aerosol scattering spectrum for 4 observing site altitudes.

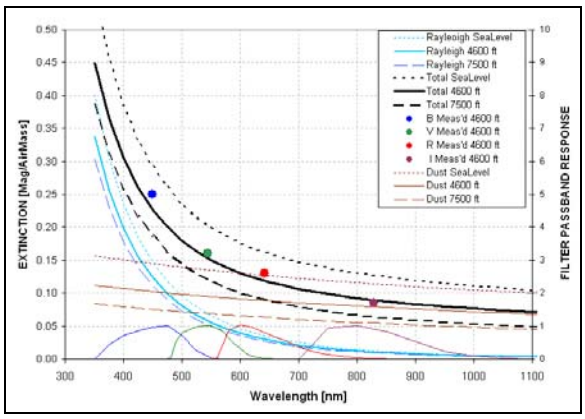

Figure 3. Sum of Rayleigh and aerosol scattering compared with measurements at a 4600-foot site.

4. Star Color Affects Zenith Extinction

Stars radiate with a blackbody spectrum, as a first approximation. The next figure shows blue and red star blackbody spectra in relation to a B-band response function.

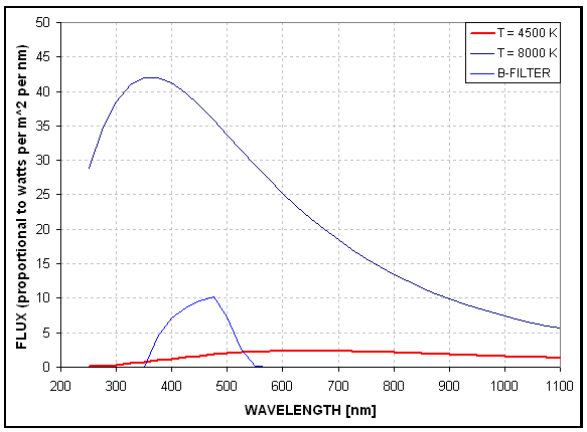

Figure 4. Blackbody spectra for blue and red stars in relation to B-band response function.

Throughout the B-filter passband the red star has increasing flux with increasing wavelength, whereas the opposite is true for the blue star. The flux-weighted wavelength for the blue and red stars is 445 nm and 467 nm, respectively. The flux-weighted extinction coefficients are 0.244 and 0.228 magnitude/air mass. In other words, a blue star fades with increasing air mass faster than a red star.

Consider the case of a target star (the one undergoing an exoplanet transit) with red and blue stars nearby that are otherwise suitable for use as a reference star. Figure 5 shows what can be expected for a lightcurve when either star is used for differential photometry reference.

Clearly, for B-band it is important to choose reference stars that are approximately the same color as the target star. Although use of R-band or I-band filters will have smaller effects than the 10 mmag systematic error shown in this figure, effects correlated with air mass have been seen using these filters.

Unfiltered observations are also subject to reference star and target star color mismatches. The next figures illustrate this. Figure 6 is a lightcurve of an exoplanet using a properly-matched reference star. The out-of-transit (OOT) baseline level is "flat."

Figure 7, however, was produced using blue stars for reference. Although the plot is less noisy, because more reference stars were used, the OOT baselines are curved. The curvature is in the way that is expected, with symmetry about transit (~5 UT).

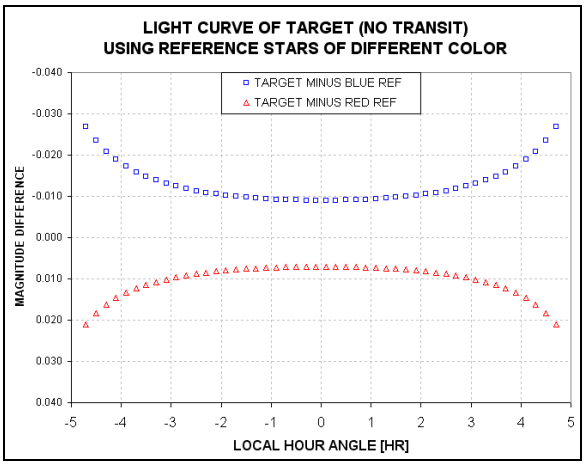

Figure 5. Model lightcurves for observations of a typical color star with a B-filter using nearby blue and red stars for reference.

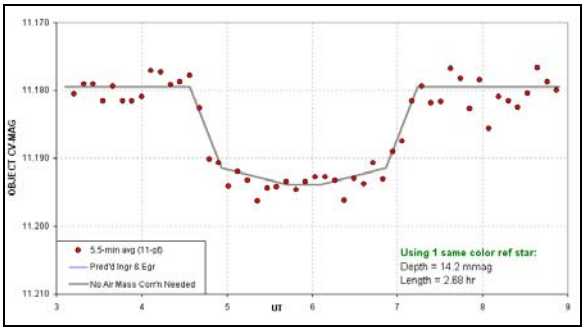

Figure 6. Measured exoplanet lightcurve using a same-color reference star.

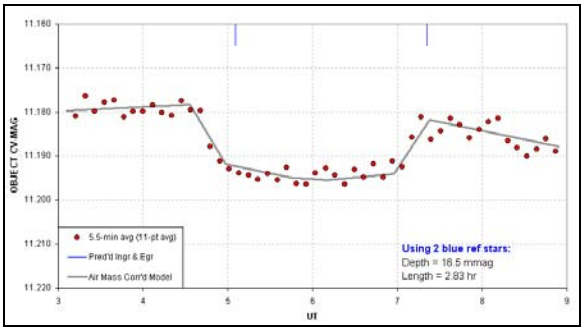

Figure 7. Measured exoplanet lightcurve using two blue reference stars.

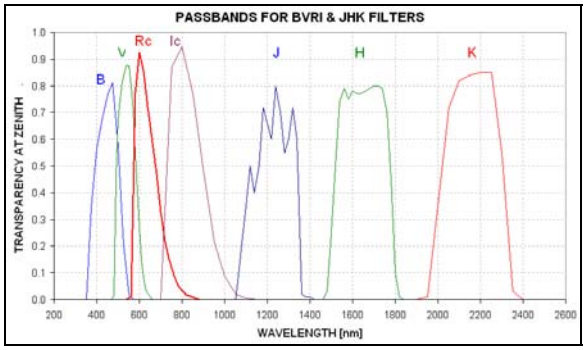

Figure 8. Passbands for BVRcIc and JHK filters, scaled to show typical zenith transparency.

The same XLT measurements were processed using a red star (not shown), and the curvature is opposite that for the blue reference stars. Readings of the three lightcurves show a systematic change of measured transit depth, length and mid-transit timing. The depth readings are 13.5, 14.4 and 16.0 mmag for use of blue, same-color and red reference stars, respectively. The transit length readings are 2.71, 2.68 and 2.74 hours, for use of blue, same-color and red reference stars. The mid-transit times are 5:56.7, 5:54.2 and 5:52.2 UT for use of blue, same-color and red reference stars, respectively. Thus, systematic effects are present at the level of 1 mmag for depth, 0.04 hour for length and 2 minutes for mid-transit times.

It therefore makes a difference whether same-color or different-color reference stars are used for processing exoplanet lightcurves.

5. Finding Same-Color Stars

Figure 8 shows typical passband shapes for BVRcIc and JHK filters. It has been shown that J-K star colors are highly correlated with B-V, V-R and R-I star colors (Caldwell et al, 1993, Warner, 2007). The correlations break-down for very red stars, but it is rare that very red stars will be sought for use as reference. Since J and K magnitudes exist for almost all stars brighter than 18th magnitude (V-band), and since J and K magnitudes are conveniently available in most star map programs (such as TheSky6 and Canopus), it is feasible, and convenient, to find same-color reference stars using only the J and K magnitudes.

6. Conclusion

One of the most-overlooked yet important requirements for achieving high quality exoplanet transit lightcurves is the use of same-color reference stars.

7. Acknowledgements

Acknowledgements are due the XO Project and Extended Team members for providing many examples of exoplanet transit lightcurves, some of which are professional quality.

8. References

Caldwell, J. A. R, Cousins, A. W. J., Ahlers, C. C., van Wamelen, P. and Maritz, E. J., "Statistical Relations between the Photometric Colours of Common Types of Stars in the UBV(RI)c, JHK and uvby Systems." (1993). *SAAO Circulars, no. 15*.

Warner, B.D. and Harris, A. W. "Asteroid Lightcurve Work at the Palmer Divide Observatory", (2007). *American Astronomical Society,* Hawaii

Study of Cepheid Variables as a Joint Spectroscopy Project

Thomas C. Smith
Dark Ridge Observatory
tcsmith@darkridgeobservatory.org

Kenneth E. Kissell,
Kissell Consultants

Abstract

In the late 1940's, P.C. Keenan and J.A. Hynek conducted exploration of the near-IR with the then available 1-N photographic plates. They noted (1950) that an O I triplet feature at 777.2 to 777.5 nm., arising from a metastable state in the oxygen atom, was particularly strong in absorption in highly luminous stars, ranging from types B8III/B8Ia through G2Ib/Ia, with equivalent widths of 0.6 to 2.3 Angstroms. It was pointed out by Keenan (as part of a detector dissertation project in 1962, on a 1.75-m telescope) that Cepheid variables live within this region of the HR diagram, and several Cepheid variable stars were selected as target stars along with several dozen stable stars in the luminosity classes III through Ia, and spectral types from late-B through early-M. The predicted variation in the triplet was observed, but not then studied in detail. The case will be made that exploitation of small amateur telescopes (perhaps as a joint campaign), equipped with the currently available spectrographs/CCD cameras, can outperform the earlier telescopes of the 2-meter class, and allow investigation of this type of spectral feature. The increase of quantum efficiency from about 2-4% to 60-80% allows a 14-20 inch system, devoting 100% to the task at hand, to tackle the targets requiring more than 2.2 meters in the days when telescope time for only a few nights per year was available. In the present instance, we would like to investigate whether the spectral feature reaches its peak absorption in phase with the maximum light output from the pulsing star, or does it lag or lead it. With the same instrument, or with a co-mounted companion, we can monitor the U, B, V, or R stellar output while collecting the spectra. Other small-telescope spectroscopy projects might be found from reviews of the literature from the mid-1900s.

1. Introduction

When astronomical spectroscopy moved beyond the limits of the early blue and green orthochromatic emulsions, to the near IR (out to 9000 A., made possible with the new P and R plates of Eastman Kodak), it was quickly learned that strong lines were present due to H, N I, O I, Mg II, and Ca II, and that these were present in windows free from atmospheric absorption. P. Merrill (1934) summarized his findings, using the 2.5-m Hooker telescope on Mt Wilson with a grating spectrograph of 33 A/mm dispersion, noting especially the strength of an oxygen triplet at 7771-7775 A, frequently referred to in the literature as the 7774 feature. This feature was noted as remarkably strong in luminous stars from late B to early G spectral types, having a combined equivalent width in excess of 2 A in luminosity classes Ia. Keenan and Hynek (1950), using the newer I-N plates and a prismatic spectrograph on the new Perkins 1.75-m reflector at only 250 A/mm dispersion, undertook a more detailed study of the triplet feature on about six dozen spectral standard stars spread across the HR diagram.

In 1961 Keenan suggested further study of this feature to one of the authors (KEK) when exploring the use of a new type of imaging detector, an S-1 image converter tube, for quantitative spectroscopy in a direct comparison with I-N and I-Z photographic plates. This was prior to the development of CCD detectors, and was part of the 1960's investments made by NSF in new detectors.

2. Prior Work on Cepheid Variables

Keenan also pointed out to the student that this region of the HR diagram contained the Cepheid variables, they being Ib supergiants, which might be studied by observing how this triplet feature varies during the pulsation cycle of a few days to several weeks, depending on the star. For example, the prototype is delta Cephei, which cycles from F5Ib to G1Ib every 5.366 days, while varying in brightness from +4.37 to +3.48 st mag in this cycle. Fig. 1 is taken from the K&H 1950 paper, and shows the boundaries of luminosity classes vs. the triplet equivalent width. If delta Cephei were to remain on the Ib trajectory of

luminosity, its O I triplet strength could be predicted to vary regularly from about 0.6 A to 1.2 A during each cycle of varying spectral type. Fig. 2, from K&H, shows spectra from F0 stars from dwarf to supergiants.

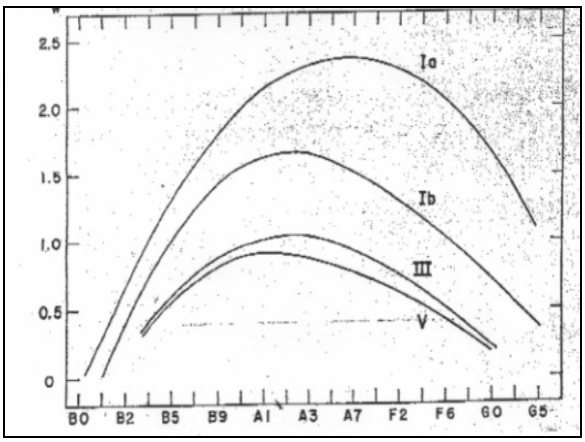

Fig. 1. Luminosity effects in the total absorption of O I 7774 feature.

Observations were made of the O I feature in delta Cephei, both image tube and I-N, during 1962

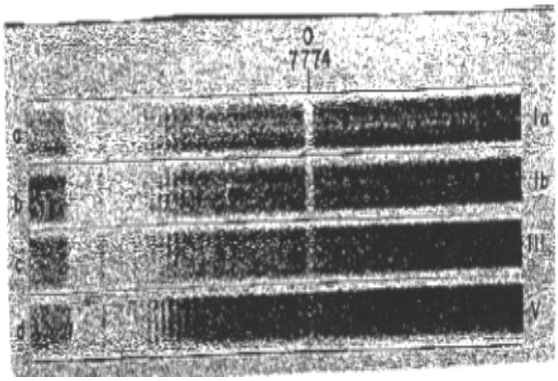

a)	**ε Aur**	**Ia**
b)	**α Leo**	**Ib**
c)	**ζ Leo**	**III**
d)	**γ Vir**	**V**

Fig. 2. The oxygen lines, 7774 A, in stars of type F0:

and 1963, along with the measures of other non-variable stars over a whole range of the HR diagram. The observations of several Cepheids were included, but these were not the main thrust of the investigation, which included stellar and solar spectra extending into the 1.2-micro-meter region, which the S-1 image tube allowed.

Fig. 3, from Kissell's dissertation (1969), shows a plot of data from both I-N (15) and image tube (17) measures of equivalent width of the O I triplet vs. brightness phase of delta Cephei, corrected to variable brightness data collected in this same time frame by an AAVSO volunteer upon my request (Marvin Baldwin, Capt. USAF, who became a very active AAVSO member).

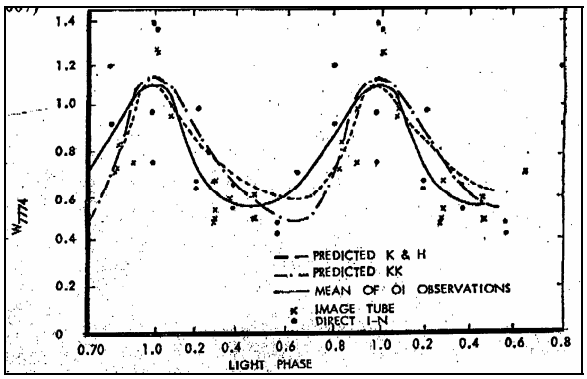

Fig. 3. Variations of O I feature at 7774 A with light phase in delta Cephei. Dashed curves are predictions based on absorption in non-variable supergiants Ib.

As is immediately apparent, the triplet strength shows strong variation with the pulsation of the star, exceeding the expected values plotted also on the figure. Unfortunately the scatter of the data taken at the dispersion used in the Perkins grating spectrograph does not allow confidence in the phase values of the maximum and minimum feature strength. Specific analyses of these data were not part of the dissertation write up (1969) or of other publications. It appears to be long overdue to explore further this interesting feature, now that many amateurs could contribute to it.

Fig. 4 shows how the brightness, temperature, stellar radius, and radial velocity vary with the phase, zero phase being the brightest. We would like to add O I triplet strength to these plots.

It is the intention of the proposed study to use current CCD detectors and SBIG grating spectrographs to obtain multiple (nearly continuous) observations at a higher resolution, so as to establish the feature strength and phase on delta Cephei, and to collect similar data on several other of the dozen Cepheids both visible in these latitudes and brighter than +7 minimum magnitude. The periods of these candidate stars range from 3.73 to 27.0 days. This study is to 'shed light' on the physics of the triplet feature, which originates from upper levels in the pulsating atmosphere in which normally metastable levels in the oxygen atom have been populated by UV excitation, but remain populated without normal collisional de-excitation.

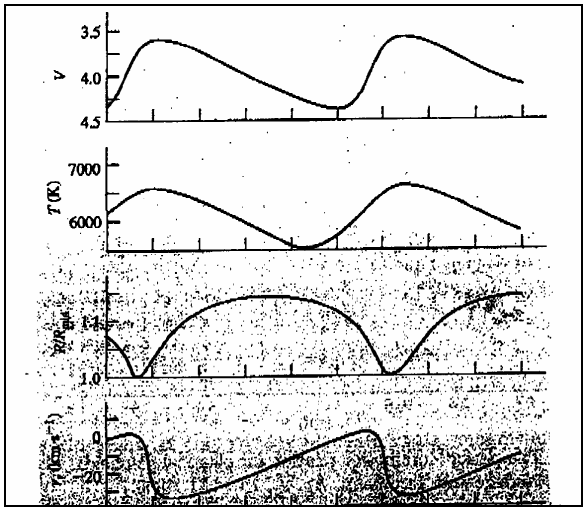

Fig. 4. Observed pulsation properties of delta Cephei.

Table I is a list of Cepheid candidates, taken from the Astronomical Almanac (2007) and it includes an epoch date value for the peak brightness (phase 0.0) from which an observer can reckon the phase at which any spectrum has been taken. We propose to validate the epochs by simultaneous photometry with the spectral collections, either by the observers themselves, or by cooperating participants. In 1963 an offset of 0.05 was needed to phase the predicted peaks to the visual measurements provided by the AAVSO.

3. Proposed Future Work

Although the immediate objective of our program is a definitive study of delta Cephei, we plan to extend the campaign to nine other Cepheids visible from the Dark Ridge Observatory, recently relocate to the dark skies of New Mexico, including eta Aquilae, zeta Geminorum, and T Monocerotis, all of which were observed for the presence of the O I feature in 1962-63, but not enough to look for their periodicity and phase. These stars will be studied so as to map the equivalent width with phase and spectral type. Equipment to be utilized at the Dark Ridge Observatory include a Meade 14" LX200GPS incorporating an SBIG SGS spectrograph fitted with an 1800 rules/mm diffraction grating.

Another class of variable stars (also of high interest to cosmologists) are the RR Lyras, also pulsating variables but about luminosity class II, and with periods much shorter than the Cepheids, about 0.7 days. The brightest of them is about 4% that of delta Cephei. We will explore RR Lyrae for the O I triplet, but it may be beyond the detailed study with our small instruments. RR Lyras are receiving some rebirth of interest by the Japanese astronomers at the Subaru facility on Mauna Kea.

Name	Right Ascension h m s	Declination ° ‘ “	Magnitude max / max	Epoch (2400000+)	Period d	Spectral Type
T Mon	06 25 37.3	+07 04 52	5.58, 6.62	43784.615	27.025	F7Iab-KIIab
RT Aur	06 29 03.0	+30 29 16	5.00, 5.82	42361.155	3.728	F4Ib-G1I
ζ Gem	07 04 33.2	+20 33 31	3.62, 4.18	43805.927	10.151	F7Ib-G3Ib-G1Ib
X Sgr	17 48 02.0	-29 49 59	4.20, 4.90	40741.70	7.013	F5-G2II
W Sgr	18 05 30.0	-29 34 45	4.29, 5.14	43374.77	7.595	F4-G2Ib
Y Sgr	18 21 49.5	-18 51 22	5.25, 6.24	40762.38	5.773	F5-G0Ib -II
FF Aql	18 58 34.8	+17 22 17	5.18, 5.68	41576.428	4.471	F5Ia-F8Ia
η Aql	19 52 51.3	+01 01 31	3.48, 4.39	36084.656	7.177	F6Ib-G4Ib
S Sge	19 56 21.7	+16 39 18	5.24, 6.04	42678.792	8.382	F6Ib-G5Ib
X Cyg	20 43 41.8	+35 36 54	5.85, 6.91	43830.387	16.386	F7Ib-G8Ib
T Vul	20 51 47.4	+28 16 44	5.41, 6.09	41705.121	4.435	F5Ib-G0Ib
δ Cep	22 29 27.1	+58 27 13	3.48, 4.37	36075.445	5.366	F5Ib-G1Ib
RR Lyr	19 25 42.3	+42 47 57	7.06, 8.12	50238.499	0.567	A5.0-F7.0

Table I. Cepheid Characteristics for Candidate Program Stars

4. References

Keenan, P.C., Hynek, J.A. (1950). *Ap. J.* **111**, 1.

Kissell, K.E. (1969). "Application of an Infrared Image Tube to Astronomical Spectroscopy," *University Microfilms*, Doc. #69-15933. Ann Arbor, MI.

Carroll & Ostlie (1996). *Introduction To Modern Astrophysics*, Addison-Wesley, p.546

The Astronomical Almanac (2007). U.S. Government Printing Office.

Lhires III High Resolution Spectrograph

Olivier Thizy
Shelyak Instruments; Les Roussets, F-38420 Revel, France; http://www.shelyak.com
AUDE association, Paris, France; http://astrosurf.com/aude
CALA; 37 rue Paul Cazeneuve, F-69008 Lyon, France
olivier.thizy@shelyak.com

Abstract

By spreading the light from celestial objects by wavelength, spectroscopists are like detectives looking for clues and identifying guilty phenomena that shape their spectra. We will review some basic principles in spectroscopy that will help, at our amateur level, to understand how spectra are shaped. We will review the Lhires III high-resolution spectrograph Mark Three that was designed to reveal line profile details and subtle changes. Then, we will do an overview of educational and scientific projects that are conducted with the Lhires III and detail the COROT Be star program and the BeSS database for which the spectrograph is a key instrument.

1. Introduction

Almost 350 years ago, when Sir Isaac Newton first saw the light from the Sun passing through a prism, he used the word "spectrum" to describe the phenomenon that revealed several colors and appeared to scientists like ghosts coming from mysterious places. It is only 150 years ago that we started to understand relationship between chemical composition and spectral lines.

Today, a majority of professional astronomical work is done using spectrographs, from distant red shifted galaxies to subtle stellar movement due to exoplanets. Surprisingly, only a few pioneer amateur astronomers have done some scientific work so far. Thanks to commercial spectrographs and CCD technology now available, several serious scientific programs can be conducted from our backyards.

2. Spectroscopy Theory

Light has the fantastic ability, even after traveling billions of kilometers, to convey information about the chemical composition, temperature, pressure, and movement of the source. This information is coded in the spectrum of the source and a spectroscopist is like a detective, looking for clues to decode the signal and unveil the truth.

A spectrum is obtained by dispersing the light from the source, a celestial object in our case, through a spectrograph. Visual observation can procure great sensation – looking at solar spectrum is a unique experience. However, astronomers record spectra for future study, usually with a CCD camera. Resolved sources display extended spectra while point sources only display a thin line. Those are “2D” spectra.

Scientists prefer to extract the density per column to display a graphical view of those spectra. A careful calibration in wavelength provides the X-axis scale and allows measurements of line profile details related to physical properties of the source (see Figure 1).

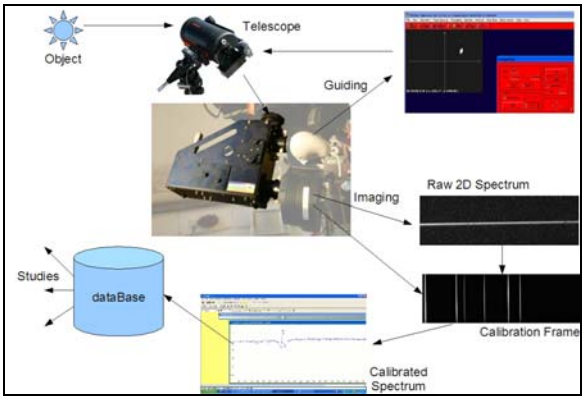

Figure 1.

Power of resolution, R, is a key parameter for a spectrograph. R is given by the equation $R = \lambda/\Delta\lambda$, where $\Delta\lambda$ is the lowest line separation that can be split and not to be confused with the dispersion of the spectrograph.

Low-resolution spectrographs record a wide spectral domain showing the overall profile of the spectrum, providing some basic information on temperature and spectral class. High-resolution spectrographs focus on a small domain but reveal line profile details providing more information on chemical

composition, radial, expansion or rotational velocities, etc.

Resolution is independent of the size of the telescope. You can have in your hand a spectrograph that has the resolution of large spectrographs on 8m telescopes! The difference is the limiting magnitude of the accessible targets.

Kirchhoff laws (Kirchhoff 1859) are the basis of spectroscopic analysis.

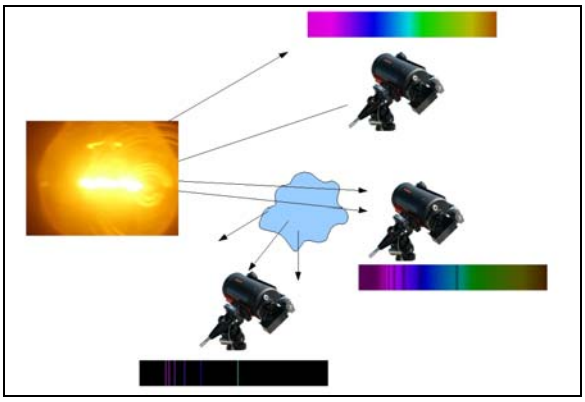

Figure 2. Kirchhoff's Laws.

1. Continuous spectra are emitted by any solid of gaseous body under high pressure and high temperature.

   A star is, under first approximation, like a black body whose continuous spectra has a shape that depends on its surface temperature, i.e., a Planck curve whose maximum is linked to temperature by Wien's law.

2. Absorption line spectra are emitted by low-pressure, low-temperature gas crossed by a continuous light that absorbs some photons. The spectra show dark lines in front of the continuous spectra.

   A stellar spectrum shows dark lines in the overall continuous spectrum. Hot stars show few lines, i.e., hydrogen lines, while cool stars display several metallic lines. The presence and profile of absorption lines depend on chemical composition and temperature as well as pressure and gravity.

3. Emission line spectra are emitted by low-pressure, high-temperature gas. Each chemical element has its own line spectra, a true identity card of its composition and state.

   For example, planetary and diffuse nebulae display emission lines. We also use spectral lamps with emission line spectra to calibrate our spectra.

Another important law in spectroscopy is the Doppler-Fizeau effect (Figure 3). An emitting source approaching the observer has its spectrum shifted toward lower wavelength (called the 'blue' side referring to the visual spectrum).

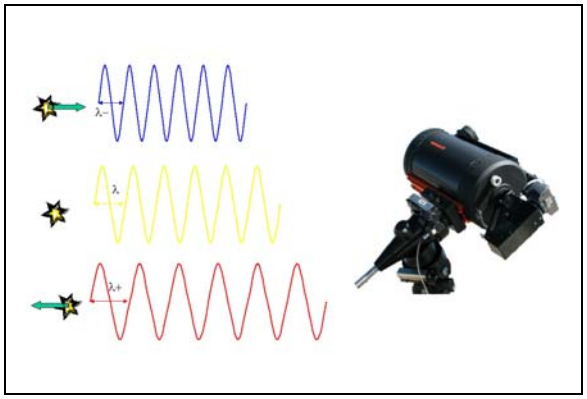

Figure 3. The Doppler Effect.

A source moving away from the observer has its spectrum shifted toward the 'red'. For non relativist sources, shift '$\Delta\lambda$' is linked to the radial velocity 'v' and the speed of light 'c' (around 300 000 km/s) by the equation

$$\Delta\lambda/\lambda o = v/c$$

The Doppler-Fizeau effect allows us to measure the speed of Earth around the sun, the radial velocities of celestial bodies, rotational speed projected toward our line of sight [called 'v~sin(i)'], or expanding velocities of ejected gas.

While analyzing in detail the information embedded in the spectra is professional work requiring time and knowledge, amateur astronomers can still do their own high-level analysis with only a few mathematical equations.

In summary, light from a celestial body gives us information about its temperature, chemical composition, physical conditions, pressure, and movements. Low-resolution spectrographs show broad features and overall spectra shape. Higher resolution spectrographs show details in spectra and line profiles and subtle changes over time.

3. Lhires III Specifications

In May 2003, a group of amateur and professional astronomers met together in Oléron to review current state of amateur spectroscopy. It quickly became clear that the resolution in commercially available equipment at that time was not high enough to see line profile changes. With support of AUDE association, a few amateurs (including Christian Buil, Fran-

Figure 4. The LHiRes III System.

çois Cochard and myself) worked on the design of a Littrow high-resolution spectrograph optimized for an 8" f/10 telescope so that many amateurs could do science from their backyard. This became after two preliminary versions the Littrow High Resolution Spectrograph Mark Three: LHIRES III (Figure 4). It was first distributed through AUDE association and then Shelyak Instruments (http://www.shelyak.com).

It was designed to be universal so it can be mounted on most amateur telescopes using a 2" (50.8mm) or a SCT (Schmidt Cassegrain Telescopes) adapter. Dispersion around Hα is 12Å/mm (0.116Å/pixel for a KAF400 CCD camera). Most CCD cameras can be attached to the Lhires III using a set of available adapters. SLR cameras can be attached, too, using a standard T-ring. Last but not least, an eyepiece can be attached to visually watch spectral lamp or solar spectra.

The Lhires III is compact (250x200x83mm) and light (1.6kg) so that it can be used with most amateur mounts. Signal loss from periodic errors along the RA axis is minimized when you align the spectrograph's slit with the RA axis.

The mirror slit can be adjusted in width but most important, it reflects the field of view toward a guiding camera (webcam, another CCD camera, etc.). This allows precise centering and continuous guiding during exposures.

4. Lhires III Performance

With the standard 2400 lines/mm grating, Lhires III's power of resolution λ/Δλ is around 17000 but can be adjusted for lower-resolution projects by simply changing the grating case, which is available in 150, 300, 600, or 1200 lines/mm. This can lower the resolution down to λ/Δλ around 600. With a Digital SLR camera, the full visible spectral domain can be shot in one part with a 300 lines/mm grating. In high resolution, around 20 parts are needed. See Table 1 for performance obtained for each available gratings

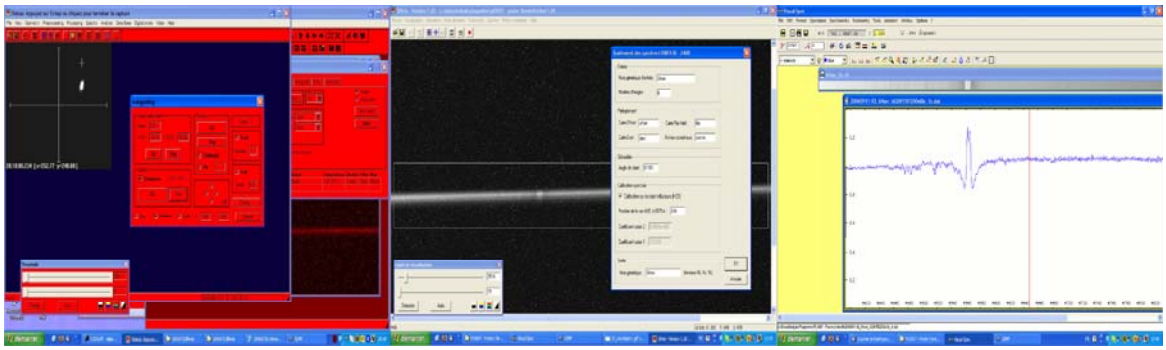

Figure 5.

		Grating – Lhires III – grooves/mm				
		2400	1200	600	300	150
Dispersion (Hα)	Å/pix	0,1	0,3	0,7	1,5	3,0
	km/s	5	17	35	75	150
Power of resolution		17000	6000	2700	1300	600
Spectral domain	Å	85	250	550	1100	2300
Limiting magnitude		5	6	7	8	9

Table 1.

(based on ETCL simulation tool for a 200mm f/10 telescope, 30µm slit, KAF0400 camera, 1h exposure, Signal/Noise of 100).

5. Spectra Processing

There are basically three steps when doing spectrography with a Lhires III (see Figure 5).

1. Acquisition
2. Extraction
3. Analysis

The Lhires III spectrograph fits between a telescope and a camera (reflex camera, CCD camera, or webcam). Spectra are captured with standard acquisition software. To center the target and to continuously guide on it, additional software may be required. Note that IRIS software, which is free, can autoguide with a webcam with a special algorithm that takes the slit into account.

Spectra extraction is a complex process. IRIS software (as well as PRIM or AudeLA/SpcAudace for example) also includes a special module for spectra processing called SpIRIS. This module allows the spectra to be corrected automatically for geometrical distortion. It can combine multiple exposures, extract spectrum with a special algorithm, and carefully calibrate spectra using atmospheric lines or integrated Neon lamp spectra. The last step of the extraction is to correct for instrumental response; this can be done in AudeLA/SpcAudace or VisualSpec for example.

Last but not least, spectral analysis is usually where the fun starts with the interpretation of line profile details. This can partially be done by amateurs with free software such as VisualSpec or SpcAudace. In any cases, relevant data should be shared with professional astronomers.

6. Projects

There are lot of projects to conduct with Lhires III spectrograph and even small size amateur telescopes. Here is a short list of projects that have high educational interests and then a focus on a professional amateur collaboration on Be Stars with the COROT program.

Usually the first spectroscopist's experience is to watch solar spectrum visually. The low-resolution mode will show main absorption lines first identified by J. Fraunhoffer. High-resolution mode will detail hundreds of absorption lines revealing some chemical composition of the Sun. This makes it a great tool to educate the public to spectroscopy. With a digital SLR camera, you can quickly record spectra of the Sun but also house lamps or laboratory spectral lamps. A very educational experience is to compare spectra of the Sun, a star, a street lamp, and burning salt. All show the Sodium doublet but at different distances!

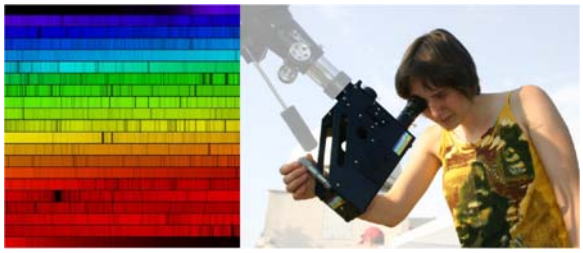

Figure 6.

Using a video camera and a small reflector, you can continuously record spectra of the sun as it passes in front of the slit. By taking a fixed wavelength in each frame, you can recompose the solar image at that wavelength. This scanning method is called spectro-heliography. It requires some hard processing work but the result is a set of solar images at different wavelengths with very narrow bandwidth.

In low-resolution mode, a simple digital SLR camera can reveal the overall profile of stellar spectra and show the variety of spectral classes. We have done, with astronomy students, the spectra of bright stars with 30 sec exposures using a 8" Schmidt-Cassegrain telescope and a Digital Rebel. High-resolution mode will show detailed absorption lines that are more and more visible as we go toward cooler stars.

Benjamin Mauclaire, a Lhires III user, has taken spectra of nebulae with students and used them to calculate temperature and electron density. We insist on the educational aspect of such observation since, through simple measurements on a spectrum, students can calculate some key parameters of the physical conditions of the nebula.

It is with the Doppler effect that spectroscopists, with a simple math formula can tell a lot of information! The FWHM of an emission line profile of a nova directly gives the speed of the expansion of the gas outward the star. Wavelength shift of stellar lines directly gives the radial velocity of the source, of course after careful correction of Earth velocity around the Sun. Following a line's swing on spectroscopic binaries will give details on those celestial bodies. Measuring the tilt of absorption line on Jupiter or Saturn will reveal the rotational speed of those planets (Figure 7). The same effect enlarges absorption lines as stars rotate around themselves.

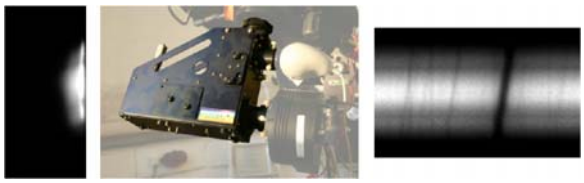

Figure 7.

These projects have been highlighted because of their educational interest. However, with a Lhires III, you can go further and record spectra that can be useful to professional astronomers. This is one of the reasons that we originally designed this high-resolution spectrograph.

While there are several areas of work such as RR Lyrae, Herbig Ae/Be objects, etc., we will focus here on the Be stars.

7. Be Stars

Be stars are hot (10000K to 30000K) B type, non-super giant luminous stars (III-V type) that show at least one Balmer emission line. Even if the star stops emitting, it keeps the Be classification. Sometimes, Helium and Iron emission lines can be seen.

The first observation of Be star spectra were done in 1866 by Secchi with beta Lyrae (a special class as it's a close binary system with mass transfer and polar jets) and gamma Cas, the perfect prototype of a Be star.

Around 15% to 20% of B stars are Be. Merrill has made a list of 410 stars, mostly Be stars (Merrill, 1933). As B stars are the largest population of naked eye stars, this makes the number of bright Be stars significant and opens the door for continuous high-resolution spectral monitoring even with small sized telescopes.

The emission line in a Be star is explained by the presence of a ring around the star (Struve 1931, Slettebak 1988). Linear radial velocity of the material can reach 300km/s, which explains the large broadening of some emission lines. Depending on the geometry and density, the emission line can be a single line, a profile with two peaks, or an absorption line with emission line(s) inside. Be stars that are seen nearly pole-on are called "Be-Shell." Some Be stars are part of a binary system and show even more complex profiles, zeta Tau (Pollmann, 2005) is a good example. Monitoring emission lines or V/R ratio (Violet/Red line intensity ratio) is easily done by amateurs. For example, the recent observations of the changing features in delta Sco (Figure 8), Miroshnichenko 2003.

How those stars create those rings is still a mystery. Fast rotational speed helps as does the presence of a companion, e.g., beta Lyrae, Figure 9. However, not all Be stars are binaries. Another possible cause are non radial pulsation (NRP) modes. Continuous monitoring of those stars would help tying photometric and spectroscopic variability (Hubert 1998). Porter and Rivinius made a detailed review of classical Be stars knowledge only few years ago (Porter 2003).

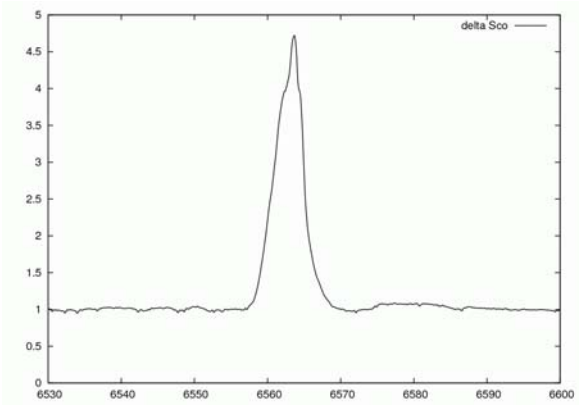

Figure 8.

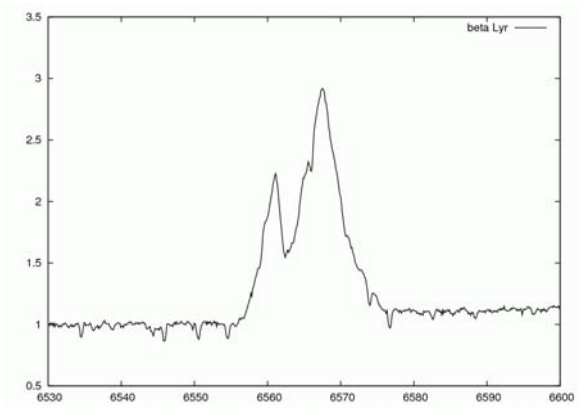

Figure 9.

In December 2006, the COROT satellite was launched. It will monitor some faint stars for exoplanets but will also monitor some bright stars for asteroseismology. Professional astronomers have targeted some Be stars for high precision continuous photometric monitoring. Parallel spectroscopic monitoring, even with amateur size telescope, is required to make that correlation. The first target has been 64 Ser (Figure 10).

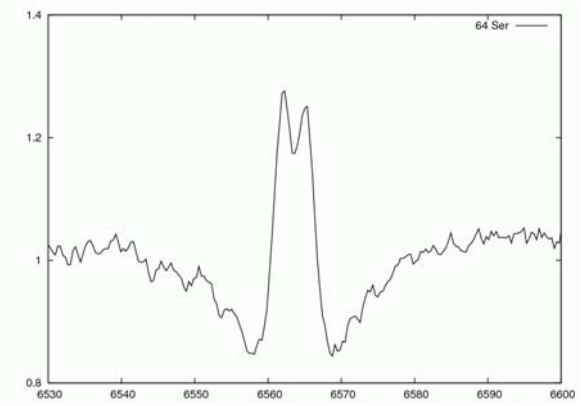

Figure 10.

In parallel to this project, a spectral database for Be Star Spectra (BeSS) has been developed by a team at "Observatoire de Paris-Meudon" with help from some amateur astronomers. This database is collecting Be Star Spectra from the two communities.

8. Further Reading

In addition to references, further reading can be found on the following web sites:

- Shelyak Instruments web site gives more information on the Lhires III spectrograph at http://www.shelyak.com/en/lhires3.html
- Spectro-L is a discussion group around amateur astronomical spectroscopy, more information at http://groups.yahoo.com/group/spectro-l
- ARAS is a portal on pro/am collaboration and can be accessed at http://www.astrosurf.com/aras
- Christian Buil maintain a dense web site at http://www.astrosurf.com/buil
- SpIRIS is a free software to process spectral images with special modules for the Lhires III: http://www.astrosurf.com/aras/spiris/spiris.htm
- VisualSpec is a free software to analyze spectra. It is available at http://astrosurf.com/vdesnoux/
- SpcAudace is a free module to process and analyze spectra, either on Windows or Linux: http://bmauclaire.free.fr/astronomie/softs/audela/spcaudace/

9. Conclusion

Amateur spectrography is at a turning if not a revolution point. More and more books are being published on the subject, equipment such as Lhires III are commercially available, and astronomers are grouping together such as the Spectro-L group. Within a short time, amateurs will be able to participate to pro-am collaboration using spectroscopic observations.

10. Acknowledgments

The author would like to thank Olivier Garde for the authorization to publish his solar spectrum and Steve Dearden for his continuous advice. Lhires III would never exist without the leadership and vision of Christian Buil, the work of François Cochard, and the support from AUDE association (André Rondi, Yvon Rieugné, Patrik Fosanelli and some others) and its president François Colas.

11. References

Cotton, A. (1899). "The Present Status of Kirchhoff's Law," *ApJ* **9**, 237.

Hubert, A.-M., Floquet, M. (1998). "Investigation of the variability of bright Be stars using HIPPARCOS photometry," *A&A* **335**, 565.

Kirchhoff (1859). Poggendorf's Annalen.

Merrill, P.-W., Burwell, C.-G. (1933). "Catalogue and Bibliography of Stars of Classes B and whose Spectra have Bright Hydrogen Lines," *ApJ* **78**, 87.

Miroshnichenko, A.-S., et al (2003). "Spectroscopy of the growing circumstellar disk in the delta Scorpii Be binary," *A&A* **408**, 305.

Planck, M. (1901). "On the Law of Distribution of Energy in the Normal Spectrum," *Annalen des Physik* **4**, 553.

Pollmann, E. (2005) "Amateur Spectroscopy of Hot Stars. Long term tracking of circumstellar emission," *Publications of the Astronomical Institute of the Czechoslovak Academy of Sciences* **93**, 14.

Porter, J.-M., Rivinius, T. (2003) "Classical Be Stars," *PASP* **115**, 1153.

Slettebak, A., "The Be stars" (1988). PASP **100**, 770.

Struve, O. (1931). "On the Origin of Bright Lines in Spectra of Stars of Class B," *ApJ* **73**, 94.

Precision UBVJH Single Channel Photometry of Epsilon Aurigae

Jeffrey L. Hopkins
Hopkins Phoenix Observatory
7812 West Clayton drive
Phoenix, Arizona 85033-2439
phxjeff@hposoft.com

Robert E. Stencel
University of Denver
Denver, Colorado
rstencel@du.edu

Abstract

First observed in the early 1980's the Hopkins Phoenix Observatory continues its UBV band observations of the long period (27.1 years) eclipsing binary star system Epsilon Aurigae. The UBV observations routinely produce standard deviations or data spread better than 0.01 magnitudes many times approaching 0.001 magnitudes. A new infrared detector has allowed the addition of precision infrared observations for the JH bands. Typical infrared observations approach a standard deviation of data spread of 0.01 magnitudes. The 2003 - 2005 seasons (Fall through Spring) of Epsilon Aurigae observations showed a 66.2 day variation that gradually increases in average and peak magnitude in the UBV bands, The 2006 season (Fall 2006 to Spring 2007) data show what appears to be a fall-back to a quiet period near maximum amplitude of V= 3.00. This paper presents the data and compares the current season to the past several seasons. The next eclipse is scheduled to begin in 2009 and an international campaign has been organized to coordinate new observations. [http://www.~hposoft.com/Campaign09.html].

1. Introduction

First observed by German astronomer J. Fritsch in 1821, this system has been observed in detail through most of the eclipses since. A concentrated effort was put forth during the 1982 - 1984 eclipse. While much was learned, many questions still went unanswered.

Most astronomers interested in Epsilon Aurigae tend to only get excited about it as the 27.1 year eclipse approaches. For many astronomers they miss the eclipse altogether. For dedicated observers this may happen twice or even three times in a lifetime. Each time great changes in astronomy have occurred. The next eclipse will be starting in 2009. While the primary eclipse is certainly interesting, the star system also has more than a few surprises out-of-eclipse.

The Hopkins Phoenix Observatory has been observing Epsilon Aurigae between the fall of 1982 and the winter of 1988 with a renewed concentrated effort beginning in the fall of 2003.

2. Why Observe Epsilon Aurigae?

Why all the interest in this long period eclipsing binary system? Aside from holding the record as being the longest known eclipsing binary star system, the object that eclipses the primary F supergiant seems to be a fantastically large opaque disk and has been called a round paving brick with a hole in the middle. The primary star is no small star either with an estimated diameter of 200 solar diameters. While that is certainly large it pales in comparison to the secondary, which is estimated at 2,000 solar diameters. Placed in our solar system where the Sun is located, even the orbit of Saturn would be millions of miles beneath the surface.

One of the problems with the Epsilon Aurigae eclipse is the determination of contact times. This is because of the out-of-eclipse variations that skew the magnitude around contact points. By extensive out-of-eclipse observations it is hoped to better understand these variations to increase the accuracy of contact time determination as well as just what is going on in the star system.

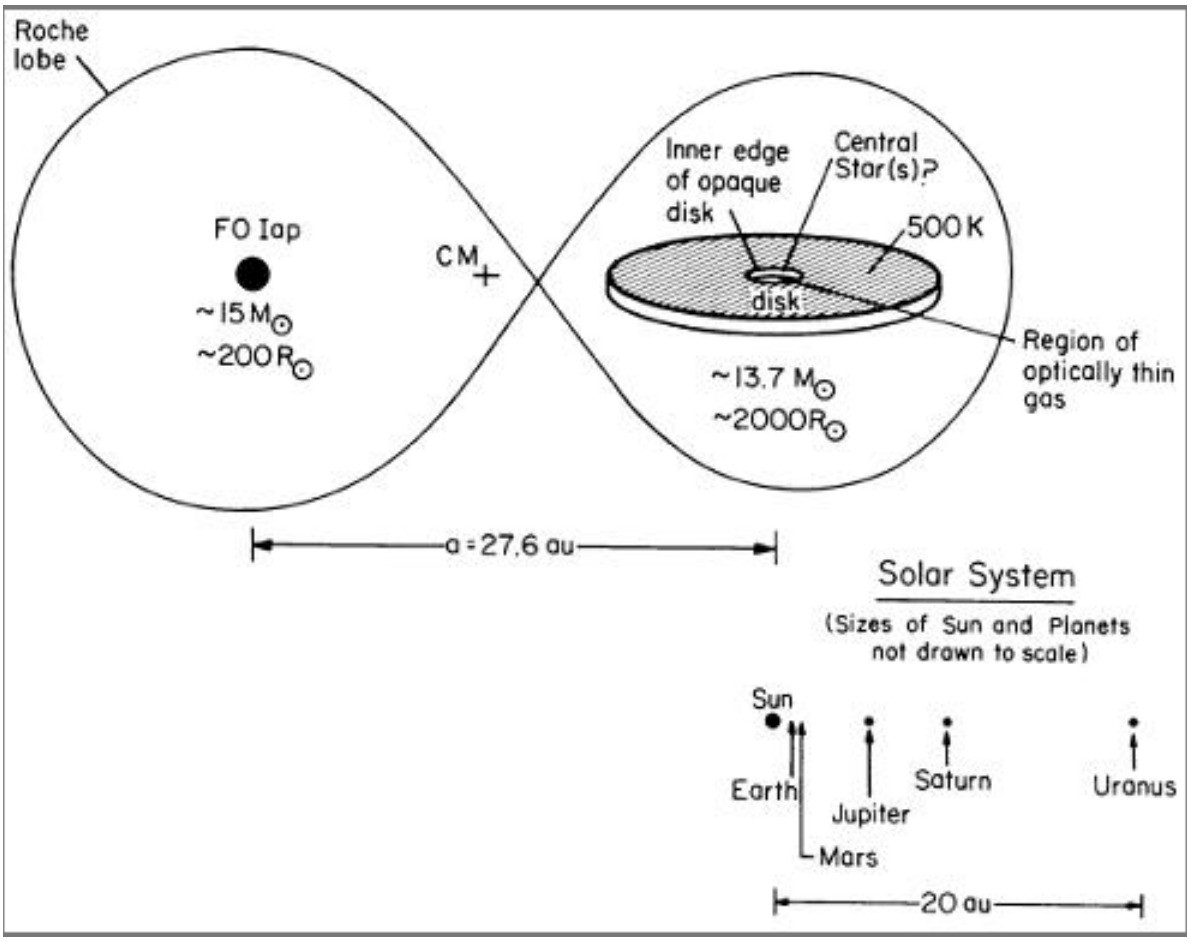

Figure 1. The epsilon Aurigae Star System (current interpretation) Carroll et al. 1991 Ap.J. 367

Figure 1 shows a diagram of the system as current understood.

3. Epsilon Aurigae Questions

The main goal for observing Epsilon Aurigae out-of-eclipse is to provide a baseline for analysis of data obtained during the coming eclipse. While the model presented above is generally accepted, the nature of the dark secondary is not well established. In addition, these pre-eclipse data pose questions as well.

What causes out-of-eclipse variations? Some possible answers are:

1. Primary star pulsations.
2. Additional eclipsing material.
3. Pulsations of the secondary.
4. Eclipsing of the binary pair in the secondary.
5. Some other phenomena.
6. Some combination of the above.

What can be deduced for the observed variations?

Why different amplitude variations in different bands?

What is the cause of the increasing / decreasing of average, maximum, and minimum amplitudes in various bands?

What causes the color changes in (B-V) and (U-B)?

4. Equipment

As reported last previously (Hopkins et al, 2006), the Hopkins Phoenix Observatory continues to use two photometric systems for observing Epsilon Aurigae. Both systems are single channel photometers. The UBV photon counting photometer uses a HPO 1P21 photomultiplier tube based photometer with an 8" C-8 f/10 SCT. The other system is for J and H band infrared photometry. That system uses an Optec SSP-4 analog photometer with a 12" LX200

GPS f/10 SCT. The SSP-4 employs a thermoelectric cooled detector, which is cooled to around -40 degrees.

5. Technique

5. 1. UBV Observations

To obtain optimum precision and accuracy a method was developed for the UBV single channel photon-counting photometry that includes taking 3 sets of star readings in each band followed by one sky reading in each band. The program star (Epsilon Aurigae) observations are bracketed by comparison star (Lambda Aurigae) readings.

5. 2. Extinction Considerations

Because these stars are nearly 5 degrees apart, extinction becomes important even when doing differential photometry. While extinction is minimized near the meridian and this is where the majority of observations have been made, it becomes increasingly important to consider an accurate extinction the further the stars are from the meridian.

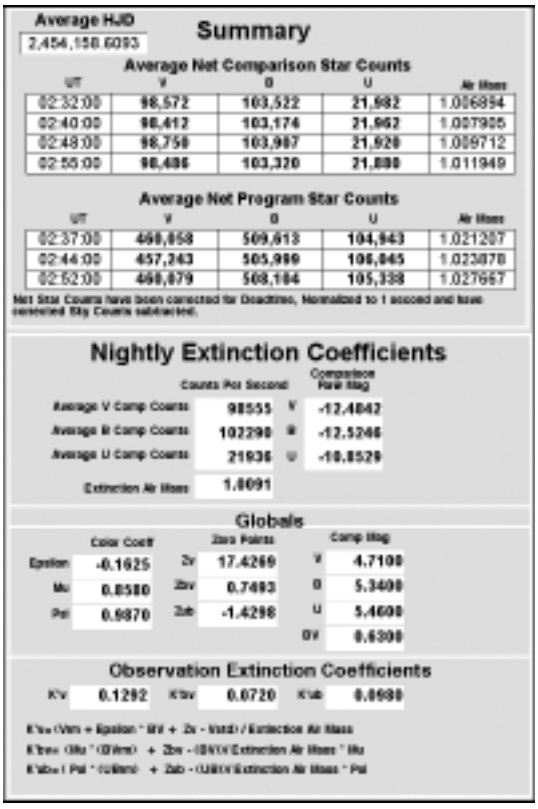

Figure 2. Typical UBV Data Entry Summary Screen

Previously, average extinction coefficients were used. To increase the accuracy it was decided to determine nightly extinction. This was done using the comparison star's nightly readings along with the star's air mass to calculate nightly K'v, K'bv and K'ub. While the use of nightly extinction coefficients as opposed to average coefficients had a minor effect on the magnitudes it proved important when tracking magnitudes in the 0.001 to 0.01 magnitude region.

Figure 2 shows a screen shot of a FileMaker Pro database program developed by HPO for UBV band photometry. This screen shot shows a summary of a night's data including Averaged Net Star Counts, HJDs and Average HJD, Air Masses and calculated Observation Extinction Coefficients.

5. 3. JH Band Infrared Observations

The SSP-4 J and H band photometry procedure is a bit different from the UBV procedure. Epsilon and Lambda Aurigae are not bright in the infrared and even with a 12" telescope the net star counts are not very high. This requires use of the SSP-4's maximum gain and 10 second integration/gate times. One big problem with the SSP-4 photometer is that when using the maximum gain of 100 and 10-second gate time, the dark counts drift considerably, sometimes over 1,000 counts in a 30-minute time span. While the variations tend to cancel out with three sets of measurements, to maximize precision and accuracy it was found that it was best to use 3 - 10 second readings of the star + sky in each band followed by single 10 second measurements of the sky in each band. To monitor the dark counts a 10-second reading is taken at the start and end of the session and between switching of the stars. Subtracting the closest dark count from the sky + dark count gives a net sky count and allows checking of the sky.

Note: The sky + dark is used when determining the net star count.

One nice feature about JH band photometry is extinction is near zero. In fact, observations can be done during close full Moon, in twilight and even daylight if the stars can be accurately found.

Figure 3 shows a screen shot of a FileMaker Pro database program developed by HPO for JH band photometry. This screen shot shows a summary of a night's data including Averaged Net Star Counts, HJDs and Average HJD, Air Masses, Dark Counts and Net Sky Counts.

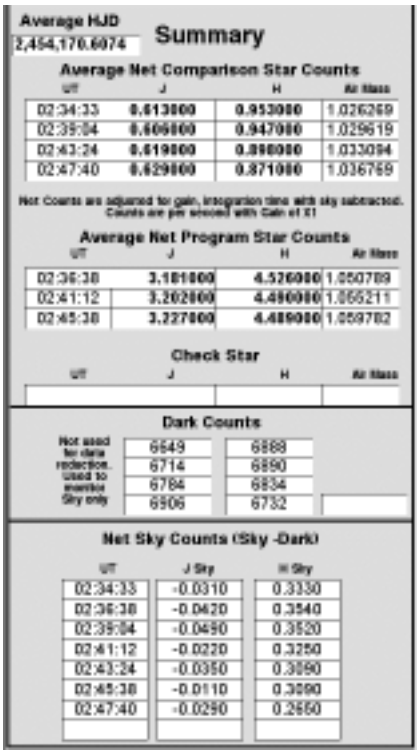

Figure 3. JH Data Entry Summary Screen

6. Reduced Data

Table 1 shows a list of sample reduced UBV data. Notice the low standard deviation (SD) data spreads.

Table 2 shows a list of sample reduced JH infrared data.

HJD							
2,450,000+	V	SD	B	SD	U	SD	X
4123.6963	3.016	.000	3.585	.004	3.700	.007	1.019
4128.6470	2.997	.002	3.564	.002	3.688	.007	1.021
4133.7414	3.005	.002	3.583	.002	3.704	.013	1.119
4135.6067	3.007	.003	3.576	.008	3.702	.011	1.037

Table 1. Sample UBV Data

HJD					
2,450,000+	J	SD	H	SD	X
126.7086	1.781	.009	1.438	.013	1.0393
127.6662	1.770	.005	1.448	.008	1.0165
128.6634	1.799	.006	1.437	.015	1.0165
135.6224	1.773	.007	1.413	.011	1.0205

Table 2. Sample JH Data

7. Lightcurve Analysis

Figures 4 and 5 show time domain plots of the V and data for 2003–2007 and 2006–2007 respectively.

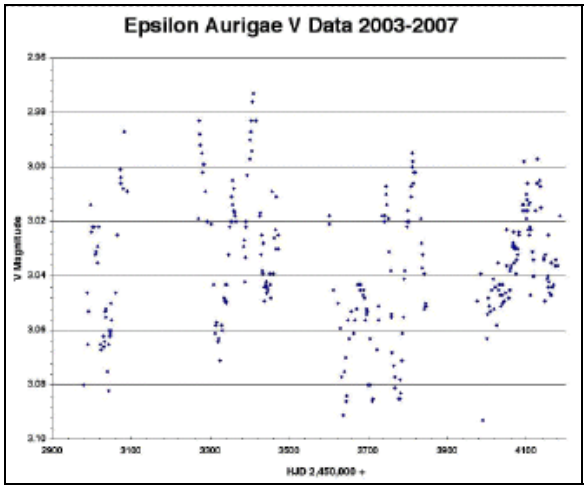

Figure 4. V Band Lightcurve(Time Domain) 2003 –2007

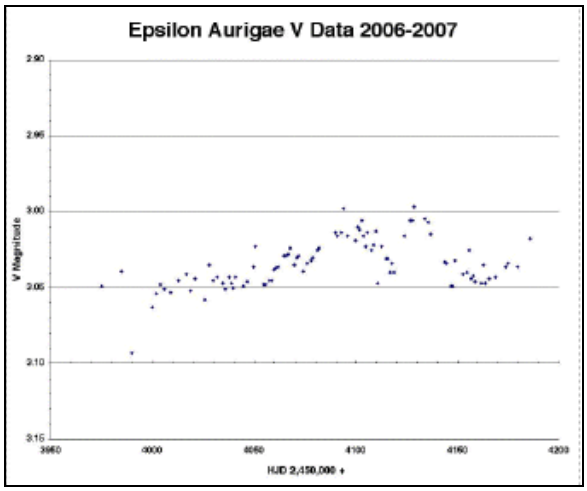

Figure 5. V Band Lightcurve (Time Domain) 2006 –2007

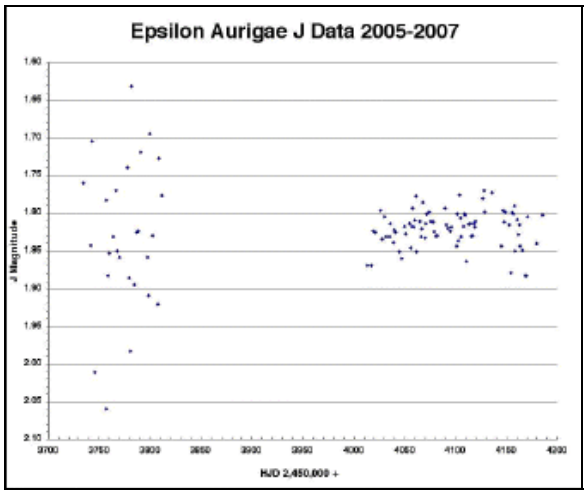

Figure 6. J Band Lightcurve (Time Domain) 2006 -2007

Figure 6 shows a time domain plot of the J band for 2005–2007. The 2005/2006 season shows considerable scatter. This was due to the instability of the smaller infrared detector in the SSP-4. The 0.3 mm detector was replaced with the large 1.0 mm and the 2006/2007 season shows more consistent data.

8. Period Analysis

Frequency domain plots were obtained using Peranso software and the Discrete Fourier Transform (DFT Deeming) technique. Other techniques were tried with similar results.

Figure 7 shows a frequency domain plot of the U Band data for the 2003–2007 period. The main frequency peak is at 164.7604 days. The second largest peak is at 66.3964 days. The 164 day peak is due to the seasonal observations (i.e., approximated start of each season is ~164 days apart).

Figure 8 shows a frequency domain plot of the B Band data for the 2003–2007 period. The V band plot is very similar. The main frequency peak is at 66.4986 days. The second largest peak is at 167.1359 days. Again the 167-day peak is due to the period of the observation seasons.

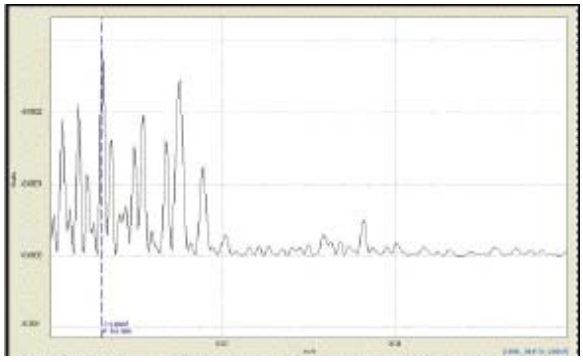

Figure 7. U Band Frequency Domain Plot 2003–2007, Cursor at 164.7604 Days.

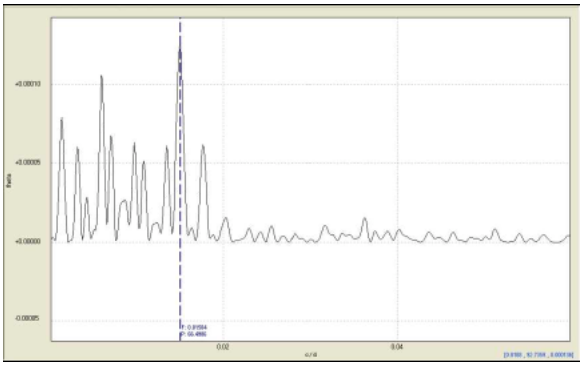

Figure 8. B Band Frequency Domain Plot 2003–2007, Cursor at 66.4986 Days.

The J and H band data was not sufficient to produce meaningful frequency domain plots. It is hoped the next two seasons will provide ample data for a detail period analysis in the infrared bands. Table 3 lists a magnitude summary of the UBV data for the 2003–2007 period. The average and mean values are simple average and mean and are not weighted. Differences between the average and mean are very small and may be more of an indication of measurement error than a real difference.

Filter	Max	Min	Delta	Average	Mean
V	2.9726	3.0927	0.1201	3.0358	3.0327
B	3.5246	3.6869	0.1623	3.6051	3.6058
U	3.6000	3.9207	0.3207	3.7275	3.7603
B-V	0.5277	0.6073	0.0796	0.5693	0.5675
U-B	0.0576	0.2687	0.2111	0.1224	0.1631

Table 3. UBV Magnitude Data Summary 2003–2007

Table 4 lists a period summary of the UBV data for the 2003 - 2007 period.

Filter	Pri Period	Sec Period
V	66.4986 days	761.7669 days
B	66.4986 days	167.1359 days
U	164.7604 days	66.3964 days
B-V	164.7604 days	295.1177 days
U-B	423.2912 days	289.5742 days

Table 4 UBV Period Data Summary 2003–2007

Table 5 lists a magnitude summary of the UBV data for the 2006 - 2007 period.

Table 6 lists a period summary of the JH data for the 2005 - 2007 period. A note of caution is in order. Because the 2005 to 2006 season used the smaller detector and the data was not consistent, a reliable set of periods for the JH bands will require at least one more season.

Filter	Max	Min	Delta	Average	Mean
V	2.9967	3.0927	0.0960	3.0340	3.0447
B	3.5434	3.6328	0.0894	3.5984	3.5881
U	3.6321	3.7719	0.1398	3.7095	3.7020
B-V	0.5277	0.5940	0.0663	0.5644	0.5608
U-B	0.0647	0.1555	0.0908	0.1111	0.1101

Table 5. UBV Data Summary 2006 -2007

Filter	Pri Period	Sec Period
J	141.8641 days	69.3131 days
H	145.1337 days	104.1014 days
J-H	150.3307 days	105.9853 days

Table 6. JH Period Data Summary 2005 –2007

9. Spectroscopy Support

H-alpha spectra are being regularly acquired by Lothar Schanne (2007) in Germany to provide a road map of the nebular emission from the binary system. This enables another dimension to be added to the revelations of the UBVJH photometry reported here. The line center velocity gives a Doppler measurement of the densest material, while the emission bump variation informs us of the movement of lower density clouds associated with one of the components. Once again, having this pre-eclipse record will help place in-eclipse variation into a useful context that largely was absent during the run up to the 1982 eclipse.

10. Conclusions

We have clearly demonstrated short term, period-like variations in the UBV lightcurves of Epsilon Aurigae. New photometry at J and H bands is underway, but signal to noise does not presently allow us to confirm similar variations. We also see strong evidence for a persistent 66.5 day period of UBV light variation with an amplitude of ~0.1 magnitude.

We find from our photometry, conducted 2003–2007 [MJD52978 - 54185], that B-V = 0.569 ± 0.012, and U-B = 0.123 ± 0.025. The B-V color of Epsilon Aurigae is not that of a normal F0 supergiant, while U-B is more nearly so. This discrepancy is not consistent with normal interstellar reddening.

Gyldenkerne (1970) reported on photometry obtained during the 1958 eclipse with a 10-inch telescope and EMI5060 photomultiplier, and transformed using calibration stars to the Johnson B and V filters. He stated the mean pre-eclipse values were V = 2.998 (N = 50 points) and B-V = 0.555 (38 points); mid-eclipse values were V = 3.767 (117), B-V = 0.575 (62), and post-eclipse values returned to V = 3.006 (31) and B-V = 0.554 (37). Furthermore the detailed a correlation between delta V and delta B-V during totality, described by the equation $\Delta(B\text{-}V) = 0.320 * \Delta V - 0.005$, where ΔV spanned ± 0.1 magnitude and $\Delta(B\text{-}V)$ spanned ± 0.05 magnitude. We see evidence for similar behavior in the present data.

Trends in the UBV lightcurve are suggestive that the outer edges of the opaque disk may be participating in an increasing amount of forward scattering of F starlight toward the observer. If the trends persist and increase during the 2007/08 and 2008/09 observing seasons, we can include those effects in more comprehensive analysis of the eclipse phenomena scheduled to start in 2009 August.

Figure 9 shows a plot of (U - B) vs. (B - V). Figure 10 shows a schematic of the star system indicating configurations before and during the eclipse.

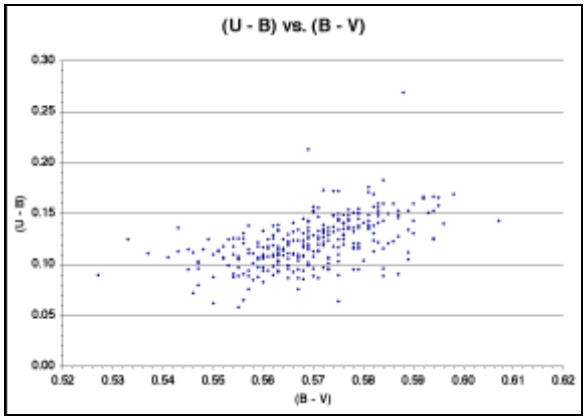

Figure 9. (U - B) vs. (B - V)

11. Epsilon Aurigae Campaign

The next eclipse of Epsilon Aurigae is fast ap-

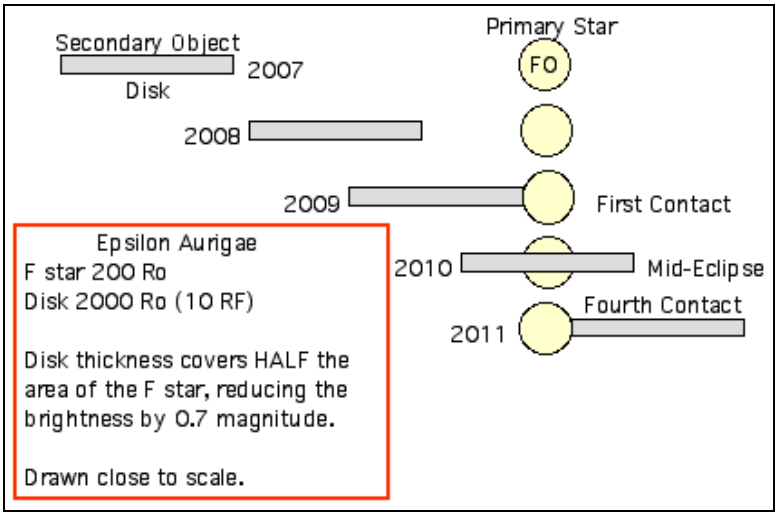

Figure 10. Epsilon Aurigae Eclipse Timing Schematic

proaching. As mentioned last year an eclipse campaign has been started with and a web site has been developed to disseminate information and coordinate efforts for the next eclipse and for events prior to the eclipse. The Epsilon Aurigae Campaign 2009 web site can be accessed at:

http://www.hposoft.com/Campaign09.html

Those interested in the eclipse are encouraged to check the web site and join the campaign. In particular we are interested in confirmation of short and intermediate variations in all photometric bands and an extension of coverage during the summer months (the higher the observer's latitude the better).

12. Other Campaigns

There are a couple of other stars systems similar to Epsilon Aurigae that bear observing. One is the 5.61-year eclipsing binary system EE Cephei. The next eclipse starts in January 0f 2009 and lasts 17 days. See references at the end of this paper for additional information. Additional information on EE Cephei can be found at:

http://www.hposoft.com/EAur09/EECephei.html

Another system is the short period (6.5 days) eclipsing binary system BM Orionis. BM Orionis is of interest because the star system produces an eclipse very similar to that of Epsilon Aurigae, but much shorter (period of only 6.5 days versus 27 years for Epsilon Aurigae). Like the eclipse of Epsilon Aurigae the BM Orionis eclipse is flat-bottomed and even has a mid-eclipse brightening. Like the secondary of the Epsilon Aurigae system the BM Orionis secondary appears to be a brick with a hole in it. This is an extremely difficult star system on which to do single channel photometry. CCD photometry is easier but still challenging. Additional information on EE Cephei can be found at:

http://www.hposoft.com/EAur09/BMOrionis.html

13. References

Hopkins, J.L, Stencel, R.E. (2006). "Single Channel UBV and JH Band Photometry of Epsilon Aurigae" in *Proceedings for the 25th Annual Conference of the Society for Astronomical Sciences*, ed. Warner et al, pp. 13-24.

Schanne, L. (2007). "Remarkable Absorption Strength Variability of the Epsilon Aurigae H-alpha Line Outside Eclipse." *IBVS* **5747**.

Baldinelli, L., Ghendini, S. (1976). "Variable Star in EE Cephei Comparison Sequence." *IBVS* **1225**.

Baldinelli, L., Ferri, A., Ghenini, S. (1981). "1980 Eclipse of EE Cephei: Lightcurve and Time of Minimum." *IBVS* **1939**.

Mikolajewski, M., Tomov, T. Graczyk, D., Kolev, D., Galan, C., Galazutdinov, G. (2006). *IBVS* **5412**.

Graczyk, D., Mikoajewski, M., Tomov T., Kolev D., Iliev, I. (2003). "The 2003 Eclipse of EE Cep is Coming: A Review of Past Eclipses." *Astron. Astrophys.* **403**, 1089-1094.

Samolyk, G. (2004). "The 2003 Eclipse of EE Cephei." *JAAVSO* **33-1**, 42-47.

Halbach, E.A. (1999). "Timing of the 1997 Eclipse of the Long Period (5.61 Years) Eclipsing Binary EE Cephei." *JAAVSO* **27-1**, 35-36.

A New Program to Search for Flare Events in Long Period Variable Lightcurves: Archived GNAT Data

Eric R. Craine
Western Research Company, Inc. and GNAT, Inc.
3275 W. Ina Road, Suite 215
Tucson, AZ 85741
ercraine@wrc-inc.com

Roger B. Culver
Department of Physics, Colorado State University and GNAT, Inc.
Fort Collins, CO 80523
gnat@lamar.colostate.edu

Adam L. Kraus
Department of Astronomy, California Institute of Technology and GNAT, Inc.
Pasadena, CA 91125
alk@astro.caltech.edu

Roy A. Tucker
Goodricke-Pigott Observatory and GNAT, Inc.
Tucson, AZ 85746
gpobs@mindspring.com

Douglas Walker
GNAT, Inc.
Litchfield Park, AZ 85340
douglas.walker@lmco.com

Robert F. Wing
Department of Astronomy, The Ohio State University and GNAT, Inc.
Columbus, OH 43210
wing@astronomy.ohio-state.edu

Abstract

Since the mid 1990s there has been an increasingly energetic debate about the reality and nature of short lived (hours to days) flare events in Long Period Variable stars. The ongoing development of a large database of lightcurves of variable stars extracted from Moving Object and Transient Event Search System (MOTESS) and Global Network of Astronomical Telescopes (GNAT) collaborative photometric survey projects offers the possibility of significantly contributing to this debate over the next few years. We describe the unique advantages of using these MOTESS-GNAT (MG) Variable Star Catalog data and outline the protocol we have developed and our progress to date. We discuss the extraction of LPVs from the MG Variable Star Catalogs, discuss their color-color diagrams, provide a summary of lightcurves developed to date, and discuss the status of a concurrent program to determine their spectral types.

1. Introduction

1. 1. GNAT

The Global Network of Astronomical Telescopes (GNAT) is modeling its system of a longitudinally distributed network of scan-mode telescopes following the designs of the Moving Object and Transient Event Search System (MOTESS), implemented at Goodricke-Pigott Observatory in Tucson, Arizona.

The MOTESS system consists of an array of three conventional Newtonian reflectors with 35-

centimeter aperture, f/5 primaries. Imaging is accomplished with thermoelectrically-cooled CCD cameras that are operated in continuous time-delay integration mode. Scanning at or near the celestial equator permits recording just over 12 square degrees of sky per hour.

In normal MOTESS operation, the three telescopes are aimed at the same declination but spread in Right Ascension at intervals of 15 to 60 minutes to produce a data stream of image triplets separated in time that reveal moving and time-varying objects. These observations, consisting of deep, unfiltered images, were originally intended for astrometric detection of asteroids.

GNAT has implemented a comprehensive data pipeline for extracting photometric measurements of all of the stars observed in each of the discrete declination bands observed with the scan-mode system. For the first declination band (designated the MG1 Survey), 48 arc minutes wide and centered at +03d18m, this has resulted in 2.5-year photometric lightcurves for 2.07 million stars with $-1 < B-R < 5$ and $R < 19$ mag.

From these stars we have created a new catalog of variable stars (the MG1 Variable Star Catalog) numbering 26,042 of which 5,271 are periodic at the 99% confidence level (Kraus et al. 2007). Only 59 of these stars were previously known to be variable and appeared as entries in the General Catalog of Variable Stars (GCVS).

Two additional surveys using MOTESS instrumentation are underway, and we anticipate adding six GNAT telescopes to the observing program. Thus, we can reasonably expect to produce data for on order of 100,000 new variable stars during the next two years.

1. 2. LPVs

Prominent among the variable stars in the MG1-VSC is the class known as Long Period Variables (LPVs). These stars are late type (M,S,C) giants with periods of $80d < P < 1000d$, and amplitudes of at least 2.5mag in the V band. The LPV lightcurves are reasonably well sampled in the MG1 data, and are generally very easily recognized by lightcurve morphology, though there are some stars that border on semi-regular types that are more difficult to conclusively categorize.

It should be noted that in the MG1 data reduction pipeline protocol there was an inherent bias against extraction of LPVs from the data. This bias arose from the need to construct a master reference catalog of stellar content in the observed declination strip, to which all subsequent stellar detections were compared. The master catalog was ultimately made from Palomar Sky Survey observations in which the images, in two band passes, were not always made on the same night. In an effort to remove spurious detections we discarded any stars in the master catalog that exhibited "impossible" colors. This condition could accrue to bona fide high amplitude LPVs whose "colors" were reported based on images well separated in time. This bias is discussed in detail in Kraus et al. (2007) and we note it here simply to clarify the small number (about 72) of candidate LPVs in the MG1-VSC. Because we have modified the means of producing the master catalog in the future, we anticipate many hundreds of new LPV discoveries in the MG2 and MG3 catalogs currently under development.

The rationale for the project discussed here is to develop a pilot program for examining large numbers of relatively long term LPV lightcurves for the presence of flaring activity.

In this paper we discuss our protocols for identifying and extracting LPVs from the source data sets, identifying flares in the lightcurves, determining spectral types of the stars and performing a statistical analysis of the flares (if any) observed.

2. Flares in LPVs

We will leave a detailed discussion of flares in LPVs for a future report on this project. For our purposes now we note that the existence of flares of duration hours to days in LPVs has been the subject of various reports since the 1980s. The evidence for such events was sparse, the data collected and analyzed was quite inhomogeneous and of the few flares reported, many were less than compelling (indeed some events reported were not flares at all, but short-lived diminutions in the lightcurve).

By the mid 1990s more convincing reports were beginning to emerge, but debate was heated not only over possible flare mechanisms, but the reality of the flares themselves. Among the most intriguing of the flare mechanisms is one described by Willson and Struck (2001) in which the flare is a consequence of interaction between the material outflows of the star and a planet that is being engulfed by the host star.

3. Identification of LPVs

Two of the authors (ERC and DW) have on several occasions visually examined all 26,042 MG1-VSC lightcurves with a goal of identifying specific types of variable stars. In this process a list of LPVs was independently compiled by the two, and comparison yielded a working list of LPVs.

Visual examination proved extremely useful for gaining a better understanding of the nature and content of the MG1-VSC, but it is an extremely tiring and slow approach.

Our next step was to run several computer sorts on the catalog in an effort to cut it to a short list of viable LPV candidates. We first sorted the list in descending order of period, and then excluded stars with P < 80d. We next sorted the list by period false alarm probability and removed those stars for which the period was highly uncertain. We then sorted this list by amplitude, and truncated it below about 1.0 mag since the unfiltered amplitudes are about half of the V amplitudes.

4. LPV Observations

The LPV observational data available in the MG1-VSC include a basic data and statistics summary, a file of reduced photometric observations, a lightcurve plot and a phased lightcurve. The summary file includes the following: RA, Dec, lightcurve amplitude, mean brightness, standard deviation about the mean, photometric error, skew of the observed data points, number of observations, log P (period), the period false alarm probability, B mag (USNO), and JHK mags (2MASS).

The photometry files are exportable to a spreadsheet program where they can be conveniently manipulated for detailed examination, including both local curve fitting and various arithmetic operations for further analysis. Included in the photometry file is a calculation of the phase of each observation, based on the period determined by the MG1 data pipeline algorithm.

5. Spectroscopy and Narrow-Band Photometry

The literature suggests that flaring in LPVs is a function of spectral type of the star; in particular there is an indication that flaring occurs preferentially in M-type Miras, as opposed to S or C type stars. It is therefore of interest, where possible, to add spectral type information to our pool of observed data. Unfortunately, it is not a trivial matter to request a series of spectroscopic observing runs at a suitably equipped observatory.

Other options more easily available to us include the following: 1) rough estimates based on (J-H) vs. (H-K) color-color diagrams, 2) dedicated small telescope spectroscopy, and 3) multi-color photometry.

In the first instance we have available JHK magnitudes for about 64% (46/72) of our program stars from 2MASS data.

At the moment small telescope spectroscopy is being explored by one of the authors (RAT) as discussed in some detail elsewhere (Tucker 2007). The instrumentation used is the Santa Barbara Instruments Group, Inc. (SBIG) SGS self-guided spectrograph, mounted on a Celestron 14 [Torrance, CA] that has been retrofit with a precision drive and privately re-figured diffraction limited optics.

The SGS spectrograph has a high-dispersion grating providing a dispersion of 1.07 Angstroms per pixel and a spectral range of 81.8nm. The low-dispersion grating provides a dispersion of 4.3 Angstroms per pixel and a spectral range of 327nm. The spectrograph may be used to obtain low-resolution spectra of objects as faint as about V = 15 mag with the Celestron 14, depending upon operating parameters, final signal-to-noise desired, and spectral class of the object being observed.

One of the authors (RFW) is using his narrow-band system to observe LPV candidate stars with the 0.9-m telescope of Cerro Tololo Inter-American Observatory in La Serena, Chile. This system, described elsewhere (Wing 1971; MacConnell et al. 1992), is an important far-red narrow-band tool for investigation of late-type M and C stars. The system defines pseudo-continuum colors, along with TiO, VO and CN band strengths, and is particularly useful for classifying M stars in our sample.

6. Preliminary Results

The LPV identification process described above yielded a working list of 72 LPV candidates, some of which are not classical Mira-type lightcurves, but are clearly long period variables meeting the other criteria for selection. An example lightcurve (Figure 1) and phased curve (Figure 2) are plotted using photometry from the MG1-VSC database. We note that for the MG1-VSC compilation, only the A and C MOTESS telescope images were reduced. The B telescope images are, however, available in the archive and in the event that a potential flare, or other interesting anomalous event, is observed, the B telescope image can also be measured for added clarification.

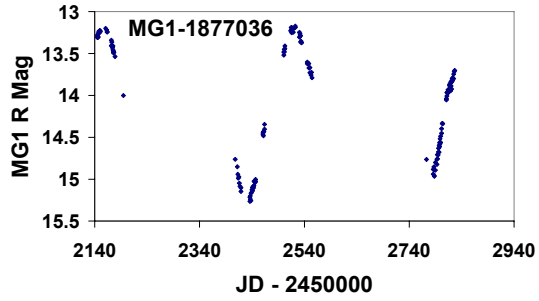

Figure 1. MG1-VSC lightcurve of LPV MG1-1877036.

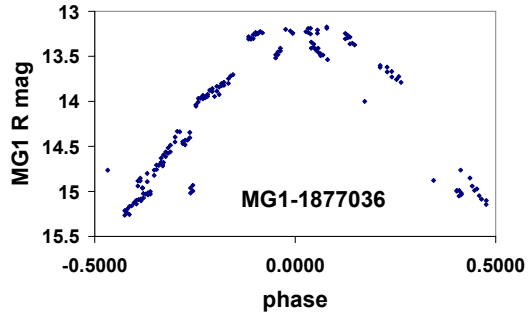

Figure 2. A phased lightcurve of LPV MG1-1877036.

It appears from Figure 2 that the shape of the lightcurve does not remain completely constant, a characteristic of these stars, since even making small changes in the period will only align parts of the curve, and the approximate period is clear from Figure 1. Nonetheless, it is possible from these data to make reasonable predictions of maxima to assist in our spectroscopic observations.

It is of some interest to consider the amplitude histogram of high amplitude stars in MG1-VSC, as shown in Figure 3. This histogram should be compared with that of Figure 1 in Wozniak et al. (2004). The disparity between these figures is caused by the aforementioned selection effect in our prototype data reduction pipeline that discriminates against extraction of large amplitude LPVs from the MG1 survey images. Because this condition has been corrected in the MG2 and MG3 survey strip data reductions, we can anticipate adding several hundreds of Mira LPVs to our candidate list upon completion of the MG2-VSC and MG3-VSC.

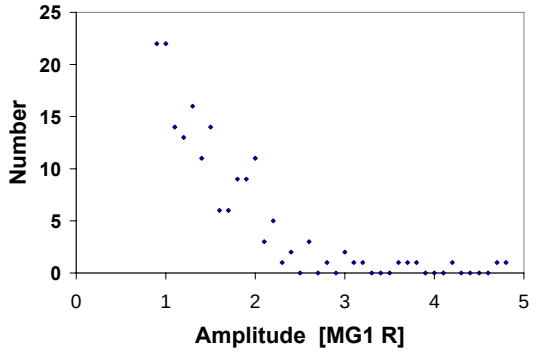

Figure 3. Histogram of amplitude distribution of a select group of high-amplitude variables in the MG1-VSC database. These are stars with very low false alarm rates in their periodogram analyses, hence likely LPV candidates.

The regions of Carbon-rich and Oxygen-rich LPVs are delineated in Cox (2000). Though not definitive, because of significant overlap of these regions, the diagram is of some utility. In particular it allows us to explore properties of stars that are at the extremes of color ranges in this diagram and address the question of whether they really belong in our candidate list.

In order to obtain spectra of the LPV candidates with the small aperture system we are using, it is necessary to observe near maximum light. We have used both the calculated period in the MG1-VSC, and visual study of the cataloged lightcurves to create a table of predictions of next maxima for the next two years.

The (J-H) and (H-K) colors of our 72 program stars are plotted in Figure 4.

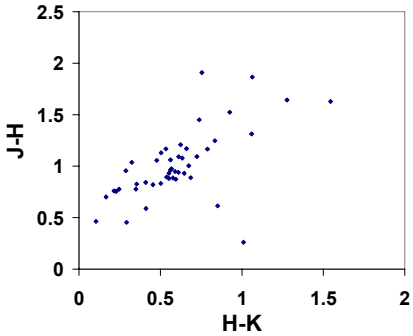

Figure 4. (J-H) vs. (H-K) color-color diagram for the LPV candidates extracted from the MG1-VSC.

At this writing we have obtained spectra for a half dozen LPV stars in our MG1-VSC list. Because of the limited light gathering power of the small system we are constrained to observing stars not much

fainter than V = 15, and it is to our advantage to tune the spectrograph to operate in the red region of the spectrum, typically about 600 – 920nm, where these red stars are bright. An example of one of these spectra appears in Figure 5.

The cool star spectral atlas of Turnshek, Turnshek, Craine and Boeshaar (1985) provides spectra of Morgan-Keenan standard stars very comparable in both resolution and wavelength coverage to the spectra we are now obtaining for our sample of LPVs. Comparing with the atlas spectra indicates that the SGS spectra are completely adequate for distinguishing M, S and C stars in our data.

We have also initiated the narrow-band photometry program at Cerro Tololo Inter-American Observatory with five stars observed to date and the next observing run scheduled for April 2007. We are at a very early stage of this observing program, but do note that all of the stars observed thus far are late type M giants (M5 – M9).

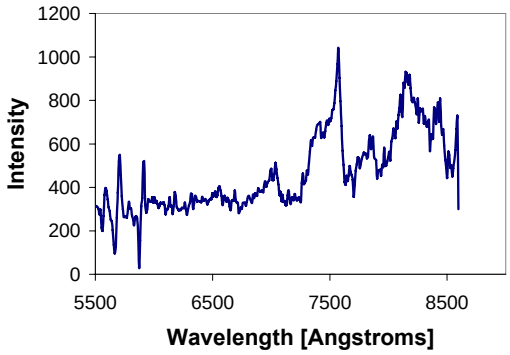

Figure 5. SGS spectrum of MG1-1291327 consistent with an M6 III LPV.

There are conflicting reports in the literature with regard to the phase of the lightcurve during which flare events are likely to be detected. Before starting the search we undertook to characterize phase coverage of our photometric observations. To accomplish this we divided the phase curves into quadrants: minimum, maximum and rising and descending legs of the phase curve. We then sorted our observations by phase and counted the number of observations in each phase.

The MG1-VSC was based on measurements of images from two of the telescopes in the MG1 survey, ideally yielding two nearly simultaneous, independent photometric measurements of each of the stars, these pairs separated by 40 minutes of time. This ideal is not always achieved: at the beginning or end of the observing season for a given star, that star may be only observable by one of the fixed telescopes in the network, or, there may be any of a number of problems with a single image, such as seeing degradation, cosmic ray events, etc.

For our initial sample of LPVs, Figure 6 shows the percent of observations in each of the minimum, ascending leg, maximum, and descending legs respectively where the observation was captured in at least one of the telescopes. Figure 7 describes the same summary of observations where images were captured in both telescopes on the same night. Thus, we have a reasonable distribution of observations across all of the phases of the LPV lightcurves.

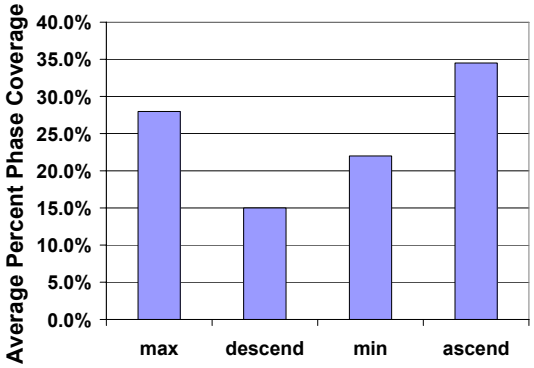

Figure 6. Average phase coverage of photometric observations with at least one telescope (100% is the sum of all of the observations).

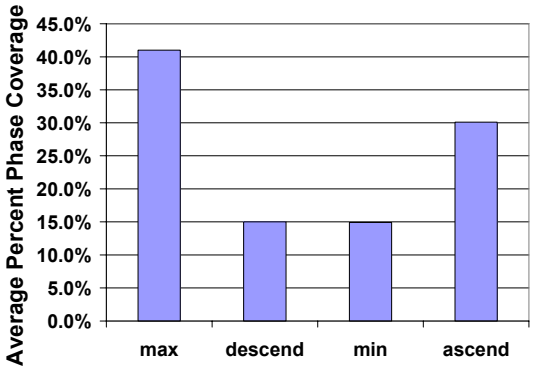

Figure 7. Average phase coverage of photometric observations with two telescopes (100% is the sum of all of the observations made with two telescopes).

Our protocol in searching for flare events is to use a spreadsheet program to plot the lightcurves, enabling fast and easy zooming on regions of interest for a higher resolution look at the lightcurve. We then visually examine the lightcurves looking for possible flares; such an event is generally easily discernable by the time it reaches amplitude 0.1-0.2 mag. Unlike some previous reports of single data point "flare

events", we require that we see the event in two of our telescopes.

Suggestive single point events can be checked by making after-the-fact measurements of the corresponding B telescope images (see Figure 8).

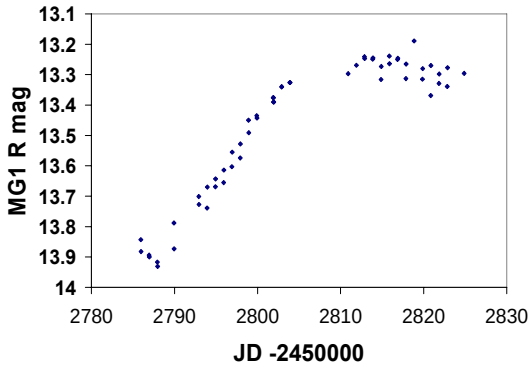

Figure 8. A portion of a maximum in the lightcurve of MG1-1639503.

In this case there is an anomalous point at JD 2452818, but it is a single point and thus not characterized as a likely flare. Upon examination of the original images it was determined that this was a spurious measurement. Most of the observations shown in Figure 8 are pairs of observations from two telescopes.

In addition to visual examination of the lightcurves, we are exploring the application of statistical algorithms for analytical extraction of candidate flare events, following methodologies suggested by Wozniak et al. (2004).

7. Conclusions

The GNAT program is producing catalogs and photometric data archives of very large numbers of newly discovered variable stars, of which many hundreds are expected to be LPVs. Our experience to date is that the phase curves of the LPVs are well sampled, usually with pairs of nearly simultaneous, independent observations, yielding an excellent data base for characterizing flaring rates.

We have initiated a supplementary program of spectroscopy and multi-color photometry to determine spectral types of most of these LPV candidates and we are refining a protocol to examine the lightcurves for short term flare events.

We expect to complete examination of the MG1-VSC candidates this year, and anticipate expanding the effort to many more LPV candidates in 2008 using the MG2-VSC and MG3-VSC databases.

8. Acknowledgements

The GNAT data pipeline work has been undertaken in stages to date primarily by ALK who was supported by the NSO Research Experiences for Undergraduates (REU) Program (2002) which is funded by the National Science Foundation, and for a second summer (2003) by support from Walker and Associates. RFW is grateful to the SMARTS Consortium for the opportunity to observe at Cerro Tololo Inter-American Observatory. Additional support for this project has been provided by Goodricke-Pigott Observatory and Western Research Company, Inc., of Tucson, AZ. We are also grateful for the support of GNAT members, both individual and institutional.

9. References

Cox, A.N. (2000). *Allen's Astrophysical Quantities*, fourth edition. pp. 163-164. Springer-Verlag, New York.

Kraus, A.L., Craine, E.R., Giampapa, M.S, Scharlach, W.W.G., Tucker, R.A. (2007). "The First MOTESS-GNAT Variable Star Survey," *A.J.* accepted for publication.

MacConnell, D.J., Wing, R.F., Costa, E. (1992). "Red supergiants in the southern Milky Way I. – Search and classification techniques," *A.J.* **104**, 821-840.

Tucker, R.A. (2007) "Observing spectra of faint astronomical objects with the Santa Barbara Instruments Group Self Guiding Spectrograph," *GNAT Journal*, www.egnat.org, in process.

Turnshek, D.E., Turnshek, D.A., Craine, E.R., Boeshaar, P.C. (1985). *An Atlas of Digital Spectra of Cool Stars.* Western Research Company, Inc., Tucson, AZ.

Willson, L.A., Struck, C. (2001). "Hot flashes in Miras," *JAAVSO* **30**, 23-30..

Wing, R.F. (1971) "A new system of narrow-band infrared photometry for late-type stars," in Conference on Late-Type Stars, *KPNO Contrib.* **554**, 145.

Wozniak, P.R., McGowan, K.E., Vestrand, W.T. (2004). "Limits on I-band microvariability of the galactic bulge Mira variables," *Ap.J.* **610**, 1038-1044.

BVRI CCD Photometry of Theta-1 Orionis A

Jeffrey L. Hopkins
Hopkins Phoenix Observatory
7812 West Clayton Drive
Phoenix, Arizona 85033-2439
phxjeff@hposoft.com

Gene A. Lucas
NiteOwl Astrophysical Observatory
15640 East Cholla Drive
Fountain Hills, Arizona 85268-4357
geneluca@ix.netcom.com

Abstract

Time-series BVRI CCD photometry data on Theta-1 Orionis A (V1016 ORI), a member of the familiar Trapezium cluster, was obtained at the Hopkins Phoenix Observatory (Phoenix, AZ) during December 2006 through February 2007. Data was acquired during two primary eclipse cycles, along with multiple out-of-eclipse observations. The observations were made with a Meade DSI Pro CCD camera and LX200 GPS 12 inch (30.5 cm) aperture telescope equipped with Johnson-Cousins filters. This paper details the observing setup, the technique, and resulting data analysis. It was noted that the estimated mid-eclipse (minimum light) point during the 02 December 2006 primary eclipse appears to have occurred several hours later than predicted from the early epoch timings. The possible secondary eclipse (which has evidently never been observed by anyone) proved to be elusive.

1. Introduction

Located in the great Orion Nebula M42, Theta-1 Orionis (more commonly known as the Trapezium) consists of several stars, the four most prominent of which form a trapezoidal geometric shape. These stars are labeled A, B, C, and D (not in order of brightness). The E and F stars do not appear in our images. Theta-1 Orionis A (V1016 Ori) is the star system of interest in this project. Theta-2 Orionis is a double star located some 100 arc seconds southwest of Theta-1. Figure 1 shows diagrams of the star locations.

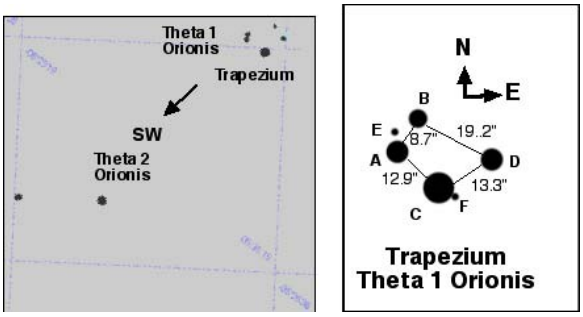

Figure 1. Theta-1 and Theta-2 Orionis Locations.

Theta-1 Orionis A and B are eclipsing binary star systems with accepted periods of 65.43233 and 6.470525 days, respectively. The other eclipsing binary system, Theta-1 Orionis B (BM Orionis) appears in the same images, so data on it were taken, too. These data may be used for another project on just that star system.

In early 1975, Lohsen (1975) was the first to report Theta-1 Orionis A as variable. The original period was determined to be 196.25 days. A few months later Strand (1975) reported a period of 196.298 days. In the spring of 1976 Lohsen (1976a) reported a refined period of 196.297 days. To add to the confusion, in December 1976, Lohsen (1976b) reported spectroscopic data suggesting a period of 392.594 days. In November 1976, Baldwin (1976) of the AAVSO, reported a period of 65.43 days, or one-third that of other reported periods. In May 1977, Franz (1976) confirmed the new period and refined it to 65.4325 days. In January 1982, Sowell and Hall (1982) reported a still finer period of 65.43233 days with an epoch of JD(hel.) 2,443,144.600. Robertson et. al. (2002) reported a possible secondary eclipse around phase = 0.58, with the possibility of the secondary event occurring between phase = 0.3 and 0.7. To date, no one has reported a definite secondary eclipse.

2. Published Data

The published data for the main Theta-1 Orionis stars is listed below:

Theta-1 Orionis A (V1016 Ori)
Alt des. HD37020, HR1893
Period, d 65.43233
V Magn. 6.72 to 7.65 (20 hours duration)*
(Suspected secondary eclipse at phase 0.3 to 0.7)
* Epoch = 2,443,144.600 (AAVSO)
* Epoch = 2,452,501.5000 (SIMBAD)
167 cycles = 10,861.76678 d
U = 5.87 B = 6.72 V = 6.72 R = 6.41 I =6.20
Prim. Eclipse (AAVSO) JD 2,454,071.410 - 1 Dec 2006; JD 2,454,136.840 - 5 February 2007
Prim. Eclipse (SIMBAD) JD 2,454,071.8872 - 2 Dec 2006; JD 2,454,137.3200 - 5 February 2007

Theta-1 Orionis B (BM Ori)
Alt des. HD37021, HR1894
Period, d 6.5470525
V Magn. 7.96 to 8.65
U = ? B = 8.20 V = 7.96 R = ? I = ?

Theta-1 Orionis C (For reference only)
Alt des. HD37022, HR1895
U = 4.188 B = 5.140 V = 5.134 R = 4.914 I = 4.734

Theta-1 Orionis D (Used as Comparison Star)
Alt des. HD37023, HR1893
U = 5.96 B = 6.78 V = 6.70 R = 6.41 I =6.22

3. HPO Equipment

BVRI CCD photometry was performed at the Hopkins Phoenix Observatory (HPO) in Phoenix, Arizona on multiple nights during the December through February 2007 observing season. A Meade® 12 inch (30.5 cm) aperture LX200 GPS telescope (Figure 2) was used at f:10 with a modified Meade Deep Sky Imager™ Pro (DSI Pro) monochrome CCD camera, equipped with an ATIK filter wheel and standard Johnson-Cousins BVRI filters. The Meade Autostar Suite™ software was used for image acquisition and subsequent processing. Data analysis was performed with FileMaker Pro database software.

4. Observing Technique

CCD photometry of the Trapezium star system is interesting, and provides some challenges. The stars are easy to find, and the two variables plus a good comparison star (star "D") are close together. At the same time, however, photometry of the Theta-1 Orionis stars proves difficult. This is due to the presence of background nebulosity, and the brightness and close spacing of the stars of interest. (theta-1 A and B are separated by less than 9 arc seconds.)

Figure 1. Hopkins Phoenix Observatory BVRI Equipment.

Single-channel photometry requires special techniques and is especially difficult. CCD photometry has proven to be a bit easier. The star images tend to become "bloated" at times, but good data can still be extracted from the images. With the setup at HPO, it was found that exposures between 0.5 and 4.0 seconds produced acceptable data. Data were taken with exposures of 0.5 seconds during November-December 2006 and 4.0 seconds during the February 2007 observations. The images were stored as FITS files. It appears the data from the 0.5-second exposures were more consistent than the longer exposures. The weather at this time in Phoenix approached freezing during the evenings.

A typical sequence was to start with the blue (B) filter and take approximately 10 images. These images were aligned and stacked (combined) by the Autostar-Envisage software. Three sets of stacked images were taken for each filter. The procedure was then repeated throughout the night. Each sequence (BVRI) took approximately 20 minutes. This seemed to work well. During the 02 December 2006 eclipse,

this resulted in nearly continuous imaging from about 9:30 pm through 3:30 am. Figure 3 shows one of us (Lucas) adjusting the filter prior to starting a new set of images.

Light box flat frames were taken at the end of each observing night. For nights using exposures longer than 1.0 second, dark frames were taken for the selected exposure time, prior to the start of the observations.

Figure 3. Adjusting Filter Wheel.

5. Images

Figures 4 and 5 show images taken with the V filter out-of-eclipse and near mid-eclipse.

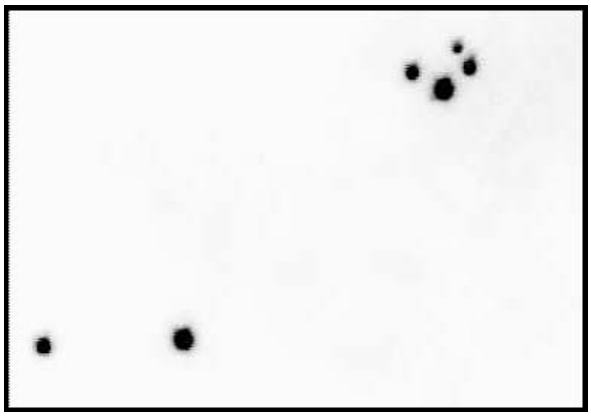

Figure 4. Theta-1 Orionis Out-of-Eclipse 01 Dec 2006 (V Filter).

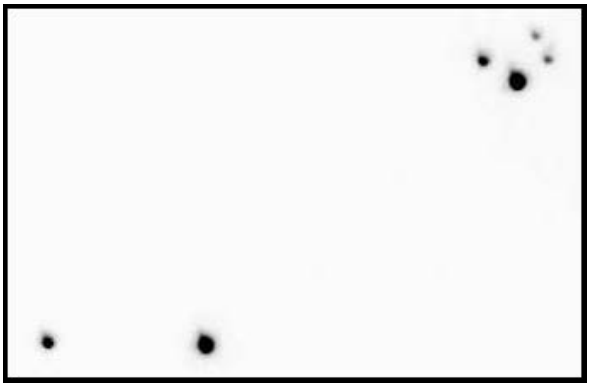

Figure 5. Theta-1 Orionis During Eclipse 02 Dec 2006 (V Filter).

During November - December 2006, a total of 33 images were taken in each filter band (out of eclipse). During the 02 December 2006 primary eclipse, 24 image sets were taken (3 sets of 10 images, stacked, in each filter). Each image (stack) was calibrated using a bias frame and flat field. Because of the short exposures (0.5 seconds), dark frames were not used. During the 05 February 2007 primary eclipse 15 images were take in each band. Each image was calibrated using a flat frame. All of the 05 February 2007 observations were taken with 4.0 seconds exposure time and a dark frame was subtracted (during imaging).

6. Data Reduction

The Meade Autostar-Envisage image processing software was used to calibrate the images and to determine differential magnitudes referenced to Theta-1 Orionis D.

Theta-1 Orionis D Reference Magnitudes

B = 6.78 V= 6.70 R = 6.41 I =6.22

The Meade Autostar image processing software created a data log, listing the times each image was taken, and the raw differential magnitudes determined during calibration, as well as other information. The data log file was then edited, and the raw magnitude data were transferred to a custom FileMaker Pro database program, developed at HPO. Figure 6 shows a sample screen shot of the HPO FileMaker Pro database. The mean time for each filter image set was calculated, as well as the average magnitudes and standard deviations. The Heliocentric Julian Date (HJD) for the observation was also calculated. The data were then exported to a Microsoft Excel spreadsheet and plotted.

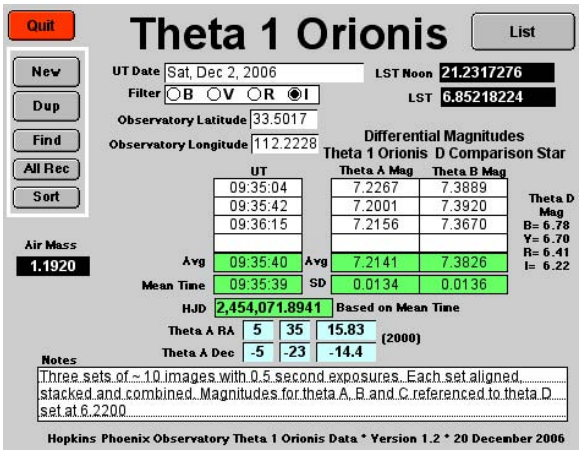

Figure 6. Custom FileMaker Pro Database.

Table 1 lists reduced data from the 02 December 2006 eclipse. (**Note:** Magnitude data has not been transformed to the standard system.)

B Filter Data		V Filter Data		R Filter Data		I Filter Data	
HJD	**Mag**	**HJD**	**Mag**	**HJD**	**Mag**	**HJD**	**Mag**
64.76930	6.7107	64.7719	6.7646	64.7739	6.4813	64.7780	6.4048
65.77410	6.7355	65.7756	6.7027	65.7773	6.5068	65.7786	6.4132
66.77003	6.7531	66.7725	6.7172	66.7754	6.4488	66.7770	6.3910
70.77159	6.6939	70.7766	6.7117	70.7783	6.4477	70.7802	6.3439
70.77327	6.6928	70.7835	6.7160	70.7820	6.5078	70.7896	6.3216
70.78521	6.7575	70.7864	6.7735	70.7880	6.4691	70.7994	6.3357
70.79435	6.7718	70.7929	6.7453	70.7914	6.4725	71.7131	6.8469
71.70745	7.2288	70.7959	6.7192	70.7977	6.4698	71.7281	6.9506
71.71631	7.2189	71.7092	7.1869	71.7247	6.9580	71.7451	6.8513
71.73670	7.3332	71.7110	7.2277	71.7426	7.0217	71.7556	6.8794
71.74776	7.3312	71.7197	7.2172	71.7523	7.0271	71.7649	6.9145
71.75894	7.3999	71.7394	7.3036	71.7632	7.0904	71.7734	6.9419
71.76689	7.4419	71.7503	7.3248	71.7706	7.1325	71.7804	6.9697
71.77558	7.4678	71.7608	7.3791	71.7786	7.1397	71.7874	6.9862
71.78231	7.4559	71.7687	7.3858	71.7857	7.1645	71.7962	7.0095
71.79036	7.5172	71.7771	7.4201	71.7940	7.1922	71.8054	7.0330
71.79938	7.5345	71.7840	7.4346	71.8036	7.2119	71.8122	7.0584
71.80724	7.5686	71.7920	7.4617	71.8104	7.2314	71.8194	7.0592
71.81416	7.6116	71.8018	7.4985	71.8178	7.2973	71.8270	7.0782
71.82181	7.6139	71.8087	7.4974	71.8253	7.3159	71.8332	7.0883
71.82891	7.6742	71.8159	7.5798	71.8318	7.3311	71.8401	7.1343
71.83527	7.6461	71.8236	7.5657	71.8383	7.3417	71.8476	7.1422
71.84282	7.6896	71.8303	7.5837	71.8457	7.3595	71.8558	7.1789
71.85056	7.6927	71.8369	7.6077	71.8543	7.3740	71.8623	7.2122
71.85746	7.7304	71.8442	7.6243	71.8607	7.3953	71.8701	7.1884
71.86473	7.7329	71.8524	7.6558	71.8683	7.4348	71.8776	7.2051
71.87255	7.7444	71.8590	7.6954	71.8759	7.4447	71.8868	7.2275
71.88216	7.7796	71.8663	7.6770	71.8854	7.4289	71.8941	7.2141
71.88936	7.7940	71.8744	7.7178	71.8923	7.4155	71.9021	7.2199
71.89594	7.7500	71.8837	7.7130	71.8994	7.4296	71.9092	7.2513
71.90411	7.7640	71.8908	7.6803	71.9074	7.4081	73.7638	6.3379
73.75887	6.7763	71.8976	7.7062	73.7620	6.4810	73.7717	6.3356
73.76622	6.7568	71.9058	7.7225	73.7703	6.5277	---	---
---	---	73.7604	6.7847	---	---	---	---
---	---	73.7685	6.7334	---	---	---	---

Table 1. Theta-1 Orionis A Observations Data. (HJD 2,454,000+)

7. Data Plots

Figure 7 shows the 02 December 2006 B filter eclipse lightcurve during ingress and the 05 February 2007 partial egress.

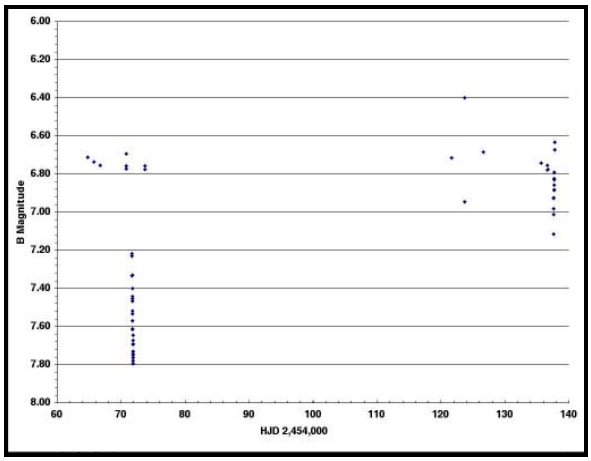

Figure 7. Theta-1 Orionis A Data Nov 2006 - Feb 2007 (B Filter).

Figure 8 shows a plot showing estimated contact times for the 02 December 2006 primary eclipse.

Event	Estimated HJD
First Contact	2,454,071.520
Second Contact	2,454,071.900
Mid-Eclipse	2,454,072.320
Third Contact	2,454,072.730

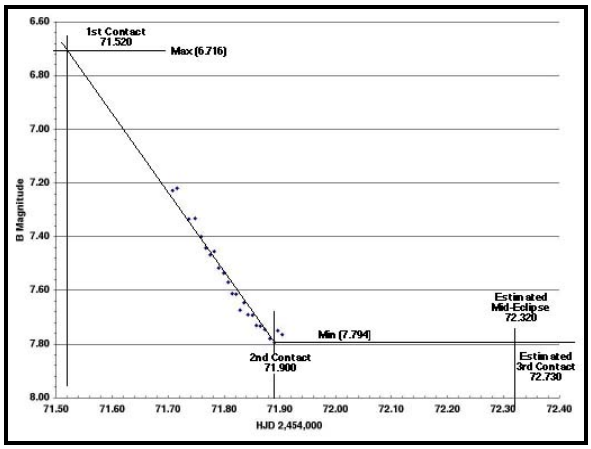

Figure 8. Theta-1 Orionis A Ingress Contact Points 02-03 December 2006 (B Filter).

Figure 9 shows a plot showing estimated contact times for the 05 February 2007 primary eclipse.

Event	Estimated HJD
Third Contact	2,454,137.185
Fourth Contact	2,454,137.760

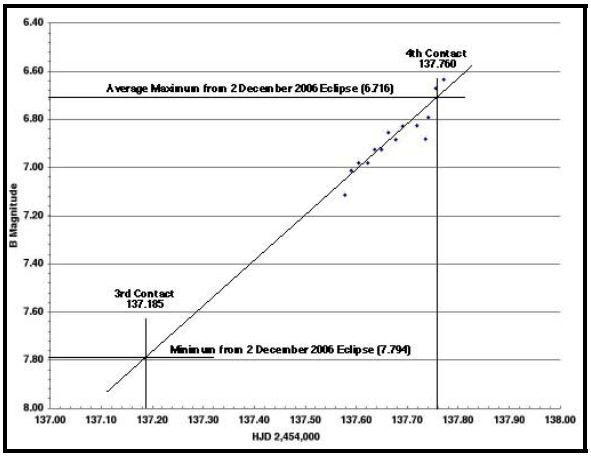

Figure 9. Theta-1 Orionis A Egress Contact Points 05 February 2007 (B Filter).

8. Analysis

Table 2 summarizes the observed magnitudes for the 2006-2007 observations. The Delta is the difference between the Avg Max and Min data (Min – Avg Max). The greatest magnitude change during the eclipse was in the V band (1.2279) while the smallest was in the R band (0.9969).

Filter	Max	Avg Max	Min	Delta	Published
B	6.4011	6.7157	7.7940	1.0783	6.72
V	6.5058	6.4947	7.7226	1.2279	6.72
R	6.2328	6.4478	7.4447	0.9969	6.41
I	6.0481	6.3582	7.3902	1.0320	6.20

Table 2. Theta-1 Orionis A 2006 -2007 Observed Magnitudes.

Table 3 summarizes the observed and estimated contact times for the 02 December 2006 primary eclipse. The earliest first contact was in the I band (HJD = 2,454,071.525) while the latest first contact was in the V band (HJD = 2,454,071.709). Mid-eclipse and third contacts were estimated to be the same in the V and I bands (HJD = 2,454,072.295 and HJD = 2,454,072.708, respectively). This is assuming a minimum primary eclipse time of 20 hours.

Filter	First	Second	Mid (Est.)	3rd (Est.)
B	071.652	071.900	072.320	072.730
V	071.709	071.875	072.295	072.708
R	071.535	071.869	072.289	072.702
I	071.525	071.875	072.295	072.708

Table 3. Contact Times for 02-December 2006 Primary Eclipse (HJD 2,454,000+).

9. Conclusions

Much was learned both about CCD photometry and the Theta-1 Orionis A star system. With the photometry system used it appears 4.0-second exposures are too long. Future observing may be done at 1.0 seconds. The 02 December 2006 data looked good, using only 0.5-second exposures. The 05 February 2007 B and I data looked good, but the V and R data was very scattered and of little value. Because the V and R data were higher counts than the B and I data leads us to believe the shorter exposure used during the 02 December 2006 eclipse is better. A compromise might be exposures of 1.0 seconds.

During the 02 December 2006 eclipse, the predicted mid-eclipse times seemed to be considerably early. The predicted time was HJD = 2,454,071.799, but from our observations, the mid-eclipse (B band) was estimated at HJD = 2,454,072.320.

Future plans are to start earlier in the next season and try to image several eclipses.

10. Acknowledgements

The research reported in this paper made use of the following Internet on-line resources:

AAVSO Julian Day Calculator:
http://www.aavso.org/observing/aids/jdcalendar.shtml

SIMBAD Astronomical Database:
http://simbad.u-strasbg.fr/simbad/

Smithsonian/NASA-ADS Astronomy Abstract Service: http://adsabs.harvard.edu/bib_abs.html

11. References

Echmar, L. (1975). "Theta-1 Ori A - A New Eclipsing Binary in the Trapezium," *IBVS* **988**.

Strand, K. Aa. (1975). "On the Variability of Theta-1 Ori A." *IBVS* **1025**.

Lohsen, E. (1976a). "Observe Theta-1 Ori A." *IBVS* **1129**.

Lohsen, E. (1976b). "A Tentative Spectroscopic Orbit of Theta-1 Ori A." *IBVS* **1211**.

Baldwin, M. (1976). "Theta-1 Ori A." IAUC 3004.

Franz, O.G. (1977). "UBV Observations of a Primary Eclipse of Theta-1 Ori A." *IBVS* **1274**.

Sowell, J.R., Hall, D.S. (1982). "Photoelectric Photometry of Theta-1 Ori A = V1016 Ori." *IBVS* **2076**.

Robertson, J.R., Stuffs, S.C., Caton, D.B. (2003). "A Light Curve of Theta-1 Ori A = V1016 Ori," *BAAS* **34**, 1096.

The Halloween Stellar Outburst of 2006 – A Nearby Microlens?

Robert Koff
CBA Colorado
Antelope Hills Observatory
980 Antelope Drive West
Bennett, CO 80102 USA
bob@antelopehillsobservatory.org

Joseph Patterson
Department of Astronomy
Columbia University
550 West 120th Street
New York, NY 10027 USA
jop@astro.columbia.edu

Thomas Krajci
CBA New Mexico
P.O. Box 1351
Cloudcroft, New Mexico 88317 USA
tom_krajci@tularosa.net

Abstract

When an experienced amateur astronomer discovered that an ordinary 11th magnitude star had brightened to 7th magnitude, other amateurs immediately followed up on the discovery. Their observations proved significant in deciphering a puzzle that garnered considerable attention among professional astronomers in the ensuing days. This paper traces the events and analysis of this highly unusual event.

1. The Discovery

On Halloween, October 31, 2006, the IAU's Central Bureau for Astronomical Telegrams sent out a notice on the internet containing observations from Akihiko Tago, a very experienced observer of novae and comets from Japan, who reported the brightening of GSC 3656-1328 from 11.8 magnitude to 7.5 magnitude (Nakano, 2006). Tago noted that the star had not varied in previous images. Two hours later, another Central Bureau Electronic Telegram was issued with a more precise position and further confirmation of the eruption (Nakano, 2006). The AAVSO quickly sent out an Alert Notice on the new variable, with the designation Var Cas 06.

Krajci and Koff, two Center for Backyard Astrophysics (CBA) observers in the western US, independently began time series observations of the new variable on November 1, within hours of the announcements. Krajci observed unfiltered, while Koff used a V filter, along with several observations in a B filter to obtain colors for the variable and potential comp stars. The two observers later coordinated their selection of a comp star.

Koff expected his observations to be consistent with a cataclysmic variable, with possible superhumps and flickering. Figure 1 shows an example of what was expected, the CV SDSS J0557+68 in outburst.

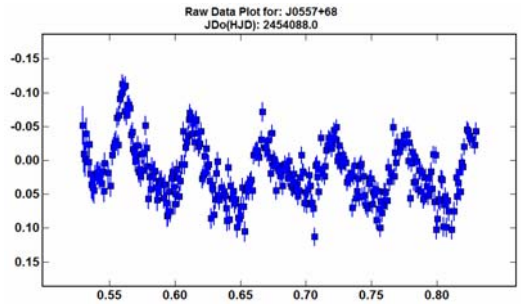

Figure 1: SDSS J0557+68 In Outburst

However, the results of the first night's time series showed a steady decline, with none of the signatures of a CV. Figure 2. The observed B-V of 0.27 was also inconsistent with a CV, which would be expected to show a B-V of close to zero. Krajci also obtained the same lightcurve results, a curve with a steadily declining magnitude of 1.5 magnitudes/day.

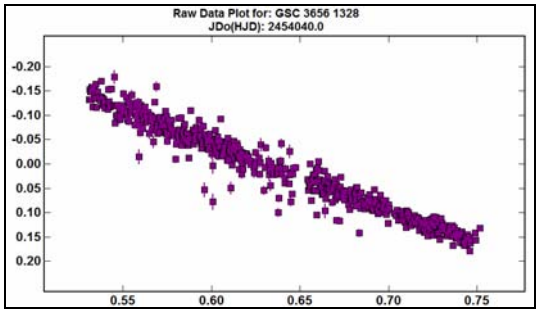

Figure 2: GSC 3656-1328, First Night of Observation

Both observers posted their findings to the CBA and AAVSO websites.

Patterson examined the observations, and noted the oddity of this variable. It did not seem to adhere to any know variable class. He sent out a notice to the CBA members on November 3 suggesting more observations of this star.

2. Observations Broaden

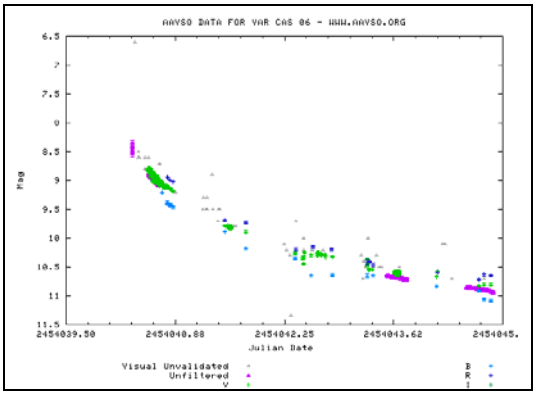

Figure 3: GSC 3656-1328, First Five Nights. www.aavso.org

By November 3, professional interest was building worldwide, as amateurs continued intensive observation. Figure 3. Patterson and his colleagues were able to schedule a target of opportunity observation from the Swift satellite, an X-ray instrument. The observations showed no detectable X-ray flux. Furthermore, Ron Remillard (MIT) reported that a search of the RXTE All-Sky Monitor showed no detectable X-ray flux before or during the outburst. This seemed to rule out a CV.

Professionals examined the available color data and arrived at a B-V value of 0.2, typical of a type A star. Such stars would not be expected to erupt like this one had. Still on November 3, Ulisse Munari of the Padova Observatory reported via another CBET that a spectrum indicated a normal A star with no indication of emission or rapid rotation (Munari, 2006).

Sergie Antipin of the Sternberg Astronomical Institute reported that a search of 400 plates from 1964 –94 showed no variation from a magnitude of 11.8, a figure that is the same as modern surveys such as Tycho, USNO, TASS, etc.

Thus, the astronomical community was left with a seemingly ordinary, constant star that had brightened four magnitudes, then begun to quickly fade. There were no x-rays, no flickering, and no apparent change in color or spectrum. In short, there was no ordinary classification for such an event.

More professional observers joined in. Images were obtained from PAIRITEL, the Peters Automated Infrared Imaging Telescope, a 1.3-meter instrument on Mt. Hopkins. The Swift satellite provided UV-band observations. Spectra were obtained by the MDM 2.4-m telescope on Kitt Peak.

Koff and Krajci, and an increasing number of other observers continued to monitor the star. But as it turned out, the initial night's observations proved critical to the solution of this enigmatic event.

3. The Explanation

The solution began to take shape. Koff and Krajci received a request from a professional astronomer in England for their data. At this point, we had several nights of observations. Figure 4. After examining the observations, he voiced the possibility that it might be a microlensing event. Soon after, Maciej Mikolajewski (Nicolaus Copernicus University) was the first to publish this proposal (Mikolajewski 2007).

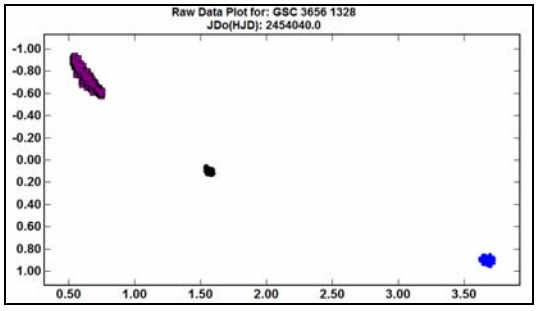

Figure 4: GSC 3656-1328, First Three Nights

A microlensing event takes place when a massive object passes between the observer and a background star. The foreground object bends space-time in such a way as to behave as a lens, focusing the light of the background object. This geometric condition allows us to study objects that would otherwise be difficult or impossible to detect. It has been used successfully in the search for extrasolar planets. These searches hunt for microlensing events and the study their lightcurves for anomalies that would indicate planets. Figure 5.

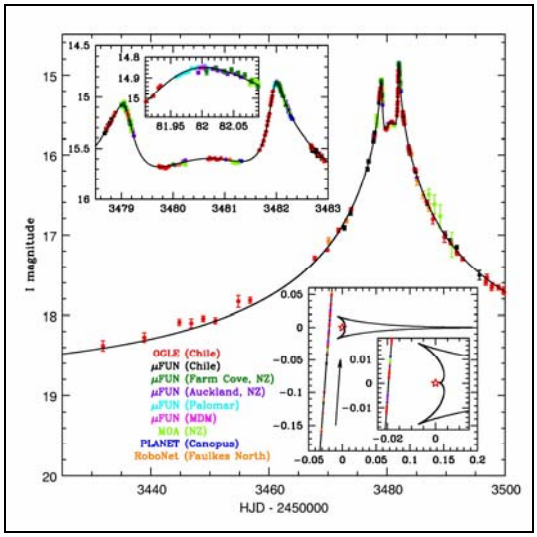

Figure 5: A Microlensing Event, from OGLE and MicroFUN

However, these searches are carried out on distant and crowded fields, such as the galactic plane or the Large Magellenic Cloud. This is because the more stars in the field of view, the better the chance of seeing a microlensing event. In addition, the probability of a microlens occurring on a given star increases with the square of the distance, so searches have concentrated on distant, and thus dim, stars.

To better analyze whether or not this was a microlens, it would be necessary to get data on the portion of the lightcurve at the beginning to the event, and at the maximum. A true microlens should show a symmetrical, achromatic curve that follows a specific mathematical shape.

A call went out for pre-Halloween images of this star. Digital camera images were received from two British amateurs, and were analyzed by Michael Richmond (Rochester Institute of Technology). Richmond was able to take these unfiltered images from short-focus cameras and extract calibrated magnitudes.

But most importantly, it turns out that the field had been imaged during test runs of the northern site of ASAS, the All-Sky Automated Survey at Haleakala, Hawaii. ASAS uses telephoto lenses to survey the entire sky every night in V and I filters. ASAS supplied a number of images of the microlens event, including five during the previously unseen rise and maximum. These observations were critical, as they filled in the missing curve with calibrated magnitudes through standard filters (Gaudi, 2007). Figure 6.

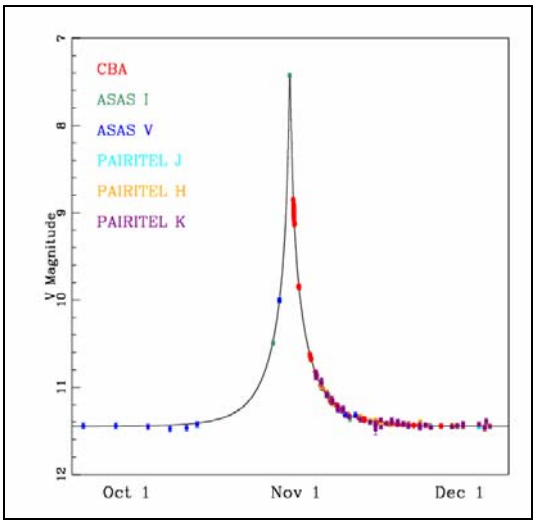

Figure 6: Lightcurve of GSC 3656-1328

4. Conclusions

All of the observations were now consistent with a microlens, and for the nearest and highest magnification event ever recorded.

An analysis of the data (Gaudi, 2007) yielded estimates of the nature of the lens object. It appears to be relatively low mass, about one/sixth that of the Sun. It is probably located about 130 pc from us, whereas GSC 3656-1328 is located at about 1 kpc distance. The lens, which may be a brown dwarf or a main sequence star, has an approximate magnitude of about 20 V. It is probably moving at a rate of about 150 mas/yr. At this rate, it may become detectable as a separate object in a few years.

By one estimate, an event involving a star this bright might occur in our sky once every 12 years. If we have to wait 12 years for the next one, and then be fortunate enough to catch it, this might not be a promising field of research. But if we can use the existing and upcoming surveys, we can increase the odds considerably by the fact that we will be examining more stars at higher magnitudes. It would seem that ASAS, Pan-Starrs, and LSST could be programmed to watch for these events in their normal

processing pipeline. It is also practical to initiate a new survey, using wide-angle cameras with CCD detectors, to monitor for microlenses and other transient events (Gaudi, 2007).

If we can detect such events, how will we follow up on them? In all likelihood, this will fall to the amateur astronomers. Only we are spread out all over the world, and only we have the telescope time and target discretion to jump on a new discovery and image it at high time resolution for days on end if necessary. In this case, by the end of 2006 Koff and Krajci had made 8000 observations, and 43 other observers including 16 other CCD observers had contributed another 11,000 observations to the AAVSO. Figure 7.

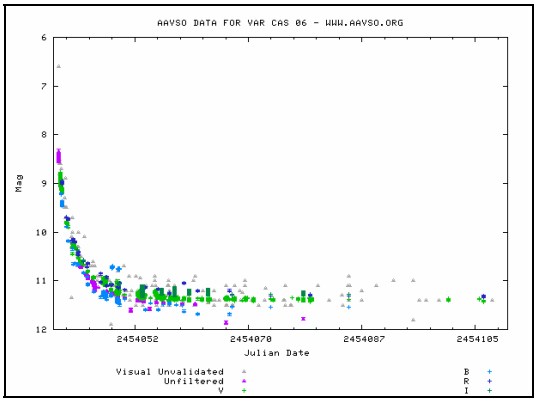

Figure 7: GSC 3656-1328, AAVSO Data www.aavso.org

It is this ability that makes us a valuable partner to the professional community. We can target any transient celestial event, be it a microlens, a variable star or an asteroid that needs intense observation. That is why we would like to encourage amateurs to learn lightcurve photometry. There are numerous projects available to you, from targets of opportunity like GSC 3656-1328 to all manner of variable stars to asteroids. It's not difficult, and seeing and publishing a lightcurve of your own observations is very satisfying.

5. Conclusions

GSC 3656-1328, the sudden brightening of an ordinary 11th magnitude star, was almost certainly a microlensing event, and the closest and brightest such event ever observed. The participation of amateur observers in the discovery and follow-up of this occurrence was key to understanding the nature of the phenomenon.

6. Acknowledgements

The authors thank the AAVSO for collecting and disseminating the thousands of observations involved in this project.

We also wish to acknowledge the many amateur and professional observers that contributed to the analysis of this unusual event.

7. References:

Gaudi, S. et al. (2007) "Discovery of a Very Bright, Nearby Gravitational Microlensing Event." *Astrophysical Journal*, submitted

Nakano, S., & Tago, A. (2006). Central Bureau Electronic Telegrams 711, 1

Nakano, S., Kadota, K., Sakurai, Y., & Waagen, E. (2006). *Central Bureau Electronic Telegrams*, 712, 1.

Munari, U., Siviero, A., Tomasella, L., & Valentini, M. (2006). *Central Bureau Electronic Telegrams*, 718, 1

Mikolajewski, et al, *The Astronomers Telegram*, 943, 1.

MicroFUN, http://www.astronomy.ohio-state.edu/~microfun/

AAVSO, http://www.aavso.org

Parameter Solutions for the System AP Leonis

Lee F. Snyder
Kings Canyon Observatory
257 Coventry Drive
Carson City, NV 89703
snyderlf@charter.net

John Lapham
Paradise View Observatory
3722 Paradise View
Carson City, NV 89703
j.lapham@sbcglobal.net

Abstract

The eclipsing binary system AP LEO is an overcontact binary of W UMa type with low surface temperature and a short period of 0.43 days and with a mass ratio well below unity. Monitoring lightcurves published in 1989 and 1993 displayed changes to this contact system uncommon in such a short period. New CCD photometric lightcurves in the V and R bands are presented. O-C values have been computed using thirteen new times of light minimums along with 62 minimums previously published in the literature. A sinusoidal trend is apparent and several authors have interpreted this small amplitude cyclic oscillation to a triple system containing a third component. This shallow sine curve is superposed on an increasing secular period. The most recent spectroscopic study classified the spectral type as F7-8 V. Photometric solutions of the lightcurve and computed parameters are compared with five other investigations of the binary system. The changes in the parameters in such a brief time indicate the orbital period variations are caused by mass transfer from the primary star to the secondary causing a decrease or change in angular momentum loss.

1. Introduction

AP Leonis was discovered as a variable by Stohmeier & Knigge in 1961 and the first photoelectric lightcurves were acquired by Mauder (1972). Zhang (1989) acquired lightcurves in 1985, 1991 and again in 1992 and 1993 and all exhibited a highly variable nature. One spectroscopic and several photometric orbital solutions have been studied by authors since the variations of the lightcurves were reported. All times of minima in the literature since 1961 have been used to construct an O-C diagram in Figure 1.

These O-C values have been computed from visual, photographic and CCD times of minima and contain a large scatter prior to April 1976 and cannot be used to compute a real period change or trend of the system. In this paper to correctly analyze the orbital trend only 62 previous CCD photometric times of minima after April 1976 were used. Thirteen new CCD times of minima, which are symmetric, were computed for this paper and have been added, Figure 2.

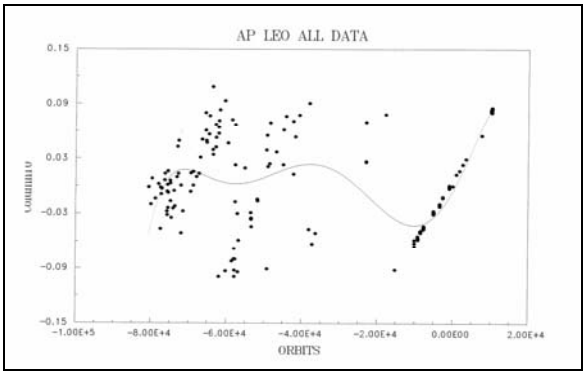

Figure 1. AP LEO All Data

The lightcurves in R and V were analyzed with Binary Maker 3 which uses the W-D code Wilson & Devinney (1971). The V lightcurve is shown in Figure 3. Photometric solutions and parameters were computed based on these symmetric lightcurves. These computed system parameters are compared with five other published papers, Cristescu (1979), Zhang (1992), Lu & Rucinski (1999), Pribulla (2003) and Qian (2007), and data collected by the Hipparcos satellite in Table 1. Accurate spectroscopic mass ra-

tio, M /M = q = 0.297 was obtained by Lu & Rucinski in 1999 and a mass ratio, q = 0.404, was computed from the 2006 lightcurve this paper. Lu & Rucincki also classified the spectral type as F7-8 V type and $M_1 \sin^3$ (i) = 1.368 M_{sun} and $M_2 \sin^3$ (i) = 0.406 M_{sun}.

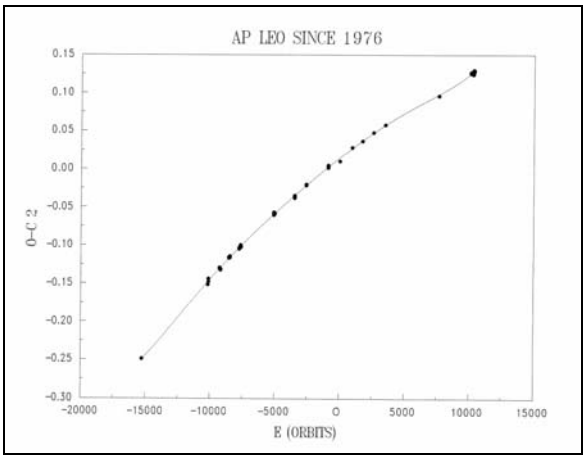

Figure 2. AP LEO Since 1976

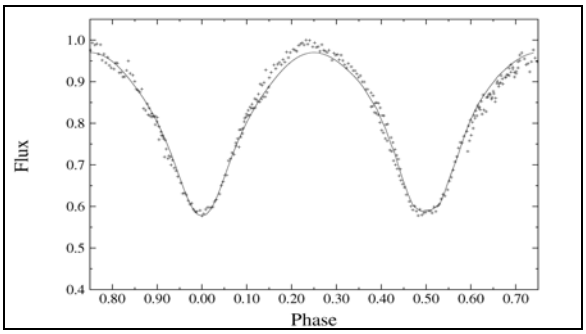

Figure 3. AP LEO Normalized Lightcurve, Polynomial Fit.

2. Observations

AP Leo was observed at two observatories during the 2006 session. The Paradise View Observatory utilizes a Meade 14" LX200GPS with an STL-1301 SBIG camera maintaining 2007mm (79") focal length and field of view of 1.49 arcsec/pixel. The Kings Canyon Observatory uses a Meade 12" LX200 Classic with an SBIG ST-9XE yielding a 1920mm (75.6") focal length and FOV of 2.18 arcsec/pixel. All data was obtained in the V and R color system approximating the standard Johnson UBVRI photometric system. Since the comparison stars are on the same CCD images as the variable, extinction corrections for the data were not made.

The lightcurve in the V band is displayed in Figure 3 and is symmetric as is the R band lightcurve. These curves are of typical W UMa-type and the depths of both minima are nearly the same. Data was obtained at the telescope using the MPO Connections Software and reduced using the MPO Canopus Software.

3. Spectroscopic and Photometric Solutions

Previous authors of the AP Leo system have used spots on the components because the lightcurves were not symmetric which required spots to make the modeling coincide with the lightcurves. Some curves also showed the O'Connell effect, O'Connell (1951), where the maximum following the primary minimum is lower than the maximum following the secondary minimum which is usually considered an indication of star spots. The lightcurve in Figure 3 is symmetric, as is the R curve, which did not require incorporating spots to adjust the modeling to fit the curve, which allowed for reliable parameters to be derived. Figure 4 displays the geometrical relationships of the surfaces of AP Leo at phase 0.24. Table 1 list five published parameters for AP Leo for comparison purposes along with some computations by Hipparcos and those parameters computed in this paper.

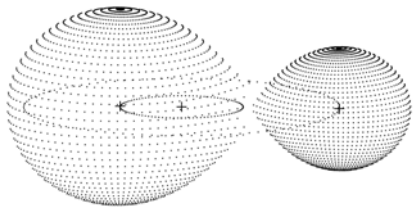

Figure 4. Geometric Structure AP Leo.

The parameters computed from the lightcurves, Figure 3, set the mass ratio to the most accurate spectroscopic values acquired by Lu & Rucinski (1990) of M_2 / M_1 = q = 0.297. Temperature for star 1 eclipsed at primary minimum was set at T_1 = 6150º K for a spectral type F7-8 V, Lu & Rucinski (1999). Limb-darkening coefficients were set at R band x_r = 0.544 and V band x_v = 0.432 and gravity-darkening coefficients $g_1 = g_2$ = 0.32. The bolometric albedo was set at $A_1 = A_2$ = 0.5. The adjustments to model the lightcurves were to the orbital inclination (i) and Temperature for star 2 = T_2. The photometric solutions carried out found the inclination of 79.6º which was close to the values derived by others and the temperatures of both stars were close but the derived mass ratio of q = 0.404 was 36% higher than the spectroscopic value. The best modeled photometric

mass ratio was determined by measuring the light-curve residuals using different ratios until the smallest sum of the squares was obtained. This is not the most accurate but is close for modeling purposes. With the mass ratio increasing from q = 0.297 to q = 0.404 would indicate mass transferring from the primary, star 1, to the secondary, star 2, which could be the cause of the Angular Momentum Gain (AMG) and orbital period increase of AMG = dP/dt = +0.044 sec yr $^{-1}$ or a period increase of +4.4 sec century^{-1}. This rapid increase in the mass ratio has occurred in seven years since 1999 and is indicated on the plot of the O-C minimum times, Figure 2, and indicates the system stars are equalizing their masses, which would increase their orbits around each other till their masses were stabilized.

4. Orbital Period Variations

The O-C diagram in Figure 1 includes all the available CCD, photoelectric and visual eclipse times of minimum and were calculated with the linear ephemeris,

$$\text{Min. I} = 2{,}449{,}428.715 + 0.4303482E \text{ days.} \quad \textbf{(1)}$$

As was stated earlier these times of minimum display a large scatter of up to ± 0.11 days. A polynomial fit indicates a small periodic cyclic sinusoidal change which has been interpreted as being caused by a triple system. These variations appear to occur every 22.5 years. A least-squares solution yields the quadratic ephemeris,

$$\begin{aligned}\text{Min. I} = {} & 2{,}449{,}428.727374 \pm 0.0058 \\ & + (0.43035022 \pm 4.424 \times 10^{-7})\, E \\ & + (2.7985 \pm 2.017 \times 10^{-6}) \times 10^{-11} E^2 \text{ days} \quad \textbf{(2)}\end{aligned}$$

A look at the O-C diagram shows another rapid linear increase in the orbital period which started April 1976 and the data is all from CCD photometric data. Considering the unreliability due to the large scatter of all the data an analysis of this increase in the period was pursued and plotted in Figure 2. The light elements, equation 1, were used to compute quadratic light elements:

$$\begin{aligned}\text{Min. I} = {} & 2{,}449{,}428.715009 \pm 0.0028 \\ & + (0.430341806 \pm 2.467 \times 10^{-7})\, E \\ & + (3.009 \times 10^{-10}) \times 10^{-10} E^2 \text{ days} \quad \textbf{(3)}\end{aligned}$$

This quadratic term reveals a continuous and constant period increase with a rate of dP/dt = +0.044125 sec yr^{-1}, which equates to a period increase of 5.11 x 10^{-6} days yr^{-1}.

5. Conclusion and Discussion

The lightcurve and period of the AP Leo system is highly variable with abrupt cyclic changes and can be classified as an overcontact W UMa-type eclipsing binary. In April 1976 an abrupt increase started and continues at present. The lightcurve indicates this increase is linear, has occurred before and is increasing at a rate of dP/dE = +6.0 x 10^{-10} days per cycle. This rate is compared to other short-period W UMa-type binaries with long-term continuous increases that have been studied. See Table 2, Wolf (2000), where this computed rate has been placed in descending order. The orbital period change of AP Leo is above the average for W UMa-type overcontact binaries and as Table 2 indicates these systems also have highly variable changes. The mass ratios of these system do not appear to be constant indicating mass transfer thru the Lagrangian point between the stars causing angular momentum gain or loss which in turn effects the orbital time of the system.

If a third body is effecting the system as some studies indicated than further investigations with lightcurves will indicate shortly a decrease in the orbital period and overtime will confirm a third body system.

This research has made use of the SIMBAD database, operated at CDS, Strasbourg, France.

PARAMETER	**CRISTESCU et al. (1979)**	**ZHANG et al. (1992)**	**Lu & Rucinski (1999)**	**QIAN et al. (2007)**	**PRIBULLA et al. (2003)**	**SNYDER THIS PAPER**	**HIPPARCOS (1997)**
Mass Ratio (solar units) q (M2/M1)	0.211	0.3013	0.297	0.297	0.078	0.404	
Omega 1				2.4134		2.586110	
Omega 2				2.4134		2.657630	
Omega inner		2.4648		2.4596		2.657630	
Omega outer		2.2820		2.2743		2.419230	
Fillout 1 %		23.5		24.9	0.23	.30	0.24
a1			2.237				
a2			0.665				
Mass (solar units) Primary			1.368		1.774		
Mass (solar units) Secondary			0.406				
Temperature (K) Primary	6608	6000		6150	6000	6250	
Temperature (K) Secondary	6586	6074		6201	6074	6200	
Orbital inclination (deg)	83.131	79.863		77.54	79.9	79.6	
Surface gravity (cm/s^2)	0.25	0.32		0.32		0.32	
x1 R				0.544		0.47	
x1 V	0.6			0.642		0.63	
x2 R				0.544		0.432	
x2 V	0.6			0.642		0.595	
Spectral type 1	G0		F7-8 V				
Spectral type 2	G2						

Table 1. Parameter Solutions AP LEO.

BINARY SYSTEM	**dP/dE x 10^{-10} days / cycle**
AP AUR	**18.13**
BX DRA	**11.12**
XY BOO	**6.20**
UZ LEO	**6.07**
AP LEO	**6.00**
V839 OPH	**3.46**
AH VIR	**2.66**
GO CYG	**2.26**
V401 CYG	**1.48**
441 BOO	**1.24**
DK CYG	**1.15**
CT ERI	**1.02**

Table 2. Rate of Long-Term Continuous Increase of Period W Uma-Type.

6. References

Bradstreet, D.H. (2004). Binary Maker 3.0, User Manual, Contact Software, Norristown, PA 19401-5505.

Cristescu, C., et al. (1979) "New elements for AP Leo." *IAU Inform. Bull. Var. Stars* **1688**, 1-3

Lifang, Lt. et al. (2002). "Period and Light-Curve Changes in AP Leonis." *PASJ.* **54**, 73-77.

Lu, W., & Rucinski, S. (1999). "Radial Velocity Studies of Close Binary Stars." *AJ* **118**, 515.

O'Connell, D. (1951). *Publ. Riverview Coll. Obs*. **2**, 5.

Perryman, M.A.C. (1997). The Hipparcos and Tycho Catalogues, ESA SP Ser. – 1200.

Pribulla, T., et al. (1999). "The Contact Binary AW Ursae Majoris as a Member of a Multiple System." *A&A* **345**, 137-148.

Qian, S.B. et al. (2007). "A new CCD Photometric Investigation of the short-Period close binary AP LEONIS." *AJ* **133**, 357-363.

Wolf, M. et al. (2000). "Period Changes in W UMa-type eclipsing binaries: DK Cygni, V401 Cygni, AD Phoenicis and Y Sextantis." *A&A Suppl Ser.* **147**, 243-249.

Yang, Y. et al. (2002). "Period Behavior of the W Ursae Majoris contact binary AH Tauri." *A&A* **390**, 555-559.

Yang, Y., et al. (2004). "RT Leonis Minoris: an Unstable W Ursae Majoris System with a Spotted Component." *Chin J. Astron. Astrophys.* **6**, 553-562.

Zhang, J.T., et al. (1992). "Period Changes of AP Leonis and its Photometric Solution." *AcASn* **33**, 131Z.

Photometry With DSLR Cameras

John E. Hoot
SSC Observatory
615 S. El Camino Real
San Clemente, CA 92672

Abstract

The emergence of DSLR cameras as cost effective astro-imaging tools prompts the author to investigate the use of DSLR cameras in making photometric measurements. The quantum efficiency, dynamic range, linearity and transformation to the standard system are explored. Observational and processing techniques unique to use of DSLRs in quantitative observation are presented. Suitability for particular observing programs is discussed.

1. Introduction

Digital single lens reflex (DSLR) cameras with high pixel counts have become the staple of professional photographers within the last five years. Entry level versions of the latest generation of these cameras are priced below $800 and offer pixel counts of 8 to 10 mega-pixels. Astro-photographs made with DSLRs appearing in popular astronomy periodicals amply demonstrate the capability of these cameras to produce excellent images. Since these cameras employ solid state CMOS or CCD photo detectors, it appeared to the author that DSLRs might be a cost effective alternative to CCD cameras for quantitative work in photometry and astrometry.

This paper presents an analysis of the DSLR camera design, implementation as it pertains to use of the camera in scientific study and presents the results of photometry performed on standard star fields and the transformation of those results onto Johnson-Cousins standard.

2. Unique and Important Characteristics

Consumer DSLRs share two of the key traits of CCD science cameras: They have linear response over a large portion of their range and they are read-out digitally, presenting an image representation amenable to quantitative analysis. They also share the less desirable trait of producing electrons in response to thermal excitation of the detector in addition to captured photons.

They differ from scientific CCD cameras in several key respects. Firstly, the cameras are not hermetically sealed and operate at ambient temperatures. The combination of properties leads to the requirement that frequent dark and bias frames must be taken to accurately calibrate images.

The active portion of these sensors is typically smaller than scientific camera. Typical pixel size range from 4.0um to 6.5um. These sensors are typically covered with micro-lenses to improve the quantum efficiency (QE) of the devices. Even so, their normal quantum efficiencies are lower than science cameras. The other consequence of the small pixel sized in these cameras is that the total captured charge capacity of DSLRs is significantly smaller than scientific cameras.

The detectors of DSLRs are universally equipped with "anti-blooming" gates. Anti-blooming limits the charge that can be accumulated by any pixel in the detector by providing a contact to the pixel pulsed with a lower electric potential than the full well potential of the cell. This causes excess current to flow out of the pixel before it spills into adjacent pixels. While this prevents unpleasant aesthetics in photographs, it leads to non-linear response of the detector as the well potential approaches the anti-blooming potential.

R	G	R	G	R	G
G	B	G	B	G	B
R	G	R	G	R	G
G	B	G	B	G	B
R	G	R	G	R	G
G	B	G	B	G	B

Figure 1: Typical Bayer Mosaic Pattern (R=red, G=green, B=blue)

The most striking difference between DSLRs and purpose built science cameras is that DSLRs have filters epitaxially deposited directly on the de-

tector in a "Bayer" pattern. The standard pattern for filter coatings are shown in Figure 1. The presence of filters on the detector is the most significant architectural difference between DSLRs and science cameras. Their presence motivates most of differences in observation techniques discussed below.

If the color filters have pass bands similar to photometric standard filters, then the DSLR is a turn-key multi-color photometric machine.

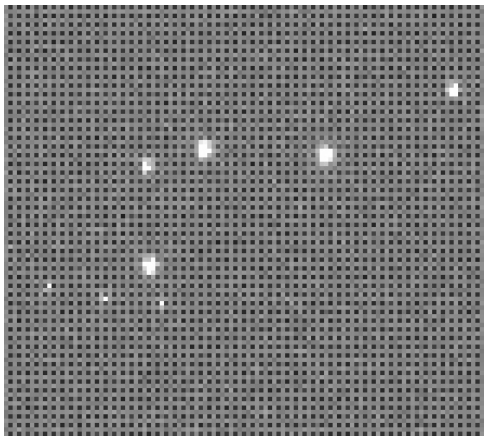

Figure 2: Raw image from Bayer filter mosaic

There are a couple of other characteristics of DSLRs that, while not unique, merit consideration in using the cameras. First, the micro lenses on the detector cause the QE of the camera to vary with the f-Ratio of the optical system to which it is attached. Slower optical systems, beyond about f7, will display lower QE than faster optical systems because the micro lenses are not strong enough to bend all of the shallower light cone into the active portion of the detector pixel.

The other consideration is that larger detectors demand better optical systems. System that performed well with smaller CCDs may display significant field curvature and vignetting when used with larger detectors.

3. Operational Considerations

Using a DSLR for photometric observation is similar to using a standard scientific CCD with the following key exception. DSLR observations are almost always made by taking a multiple sequence of short exposures and combining them. There are a number of reasons for this approach. Primarily, the smaller dynamic range and higher thermal electric response effectively limit exposure times in order to keep the objects of interest within the linear range of the detector. Additionally, depending on the color you are sampling, only one in four, or two in four pixels on each image is of a given color. You want the seeing and tracking errors of many images to "drizzle" together into normal point spread function (PSF).

On the positive side, DSLRs are completely self-contained. No computer or electronics more complicated than an electronic cable release are required for making observation. After working with progressively more complicated software, cabling, cooling, and filter wheels, this is a refreshing change. If you are planning an extended session, extra memory cards and batteries, or an external power supply will be required.

When making exposures with DSLRs, all data should be stored in the camera's RAW/Uncompressed mode. The default for DSLRs is typically JPEG, an encoding system that discards information to achieve higher compression rates. Even TIF and other lossless encodings may apply non-linear contrast stretch, and noise suppression that discards portions of the image data.

4. DSLR Performance

DSLR cameras offer an extraordinary value in many respects. Because they are produced for the mass markets, manufacturers can, and do, spend phenomenal amount of money on design, development and custom tooling that boutique science camera makers simply cannot afford. The resulting performance numbers support this observation. Figure 3 provides comparison of quantum efficiencies between DSLR cameras and other available cameras.

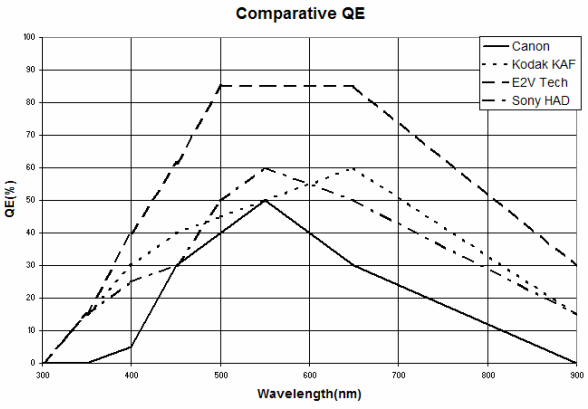

Figure 3: Relative Quantum Efficiencies

These curves show that while the QE of DSLRs falls below other cameras, the QE is still good enough to prove useful. Note that these figures are based on removing the manufacturer's supplied IR blocking filter. On all commercial cameras, except

Camera	Sensor	Class	Price	photons per $	X	Y	Pix Size	Total Area	Photos@flux w/ filters	Photons/ mm^2
Canon EOS	Propietary	Front Illum Filter	700	875.49	3456	2304	0.00645	331.27	612840.37	1850.00
SBIG ST1100M	KAF-1100ME	Front Illum Filter	9200	296.99	4096	2730	0.009	905.75	2732341.25	3016.67
Meade DSI	Sony HAD	Front Illum Filter	299	158.95	640	492	0.0075	17.71	47527.20	2683.33
Meade DSI-II	Sony HAD	Front Illum Filter	599	138.05	748	577	0.00845	30.82	82692.37	2683.33
Apogee U42	E2V-42	Thinned Back	39000	84.06	2048	2048	0.013	708.84	3278372.86	4625.00
SBIG ST-8	KAF-1602ME	Front Illum Filter	5200	73.91	1536	1024	0.009	127.40	384329.32	3016.67
Apogee U47	E2V-47	Thinned Back	11200	73.18	1024	1024	0.013	177.21	819593.22	4625.00
SBIG ST-7	KAF-402ME	Front Illum Filter	2700	35.59	768	512	0.009	31.85	96082.33	3016.67

Table 1: Camera effectiveness expressed in Photons/Dollars/Second

the Canon D20a, the manufacturer's filter has a cut-off point that excludes Hydrogen Alpha emissions.

Clearly, these QE numbers show that if you are looking for a detector to operate at the edge of delectability for your optics, a DSLR is not your choice, but for many other programs, it may be adequate. The real figure of merit for a DSLR camera is Photons/Dollar/Second. If you use this metric to evaluate cameras, the DLSR is hard to beat.

Table 1 shows the analysis of DSLRs vs. a variety of science cameras with filters using the Photons/Dollars/Second metric. It assumes a uniform flux (photons/nm) falling on the detector. Using this metric, you can see that the large detector area coupled with its lower cost propels the DSLR to the top of the list. Even for projects that need to work out at dim magnitudes, the price difference between a large back illuminated detector and DSLR might be more profitably spent on larger optics, at least up to 20" glass.

Another figure of merit for cameras where DSLRs shine is Signal to Noise Ratios (SNR). QE is worthless unless the noise is low enough to make the SNR of the camera superior. Table 2 shows a comparison of readout noise and gain for a variety of cameras. The DSLRs all display very low read noise values.

Camera	ISO/Gain	e-/ADU	Read Noise (e- rms)	Reference
Canon 10D	400	2.5	11	Buil
Canon 20D	400	3.1	7	Buil
Canon 300D	400	2.8	12	Lovejoy
Canon 350D	400	2.2	6	Buil
Nikon D70	400	3.0	13	Buil
Sony HAD	n/a	0.8	12	SONY
SBIG ST7/8	n/a	2.3	15	SBIG

Table 2: DSLR Read Noise Comparison

5. Photometry Performance Tests

The analysis above indicates that DSLRs have excellent potential to perform quantitative photometric and astrometric observations. To ascertain how well the cameras actually perform photometry, I set about making a series of observations of Landolt standard star fields using a Canon EOS 350D camera. The camera has an 8 Mega-pixel detector composed of 6.4um pixels that have a factory applied RGB Bayer filer array deposited on the detector. Observations were made on two separate new moon evenings with near photometric conditions. The observations were made with geometrically increasing exposure times and across a wide range of air masses between 1.19 and 2.0. Landolt fields SA100xxx .. SA105xxx were observed during the program.

Observation data was converted from Canon RAW data format to FITS floating point representation using Canon and Meade image processing software. All subsequent data reductions and analysis were then performed using IRAF 2.13 Beta running under the PC-CygWin environment.

Observation and calibration images were split into 3 separate R, G and B images using flux conserving techniques. Calibration images for each color field were combined and applied to observations. Each field was measured by taking eight exposures and averaging these together after they had been calibrated and co-aligned. For the purpose of data reduction each of these composite images was treated as a single photometric observation with an air mass of that of the middle of the sequence.

Photometric measurements of each field were performed using DAOPHOT point spread photometry. Observational data was taken in each of the color bands. The basic working assumption being that the camera's native red, green and blue responses would approximate Johnson-Cousins standard R,V, and B band responses respectively.

These observations were then fitted for extinction and zero-points using a "least squares" best fit method. These raw instrumental readings were then plotted against the Landolt magnitudes in Figures 4, 5 and 6.

These instrumental fits have RMS errors of 0.347, 0.134 and 0.236 Mag. for B,V and R bands respectively.

For the V color band an attempt was made to determine a single color correction term to transform the observations onto the standard system. The result was again plotted against the Landolt standard value and shown as Figure 7.

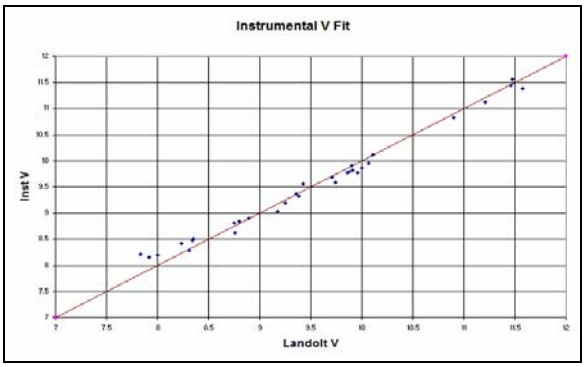

Figure 4: Instrumental V Fit

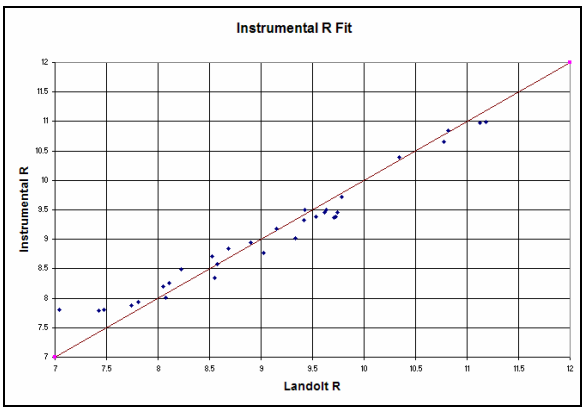

Figure 5: Instrumental R Fit

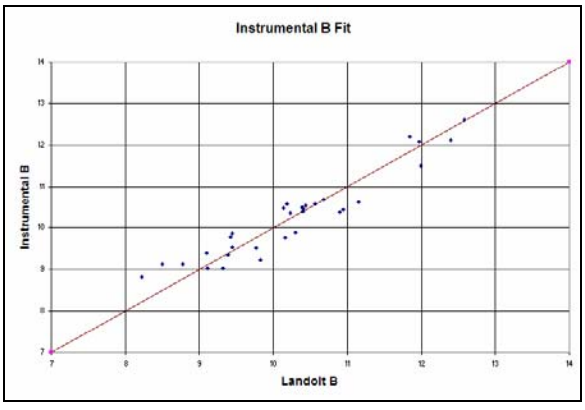

Figure 6: Instrumental B Fit

After refitting the V band magnitudes using the instrumental V-R term for color correction, the RMS error value dropped from 0.134 Mag. to 0.132 Mag.

6. Discussion of Results

The attempt at chromatic correction of the V-Band response must be categorized as a failure given the average statistical uncertainty of the instrumental photometry was 0.003 Mag. and the incremental improvement of the photometry was only 0.002 Mag.

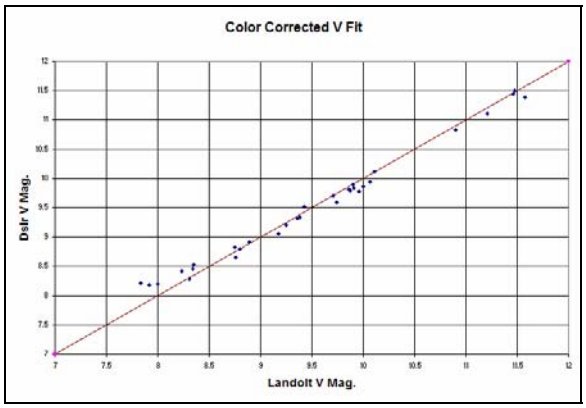

Figure 7: Color Corrected V Fit

I must conclude that the fit problems were more likely a result of another systematic effect. Two separate plots support this analysis. A scatter plot of error vs. color index shown as Figure 8 suggests no significant relationship between color and error. While Figure 9 showing error as a function of magnitude suggests another cause for the low quality of the fit.

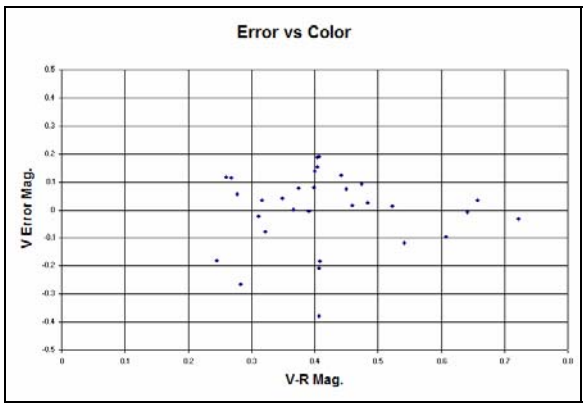

Figure 8: Error vs. Color Plot

Overlaid on Figure 9 is a 3rd order polynomial fit of absolute error as a function of magnitude. It clearly shows that for objects in the range of 9.0 to 11.5 magnitude absolute photometry errors are on the

order 0.05 magnitude. But for objects brighter than magnitude 9.0, systematic errors increase rapidly with magnitudes being systematically under estimated. This pattern of errors leads me to conclude that, despite earlier admonitions, I was a victim of non-linear detector response resulting from the presence of anti-blooming structures in the detector.

I have considered reanalysis of this data set after exclusion of observations with fluxes yielding magnitudes brighter than 9.0, but I feel the resulting sample size would be too small to provide strong support of any conclusion.

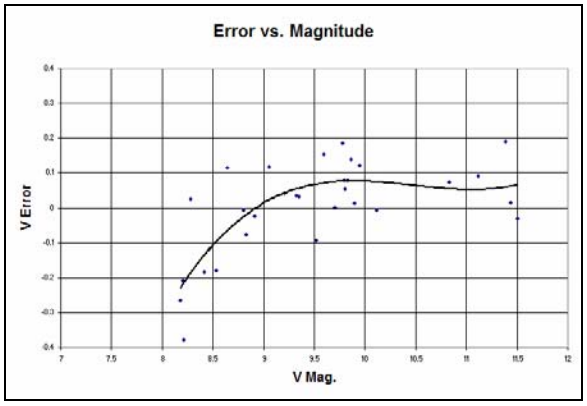

Figure 9: Error vs. Magnitude with 3rd order fit

7. Conclusions

Based on the results above, I think several conclusions can be drawn. Firstly, no single exposure set taken with this DSLR family of camera can accurately span more than 2.5 magnitudes. That particular restriction does not preclude performing very accurate, multi-band differential photometry. All that is required to perform milli-magnitude differential photometry is care to assure that target, check and comparison stars are within a 2.5 magnitude range and that the exposures used keeps all observed stars well within the linear regime of the camera.

Secondly, I would assert based on these results, that, subject to dynamic range limitations, the Green filter set closely approximates the Johnson-Cousins V band.

Third, data would indicate that the instrumental blue filter response may not extend far enough into the shorter wavelengths to easily transform onto the standard system. Still, the presence of color information in single frame exposures provides the tools necessary to select reasonable comparison stars in differential photometry.

Fourth, the work here begs for follow up work using geometrically scaled exposure sets to more fully characterize the chromatic effects of the camera.

With the constraints indicated above, I conclude that DSLRs are very well suited to programs of differential photometry. They also offer excellent opportunities to perform large surveys with modest optical systems.

The key to using the cameras in survey applications will be to take multiple exposures of geometrically increasing duration, where each exposure goes approximately 2.0 magnitudes deeper than its predecessor. By carefully limiting the magnitude selection from each exposure group to 2.0 magnitudes, centered the linear portion of the detectors, wider dynamic ranges can be surveyed without loss of precision.

The practice will lead to more exposure and processing time to reduce data from any survey. As in other survey work, the design of the backend data stream processing will be resource intensive. It will require the same level of automation and online storage as any other program yielding equivalent volumes of raw data.

8. References

Buil, C. (2007). "Spectroscopy, CCD and Astronomy." http://www.astrosurf.com/buil.

Bessell, M.S. (1990) "UVBIR Passbands", *PASP* **102,** 1181-1199.

Desnoux, V. (2006) "Nikon Astronomy Imaging," http://valerie.desnoux.free.fr/neat/nikonD70.htm,.

E2V Technologies (2002). *CCD42-40 Ceramic AIMO Back Illuminated Compact Package High Performance CCD Sensor,* Essex, England.

Eastman Kodak Company (2000). *KAF-1602E Full Frame Image Sensor,* Rochester, New York.

Johnson, H.L, Morgan, W.W. (1953). "Fundamental Stellar Photometry Standards Of Spectral Type On The Revised System Of The Yerkes Spectral Atlas," *ApJ* **117,** 313-352.

Landolt, A.U. (1983). "UBVRI Photometric Standard Stars Around The Celestial Equator," *ApJ* **88**, 439-460.

Lovejoy, T., (2006). "DSLR's For Astrophotography-Tech Notes", http://www.pbase.com/terrylovejoy/dslr_tech.

Sony Corp. (2006). *ICX489AQF High Resolution 7.24M Pixel CCD Sensor*, Tokyo, Japan.

Stetson, P.B. (1987). "DAOPHOT - A Computer Program For Crowded-Field Stellar Photometry," *PASP* ***99,*** 191-222.

CCD Video Photography and Analysis of Comet Schwassman-Wachman 73P Fragments B & C Using the Low-Cost Meade DSI Camera

Steve Gifford
1012 S. Crown Key Ct., Gilbert, AZ 85233
stevegifford@cox.net

Abstract

Near Earth Object Comet Schwassman-Wachman 73P had its closed approach to Earth on May 12, 2006. 874 8-second CCD exposures were collected for fragment B using the un-cooled low-cost Meade DSI Camera Model 1. These images have been extensively processed and made into a dramatic video that captures over 2 hour's movement of the comet through a star field. This paper discusses image processing techniques such as image registration, automatic flat fielding, image restoration and estimation of the comet's position using tracking algorithms.

1. Introduction

On the morning of May 12, 2006, Comet Schwassman-Wachman 73P came within 0.08 AU of planet Earth. This periodic comet (5.3 yrs) has an estimated diameter of 600-1100 M. An impact of this NEO into Earth would be disastrous. The potential of impact will reoccur in 2022 with an even closer approach. In 1995, the comet broke into 5 large pieces and during the latest pass broke into many smaller components.

CCD images were collected during the time of closest approach. The objective of this paper is to present the data and analysis of this NEO as well as signal processing techniques used to process the data. Details of the equipment are as follows:

Location: Gilbert, AZ (16 mi. S.E. of Phoenix)
Schwassman-Wachman 73P Fragment B
8" LX-200 F6.3 Classic w/F3.3 focal reducer
Modified Meade Equatorial Wedge
Meade DSI Model 1 CCD Camera (648x488)
CCD FOV: 42' x 32'; I Filter
Center CCD: RA 20:01:08, DEC +37 52' 58".
CCD Orientation: Landscape + 45° CCW
874 8-sec exposures taken
Start: 3:11A.M. On May 12, 2006 MST (-7 hrs)
End: 5:24 A.M. at Morning Twilight
No tracking of the mount was used.
Ambient Temperature: 57° F-64° F
4.7"/pixel
Clear Skies but Full Moon

Images and data were also taken for comet fragment C at earlier dates. Details in this report are for fragment B unless stated otherwise.

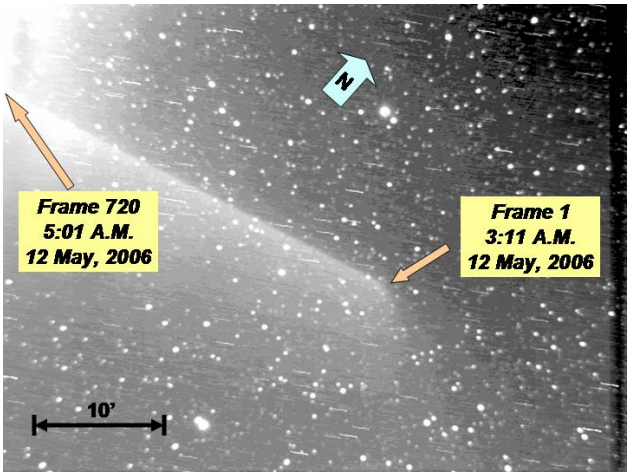

Figure 1. Comet Schwassman-Wachman 73P Fragment B Stack of Unprocessed 720 8 Second Exposures

2. Observations

The time of closest approach to Earth for Comet Schwassman-Wachman 73P occurred on May 12, 2006. 874 images were taken for 73P Fragment B starting at 3:11 A.M MST and ending during morning twilight at 5:24 A.M. MST. The CCD camera used was the un-cooled Meade DSI Pro Model 1 (648 x 480) with the 'I' filter. The field of view for the equatorially mounted 8" LX200 F6.3 Classic telescope was expanded to 42'x32' by using an F3.3 focal reducer. 60 dark frames were collected and averaged to

create a static master dark frame before the comet image collection phase. The location of equipment was not optimal since our site was only 16 miles from brightly illuminated metropolitan Phoenix, AZ and the ambient desert temperature varied from 57° F to 64° F over the 2 hour comet data collection session. The Moon was full. Since no guide star tracking of the mount was used, careful alignment of the telescope was performed by using the drift test for a star above and a star to the East. Each of the 874 images collected consisted of a single 8 second exposure with the master dark frame automatically subtracted. No saturation of the comet nucleus occurred with the 8 second exposure; however, a few of the stars were slightly saturated. Many days and nights of preplanning were required to collect the desired images. The program 'Starry Night Pro 4.5' was used to simulated the comet position and FOV. Using this information, the center of the FOV for the comet collection session was set statically to: RA 20:01:08, DEC +37 52' 58".

Several factors made the post-processing of the comet images difficult as can be demonstrated by analyzing the unprocessed images in Figures 1 and 2. The brightly illuminated location of suburban Phoenix and the low-altitude (1100') reduced the image signal to noise ratio. The near worst case position of the waxing gibbous Moon, 13.9 days old and 99.3% illumination created a time dependent glare into the aperture of the telescope. The un-cooled CCD camera itself was responsible for much of the image degradation. A better solution for a CCD camera would be one in which the CCD detector is cooled to a stable temperature 20° - 30° C below ambient. Such temperature regulated CCD chips exhibit stable low dark currents. The warm time-varying desert temperature from 57° F to 64° F, static dark master subtraction and an un-cooled CCD camera resulted in dynamic flat field distortions as a function of the point in time that each of the 874 images were recorded. An extremely small drift in the mount resulted in a 3' displacement over the course of collecting 874 images that required over 2 hours of data collection.

3. Image Post-Processing

The raw images shown in Figures 1 and 2 can be improved upon by using image processing techniques. The time-varying flat field can be estimated and removed, but the comet signal makes this difficult. The task was accomplished by computing the median value of each 31x31 pixel block as shown in Figure 3, cutting out the area around the comet leaving a hole where the comet would normally be, interpolating across the hole and then upsampling the image by 31 to get the resulting 648 x 488 pixel image as shown in Figure 4. This process was separately performed for each image.

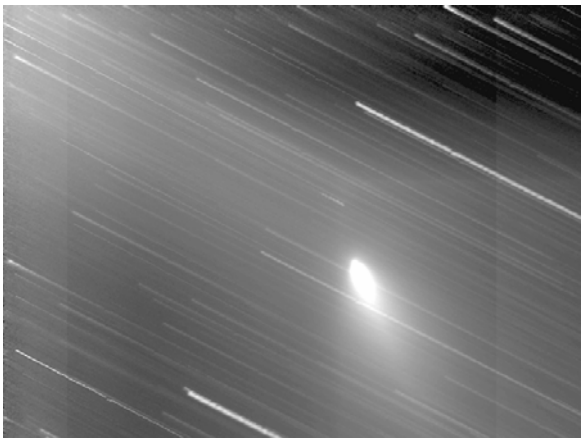

Figure 2. Comet Schwassman-Wachman 73P Fragment B Stack of Unprocessed 720 8 Second Exposures

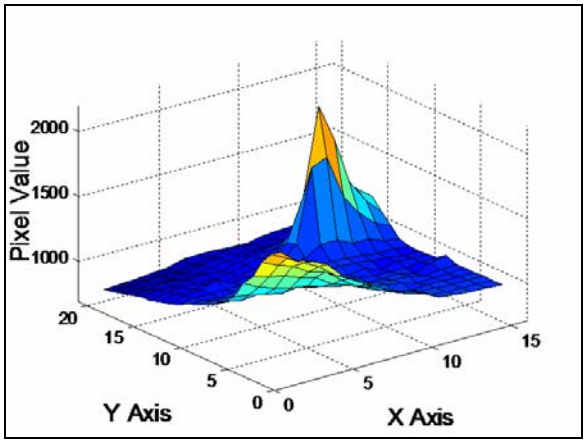

Figure 3. Initial Automatic Flat Field for Image 1

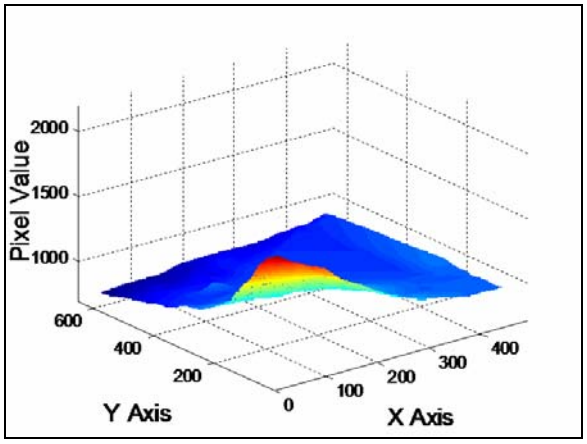

Figure 4. Corrected Automatic Flat Field for Image 1

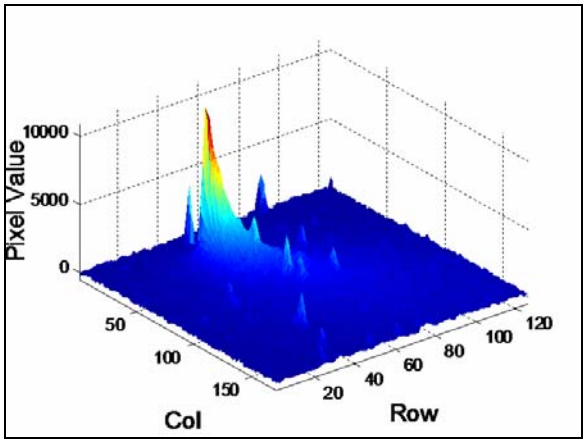

Figure 5: Comet Extraction With Stars for Frame 1

Figure 5 shows the extracted comet with the stars. The stars in the comet image can be removed with the following process: Carefully align images 1 through 200. For each of the pixels find the median value for frames 1 through 200 and create a new image composed of the median values. The comet has been removed from this image. Subtract the image from frame 1. The result is the comet image with the stars removed as shown in Figure 6. Now a brightness measurement can be made of the comet without the stars in the comet field.

Another impairment to the collected images is a uneven bias for odd vs. even rows. Figure 7 shows the results of an analysis of this problem. A curve fit was computed for the median of the odd rows and also for the even rows. The bias in each odd and even row was adjusted so the new bias was the average bias. The corrected bias is shown as the middle curve in Figure 7. This fix removed strong horizontal lines in the image.

Bad pixels in the images were repaired as follows: Image darks were performed for multiple exposure times. Figure 8 shows an example for 400 pixels. Note that most of the pixels near the bottom of the graph behave in a similar manner, but some of the pixels exhibit poor dark current characteristics. A statistical analysis was performed of the 316,224 pixels on the CCD to identify the bad pixels. Pixels that varied more than 0.5σ from the mean were classified as bad and their location was placed in a file. The bad pixels in each of the comet images were repaired by replacing the bad pixel with the median value of the surrounding pixels.

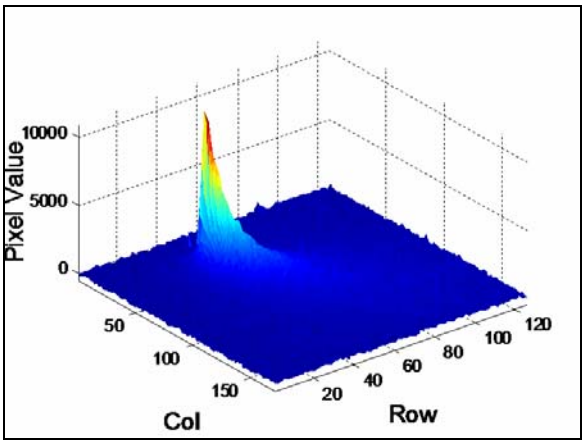

Figure 6. Comet Extraction Without Stars for Frame 1

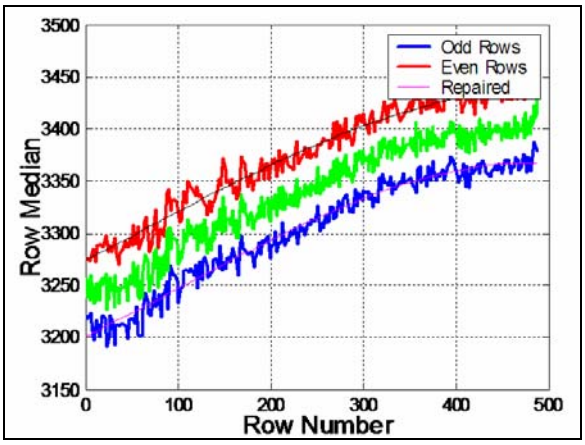

Figure 7. CCD Row Bias Correction

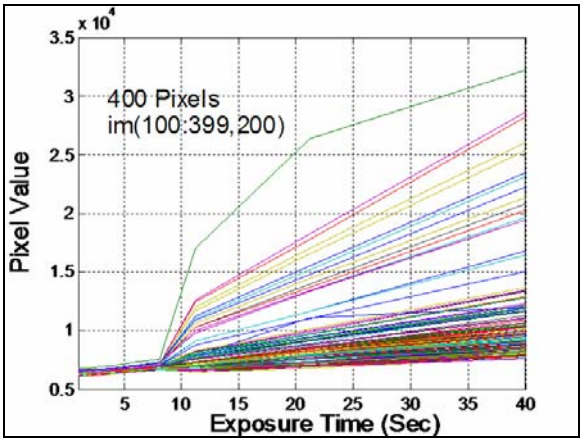

Figure 8. Bad Pixel Analysis

4. Results

Image restoration as outlined in the previous section was applied to the unprocessed photos frames 1

to 200 to create the composite stacked image shown in Figure 9. Compare this image with that in Figure 1. Substantial improvement in flattening the image and enhanced detail of the comet is visible. These image processing algorithms often require excessive amounts of memory, so the image stack size was reduced to 200 frames from the original 720 frames.

Figure 9. Corrected Figure 1 Image (Frames 1-200)

Now compare Figure 10 with Figure 2. Again, the image has improved. The results in Figure 10 were achieved by computing the comet position using sub-pixel accuracy (Figure 12), images 1 through 360 were upsampled 2x to allow more accurate stacking, the images were then stacked using the comet position and then cropped. Note that this image is 2X compared with Figure 2.

Figure 10. Corrected Figure 2 Image (Frames 1-360)

Figure 11 shows a 3D representation of the image in Figure 10. Note the large peak associated with the nucleus of the comet and the long tail that extends to the bottom and beyond the edge of the photo.

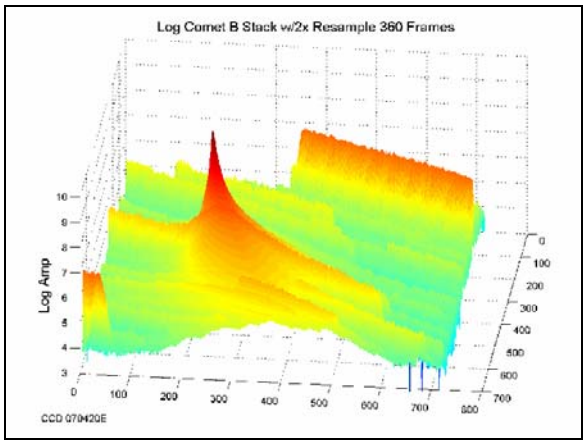

Figure 11. 3D Log Amplitude Plot of Figure 10

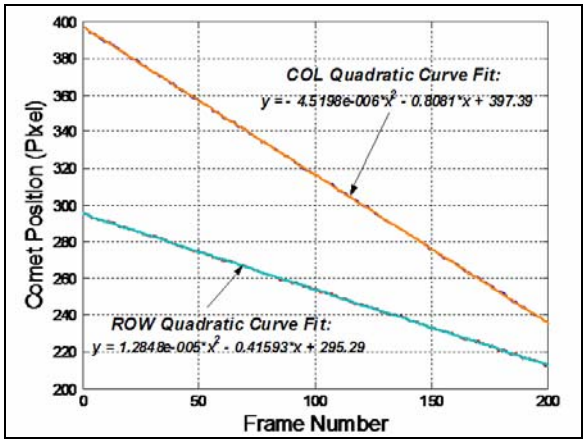

Figure 12. Comet Position Vs. Frame Number

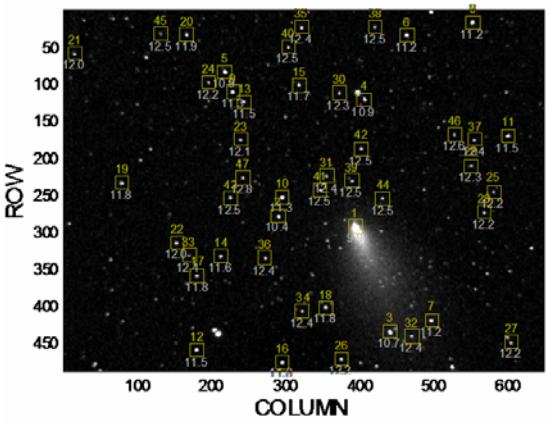

Figure 13. Star & Comet Brightness

The comet brightness was measured as shown in Figure 13 to a value of 9.9. This measurement only

took light from the comet nucleus into account. The total comet brightness would be much more substantial, perhaps as bright as 6.6 as reported by many observers at the time. The brightness of the surrounding stars was checked with MPO Canopus and compare favorable to within ±0.2 magnitude.

A CCD linearity test was performed with the Meade DSI camera using a custom made flat box. The results are shown in Figure 14 for 400 pixels. Results indicate that the CCD detector is very linear up to values of 60,000 counts.

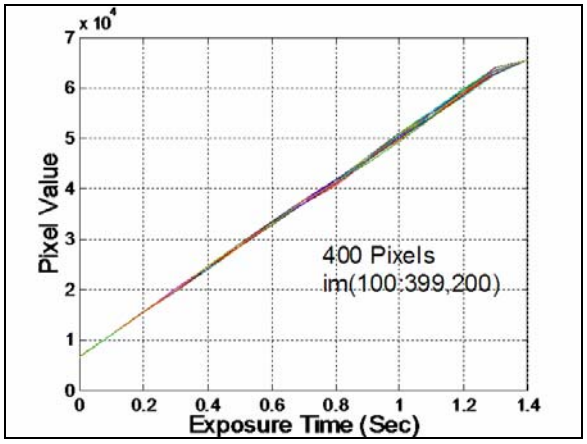

Figure 14. CCD Linearity Test

The image processing steps described in this paper was used to process 360 frames of the comet B fragment. These corrected image frames have been assembled into a movie showing the movement of the comet through the star field (Figure 1). Contact the author at the email address shown at the front of this paper for more information concerning the comet movie.

5. Conclusion

This paper indicates that careful image correction can substantially enhance the value of images both in terms of intrinsic beauty and their application to the acquisition of scientific knowledge. It is possible for low-cost astronomical equipment to be useful in the pursuit of knowledge, but patience is required to accurately extract information.

6. Acknowledgements

Many thanks to members of the SAS organization including Brian Warner's help with MPO Canopus for brightness reference measurements, to Jerry Foote, for an excellent reference to CCD technology, and to Richard Berry & James Burnell on the best reference for astronomical image processing.

7. References

Foote, Jerry, "CCD Essential Workshop", *Symposium on Telescope Science*, May 23-25, 2006, Big Bear Lake, CA.

Berry, R. and Burnell, J., "Astronomical Image Processing," Willman-Bell, Inc.

Warner, B.D., MPO Canopus Software, BDW Publishing.

Initial Efforts at Asteroid Lightcurve Inversion

Brian D. Warner
Palmer Divide Observatory
17995 Bakers Farm Rd.
Colorado Springs, CO 80908
brian@MinorPlanetObserver.com

Abstract

The problem of determining the shape of an asteroid from its lightcurve has been studied for many years. Henry Norris Russell presented a paper in 1906 that said it couldn't be done with any certainty. However, further study during the 20th century said otherwise and several methods were developed that had various levels of success. In the last several years, many asteroid shape and spin axis models have been produced using methods pioneered by Mikko Kaasalainen and others. The author has converted the original FORTRAN and C code of Kaasalainen and Durech so that it is available to anyone wanting to develop their own inversion program. Models based on lightcurves the author and others have obtained are shown.

1. Introduction

Imagine an asteroid painted with alternate sections of black and white, such as shown in Figure 1. Now rotate the asteroid and measure the reflected light. Assuming the object reflects light geometrically, this "asteroid" will show no lightcurve variations over its rotation.

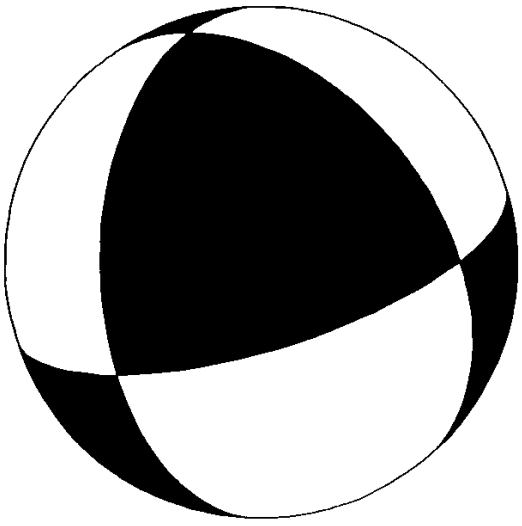

Figure 1. A sphere painted so that it will have a zero-amplitude lightcurve. After Magnusson et al (1989).

This logic of being able to paint (change the albedo) any object in specific ways lead Henry Norris Russell to conclude in his famous 1906 paper that it was very improbable that one could determine the shape of an asteroid from its lightcurve alone. In fact, one could paint an asteroid so that it was faintest when seen with its largest surface profile and brightest when seen with its smallest profile.

However, despite what would prove to be an incorrect assessment of the chances for success, that paper did contain some important conclusions that proved useful in later studies of the inversion problem, i.e., those concerning albedo variations and scattering law. In particular, he showed that it was theoretically always possible to determine the position of the asteroid's equator.

Eventually, it came to be accepted that asteroids are not painted like checkerboards but are, for the most part, painted a uniform gray, or least to a first order sufficient to find a reasonable model of the spin axis and shape. For a more complete discussion of the history of lightcurve inversion and the various methods that developed prior those of Kaasalainen et al, the reader is referred to the chapter in *Asteroids II* by Magnusson et al.

2. Shape versus Spin Axis

Before going on, it's important to distinguish the differences and importance of what can be learned from an asteroid's lightcurve.

The first is the orientation of the spin axis of the asteroid and its exact rotation rate. In fact, this is really the more important information over the shape of the asteroid, the fact that finding and showing the shape is much more dramatic.

The spin axis is given as the ecliptic coordinates, longitude and latitude, of the direction in which the north pole of the spin axis (+Z) is pointing. If the

latitude is 0°, then the equatorial plane of the asteroid is coincident with the plane of the ecliptic.

If the orbit of the asteroid also has a very small inclination to the ecliptic, then we not see much change in the shape of lightcurve except for those caused by the variations at large phase angles when shadows on the asteroid become longer and change shape.

If the latitude is near 90°, then at some apparitions, we'll see the asteroid nearly pole-on at other others we'll see it "broadside". This allows for even more dramatic changes in the shape and amplitude of the lightcurve at different apparitions.

Why is the spin axis more important? More and more its being accepted that thermal re-radiation of sunlight, the so-called YORP effect, is the primary force behind the formation of binary asteroids for smaller objects and the excess of fast and slow rotators among the MBA and NEO populations.

In the case of the Koronis family (see, for example, Slivan 2003), some of its members have been forced into a narrow grouping of orientations, i.e., their spin axes are somewhat parallel. The careful modeling of spin axes for all asteroids and, in particular, families or groups with smaller members will allow refining the theories on the YORP effect.

Two recent example of how sunlight can affect asteroid rotation rates were presented by Kaasalainen et al (2007) and Lowry et al (2007). In both these papers, the authors gave proof that the YORP effect was indeed causing the asteroid spin rates to increase.

3. Modern Lightcurve Inversion

In 2001 Mikko Kaasalainen and his colleagues published two important papers that helped revolutionize the lightcurve inversion process. These two papers presented the problem as a matter of finding a convex shape that, when appropriate scattering laws were applied, would reproduce an asteroid's lightcurve at any given epoch.

The most important point is that the modeling process deals only with convex shapes and does not attempt to model concavities such as large craters or saddles directly. Instead, these areas appear as large flat areas in the final model. A good example is 433 Eros with its large saddle. In that case, the shape model shows a large flat area where the saddle would be.

For analogy, consider the model to be the shape of the "wrapping paper" put around the object with the paper stretching over the large concavities and not trying to fill them in. Kaasalainen showed that this approach not only produced good results but that the solutions were more stable.

Since these papers, many have followed using the algorithms involved so that models (spin axis and shape) are now available for more than 100 asteroids. What's more, those models for which there are direct comparisons against detailed occultation results or images from spacecraft or adaptive optics on large telescopes agree well within the given errors.

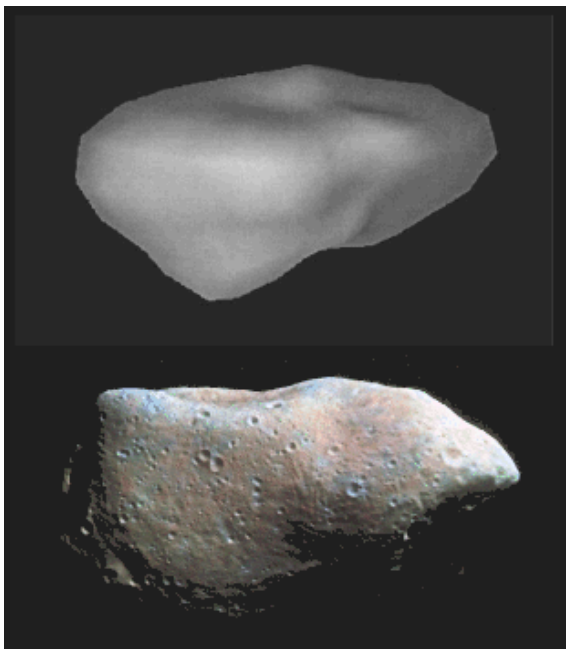

Figure 2. Comparison on model by Kaasalainen (top) and Galileo image of 953 Gaspra. Kaasalainen/NASA.

The rest of this section is based largely on the introductory material provided in the documentation for LCInvert from Bdw Publishing, but it is not specific to that program. Instead, it is a primer on asteroid modeling and can be applied when using programs based on the free open source code.

3. 1. Free Modeling Source Code

The core libraries developed by Kaasalainen and Durech are available as free, open-source files written in C or Delphi, the latter using Delphi TObjects in place of large static arrays. The source code, including the aforementioned documentation, can be downloaded from

http://www.minorplanetobserver.com/MPOSoftware/Inversion_SourceCode.htm

Please observe the open source license agreement.

3. 2. Model with Care

It is very important to emphasize that lightcurve inversion is not a simple, straightforward process and is fraught with many more pitfalls than might ever be encountered when finding the period of a lightcurve. ***It is very easy to reach false conclusions.*** A certain amount of data is required that meets specific requirements.

To answer the most common question right off: You cannot get the shape or spin axis of a main-belt asteroid from data during a single apparition. It just cannot be done. An NEO that goes through a significant change in phase angle and viewing aspect during a single apparition might be an exception, but only if there is sufficient data.

For example, the model in Figure 3 was the result of doing a search and assuming the model with the best fit, i.e., the lowest ChiSq value, was a valid solution. In this case, all the ChiSq values were very similar, which is an almost sure indication that the available data cannot generate a good model.

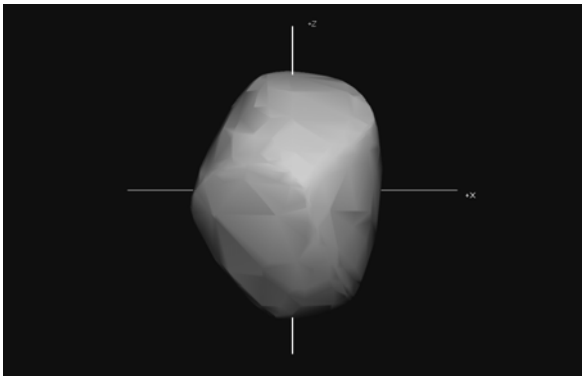

Figure 3. A bad shape model. The spin axis parallels the long axis of the asteroid.

3. 3. Relative versus Absolute Data

Absolute (or calibrated) data means that all the magnitudes (or intensities) have been put on a common system. This system can be internal or it can be one of the standard magnitude bands such as Johnson V. In addition, the data should be corrected to unity distance by applying, for magnitudes,

$$-5 \log(\Delta r)$$

Where Δ is the asteroid-Earth distance and r is the asteroid-Sun distance, in AU.

If data in different lightcurves are absolute (calibrated), they should not be shifted by arbitrary amounts within themselves to get the different curves to match. Supposedly, by virtue of being calibrated, they already do so.

In fact, you can take so-called "absolute data" (many times it is said to be but really isn't) and back out the unity distance correction if it was applied. The data set *can then be used as a relative data set*. This is done quite frequently since it is ***strongly*** recommended that only relative data sets be used when doing modeling.

Calibration is needed only for the sparse data sets anticipated from the Pan-STARRS and other surveys. In those cases, the observations will be made over many years and so the data need to be put on some sort of standard magnitude system.

Such calibration is sometimes required even during a single apparition. For example, if the asteroid has a long period, i.e., days or months. Getting the individual runs to align properly requires putting the data on a standard system, even if only internal. Again, once the entire data set is calibrated within itself, it is usually treated as a single relative set.

As you might gather from the above, a relative set of data has not formally been put on an internal or standard system. As often occurs with amateur (and even some professional work), data from several different nights are arbitrarily shifted to get a best fit. ***This is still relative data***, by virtue that the shifts are arbitrary. So, in general, amateurs are already providing the necessary lightcurve data required for modeling.

The ability to use relative data is what makes amateur work important and easy to incorporate within the planned efforts to use so-called sparse data sets generated by the large surveys to produce possibly thousands of shape and spin axis models in the first decade of the Pan-STARRS survey.

In short, the sparse data sets will generate good solutions in almost all cases. However, for refined solutions and to resolve unusual case (possible binary, etc.), dense lightcurves will be required. This is where the amateur community will fill in the gaps – by supplying just a few dense lightcurves of a given object. Of course, Pan-STARRS will reach much fainter than most amateurs, but there will still be more than enough work to occupy dozens observers for many years.

3. 4. Summary of Data Requirements

1. Lightcurves of sufficiently different geometries are required. (Which is why you can't get a good solution for a main-belt asteroid from one apparition since the viewing geometry is near the same for the whole apparition).

2. Lightcurves within the data set should cover a range of phase angles, including some at phase angles of >10° and, for an even better solution, >20°.

3. The range of geometries and phase angle coverage is more important than the density of the data set, though excessively sparse lightcurves may be a hindrance.

4. Removing nearly redundant curves (in date) or bad (too sparse, high noise) can help remove biases and is more expedient than trying to apply weighting to individual curves.

5. The synodic period must be known to a sufficient degree of precision. The smallest separation ΔP of local minima in the period parameter space is roughly given by

$$\Delta P \approx 0.5 \frac{P^2}{\Delta t}$$

where Δt is the full epoch range of the data set. This derives from the fact that the maxima and minima of a double-sinusoidal lightcurve for periods P and P ± ΔP are at the same epochs after Δt time.

The period and time span must be in the same units. The result is in those same units.

For a good solution, the initial period in the search should differ from the true sidereal period by no more than the ΔP given in the formula above. For example, assume the period is 6.0000 hr (0.25000 d) and that the observations span a range of five years, or about 1800 days. In this case, ΔP is about 0.0004 hr. If the span of data covers 30 years, about 11,000 days, then ΔP is about 0.000007 hr. If these levels of precision are not possible, then you should do a period scan based on the period_scan C or Delphi source code.

To put it in a nutshell, pole, period and the photometric convex hull of the object overwhelmingly dominate lightcurve morphology. Concavities and scatter properties are, in a way, comparable to noise: even thought changing them does change the lightcurves somewhat in the direct problem, the solution of the inverse problem does not change much since there are no notably different convex shapes that could model the lightcurves better. The well-posedness and stability of the inversion procedure is thus a result of the convex formulation.

3. 5. Regularization Weight and Albedo Variations

One of the input parameters for the model search is a weighting factor given to the "dark facet". This facet is added as an absolute lightcurve (regardless of the data being used) that forces the model to be convex. *It has no effect on the lightcurve of the resulting model*.

The initial modeling process generates a file that includes the area and XYZ coordinates of the normal to the area. For a good result, the area of the dark facet must be less than 1% of the total area. If the area is too large, increasing the weight factor should decrease the size of the dark facet. This is particularly true if the Z-component of the normal of the dark facet is large, i.e., the normal is generally pointing up or down.

However, if the dark facet area remains large with increased weighting and it's normal is closer to right angles to the spin axis than not, this means there very likely a real albedo feature on the asteroid – a particularly bright or dark spot . This is very rare but does happen. In this case, increasing the weight doesn't fix the area problem and worsens the fit.

In this regard, use the ChiSq value of the fit for the model in comparison to that from other models to find the best model.

4. Sources for Modeling Data

Unfortunately, there is no great repository of asteroid lightcurve data such as there is for astrometry with the Minor Planet Center. The closest thing right now is the Standard Asteroid Photometry Catalog (SAPC) developed by Torppa et al

http://www.astro.helsinki.fi/SAPC/index.jsp

The example below shows a typical data set found on the SAPC site. It's important to note several critical fields in the header before you adapt the data for use in a modeling program.

First is "LT CORRECTED." The core libraries require that the Julian Date for the data be light-time corrected. If the given data are not corrected, that correction must be applied before modeling begins.

Next is "ABS PHOTOMETRY." If this is True, then the data has been converted to a standard system, be it the typical Johnson-Cousins, or some internal system. While the core libraries can handle combined lightcurve sets that contain absolute and relative data, it's best to put treat them all as relative data. As noted in the previous section, a calibrated (absolute) data set is often treated as being relative. The

```
*****************************
OBJECT    : 2,  , Pallas
LIGHTCURVE       : 271
COLUMNS          : # Visual Error
LT CORRECTED     : false
ABS PHOTOMETRY   : false
*****************************
OBSERVING TIME   : 2441780.585081     (Sun Apr 08 04:02:31 EET 1973)
LOCATION  : E   5.71 +43.93 Observatoire de Haute-Provence, France
REFERENCE : Lustig and Hahn (1976)
INFORMATION      :
    UPDATE........: 0
    OBSERVING TIME: 1973 Apr  8.1
GEOMETRY:
   epoch  : 2441780.585081     (Sun Apr 08 04:02:31 EET 1973)
   Earth  : -0.949737225310019 -0.317430659536775 -1.99850829998031E-5
   object : -2.05435606514992 -1.32150929163441 1.07575905867397
ASPECT DATA      : 2.6691 1.8399 14.6 222.3 35.8 2441780.585081
DATA:
2441780.585081   8.192  0.0
2441780.586782   8.188  0.0
2441780.58853    8.182  0.0
2441780.590949   8.186  0.0
2441780.592373   8.189  0.0
```

Sample of Data from SAPC site

only disadvantage is that absolute data does allow fixing the "height" (Z-axis depth) of the asteroid while relative data does not, meaning a model using only relative data can find only the a/b ratio of the shape but not a/c or b/c.

Finally, there can be a "REDUCED" field. If not included, this implies the value is False. If the field is included and set to True, then the data have been set to unity distance by applying

$$-5 \log(Rr)$$

Where R is the asteroid's sun distance and r is the distance from Earth in AU.

If True, this correction must be removed if the data are being treated as relative and not absolute.

4. 1. Basic Data Requirements

In addition to the light-time corrected Julian Date and a magnitude, differential or "absolute" (not the same as absolute data), the input data files must contain the *asteroidcentric* XYZ ecliptic rectangular coordinates of the Sun and Earth.

Note that the Sun values are the negative of the heliocentric ecliptic coordinates of the asteroid. The Earth values are found by finding the vector sum of those coordinates and the geocentric ecliptic XYZ coordinates of the asteroid. The MPO LCInvert program computes these values and places them in the input data files automatically.

The free source code includes properly formatted sample files. The included documentation covers these requirements in more detail as well as provides a tutorial for preparing the data for LCInvert. The beginning part of that tutorial can be applied when creating data files for a different modeling program.

5. The Modeling Process

Once the data have been prepared, the modeling process begins. Even on today's fast desktop computers, do not expect to have instantaneous results. In some cases, it can take several hours for a single step within the process. However, the end result is what matters and doing it by hand is not an option.

5. 1. Finding the Period

As noted in Section 2, you must know the synodic rotation period of the asteroid to a very high degree of precision. Using a low precision period or one that's entirely wrong is a complete waste of computer time and, save only with "Lottery-Winning Luck", will produce completely wrong results.

The open source code contains a file that does the period search using the same data that you use for the initial modeling stage. It helps to have a good estimate of the period from other sources, such as Fourier analysis on the data set or previously published work. Note again that any of these sources must be both accurate and precise.

If using Fourier analysis on multiple lightcurves over several apparitions, remember that the synodic rate can change during a single apparition. Break the lightcurves into sets of about the same date and find as precise of periods as possible for each set. Use the average of those periods as the center point of your search and the spread of the values to dictate the range of periods to be searched.

5. 2. Finding the Gaussian Shape Areas

The initial step of the modeling process starts with a near sphere cut into a number of rows with so many facets per row. The first step of the modeling process converts those facets from their original size and orientation to a set of areas and outward normals that duplicate the lightcurve data. Two forms of scattering are included in the modeling.

Several initial conditions must be set before stating this phase of modeling. This includes an initial estimate of the ecliptic longitude and latitude of the pole as well as the period. The last can be taken from the period search or other sources. If previous work has been published for the asteroid being studied, the longitude and latitude can be taken from there as well.

However, it may be a good idea to search for alternate solutions, especially if the inclination of the asteroid orbit is small, i.e., it is nearly on the same plane as the ecliptic. In this case, there can be an ambiguity in the solution where the true longitude is about 180° from the one found.

Quick mention will be made of one parameter, that is the size of the "dark area" that is required to assure that the final shape is a closed convex hull. See "Regularization Weight and Albedo Variations" above for a discussion about this value. It is critical to being able to find a proper model.

The others parameters will not be discussed in detail here. Instead, the reader is referred to the documentation included in the open source code libraries.

The MPO LCInvert program allows searching a grid of 15 possible longitude/latitude combinations and reports the ChiSq and area of the dark area. A grouping of the derived pole solution along with lowest ChiSq values gives a good sense of the quality of the solution. It would be a good idea for any modeling program to include such a grid search, especially for those times when there are no previously reported pole solutions available.

This process takes the least amount of time of all the steps with, usually, about 50 iteration steps being used. Sometime a higher value, e.g., 100, will provide a better model, but – of course – doing so extends the time to complete this step.

Naturally, if a grid search of pole solutions is implemented, then the time for this step is increased considerably. However, if such a search means finding a highly probable solution for final modeling, the extra time for this step is worth it.

5. 3. The Minkowski Reduction

The previous step does not define a closed convex hull, only a set of areas and their directions. These must be put together, like a jigsaw puzzle, into a final closed form that fits the lightcurve data. This is done using the Minkowski source code file and can take a considerable amount of time. This is actually a very elegant process (only a mathematician would say that) and the reader is encouraged to read the two 2001 Kaasalainen papers to learn more about it.

The Minkowski method generates a file that contains two sets of data: the XYZ coordinates of the vertices of the set of polygons that form the final shape and the indices for the vertices that form each of the shapes.

Many 3-D modeling programs cannot handle polygonal shapes for creating a 3-D model but can use triangles. A simple routine in the source code libraries splits the Minkowski polygons into a, usually, larger number of triangles. These can then be used for 3-D rendering.

6. Modeling Results

The first attempts at modeling were to duplicate previously published work by Kaasalainen and others. Many subtleties were learned and some not so small mistakes made. However, there is no better teacher than experience and it was extremely gratifying to get the same results – eventually.

6. 1. 2 Pallas

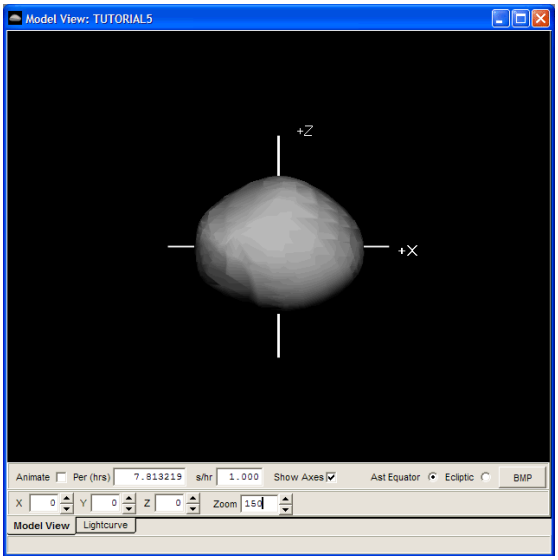

Figure 4. A model for 2 Pallas generated with LCInvert.

Torppa et al (2003) used data from the SAPC web site to determine the pole and shape for the second largest main-belt asteroid (or largest if Ceres is the only dwarf planet in the main belt and so not part of the group of small solar system bodies that includes asteroids). Their findings were:

```
Pole (long): 35°
Pole (lat): -12°
Period: 7.813225 hr
```

Using the same data set, my results were:

```
Pole (long): 35.3
Pole (lat): -15.2
Period: 7.81321904
```

Given its size, the asteroid is, as expected, somewhat spherical in shape.

6. 2. 43 Ariadne

Kaasalainen et al (2002) used data from the Uppsala Catalog (available via the SAPC site) to determine its model. Their data is part of the open source code distribution so it would be natural that my findings matched theirs. It was good to have that control since not matching the model when developing the open source Delphi code was an indication that something had been lost in translation.

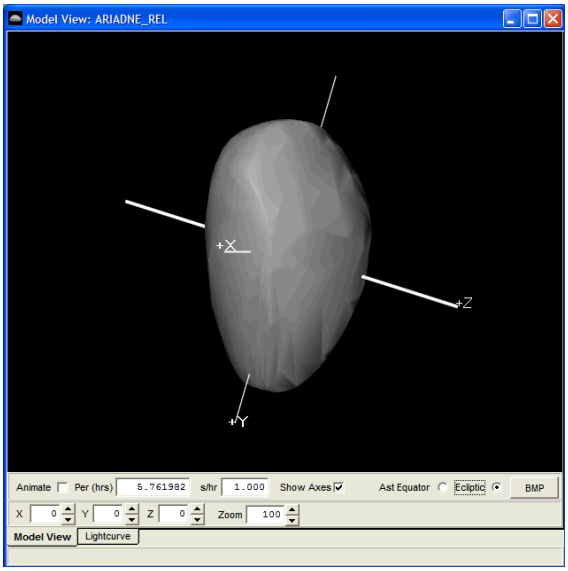

Figure 5. The model for 43 Ariadne as generated by LCInvert. The view is from the plane of the ecliptic looking towards the center of the asteroid. The sun is behind the observer.

Figure 5 shows the model as seen on the plane of the ecliptic. This shows the true orientation of the spin axis and the sense of rotation, which is always counter clockwise as viewed from above the north pole. Figure 7 shows the view from above the asteroid's equator at local noon at its "prime meridian."

```
Pole (long/l253°
Pole (lat): -15°
Period: 5.761986 hr
```

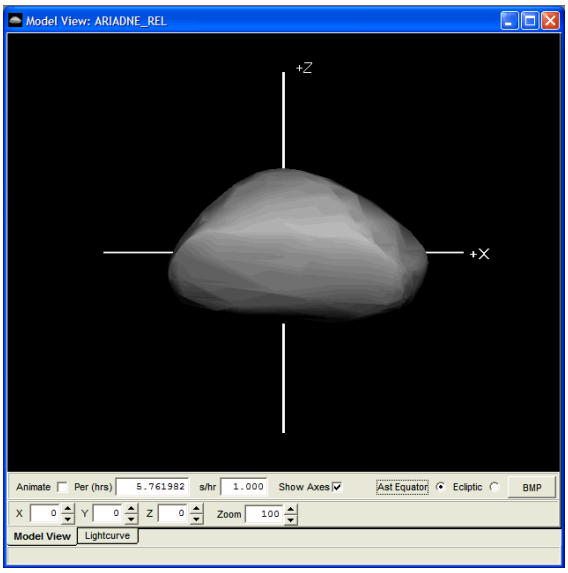

Figure 6. The model for 43 Ariadne as generated by LCInvert. The view is from above the subsolar point on the asteroid's equator at 0° rotation ("prime meridian").

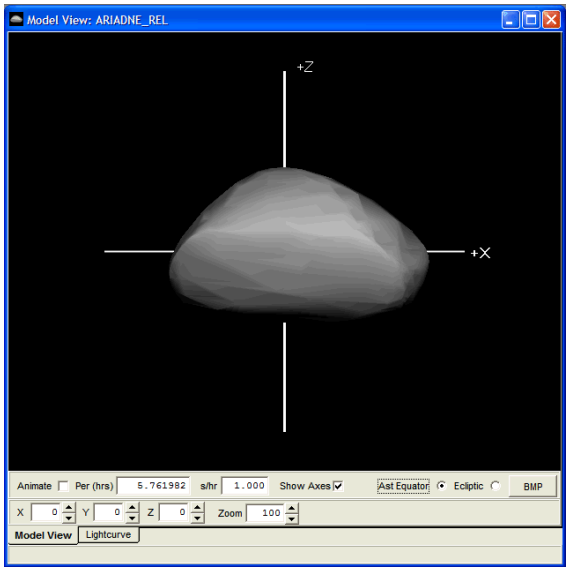

Figure 7. The model for 43 Ariadne as generated by LCInvert. The view is from above the subsolar point on the asteroid's equator at 0° rotation ("prime meridian").

7. 1600 Vyssotsky

Once two known models were re-created, the next test was to work with data on an asteroid that was not previously modeled. This turned out to be the Hungaria asteroid, 1600 Vyssotsky. Lightcurves covering three apparitions were obtained by the author and other observers (Warner 1999, Warner 2006).

The viewing aspects were significantly different in one apparition, which led to hopes that a good model could be obtained. Unfortunately, that was not the case. The ChiSq values for the various solutions did not show a clear-cut solution. This was supported by the fact that the 15-position grid search did not show any substantial grouping of pole solutions.

The two best models (lowest ChiSq) had the following solutions:

Longitude: 113.7
Latitude: +14.5
Sidereal Period: 3.19997896

Shown in Figure 8

Longitude: 272.6
Latitude: –46.9
Sidereal Period: 3.19997909

Shown in Figure 9. The two periods are essentially identical but the pole solutions are dramatically different.

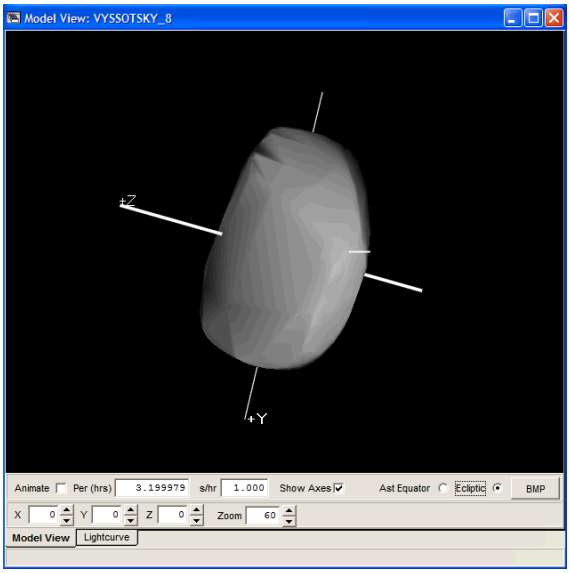

Figure 8. A model for 1600 Vyssotksy using the ecliptic view, which is from the plane of the ecliptic looking towards the center of the asteroid. The sun is behind the observer.

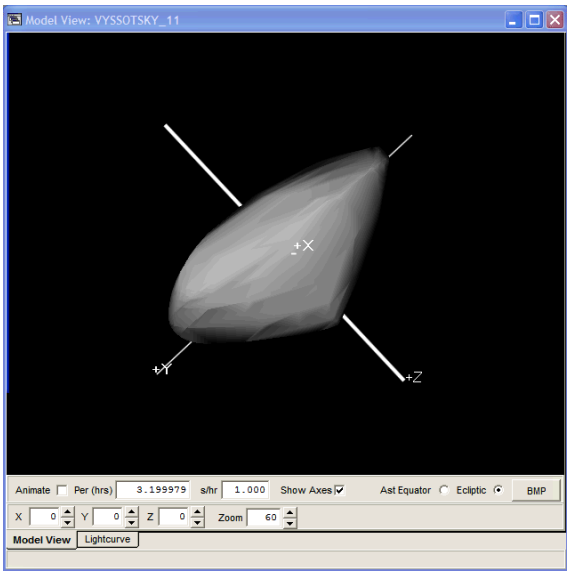

Figure 9. An alternate model for 1600 Vyssotsky. There were insufficient data to find a consistent model.

One way to check the solution is to fit a lightcurve from the model to the actual data. Figure 10 shows such a comparison. As you can see, the actual and theoretical curves fit very well. However, this alone does not mean that the correct model was found.

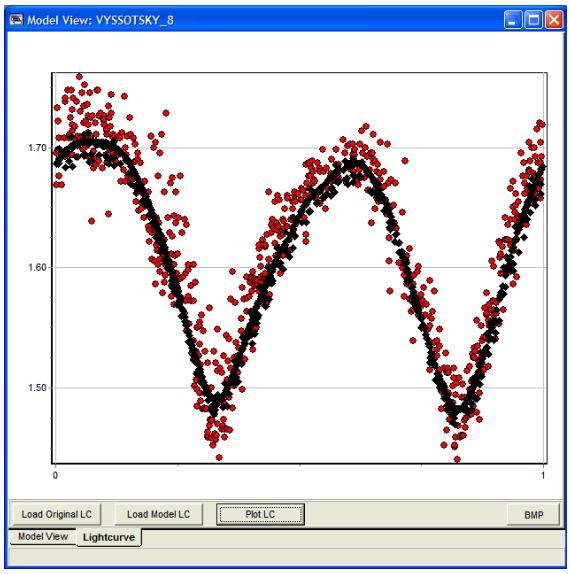

Figure 10. Comparing the model lightcurve to the original data. The red dots represent the original data while the black dots represent the model. The November 2005 data produced nearly identical comparison plots with the theoretical model.

Both models shown above produced nearly identical comparison plots. The ChiSq value for neither model was significantly different from the other. This is the better test, i.e., that one model have a ChiSq solution that is at least 10-20% better than any other solution.

8. Conclusion

While working asteroid lightcurve inversions is not a simple process and yields "bad" results more often than good results, it is no longer strictly for professional astronomers. There are many asteroids wanting only another apparition or two before a model can be found. Amateurs have access to most of the data available, and so they are not shut out from this important field of research.

Furthermore, with the large surveys such as Pan-STARRS coming on line, the work for amateurs will be even more important. It is they who can provide the dense lightcurves, concentrated data runs that are used in conjunction with the sparse data sets provided by the surveys that will produce the best possible results. The sparse data sets can find good models for thousands of objects but they cannot resolve questionable results. That will be the role of the amateur.

The large surveys may be limited in how bright they can go, leaving open for those with more modest equipment, still hundreds of asteroids where amateur work can dominate.

The collection of data is vital to the advancement of asteroid research. However, analysis is just as important and, for many, provides the extra incentive that compensates for the sometimes drudgery of taking and measuring images. Being able to participate fully in both sides of scientific endeavor allows the amateur to become not just a participant but a significant and vital collaborator.

9. Acknowledgements

My thanks go to Mikko Kaasalainen and Josef Durech for their extensive help with converting the core inversion libraries and understanding as much as I could of the lightcurve inversion process.

Funding for work at the Palmer Divide Observatory was provided by NASA grants NNG06GI32G and NNX06AB30G, National Science Foundation grant AST-0607505, and by a 2007 Gene Shoemaker NEO Grant from the Planetary Society.

10. References

Burns, J.A., Tedesco, E.F. (1979) "Asteroid Lightcurves: Results for Rotations and Shapes" in *Asteroids*, ed. Gehrels T. pp. 494-527. University of Arizona Press.

Cunningham, C. (1998) "Shapes" in *Introduction to Asteroids*, pp. 77-82. Willmann-Bell.

Kaasalainen, J., Torppa, J. (2001) "Optimization Methods for Asteroid Lightcurve Inversion: I. Shape Determination". *Icarus* **153**, 24-36.

Kaasalainen, J., Torppa, J., Muinonen, K. (2001) "Optimization Methods for Asteroid Lightcurve Inversion: II. The Complete Inverse Problem". *Icarus* **153**, 37-51.

Kaasalainen, M., Mottola, S. Fulchignoni, M. (2002) "Asteroid Models from Disk-integrated Data" in Asteroids III, ed. Bottke, W.F., Cellino, A., Paollicchi, P., Binzel, R. pp. 139-150. University of Arizona Press.

Kaasalainen, M., Durech, J., Warner, B.D., Krugly, Y.N., Gaftonyuk, N.M. (2007) "Acceleration of the Rotation of Asteroid 1862 Apollo by Radiation Torques. *Nature* DOI:10.1038/nature05614.

Kaasalainen, M., http://www.rni.helsinki.fi/~mjk/asteroids.html (see the FAQ and the numerous references).

Lowry, S.C., Fitzsimmons, A., Pravec, P., Vokrouhlicky, D., Boehnhardt, H., Taylor, P.A., Galád, A., Irwin, M., Irwin, J., Kusnirák, P. (2007) "Direct Detection of the Asteroidal YORP Effect". *Science* DOI: 10.1126/science.1139040.

Magnusson, P., Barucci, M.A., Drummond, J.D., Lumme, K., Ostro, S.J., Surdej, J., Taylor, R.C., Zappala, V. (1989) "Determination of Pole Orientations and Shapes of Asteroids" in Asteroids II, ed. Binzel, R., Gehrels, T., Matthews, M.S. pp. 66-97. 1989. University of Arizona Press.

Russell, H.N. (1906) "On the light-variations of Asteroids and Satellites", *Astronomy and Astrophysics* **149**, 186-194.

Slivan, S.M., Binzel, R.P., Crespo da Silva, L.D., Kaasalainen, M., Lyndaker, M.M., Krčo, M. (2003) "Spin vectors in the Koronis Family: Comprehensive Results from Two Independent Analyses of 213 Rotation Lightcurves". *Icarus* **162**, 285-307.

Taylor, R.C., (1979) "Pole Orientations of Asteroids" in *Asteroids*, ed. Gehrels, T. pp 480-493. University of Arizona Press.

Torppa, J., Kaasalainen, M., Michalowski, T., Kwiatkowski, T., Kryszczynska, A., Denchev, P., Kowalski, R. (2003) "Shapes and Rotational Properties of Thirty Asteroids from Photometric Data", *Icarus* **164**, 346-383.

Warner, B.D. (1999) *Minor Planet Bull.* **26**, 31-33.

Warner, B.D., Pray, D.P., Dyvig, R., Reddy, V. (2006) *Minor Planet Bull.* **33**, 45-46.

Variable Star Photometry at West Challow Observatory

David Boyd
BAAVSS and CBA Oxford
5 Silver Lane, West Challow, Wantage, OX12 9TX, UK
drsboyd@dsl.pipex.com

Abstract

This paper describes the facilities and observing programme of a small personal observatory set up in the UK for CCD photometry of variable stars. Its development has been driven by the belief that committed amateurs can make a valuable scientific contribution to the study of variable stars. Observing projects carried out at WCO are described including examples of Pro-Am collaboration and contributions to the observing programmes of the BAAVSS, AAVSO and CBA.

1. Introduction

As someone with a scientific background, I have always been interested in the potential of amateur astronomers to make scientifically useful contributions to the subject. The availability of affordable CCD cameras coupled with computer controlled telescopes offered me the opportunity I had been looking for. After investigating various possible areas I finally settled on measuring variable stars.

I live in the centre of southern England in a region called the Vale of the White Horse. It is named after a Bronze Age stylised representation of a horse, about 375 feet long, carved into the chalk on a nearby hillside some 3000 years ago, no one really knows why. The countryside is a shallow basin formed over millennia by the River Thames which flows through the Vale. The climate is generally mild, it rarely goes below –5C, and the weather is consistently variable. My observing log shows that during 2005 I recorded usable images on 115 nights, while in 2006 the figure was 96 nights.

2. Equipment

West Challow Observatory, named after my small village of about 50 houses which is listed in the Doomsday Book of 1086AD, was originally established in 1998 after many years of using portable telescopes for purely visual observing. It has been equipped in turn with a 0.06-m refractor, 0.1-m and 0.25-m Newtonian reflectors and now a 0.35-m SCT, all on pier-mounted GEMs and housed in a simple run-off shed. The 0.35-m is equipped with a JMI remote-controlled focuser, an Optec 2x focal reducer, a True Technology filter wheel with Schuler BVI and Clear filters, and a dew heater (Figure 1).

Figure 1: 0.35-m SCT with SXV-H9 CCD camera

I use Starlight Xpress cameras, originally a HX 516 and now a SXV-H9. They have the useful characteristic of extremely low and virtually exposure-independent dark current. The SXV-H9 camera is normally used in 2x2 binned mode which gives a field of about 16x12 arcmin and a pixel size of 1.4 arcsec/pixel. Seeing at the site is typically in the range 3-5 arcsec FWHM. All cables run underground into a small hut which is the observatory 'control room' containing power supplies, computer, etc. The mount is controlled using Guide and the camera and filter wheel with AstroArt. Focusing is controlled manually and regularly monitored during a long run to correct for thermally induced changes in the position of the focal point. Flat fielding is carried out using a white screen

illuminated with a fluorescent lamp and imaged through a translucent sheet. Comparisons with sky flats indicate that the differences are acceptably small (resulting magnitude differences are <0.005).

3. Data analysis

When I started I found analysing time-series of images manually a real chore. A conversation with Richard Berry at the British Astronomical Association (BAA) Winchester conference in 2000 brought relief, AIP4WIN was about to be launched. It would be hard to underestimate the empowerment this software has brought to amateur CCD photometrists at modest cost. However it also created another problem: how to use the output files of measurements which it produced. I started developing an Excel spreadsheet for this which eventually grew into a family of tools for analysing both filtered and unfiltered observations, including transformations where appropriate, and for calculating differential magnitudes with as realistic an estimate of the error as possible. This was later extended by Andy Wilson, an experienced VB programmer, to include macros which made it more user friendly. It has been widely distributed and used within the BAA Variable Star Section (BAAVSS) [2].

With the advent of AIP4WIN v2 [1], and the possibility of easily measuring multiple comparison stars, I re-engineered the spreadsheets to implement a version of weighted ensemble photometry. The methodology for doing this is the subject of a poster paper at the symposium. This revised spreadsheet has also been enhanced by Andy and distributed to users running AIP4WIN v2.

Besides calculating magnitudes and errors, the spreadsheet produces several plots (Figure 2). These show the derived magnitudes and errors for the variable and each of the comparison stars and also the behaviour of the mean image zero point and its error during the run, a good way of spotting changing conditions and problem images. Variation of a comparison star by only a few hundredths of a magnitude is usually apparent enabling it to be eliminated from the ensemble. The spreadsheet also generates the output formats required by the BAAVSS, the American Association of Variable Star Observers (AAVSO) [3] and the Centre for Backyard Astrophysics (CBA) [4].

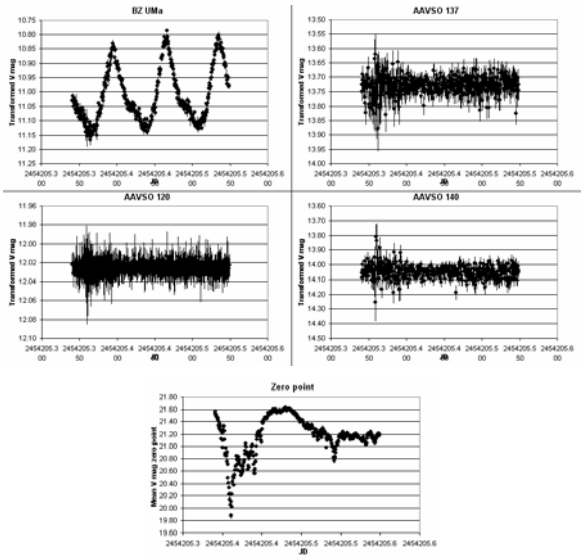

Figure 2: Variable and comparison light curves and image zero point plot

As a general rule, I carry out at least a preliminary analysis of all my observing runs as they progress to ensure that everything is working properly, that focus is being maintained, and to check what the variable is doing. It is quite exciting to think you might be the first person ever to see superhumps in the light curve of a particular dwarf nova. For a few minutes, until you email your discovery to others in the community, you are the only person in the world who knows the true nature of that star.

4. The Learning Curve

Developing the necessary skills in CCD photometry has been a gradual learning process. Understanding calibration and filter transformations, and developing consistency in operating equipment and analysing data, eventually builds confidence that the variations you see are intrinsic to the object being observed, subject of course to the inherent limitations of your equipment, the observing conditions and statistical uncertainty. Under reasonable conditions with an unfiltered 60 sec exposure I find I can measure mag 14.5 stars with SNR ~100, mag 16 with SNR ~50 and mag 17 with SNR ~20. A V-filter reduces these figures by around 1 to 1.5 mags. I have tried to capture my experiences in climbing this learning curve in a Beginners' Guide to Measuring Variable Stars which is published by the BAAVSS [5].

Once you are regularly submitting observations to one of the international variable star databases, the logical next step is to consider publishing an analysis of your results. This is a good way to teach yourself

about the current state of variable star research since you have to present your results within the context of existing knowledge and previous published work. I have also found it a good way of developing working relationships with other observers since combining the results of several observers will almost always produce a better and more complete analysis.

5. Observing Programme

The observing programmes of the BAAVSS, AAVSO and CBA offer a wide variety of observing challenges sufficient to exercise the skills of any observer. Like all beginners I dabbled in various ventures but have gradually migrated towards generating time-series light curves for various purposes including planned collaborative research programmes and observing targets of opportunity. The ability to switch immediately to observing a new target such as a just-announced outbursting CV without reference to a telescope allocation panel is one of the benefits of being an amateur astronomer.

In the remainder of this paper I will briefly mention five areas in which I have been active recently:

1) monitoring ephemerides of eclipsing SW Sex stars;
2) measuring periods in outbursting dwarf novae;
3) following the decline of novae;
4) discovering new variable stars;
5) developing comparison star sequences.

6. Monitoring Ephemerides of Eclipsing SW Sex Stars

Among the CVs found by the Hamburg Quasar Survey team are several SW Sex variables, some of which are eclipsing [6]. It is now some time since the ephemerides of these stars were first measured. In the course of writing a new paper on them, the team wanted to check whether the original ephemerides were still accurate. At the request of Dr Boris Gaensicke at Warwick University, I measured eclipse timings and compared them with predictions to see whether there was a discrepancy. These observations were made unfiltered to maximise signal-to-noise in the light curve.

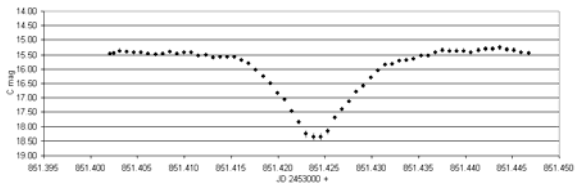

Figure 3: Eclipse light curve for HS 0728+6738

Figure 3 shows a typical eclipse light curve from which the time of minimum is extracted by a quadratic analysis, if necessary corrected for asymmetry in the shape of the eclipse. A heliocentric correction is then applied to the observed time. In most cases the time of minimum could be determined with a precision better than 20 sec.

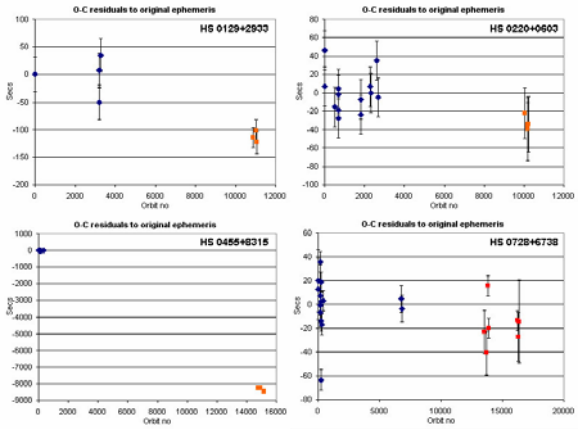

Figure 4: O-C diagrams for 4 eclipsing SW Sex stars

Figure 4 shows O-C (observed minus calculated) diagrams of the difference between the observed and predicted times of eclipse for four of these variables. The data points to the left of centre are those used to determine the original ephemerides, those to the right are my measurements. It was clear that in all these cases the published ephemeris needed to be revised, in most cases by a small amount but in one case substantially. The updated values are included in a paper currently being published [7]. This project is continuing and being expanded to check the ephemerides of a larger set of eclipsing SW Sex variables. It appears that many of those will need to be updated. In the longer term, we will also be looking for any departure from a linear ephemeris in these stars, as has been seen for example in OY Car.

7. Measuring Periods in Outbursting UGSU Dwarf Novae

The Sloan Digital Sky Survey has also been a fruitful source of new CVs. Many of these are faint in quiescence (~18th mag) but outbursts of eclipsing systems, when they occur, provide an opportunity to refine their orbital periods. An example of this is SDSS J170213.26+322954.1, for which the first photometry was obtained by Arne Henden at the USNO Flagstaff Station in 2003. At that time the orbital period was determined to be ~2.5 hrs. During its first observed outburst in 2005, by measuring the times of 13 eclipses and combining these with

Henden's original observations, Arto Oksanen and I were able to refine the orbital period to a precision of about 1 msec. We also detected superhumps and measured their period and so were able to calculate ε, the superhump period excess for this system [8]. There are various published empirical relationships between ε and q, the mass ratio of the binary, which then enable q to be estimated.

It is always exciting to make the first observation of superhumps in the light curve of a CV in outburst as this confirms its UGSU classification. During the past year I have been fortunate to observe superhumps for the first time in V1316 Cyg, V337 Cyg, Var Cam 06 and SDSSp J082409.73+493124.4. The June 2006 superoutburst of V1316 Cyg was particularly well observed by the CBA community and a comprehensive report on this will shortly be published. Figure 5 shows the first observation of superhumps in V1316 Cyg.

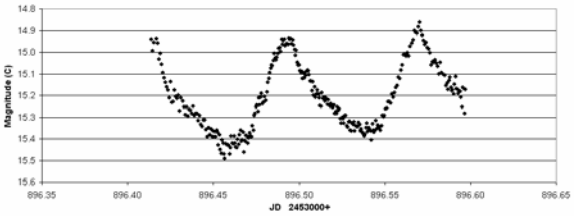

Figure 5: Superhumps in V1316 Cyg on 2006 June 9

By combining data from several observers it may be possible to measure the periods of both common superhumps, which occur in the early stage of an outburst, and late superhumps, which have a slightly shorter period and usually follow a change in phase of the superhump signal. Tonny Vanmunster's period analysis software Peranso [9] has been invaluable in enabling these analyses. It is the accessibility of software such as this, previously only available in professional astronomical software suites, which has empowered today's amateur astronomers to be able to make scientifically useful contributions.

An interesting recent observation was obtained during the first and long-awaited superoutburst of the dwarf nova BZ UMa in April 2007. At the peak of the outburst on 14 April, when the superhump amplitude was greatest at ~0.3 mag, the V–Ic colour index apparently varied in phase with the superhumps in V and Ic with amplitude ~0.02 mag becoming bluer at the superhump peaks and redder in the troughs. The superhump period in V on that day was 0.0702+/-0.0008d. Figure 6 shows light curves in V, Ic and V–Ic. At the time of writing, analysis of the data from this superoutburst continues.

An additional benefit of performing long time-series runs is the ability to use them to analyse the flickering behaviour of CVs. This stochastic process is believed to be associated with irregularity in the transfer of material either into or out of the accretion disc. The scalegram analysis technique described by Fritz and Bruch [10] has been applied to my data for several CVs by Chris Lloyd of the Open University. The slope and height parameters α and Σ which characterise the flickering behaviour of a CV can be determined from the scalegram. When plotted in α – Σ space, different types of CV tend to fall into distinct clusters, thus providing an additional clue to the nature of an unclassified CV. Figure 7 shows a scalegram containing several time-series runs on V1363 Cyg (sloping lines) together with a comparison star from the same images (horizontal lines). The positive slope of the lines for V1363 Cyg indicates that it generates more flickering power at longer rather than shorter timescales.

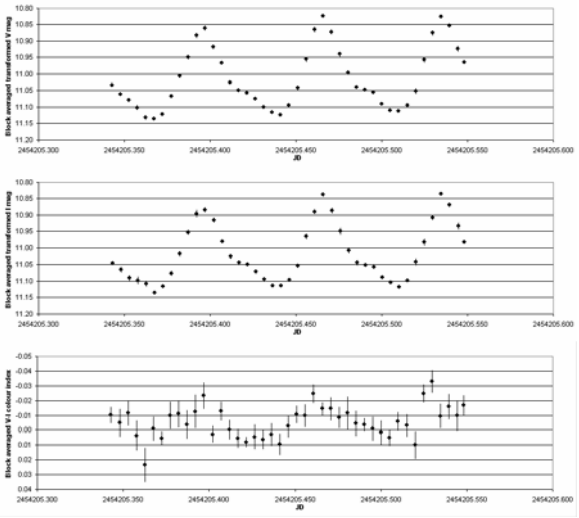

Figure 6: Light curves in V, Ic and V–Ic for BZ UMa on 2007 April 14 (each data point is an average of 10 measurements, 2 cycles are shown)

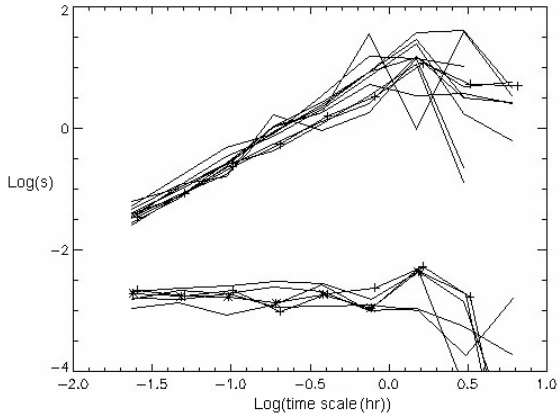

Figure 7: Scalegram for V1363 Cyg (upper lines) and a comparison star (lower lines)

8. Following the Decline of Novae

It is both interesting and useful to follow the decline of novae as every one is different and often they do unexpected things. A recent example is V2362 Cyg which peaked around mag 8 in April 2006 then declined rapidly for 3 months before rising and declining again. 12 months later, it remains 5 magnitudes brighter than its expected quiescent level. Nova experts are still debating what might be going on in this system. Using filters to observe at more than one wavelength, it is possible to detect colour changes which indicate physical processes such as the emission of dust.

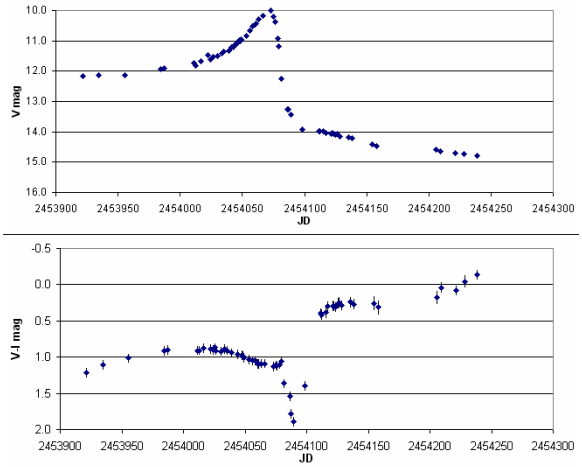

Figure 8: V light curve and V–Ic colour index for V2362 Cyg

Figure 8 shows my measurements of the V magnitude and V–Ic colour index of the nova since June 2006. Magnitudes have been corrected to account for the nearby mag 15 star which is also included within the photometry aperture. There was an emission of dust in early December (JD ~2454075) which produced a rapid fading and a temporary reddening in the colour index.

9. Discovering New Variable Stars

It is not unusual to find that comparison stars in a variable chart originally developed for visual use are actually variable at the level of a few hundredths of a magnitude. One advantage of using several comparison stars is that this low level variation may be recognised and the variable comparison star not used if high accuracy is required.

One example I found in 2005 was GSC 3132-1448 in Lyra (RA 19h 06m 46.60s, Dec +44° 01′ 46.30″, J2000) which is the star marked 131 in the AAVSO chart for MV Lyr. This appears to be an eclipsing binary of magnitude 13.1V with a primary eclipse depth of ~0.2 mag and the intriguing (and rather frustrating) period of 7 days +/- 1 min (Figure 9). Tom Krajci and Bart Staels have helped me put this light curve together. Efforts to confirm its nature by getting observations of the secondary eclipse continue.

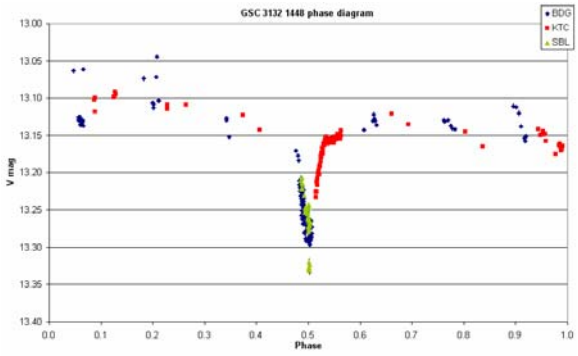

Figure 9: Phase diagram for GSC 3132-1448

Another is the star TYC 3181-1907 in Cygnus (RA 21h 11m 44.99s, Dec +44° 45' 30.4", J2000) which has been marked as a comparison star in some charts for the nova V2362 Cyg. I obtained several long runs on this star over a 6 month period while looking (unsuccessfully) for periodicity in the nova. Its mean magnitude is 11.63V and its V-Ic colour index is 0.46. Arne Henden had also collected about 250 measurements of the same star which he kindly gave me. Period analysis of all of this data shows that it has a full amplitude of ~0.08 mag and a likely period of 2.92 days. Figure 10 shows a phase diagram assuming this period.

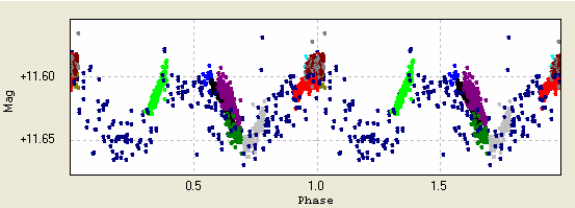

Figure 10: Phase diagram for TYC 3181-1907

10. Developing Comparison Star Sequences

Improving existing charts and developing comparison star sequences for new variables is an important and ongoing task. Observers with filters who are able to transform their results to the standard Johnson-Cousins photometric system can contribute to this work. As conditions in the UK are rarely suitable for all-sky photometry, I have used Hipparcos stars whose derived Johnson V magnitudes are accurate to around 0.01 mag to define zero-points in V [11]. This is good enough to produce charts for visual use. As this activity usually involves comparing measurements with other experienced observers, it is a good way to build confidence in your observing technique and to fine tune your analysis procedures.

11. Conclusion

Developing the necessary skills and observing procedures to measure variable stars using CCD photometry is a very enjoyable but quite demanding challenge. The more you learn, the more you realise there is to learn. However, well motivated amateurs prepared to invest the effort can contribute much to the science of variable stars and derive great satisfaction in the process.

12. Acknowledgements

I gratefully acknowledge the support and encouragement of many colleagues, too numerous to mention individually, in all of the organisations mentioned in the paper. Without their willingness to share their experience, I would have taken much longer to climb the learning curve. My thanks are due also to several professional astronomers including Boris Gaensicke, Chris Lloyd and Arne Henden who have taken time to point me in useful directions and provide invaluable advice.

I am grateful to the Royal Astronomical Society for the award of an RAS Grant which has supported my participation in the Symposium and to the British Astronomical Association for a Ridley Grant which assisted development of my observing equipment.

13. References

[1] Berry R. & Burnell J., The Handbook of Astronomical Image Processing, 2nd Edition, Willmann-Bell (2005)

[2] BAAVSS, http://www.britastro.org/vss/

[3] AAVSO, http://aavso.org/

[4] CBA, http://cba.phys.columbia.edu/

[5] Boyd D., Ed., Measuring Variable Stars Using a CCD Camera: A Beginner's Guide, ISBN 0-902749-17-X, BAAVSS (2005)

[6] Hamburg Quasar Survey, http://deneb.astro.warwick.ac.uk/phsdaj/HQS_Public/HQS_Public.html

[7] Rodriguez-Gil P., Gaensicke B. T., Hagen H.-J., Araujo-Betancor S., Aungwerojwit A., Allende Prieto C., Boyd D., Casares J., Engels D., Giannakis O., Harlaftis E. T., Kube J., Lehto H., Martinez-Pais I. G., Schwarz R., Skidmore W., Staude A., Torres M. A. P., SW Sextantis stars: the dominant population of CVs with orbital periods between 3-4 hours, Mon. Not. R. Astron. Soc., 377, 1747 (2007)

[8] Boyd D., Oksanen A., Henden A., Measuring the orbital and superhump periods of the eclipsing cataclysmic variable SDSS J170213.26+322954.1, J. Br. Astron. Assoc., 116, 4, 187 (2006)

[9] Vanmunster T., PERANSO, http://www.peranso.com

[10 Fritz T., Bruch A., Studies of flickering in cataclysmic variables: IV Wavelet transforms of flickering light curves, Astron. Astrophys., 332, 586 (1998)

[11] Miles R., Asteroid Phase Curves: New Opportunities for Amateur Observers, Proceedings of SAS Symposium (2005)

Selective Availability of Astronomical Data

P. R. McCullough
Space Telescope Science Institute
3700 San Martin Dr., Baltimore MD 21218
pmcc@stsci.edu

Abstract

We discuss potential advantages and disadvantages of selective availability of astronomical data. Selective availability would enable prompt dissemination of data to the community at large by maintaining the proprietary nature of only selective characteristics of the data to only a select set of persons. For the purpose of illustration, we present a simplistic example of an algorithm that modifies a two-dimensional image such that it corrupts stellar photometry of specific (bright) stars while preserving other characteristics such as stellar astrometry. We advocate that the astronomical community already could benefit from selective availability, and we suggest that the need will increase in time as ever-larger volumes of data are collected but not disseminated in a timely fashion for lack of appropriate algorithms to create selective availability.

1. Introduction

The term "selective availability" (SA) refers to the intentional masking of certain characteristics of data to be made publicly available while retaining those characteristics for authorized users, typically by some form of encryption. For example, in the U.S. global positioning system (GPS), pseudo-random deviations were introduced into the satellite signals to reduce the accuracy of positions on Earth, i.e. longitude and latitude, available to those users that lack the knowledge of the pseudo-random deviates. The SA for the U.S. GPS system was de-activated on May 1, 2000, because the advantages of doing so outweighed the disadvantages.

(http://www.ngs.noaa.gov/FGCS/info/sans_SA/)

Civilian users of GPS would benefit by the ~10-times better precision of positions without SA compared to with SA, while the US could still deny GPS on a regional basis as necessary for national security using alternatives to SA.

In this paper, we introduce "Alice" as an astronomer with rights to data in its original full-fidelity form (hereafter, O-data), and "Bob" as another astronomer who wishes to have access to the O-data in some form (hereafter, SA-data) that is useful to him and agreeable to Alice. The SA concept we propose here enables Bob's access; otherwise, Bob would have access only at Alice's discretion or alternatively he could wait until Alice's proprietary period expires. Selective availability generally is not applied to astronomical data; typical practice is described in this paragraph. Availability is accomplished with a single bit: either a person has access to data in all its intrinsic fidelity, or the person does not have access to the data at all. The bit is active for a so-called proprietary period, which begins when the data are obtained and extends for a period of time specified in the observing proposal. The nominal proprietary period is 18 months, which allows an investigator to analyze the data and potentially obtain additional data in a second observing season, if necessary, prior to publication.

The proprietary period can be longer or shorter than its nominal value, depending on circumstances. For example, data may be collected over an extended period of time to enable the intended science goals. For example, NASA's Kepler mission requires at least three years of observing to confirm multiple transits of extrasolar Earths, so its investigators may justifiably request to retain their proprietary rights for at least that duration. As another example, spectra obtained at the Keck observatory for the purpose of radial-velocity detection of extrasolar planets have been archived in a form where the section of the spectra with iodine absorption lines (used as radial velocity fiducials) has a longer proprietary period than the rest of the spectra, in order to allow the principal investigators time to see oscillations in the radial velocities associated with planets that can have many-year periods (Beichman p.c.; see also http://www2.keck.hawaii.edu/koa/public/koa.php).

The XO Project, and others like it, aim to discover transiting planets via photometric monitoring of hundreds of thousands of stars and have accumulated multiple terapixel sets of images of significant fractions of the sky that could be useful for a number

of other fields of astronomy (McCullough et al. 2006 and references therein). However, only a small fraction of those images have been released to the public domain, because the teams that have labored to produce the data continue to analyze them to find additional transiting planets. At the other extreme, data have no proprietary period; for example, observing time with major observatories that is awarded via Director's discretion traditionally is afforded zero proprietary period – the Hubble Deep Field and the Ultra Deep Field are examples.

If "Alice" could apply a SA algorithm that would corrupt all stellar photometry by 3% rms, she could be confident that releasing the data in that form would retain to herself the ability to detect planetary transits which typically are less than 2% in depth. Another astronomer, "Bob" could use the XO data in its SA-form for other purposes, such as studying larger-amplitude variable stars, detecting moving objects such as near-earth asteroids or comets, studying diffuse objects such as galaxies, zodiacal light, or artificial light pollution, or studying rare transients such as optical counter parts to gamma-ray bursts (e.g. Paczynski 2006).

For the purpose of illustration, we present a simplistic example of an algorithm that modifies a two-dimensional image such that it corrupts stellar photometry of specific (bright) stars while preserving other characteristics such as stellar astrometry. Trivial algorithms for SA of tabular data can be effective also.

2. Lossy Compression as a SA Algorithm

The desirable property of lossy compression (e.g. HCOMPRESS, White, Postman, & Lattanzi 1992) usually is the reduction in file size in bytes for a given image size in pixels. For a typical image from the XO survey, HCOMPRESS increases noise by 0 (i.e. lossless compression), 0.5, and 1.6 millimag rms for aperture photometry with a radius of 3 pixels of bright stars at corresponding file-size compression factors of 1.8, 3.8, and 7.5, respectively. Scintillation noise for the same images is 2 to 4 millimags rms, depending on atmospheric conditions, so potentially one could use lossy compression without significant loss of photometric accuracy. However, to be certain one wouldn't later regret irreversibly lossy-compressing images (i.e. not saving the uncompressed data), very extensive testing would be required, so for critical scientific data, astronomers tend not to use lossy compression. The benefits of reduced disk storage space and transmission bandwidth are outweighed by the cost of that testing. Also, the cost, volume, and mass of disk storage all decrease approximately a factor of two every two years, so the smaller file size benefit of lossy compression is largely ephemeral.

Lossy compression also could be a practical SA algorithm to corrupt stellar photometry. However, lossy compression is a blunt tool for SA, because while it does corrupt stellar photometry by somewhat predictable amounts, it simultaneously corrupts astrometry and surface brightness of extended objects. Ideally, the SA could be turned on and off with a small encryption key, a.k.a. a password, that would transform the SA-data to its original form, i.e. O-data. Lossy compression algorithms, by definition, are irreversible, so they would not satisfy the desire for such a key. However, if such a key-based SA algorithm could be implemented, it would provide an incentive for astronomers to release to the public domain keyed-SA data, because the public domain could provide a robust backup for and access to the O-data. We imagine Alice might use the keyed-SA data herself and use the key whenever she wished to obtain the data with full fidelity.

The PHOTZIP algorithm was designed to losslessly retain the pixel values near stars while lossy-compressing regions of sky without stars, all in a user-selectable and predictable manner (Shamir & Nemiro 2005). The PHOTZIP algorithm thus may be an algorithm to achieve SA for the photometry of galaxies or other diffuse objects while allowing public access to stellar (or more exactly, point-like object) photometry (i.e. PHOTZIP as a SA algorithm would have the "opposite" goal of the algorithm described in Section 3.1).

3. Examples of SA algorithms

3. 1. SA Algorithm for Photometry

The following is a simplistic algorithm for SA of precision photometry of bright stars in a 2-D image. The objectives of this SA algorithm are

1. SA-data will differ from O-data only at specifically identified pixels.
2. Photometry of SA-affected stars will differ from that of O-data by a predictable random fraction.
3. Astrometry of all stars, including the SA-affected stars, will not be affected.
4. SA-data could be converted to O-data by anyone that knew the encryption key.

The proposed algorithm would fist identify which stars are desired to be subject to SA. They could be identified by coordinates or a parameteriza-

tion of their brightness or other characteristics. An associated table would store the (x,y) coordinates of a fiducial "center" pixel associated with each star subject to SA. Pixels within a specified vicinity of the tabulated pixels would be adjusted as part of the SA procedure, and all other pixels would be unaffected. The algorithm would solve for the "sky" value within each star's vicinity and store that with the coordinates of the center pixel. The SA algorithm would generate a unique semi-infinite series of pseudo-random numbers from the encryption key. For each set of pixels associated with each star, the SA algorithm would subtract the sky value (a scalar), multiply the residuals (a vector of a few pixel values) by the next pseudo-random number (a scalar), add back the sky value and replace the appropriate pixels with the SA-adjusted values. Because the pixel coordinates and sky values are stored, and because the random numbers are pseudo-random (i.e. reproducible), the SA-data can be converted to an identical copy of the O-data by anyone who knows the encryption key. For the special circumstance of overlapping SA-affected regions around nearby stars, the order of the stars will be important and the inversion algorithm will need to operate on the stars in the correct (reverse) order.

The above algorithm can be described in equations as follows. Let I be the O-data value of a pixel in common between two stars (The algorithm can be generalized to pixels that are associated with one, two, or more than two stars), identified by their sequence indices m and n. The SA-algorithm converts I to I' and then to I" by the following linear equations:

$$I' = R_m (I - S_m) + S_m \qquad (1)$$

$$I'' = R_n(I' - S_n) + S_n \qquad (2)$$

where the S are the sky values and the R are the pseudo-random numbers, equal to 1 + ε where ε is a normally distributed pseudo-random number of zero mean and specified standard deviation (e.g. 0.03). In order to recover the original pixel value, I from the SA-value I'', S_m, S_n, R_m, and R_n, the intermediate value I' should be recovered first from I'', S_n, and R_n, then the I can be recovered from I', S_m, and R_n.

The simple algorithm described above should permit SA of photometry while retaining astrometry to a high degree of precision. Astrometry should not be affected significantly because all the pixels within a region of interest associated with a specific star are multiplied by the same pseudo-random number (R) after the sky has been subtracted (and later restored). Differences between a specific stellar astrometry algorithm and the algorithm used to determine the sky value (S) could perturb the astrometry to some degree. That possibility and the circumstance of pixels being shared by multiple stars both suggest that some empirical testing would be required to measure empirically the effect the proposed algorithm, designed for SA of photometry, would have on astrometry. Presumably the proposed algorithm's effects, if any, on galaxies or extended structures would be insignificant, because as we have imagined its implementation, only pixels within approximately one or two FWHM of bright stars would be SA-adjusted, and only by multiplying them by scalars of order 1 + ε.

A significant improvement in the proposed algorithm would be elimination of the table of affected pixels and associated sky values. If the elements of the table could be algorithmically generated uniquely from both the SA-data and the O-data, then no separate table would be required, which would eliminate the need for a separate table. We encourage the reader to consider how to accomplish this improvement.

3. 2. SA Algorithm for Astrometry

An algorithm that would provide SA of astrometry while not affecting aperture photometry could move counts from some pixels to other pixels, all within the PSF and the photometric aperture. We leave it as an exercise to the reader to design such an algorithm with similar objectives as those enumerated for photometry in Section 3.1 (The author has not completed that exercise himself).

3. 3. SA Algorithm for Tabular Data

The SA algorithms for tabular data can trivially simple, because the various parameters are separate already. For example, a table of photometric and astrometric measurements can easily have one or the other (or both) SA-adjusted by applying (i.e. adding or multiplying as appropriate) a sequence of pseudo-random deviates to each value in the table.

4. Discussion

Potential advantages of SA could be:

1. Bob will have access to SA-data sooner than he'd have access to O-data. Bob's interest may be purely complementary science enabled directly by the SA-data, or his interest might be planning similar observations.
2. Alice enables additional science earlier than if she held all her data for their proprietary period.
3. SA may foster collaborations, by providing a means for Bob to realize and to demonstrate to

Alice that his own analysis or complementary data can add value to Alice's SA-data and by inference also her O-data.

4. Alice could benefit from an archive of her SA-data because she can use it as an alternative user interface to her O-data, because she knows the decryption key. Alice can use the SA-data as a backup, either the sole copy or a copy redundant to her own.

Potential disadvantages of SA could be

1. The traditional proprietary period is simple to implement and to understand, whereas SA-data are more complicated to create and to understand.
2. Some may have the opinion that the intentional corruption of data (i.e. from an SA algorithm) is antithetical to science.
3. The community, journals, or referees may not trust SA-data or conclusions based upon them.
4. SA-data could be mis-interpreted in a manner that O-data would not be.
5. Scientific data products based upon SA-data could be considered ephemeral.
6. The SA-data products may require updating when the associated O-data became available.
7. Two "strains" of subsidiary data products potentially may co-exist in the literature.

The latter disadvantages (items 5-7) of SA would apply equally to the current practice at STScI of "on-the-fly reprocessing" in which the archive provides data that has been calibrated with the latest, and presumably best available, reference files (e.g. flat fields) and algorithms (e.g. cosmic ray identification). The latter practice shares some of the same motivation as SA, specifically to disseminate data known to be of lower fidelity sooner than data of higher fidelity to be made available at some time in the future.

5. Conclusions

The main purpose of this draft manuscript is to foster discussions of the potential advantages and disadvantages of selective availability (SA) of astronomical data prior to revising and publishing it in a journal. A auxiliary purpose is to encourage others to create and test superior SA algorithms. Comments, opinions, suggestions, and questions are welcome.

6. References

McCullough, P. R., et al. (2006). *ApJ* **648**, 1228.

Paczynski, B. (2006) *PASP* **118**, 1621.

Shamir, L., Nemiroff, R. J. (2005) *AJ* **129**, 539.

White, R.L., Postman, M., Lattanzi, M.G. (1992). *ASSL* **174**: Digitized Optical Sky Surveys, 167.

Developing an Undergraduate Astronomical Research Program

Russell M. Genet
Cuesta College, California Polytechnic State University, and Orion Observatory
4995 Santa Margarita Lake Road, Santa Margarita, CA 93453
rgenet@calpoly.edu or *russmgenet@aol.com*

Abstract

Time-series astronomical photometry is an area of scientific research well suited to amateurs and undergraduates, and their backyard and campus observatories. I describe two past one-semester community college research programs, one six year ago and one last fall (2006), as well as a program planned for this coming fall (2007). The 2001 program, a course at Central Arizona College, utilized a robotic telescope at the Fairborn Observatory. Results were presented at the 200th meeting of the American Astronomical Society. This past fall, three students, in a 17-week, one-semester course at Cuesta College, were able to plan a research program, make several thousand CCD photometric observations, reduce and analyze their data, write up their results and, on the last day of class, send their paper off to a refereed journal, the *JAAVSO*. A course is being offered this coming fall (2007) that will involve about a dozen students (including high school students), several local amateur astronomers, and at least three CCD-equipped semi-automatic telescopes. Potential solutions to "scaling up" challenges created by increased class size are discussed.

1. Amateur Research

Two decades ago, at the Eighth Annual Fairborn-IAPPP Symposium, *New Generation Small Telescopes*, held at the Saguaro Lake Ranch in Arizona, Robert A. Stebbins, a sociologist from the University of Calgary, stated the following:

> In the wider community, the thought that amateurs might contribute anything other than, perhaps, money and goodwill to professional science is only slightly less than preposterous. Science, according to the popular conception, is a highly technical and oftentimes abstract undertaking mastered only by [those] with a unique bent for intellectual esoterica and a passion for such cloisters as the library and the laboratory. The scientist is a special strain of humanity who develops into a social curiosity after years of specialized education and unstinting dedication to the solutions of problems so arcane that the average citizen can only marvel at their incomprehensibility. This is the public's image of science and the profession of scientists.
>
> That some people might try from time to time to enter this lofty realm purely for the fun of it, for leisure, is even more inscrutable than science itself and the professionals who work there. And when some of these leisure-seeking "eccentrics" indicate that they occasionally contribute something new to the science they are pursuing, the man in the street is more likely than not to disintegrate in utter disbelief. Science is for the spectacled, half-bald, wild-eyed genius, not for the ordinary being who lives next door. (Stebbins 1987.)

Stebbins went on to remark that "notwithstanding these stereotypes, amateur scientists abound." He suggested they had, over the years, "made important contributions to archeology, ornithology, and astronomy."

Almost a decade before the conference at Saguaro Lake Ranch, I had conducted my own informal survey of amateur science and had selected astronomy as the field most likely to result in published papers—the hallmark of science. I had examined every paper in five years of a leading publication, the *Astronomical Journal*, asking myself, as I reviewed each paper, could I have accomplished this research? Writing many of the papers would have required a theoretical background beyond my grasp, while others would have required making observations through telescopes much larger than I could afford to purchase or build. Over two-dozen papers caught my attention, however. All were photoelectric observations of variable stars or asteroids with telescopes of 16-inch aperture or less.

It should not have been surprising that time-series photometry appeared to be the major contribution of smaller telescopes to astronomical science. Photometry makes efficient use of the meager photons available to smaller telescopes, while time-series observations are well suited to those who operate their own observatory.

2. Undergraduate Student Research

The public perception of undergraduate student researchers is similar to its perception of amateur researchers. It is, of course, well accepted that graduate science majors should conduct research. In fact, they must prove themselves capable of original research if they are to receive a doctoral degree. But it is not widely recognized, as is the case with amateurs, that undergraduate students, including non-science majors, are quite capable of conducting scientific research and that they, their schools, and their local communities—not to mention the larger scientific community—all benefit from undergraduate scientific research.

While it is entirely appropriate that undergraduate students should learn the essentials of one or more of the sciences in lecture courses, as well as master basic laboratory skills while conducting "experiments" with known outcomes, they may, in this process, obtain a distorted view of science and scientists. Science, after all, is primarily concerned with the unknown, not the known. While it could be argued that science majors will, soon enough, be exposed to research in graduate school, might they benefit if exposed to research while still undergraduates? Would non-science undergraduate majors gain an entirely different impression of science if they participated in actual research?

An increasing number of schools recognize the positive contributions undergraduate research can make to student learning and the furtherance of the true sprit of science—exploration of the unknown—on the campus and also within the local community. In this paper I discuss my own experience with undergraduate research at community colleges.

3. Research Program I: Cepheids

Six years ago, while teaching astronomy and mathematics at the Superstition Mountain campus of Central Arizona College, I organized, with the assistance of Cheryl Genet, a one-semester astronomical research class (Fall 2001). Nine students were formed into three teams. All three teams chose to observe bright Cepheid stars using a robotic telescope at the Fairborn Observatory in southern Arizona.

Astronomer Kenneth Kissell discussed the project with the students during several conference calls and assisted them in selecting appropriate Cepheids. Michael Seeds, the Principal Astronomer for the Phoenix-10 robotic telescope at the Fairborn Observatory, also spoke with the students during conference calls and helped them with their observational requests. Douglas Hall aided the students in selecting appropriate comparison and check stars, while Louis Boyd operated the robotic telescope.

The Phoenix-10 robotic telescope obtained the student-requested UBV photometric observations of the selected Cepheids. Results became available toward the end of the semester and, in several late-night sessions, the students tabulated and plotted differential magnitudes as time series which, of course, appeared quite random. They then produced phase plots and, as if by magic, the Cepheid lightcurves appeared. They were most impressed!

One student, only 16 years old at the time, presented his results on T Vul at the 200th meeting of the American Astronomical Society (Lappa 2002). Cheryl Genet presented her results on U Aql (Genet 2002) at the same meeting, while Cheryl and I described the research course itself (Genet and Genet 2002).

4. Research Program II: GNAT

The following year, Cheryl and I moved to California's Central Coast (near San Luis Obispo) to be near her aging parents. I established the Orion Observatory and equipped it with a 10-inch Meade LX-200 telescope and SBIG ST-8 CCD camera. Thomas Smith, at the nearby Dark Ridge Observatory, and I collaborated in observations of short-period W UMa eclipsing binaries. I also taught introductory astronomy part time at nearby Cuesta College,

Cuesta College seemed to be an appropriate venue for another community college astronomical research course, and I was allowed to offer such a course as a physics research seminar in the fall of 2006. Three students— Neelie Jaggi, Casey Milne, and Noll Roberts—worked together as a team to obtain lightcurves and determine the periods of GNAT MG1 catalog stars whose periods, due to heavy aliasing, were unknown. CCD photometry was obtained on nine MG1 stars at the Orion Observatory. Two were found to be continuously variable, and their periods were determined with precision. The students wrote up their results, obtained reviews, and submitted their paper to the *Journal of the American Association of Variable Star Observers,* a respected, refereed journal, for the editor's consideration (Roberts et al 2006). This research was also summarized at the 209th meeting of the American Astronomical Society (Roberts et al 2007).

The three keys to the student's success were: (1) the considerable help of an experienced local amateur astronomer, Thomas Smith; (2) suggested observational candidates, assistance, and visits by the director of the Global Network of Astronomical Telescopes (GNAT) program, Eric Craine, and (3) much

hard work by the students themselves. Cuesta College faculty and staff were very supportive of this "pilot" program, although it was understood that any repeat of the course, to be viable, would need to enroll a dozen students.

5. Research Program III: Scaling Up

Cuesta College has scheduled a second physics research seminar for this coming fall (2007). We plan, again, to observe potential short-term variables selected from the GNAT MG1 catalog. We also plan to obtain an asteroid lightcurve and determine its rotational period. This research seminar should involve about a dozen students (including a few high school students and several local amateur astronomers) and several CCD-equipped, semi-automatic telescopes. Potential solutions to problems in "scaling-up" last fall's pilot program are discussed below.

A single research team of a dozen or more students would be unwieldy, so the research seminar will be organized around multiple teams—each provided with the use of its own CCD-equipped, go-to telescope. A student, Brittany McCrigler, loaned the Orion Observatory a Meade 12-inch LX-200, and the observatory supplied a permanent pier, equatorial wedge, and guidescope for this telescope. Two additional CCD cameras with built-in B, V, and I filters (SBIG ST402) were purchased with funds granted by the American Astronomical Society. James Carlisle, at the Hill House Observatory in nearby Atascadero, recently purchased a Meade 14-inch RCX 400 telescope and SBIG ST402 camera. He will make these available at his observatory to one of the teams. Finally, Tom Smith will be providing time (remotely) on his 14-inch LX-200 GPS telescope from the Dark Ridge Observatory's new home under the clear skies of New Mexico.

Last fall, the single team with just three students was able to use the computer and software at the Orion Observatory for data reduction and analysis, although this required considerable student travel. Such an arrangement would be cumbersome for a seminar with a dozen students, multiple teams, and telescopes at several different locations. It would be more efficient for each student to have reduction and analysis software installed on their own laptop computer, which they could take to the weekly seminar meetings for software instruction, to observing runs to retrieve data and, of course, to their homes for data reduction and analysis.

There are many excellent software programs available for the reduction and analysis of time-series CCD photometry that can be installed on laptop PCs. These include Maxim-DL, AIP4WIN, CCD Soft, and MIRA. In choosing software for this coming fall's research seminar, two factors were paramount: (1) completeness in terms of reduction and analysis for both variable star and rotating asteroid time-series photometry, including period determination; and (2) low cost per student. MPO Canopus/Photometric Reduction software was chosen for the seminar this coming fall. It met our technical requirements and its cost (educational license for five students) is only $13 per student.

Last fall, students learned the basics of CCD photometry and lightcurve analysis through informal discussions at the Orion Observatory. The seminar this coming fall will, instead, meet formally every Monday evening at Cuesta College where students will learn the fundamentals of time-series photometry via lectures. A textbook, *A Practical Guide to Lightcurve Photometry and Analysis* (Warner 2006), will provide the essentials of variable star and asteroid time-series CCD photometry and analysis. This book is available from Amazon for less than $40.

This coming fall's research seminar will not only include Cuesta College students taking other courses at the college, but also a number of high school students enrolling in this research seminar as their first college course. In addition, several seasoned observers—members of the Central Coast Astronomical Society—will be enrolling in the course. Finally, we expect a few undergraduate students from California Polytechnic State University to participate. The mix of high school students, community college students, university undergraduate students, and local amateur astronomers should not only be enriching to all concerned, but should help to inform and involve the local community with respect to the rewards (and tribulations) of scientific research.

Three preparatory activities are being undertaken prior to this fall's research seminar. They are: (1) an informal spring student research effort; (2) a conference, *Time Series Astronomical Photometry,* 22-24 June, at California Polytechnic State University; and (3) a two-day training workshop on MPO Canopus/Photometric Reduction software that will be taught by Brian Warner July 27-28 at a workshop in Ft. Collins, Colorado.

6. Conclusions

Amateurs, undergraduate college students, and high school students are quite capable of scientific research and have, for years, been successfully completing projects resulting in published papers. Time-series CCD photometry of intrinsically variable stars, eclipsing binaries, asteroids, and planets transiting distant stars are a particularly fertile area for such

research because the combination of compact Schmidt-Cassegrain go-to telescopes, highly sensitive CCD cameras, and very capable personal computers has transformed backyard and college campus observatories into powerful scientific research facilities.

Large-scale automated surveys at a number of professional observatories have uncovered tantalizing hints of astronomical objects whose true nature can be determined through the dedicated time-series CCD photometry that properly-equipped amateur and campus observatories can provide. Affordable, high-tech telescopes, cameras, and computers have opened the door wide to amateurs and students who wish to conduct cutting-edge scientific research.

Of course there is a catch—there always is! Science is never easy. A basic understanding of CCD photometry of variable stars and asteroids is required. CCD time-series photometry also requires understanding and operating highly complex (albeit affordable) equipment. Observations must be made for many hours on multiple nights. Gigabytes of data have to be reduced and analyzed with sophisticated software. Finally, results must be described in a paper, the paper reviewed by outside experts, rewritten, and submitted for publication. In the upcoming Fall 2007 research seminar discussed above, all this will, as in last fall's course, have to be accomplished by busy students within the confines of a single semester.

Although daunting, the rewards of successfully completed undergraduate (and high school) research are significant. As coauthors of published scientific research papers, students not only receive a boost with respect to their future educational opportunities, but gain an understanding of the true nature of science and an appreciation of how research is actually conducted. The word gets around; there are other areas besides football and basketball where students can shine!

7. Acknowledgements

I am pleased to acknowledge the assistance of several individuals in scheduling, organizing and conducting last fall's research seminar. Thomas Smith (Dark Ridge Observatory); Eric Craine (GNAT Program); Kathie Jimison, Cathie Babb, and Pat Len (Cuesta College); Kenneth Kissell (Kissell Associates); and, especially, the course's three students, Neelie Jaggi, Casey Milne, and Noll Roberts (Cuesta College), all helped to make this course possible. Also, my thanks, in advance, to those who are helping pave the way for this coming fall's research seminar.

This research was partially supported by a grant from the American Astronomical Society.

8. References

Genet, C.L. (2002). "Photoelectric Photometry of the Bright Cepheid U Aql." *BAAS* **34**, 7.01.

Genet, R.M. Genet, C.L. (2002) "Community College Class Devoted to Astronomical Research." *BAAS* **34**, 13.08.

Lapa, K. (2002). "Observations of the Cepheid T Vul." *BAAS* **34**, 7.02.

Roberts, N., Milne, C., Jaggi, N. (2006). "Light Curves of Two GNAT MG1 Survey Stars." *JAAVSO*, submitted.

Roberts, N., Jaggi, N., Milne, C. (2007). "GNAT Student Follow-up Pilot Project." *BAAS* **39**, 162.09.

Stebbins, R.A. (1987). "Amateurs and Their Place in Professional Science." In *New Generation Small Telescopes* (D.S. Hayes, D.R. Genet, R.M. Genet, eds), Fairborn Press, Mesa, AZ.

Warner, B.D. (2006). *A Practical Guide to Lightcurve Photometry and Analysis.* Springer, New York.

Imaging Automation

Jerry D. Horne
3055 Lynview Drive
San Jose, CA 95148
jdhorne@hotmail.com

Abstract

Multiple software programs, techniques, scripts, and related routines now exist to automate much of the work of taking, processing, analyzing, and extracting data from CCD Images. Five categories of such software programs are examined. The automation capability of Maxim DL and the ASCOM modules is demonstrated, together with specific examples of automation routines to control a telescope, take and process images.

1. Introduction

The term *image automation* can be used in the sense that multiple images can be processed, or multiple operations can be performed, with minimal or no operator interaction. In automating these tasks, this paper will look at what can be done to more quickly take, process, and extract data from, a large number of images. The idea of Imaging Automation was documented thirty years ago by Bijaoui et al (1977), and now routines now exist to handle everything from positioning the telescope, setting filters, exposing images, processing images, and analyzing data.

2. Types of Automation

For the serious amateur and professional astronomer, there appear to be five categories of image automation software available. These software categories range from sophisticated commercial programs, backed by customer response teams, to one-of-a kind scripts written by an amateur astronomer, simply trying to find a way to solve a particular imaging or observing problem.

2. 1. Automation Category 1

This category concerns commercial software programs that both control multiple CCD cameras and allows the user to do at least some image processing. These are usually Windows based programs, often written in C++, usually cost hundreds of U.S. Dollars, and are sold by various vendors. These programs can operate on multiple images simultaneously, have the ability to create and utilize master frames for processing. Some can run scripts or plug-ins, and have ability to integrate with other software programs (e.g. the Sky®) and hardware (telescopes, filter wheels, mounts, etc). One program even has the ability to record commands and play them back. Examples programs able to interface with a number of cameras are Maxim DL/CCD® (2007), Astro Art®, and CCDSoft®. Examples of more proprietary, and somewhat less capable programs, are that software included with specific CCD cameras such as Starlight Xpress, or the Meade DSI.

2. 2. Automation Category 2

The second category of automation utilizes the scripting ability of other commercial programs and/or common software and hardware interfaces to provide another level of automation and specialization. In a sense, these so called "3rd party" programs provide the glue to stick together a variety of software and hardware in a coherent and structured manner. They represent perhaps the ultimate in a user's ability to automate imaging operations.

Typical abilities of such software include automatically taking the images from observing lists, focusing, filter selection, automated dark, flats, and bias images, open/closing and moving the dome, monitoring weather instruments, measuring seeing and image quality, parking the telescope, and warning the operator of error or unusual conditions. Some software even allows multiple user and internet access to an imaging setup.

Examples of this are ACP®, CCD Commander® (2007), and CCD Autopilot® (CCDWare 2007) We also place in this category, the modules of ASCOM (2007), the Astronomy Common Object Modules, since they provide access by multiple programs to multiple types of hardware.

2. 3. Automation Category 3

In this third category of automation software, the programs are designed specifically for image processing, with no hardware control capabilities. These programs can operate on multiple images simultaneously, have the ability to create and utilize master frames for processing, have the ability to extract photometric observations, have multiple filter and processing algorithms, and can usually read and write multiple file formats.

Obvious examples are AIP4Win® Mira®, Canopus®, IRAF® (2007), and a version of Maxim DL®, together with other lesser know programs such as Iris, Cadet; much older programs such a Super Fix or DAOPHOT, and even a Spanish-language program such as Laia.

2. 4. Automation Category 4

This fourth category concerns software tools and spreadsheets designed to perform a specific task related to observing and imaging such as Julian Date conversion, data analysis tasks, or converting one image format to another. These tools are usually provided as shareware or commercial software.

Examples of this category would be Lew Cook's spreadsheet tools (Cook 2007), software from the AAVSO such as *PC Obs* or *WWZ*, Ron Wodaski's tools (Wodaski 2002), or Tony Vanmunster's period analysis software, *Peranso* (Vanmunster 2003).

2. 5. Automation Category 5

The fifth and final category of automation is made up of non-commercial, individually written scripts, plug-ins or stand-alone programs that usually access either the scripting ability of other software programs, and/or the drivers associated with specific hardware. This is probably the most diverse software category, with its members ranging from fairly sophisticated tools to VB scripts that perform a very limited function. These scripts, tools, or sometimes just bits of code are usually available over the internet as shareware or freeware, and may or not have user support or license issues, and of course may or not work for particular applications.

Examples of items in this category are automated photometric extraction, image processing tools, telescope and observing routines, or color and image adjustment software.

3. Automation Requirements

For astronomers wishing to automate a specific imaging task, there appear to be a few obvious requirements. First, one must be able to get the computer to command, or talk to the camera, telescope, or accessory. Secondly, you must be able to monitor or receive feedback from this same hardware. Both of these requirements imply using some sort of programming language or interface to the hardware involved, usually interacting with the hardware driver.

When considering the development of a specific automation task, using Maxim DL®, by Diffraction Limited, provides such an interface, since it has a scripting interface, for both Visual Basic and Visual C++, it can meet a wide range of automation needs, and it has a wealth of embedded commands and functions for the camera, telescope, and for image processing. An automation routine in Maxim DL can be developed as a stand-alone executable program, a plug-in, or a visual basic script, depending on the sophistication of the program, its data storage and access needs, and the ability of the observer/programmer.

A simple automation routine can be run with Maxim DL's ***Run Script*** function, selectable from the File Menu. Similarly Maxim DL's Plug-ins are added and activated via the top level pull-down ***Plug In*** menu. For stand-alone executable programs, the decision to use Visual Basic or Visual C++ is a usually stems from the programmers preference and abil-

```
Dim WithEvents Cam As CCDCamera          'Camera object
Public LX200_Int As POTH.Telescope       'LX200 Interface Object from ASCOM
Public PPP As PinPoint.Plate             'Pinpoint solution object
Public MaximApp As MaxIm.Application      'maxim application object
Public MaximDoc1, MaximDoc2 As Document  'image document objects
Public Tel_u As DriverHelper.Util        'Telescope Utlities Object from ASCOM
```

```
Set Cam = CreateObject("Maxim.CCDCamera")          'Instantiate CCD camera object
Set LX200_Int = CreateObject("POTH.Telescope")     'instantiate telescope driver
Set PPP = CreateObject("PinPoint.Plate")           'Instantiate Pinpoint Plate Object
Set MaximApp = CreateObject("Maxim.Application")   'Instantiate Application
Set MaximDoc1 = CreateObject("Maxim.Document")     'Instantiate 1st Maxim Document
Set MaximDoc2 = CreateObject("Maxim.Document")     'Instantiate a 2nd Maxim Document
Set Tel_u = CreateObject("DriverHelper.Util")      'Instantiate telescope driver utilities object
```

ity, although certain embedded Maxim DL commands, require a variant-type array data structure, that is handled easiest in Visual Basic, and VB is used for the examples in this paper.

An important extension to Maxim DL's routines come from the Astronomy Common Object Model (ASCOM) modules, developed by Bob Denny, and others. Multiple objects from the ASCOM modules can be coupled with Maxim DL to provide extend a programs access to specific telescope mounts, focusers, and observatory interfaces.

4. Examples of Automation

The key software interface components for Maxim DL is its application and document objects. The application object provides for camera and telescope connections, while the Document object provides access to a variety of functions including image calibration, alignment, photometry, image filtering, and other measurements. The ASCOM modules provide other objects which help implement automation routines.

Typically, the object that the programmer intends to use must first be declared as a local or global variable, then instantiated before use. For example the Maxim DL and ASCOM objects for a camera, telescope, pinpoint plate, application, and document are declared (in VB) as shown in the first box below while the objects are, instantiated as shown in the second box below.

4. 1. Connecting to Telescope and Camera

As a simple example of automation, a script can be used to connect these declared and instantiated objects to the CCD camera and telescope as follows.

In this code example, the telescope and CCD hardware connection is made simply by setting the value of the object connection property to *true*.

```
'-------------- Connect Hardware --------------------
' Description:  This routine connects the
‘ ccd and telescope
'
' Inputs:
'          None
' Outputs: None
‘
‘ Calls:
‘        Cam.LinkEnabled
‘        LX200_Int.Connected
'   ------------------------
Private Sub ConnectHardware

 ‘connect to telescope
   LX200_Int.Connected = True

  ‘connect to CCD
   Cam.LinkEnabled = True
End Sub
```

4. 2. Taking Images

In terms of imaging, there are two basic methods for taking such images using Maxim's scripting capability, either exposing a single image at a time, or using its intrinsic sequence function.

The following two scripts shows an example of taking a single image, and then waiting for the CCD camera to download the image. The exposure routine returns a value which can be used to test the success or failure of the command.

Alternately, a different routine can be used to start an image sequence that has been previously defined in Maxim DL and saved to a file. The sequence file contains the exposure time, exposure type, filter, and other information.

```
'----------------- Take Single Image ------------------
-
'
' Description:  This routine commands the
‘ camera to take an image
'
' Inputs:
‘
'    Image_Duration:
‘          single_exposure time in seconds
'    Image_Type:
‘         integer_Type of image (1 = light, 0 =
dark)
‘   Filter_type :
‘       integer_filter number to use (if applicable)
' Outputs: None
‘
‘ Calls:
‘         Cam.Expose
‘
'     --------------------------
Private Sub TakeImage (Image_Duration As
single, Image_type As integer, Filter_type as
integer)

‘return value for image routine
   Dim temp_result as Boolean

‘take the image
   temp_result = Cam.Expose(Image_Duration,
       Image_type,Filter_type)

' wait for image ready
Do While CCD_ImageDone = False
 ‘allow other processes to continue
   DoEvents
Loop
End Sub
```

```
'------------- Start Sequence  -----------------------
'
' Description:  This routine starts an imaging
sequence
'
' Inputs:
'      Sequence_file:
‘         string_full path and filename of saved
sequence file
‘
' Outputs: None
‘ Calls:
‘       Cam.StartSequence
'       -------------------------
Private Sub TakeSequence (Sequence_file As
String)

   Cam.StartSequence(Sequence_file)

      End Sub
```

4. 3. Loading and Aligning Images

```
'---------- Load and Align Files ----------
'
' Description:  This routine handles ‘alignment
of the reference and image ‘files
'
' Inputs:
'    File1:
‘    string_Reference File path and name
‘
'    File2:
‘      string_Image File path and name
‘
' Outputs: None
' Calls: MaximDoc1.OpenFile
'          MaximDoc2.OpenFile
'          MaximDoc1.AlignImages
'    -------------------------
Private Sub LoadandAlign(ByVal File1 As
String,
     ByVal File2 As String)

'load reference file into the doc object
    Call MaximDoc1.OpenFile(File1)

'load image file
    Call MaximDoc2.OpenFile(File2)

'don't abort program for align problem
   On Error Resume Next

'call Maxim routine to align them
     Call MaximDoc1.AlignImages(1, False)

End Sub
```

An example of using the document object is shown in a routine to load and align images. Maxim DL provides software access to standard FITS load functions and image align routines.

The code segment in Visual Basic shown above is used to load and align two images. The routine takes as input two complete file names.

4. 4. Astrometric Solve

An automation routine to astro-metrically solve an image using a large star catalog such as GSC, is shown in the following VB code segment by using the Pinpoint Engine within Maxim DL. The routine takes as input the image file name and the approximate RA and Dec of the center of the image.

```
'---------------------- Solve Image ----------------------
'
' Description:  This routine handles the
astrometric
‘   solve of the image
'
' Inputs:
'   RA:
‘     single_approximate Right Ascension
‘     coordinates of center of image
'   Dec:
‘      single_approximate Right Ascension
coordinates
‘      of center of image
'   File1:
‘      string_Image File path and name
' Outputs: None
' Calls: PPP.FindImageStars
‘           PPP.FindCatalogStars
‘           PPP.Solve
'     -------------------------

Private Sub SolveImage(ByVal File1 As String,
  ByVal RA As Single, ByVal Dec As Single)
 'attach image to pinpoint engine
     PPP.AttachFITS (File1)

  ‘ Tell PinPoint where the telescope is pointing
   ‘in RA                                    '
      PPP.RightAscension = RA
    ‘in Dec
      PPP.Declination = Dec

    ‘set image parameters for the CCD
    ‘Horizontal
      PPP.ArcsecPerPixelHoriz = 1.13
    ‘Vertical
      PPP.ArcsecPerPixelVert = 1.09

   'find the stars in the image
      PPP.FindImageStars
   'get the stars from the catalog
       PPP.FindCatalogStars

   ‘solve the image
      PPP.Solve

End Sub
```

4. 5. Stacking Images

Stacking images is useful for a variety of purposes and can be accomplished via an automation routine. The following routine stacks a series of images in a given directory, using Maxim DL's auto-star matching routine, and saves the resulting combined image.

```
‘---------- Stack Images ----------
" Description:  This routine handles the
combining  or stacking of images
'
' Inputs:
'    temp_filemask:
‘     String_full path & mask of files to be
stacked
‘     (e.g. C:\temp\m57*.fts)
‘    save_filename:  String_full path and name
‘    of stacked image file
'
' Outputs: None
' Calls: MaximDoc1.OpenFile
‘          MaximDoc1.CombineFiles
‘          MaximDoc1.SaveFile
‘  -------------------------
Private Sub Stack_Images(temp_filemask As
String,  save_filename As String)

'Directory of files to stack
   Dim file_Dir As String
‘ first file name
  Dim temp_filename As String

'get path of files
      file_Dir = Mid(temp_filemask, 1,
Len(temp_filemask) - 5)
‘get first file name
   temp_filename = Dir(temp_filemask)
 ‘build path and filename
    temp_filename = file_Dir & temp_filename
 'load the file into the document object
    Call MaximDoc.OpenFile(temp_filename)
 ‘allow for error result from Maxim on stacking
    On Error Resume Next

‘combine with other files in directory
‘ using auto-star matching
    Call MaximDoc.CombineFiles(file_mask, 1,
False, 0, False)

 '   Save the file as 32-bit fits
    MaximDoc.SaveFile(save_filename,
mxFITS, False, 2, 0)
Exit Sub
```

4. 6. Photometry

```
'------ Perform Photometric Measurement -------
------
" Description:  This routine measures the
‘magnitude  of the variable star in an image
'
' Inputs:
'  VarX:  integer_X coordinates of the variable
star
‘  VarY: integer_Y coordinates of the variable
star
'  CX:   integer_X coords of the comparison
star
‘  CY:  integer_Y coords of the comparison
‘  CM:  single_magnitude of the comparison
star
‘
' Outputs: single_magnitude of the variable
star
' Calls:
‘   MaximDoc2.CalcInformation
'       -------------------------
Private Function GetPhotometry(VarX, VarY,
CX, CY,  CM As Integer) As Single

Dim Star_Info As Variant   ‘  storage for star
info
Dim Var_Int, As Double  ‘ variable star
intensity
Dim Comp_Int As Double ‘comp star intensity
Dim MV As Single   ‘measured mag of var star
Dim MRings(2) As Integer    ‘rings setup

   MRings(0) = 6        ‘ aperture setting
   MRings(1) = 3        ‘gap setting
   MRings(2) = 6        ‘annulus
‘Get variable star data from image
   Star_Info =
MaximDoc2.CalcInformation(VarX, VarY,
MRings)
   Var_Int = Star_Info(11)  ‘Get intensity of var

‘Get comparison star data
    Star_Info =
MaximDoc2.CalcInformation(CX1, CY1,
MRings)
‘Get intensity of Comparison star
    Comp_Int = Star_Info(11)
‘Calculate magnitude of variable star
    MV = CM - 2.5 * Log10(Var_Int / Comp_Int)
‘return the calculated magnitude
```

To perform photometry, an automation routine needs to measure intensities and magnitude of various stars.

The above routine calculates the magnitude of a star in an image, given the X & Y pixel location of the variable, the X & Y pixel location of a comparison star, and the known magnitude of a single comparison star.

For differential photometry, there are of multiple methods for determining the magnitude of the variable star. Three examples that could be incorporated into an automated photometry routine are:

1) Basic V-C: the magnitude of the variable found by using a single comparison star:

$V = (v - c) + C$ {e.g. V = 3.7 + 12.5 }

2) Average = Mean of variable magnitudes found using multiple comparison stars:

$V_i = (v - c)_i + C_i$ {e.g. V_i = 3.7 + 12.5 }

Then:

$$V = \left(\sum_{i=1}^{n} V_i\right) / i$$

{e.g. V = (16.2 + 16.3 + 16.4) / 3 }

3) Aggregate – combining all comparison star intensities and magnitudes to form a virtual star to compare with the variable:

$$C_{(total)} = (-2.5)\text{Log10}\left(\sum_{i=1}^{n} 10^{(-Ci/2.5)}\right)$$

{sum comparison magnitudes}

$$I(total) = \sum_{i=1}^{n} I_i$$

{sum intensities}

Then:

$$V_{agg} = -2.5\ \text{Log10}\ (I_v / I_{(total)}) + C_{(total)}$$

{find var mag}

4. 7. Park and Unpark

Automation routines can be utilized to add features to a telescope, that are not part of it intrinsic command set. An automated park and unpark routine for the Meade LX200 telescope can be implemented using Maxim DL and a telescope driver from the ASCOM modules. This can be implemented as follows using the instantiation of the LX200 interface module declared here as LX200_Int.

```
'---------- Park Command ----------
" Description:  This routine parks the LX200 at the ‘  local hour angle and a given Dec.
'
' Inputs:
'    Horizon_Dec:
‘      integer_Value of Dec to park scope at
' Outputs: None
' Calls:
‘   LX200_Int. SiderealTime
‘   LX200_Int.SlewToCoordinatesAsynch
‘   LX200_Int.Slewing
‘   LX200_Int.CommandBlind
'          -------------------------
Private Sub Park_LX200(Horizon_Dec As Integer)

'storage for RA, DEC, local hour angle
    Dim RA, Dec, LMST  As Variant
'get the current hour angle
     LMST = LX200_Int.SiderealTime
'set the target RA to the hour angle
     RA = LMST
  'set the target Dec to the local horizon
      Dec = Horizon_Dec
'slew the telescope to the target coords
Call LX200_Int.SlewToCoordinatesAsync(RA, Dec)
'wait for slew to complete
  Do While LX200_Int.Slewing = True
      DoEvents
   Loop
'Set Land Mode to turn off tracking
   Call LX200_Int.CommandBlind("#:AL#")
Exit Sub
```

```
'------------ Un-Park Command ---------------------
-
' Description:  This routine un parks the LX200
‘and places the telescope at the local hour
‘angle  and zero Dec - the normal start
‘alignment position
'
' Inputs:
'          Horizon_Dec:
‘  integer_Value of Declination telescope was
‘ parked at ‘   (the horizon at a given latitude)
‘
' Outputs: None
' Calls:
‘   LX200_Int. SlewToCoordinatesAsynch
‘   LX200_Int.SlewToCoordinatesAsynch
‘   LX200_Int.Slewing
'                          ---------------------------
Private Sub UnPark_LX200(Horizon_Dec As
Integer)
  'storage for RA, DEC, local hour angle
     Dim RA, LMST As Variant
    Dim Dec As Double

  'Set Polar Mode to turn on tracking
      Call LX200_Int.CommandBlind("#:AP#")
  'Get current start up RA = LMST
      RA = LX200_Int.RightAscension
  'Set the target Dec
      Dec = 0#
 'sync the telescope to parked coord.
    Call LX200_Int.SyncToCoordinates(RA,
Horizon_Dec)
  'move scope to target = RA=HA, Dec = 0
    Call
LX200_Int.SlewToCoordinatesAsync(RA, Dec)
  'wait for slew to complete
  Do While LX200_Int.Slewing = True
       DoEvents
  Loop
Exit Sub
```

5. Conclusion

Today’s serious amateur and professional astronomers have a wealth of software automation routines that can greatly simply and speed up the collection of images and processing of data. The various automation programs appear to fall into five categories, according to their abilities and design. These programs are available from commercial vendors, or in some cases they exist as shareware or freeware. With a little bit of experience and skill, an astronomer can also craft his own automation routines using the scripting ability of a program like Maxim DL. Like anything else in Astronomy, all it takes is practice and patience.

6. References

ASCOM (2007). Astronomy Common Object Model. http://ascom-standards.org/

Bartels, M. (2003). ASCOM Talk List. http://ascom-standards.org/BartelsOpEd.html

Bijaoui, A, Marchal, J, Ounnas, C. (1977). *Astron and Astrophys* **65,** 71-75.

Cook, L. (2007). http://www.geocities.com/lcoo/

Maxim DL (2007). http://www.cyanogen.com/products/maxim_extras.htm

IRAF (2007). http://iraf.noao.edu/

CCDWare (2007). http://www.ccdware.com/

CCD Commander (2007). http://ccdcommander.astromatt.com/

Wodaski, R. (2002). *The New CCD Astronomy*, New Astronomy Press.

Vanmunster, T. (2003). Peranso. http://users.skynet.be/fa079980/peranso/index.htm

Fast Photometry

John Menke
22500 Old Hundred Rd
Barnesville, MD 20838
John@menkescientific.com

Abstract

Fast photometry is measuring changes in brightness in the range of several seconds down to a few milliseconds or faster. Increasingly, asteroid and lunar occultation measurements are carried out using camcorders or video cameras. These can be very inexpensive, and allow event timing to about .02 sec. GPS timing signals, good to a microsecond or better, can be combined with video or photometers to allow UTC timing to as good as the sensing device allows. Beyond video cameras that are usually limited to event timing, there is also a role for amateurs to explore true high speed photometry. I will describe use of several inexpensive devices that allow an amateur to conduct fast photometry. I include observing results from this equipment as used in occultation and scintillation studies, and will discuss some of the possible areas of amateur work.

1. Introduction

So what is fast photometry? Fast photometry is the process of measuring brightness that varies at a "high" rate. "Slow" photometry is measuring at a rate slow enough for conventional methods (formerly film, now CCD cameras) to give good results. Normally, we want to measure to some specified precision within a specified time. Measuring a 1% change in brightness of a faint star in a millisecond is a very different problem from taking a minute to measure a 10% change of a bright star. We will fairly arbitrarily say that "fast photometry" means measuring intensity changes occurring faster than about 1 minute. In this paper, I report measurements at 1ms, but some fast photometry is done at the microsecond rate.

What kind of equipment and techniques are feasible for amateurs to use to do fast photometry? And what are some of the phenomena that require these techniques? And what do the data really look like?

2. Equipment

2. 1. Telescope

Most astronomy phenomena require a telescope to gather enough light to measure. As we shall discuss, in the fast photometry regime, you may be surprised to discover that chief problem may not be that the objects are too faint. Rather, even for bright objects, the atmospheric scintillation sets a limit on the precision of a brightness measurement that may be made at a particular speed. As usual, the bigger the scope, the more light there is to use (almost always a good thing) AND the more scintillation will be averaged. The work reported here has been done with a C11 on an AP mount (but I look forward to my fast Newtonian 18in. f3.5).

2. 2. CCD Cameras

Most CCD cameras these days operate with shutters that will operate in 0.1 sec or faster. While the full frame download time may be 1-10 sec or longer, one can often operate with partial or sub-frames and achieve download times down to 1 sec or even a bit faster. Thus, a CCD camera may operate at close to 1Hz. Note, however, that using a subframe will probably prevent you from having a suitable comparison star in the field--you are then in almost the same boat as a person with a standard one-channel photometer.

2. 3. Photometer

A photometer uses a photosensitive device (silicon diode, photomultiplier, etc.) to convert light to an electric current that can be measured. A silicon diode is similar to a single pixel in a CCD, but whereas the CCD accumulates charge for a delayed readout, the photometer detector reads out continuously. There is always a tradeoff of speed vs. sensitivity: the widely used Optec photometers using silicon diodes achieve fairly high sensitivity by foregoing operation faster than about 1 sec response. However, it is entirely feasible to build a homemade fast photometer. My own, shown in Fig. 1, cost about $50 in parts, and uses a 1mm square silicon photodiode (see References). I designed it more for speed than sensitivity, achieving about 2 ms rise time with an internal noise roughly equal to a mag 9.5 star in a C11. The output

of the photometer is digitized and sent over a serial link to a PC for recording and analysis. I used this instrument for many of the data in this paper.

Figure 1. Fast photometer Equipment

To reduce background light from nearby stars and skyglow, one normally operates the photometer with a diaphragm to limit the field of view (I used about 1 a-min). The smaller the field, the more challenging is the tracking. Most photometers do not let you see whether the image is landing on the sensor--i.e., you only see the resulting intensity whether the change is due to a tracking error or a cloud passing by. Thus, an excellent mount is a big plus in photometry (conversely, a big advantage of using CCD or video is that there is less need for accurate telescope pointing and tracking).

2. 4. Video Camera

For some work, a camcorder can be used either aimed at the target or even through a telescope. But one can also use an inexpensive video camera and feed the image from a telescope into a camcorder for recording, or directly into a computer for recording and analysis frame by frame. In any case, the best time resolution is 1/60 sec (17ms) with 8 bit digitization. Video can eat even hard-drive storage very fast (a mere one hour of video can be tens of 25GB).

2. 5. Human Eye

The human eye's best feature is that it is pretty sensitive, portable, and has no wires or batteries. But it does weigh a lot (especially as it gets older), and is only good to about 0.2 sec time resolution. The eye is especially useful for transient, one time events. For example, the eye can be used with a telescope to observe asteroid occultations, and can easily discriminate one star from many.

2. 6. Timing

Many events require only approximate timing (>1 sec), but some events or experiments require very accurate timing. There are pros and cons of using WWV, telephone, and computer time based on the Internet. Internet/PC-based timing sources frequently are off by as much as one second. While the display on a GPS is frequently wrong by many seconds, GPS modules are available that output a UTC pulse every second with an accuracy of a microsecond or better. One entrepreneur has developed a device for imprinting this time on raw video for use in asteroid occultation work (see References). I built a related device for time stamping digital data from the photometer, or for use in visual occultation work (cost about $50 plus another $75 for the GPS module, and good to about 1ms).

3. Phenomena

There is a huge range of phenomena to observe in the "fast photometry" category, only a few of which have been explored widely be amateurs. In a few areas, amateurs can contribute to the science (e.g., asteroid occultations), while in others, at least at this time, the benefit is in learning how to do the measurements. However, if more people worked this area, it is likely that we would learn how amateurs might contribute to new areas in the science.

Here is a sampling of some of the interesting high-speed photometry measurements (some of which I have done or am planning).

3. 1. Lunar Occultations, Grazing and Total

These are fun to watch, and highly organized. David Dunham and others have developed a wonderful network of observers, with extensive website support on suitable targets, recommended methods, a convenient place to send data to be analyzed and combined. A good website to start from is http://iota.jhuapl.edu/exped.htm and follow links from there. Equipment may be portable, telescopes in the 4-12 inch range, and observation is usually visual or with video.

3. 2. Asteroid Occultations

Because asteroid occultations give direct information on the size and shape of the objects, this field is now being aggressively developed, again by Dunham and friends. Like grazing lunar events, the

event is usually studied by a series of observers spread out over the relatively narrow (20-100 mile) predicted track. Watching a star wink out when crossed by an asteroid would be cool: I've been wiped out by weather 7/7 of my recent attempts. Observation methods are similar to lunar occultations.

3. 3. Pulsars

Pulsars rotate at rates from 1ms to about 1 second. But they are usually faint (though the Crab is at 8.5mag), and may be embedded in nebulosity. The photocurves cannot generally be detected directly, but require substantial effort to pull out of the background noise. Note that the Crab at 33ms is well inside the range of atmosphere scintillation effects, and also happens to be 1/2 the 60Hz rate, a potential source of interference.

3. 4. Planetary Occultations

Detecting the Saturn ring gaps and ring structure, Uranus rings, inferring atmospheric structure and similar studies can be done as a planet passes in front of a star. The big problem is that the light of the planet tends to overwhelm the fainter star. Some relatively rare events should be observable with amateur equipment, but predictable events are not likely to produce science opportunities for amateurs. But wouldn't it be fun to record the central flash from atmospheric focusing of light a billion miles away!

3. 5. Solar variations

The five-minute oscillations in the sun, and variations thereon, are potential experiments. Obviously, getting enough light is not the problem--the tiny size of the effect is the problem.

3. 6. Cataclysmic and Irregular Variables

Professionals and amateurs follow these objects, usually looking for relatively slow variations (egg, 60 sec). Because the observations are often of long duration, the data requirements are high.

3. 7. Gamma Ray Bursters

Amateurs are doing great work on GRBs, with time resolutions usually in the one-minute range. Most GRBs are faint, so it will be very difficult to have enough signal to do true fast photometry.

3. 8. Atmospheric Studies

Stars are a wonderful probe for our own atmosphere: we can use them to learn more about all those interesting motions of the air that we like to complain about. I will describe work I have done in this area.

3. 9. Other Fast Variations in Starlight

There are recurrent claims for observing very transient stellar phenomena, e.g., "XYZ star tripled in brightness for three seconds". Most of us have been "sure" we have seen such events…out of the corners of our eyes. On the other hand, extensive studies have verified very little of this. Unless we know of a good candidate, we are likely never to make a positive observation (at least, one that will stand up to scrutiny).

But some of us have always wondered about why more stars don't produce fast photometric signals. It does seem hard to believe that binaries can be rotating so close and so fast without violent disturbances of the atmosphere that can be observed. While the signals might be small, we know we can take lots of data and then spend computer time searching for signals. While there seem to be few such targets suitable for amateurs, as an example I will report on one of my own investigations in this area.

This list is NOT all inclusive. There are many objects that show fast intensity changes. However, most of the interesting ones are under constant investigation by professionals, where to add to the science requires professional level equipment and expertise. However, there are many bright people out there, and it is very likely that someone in this room will identify some new fast photometry area for pro-am research. And beside, it is a very interesting field!

4. Fun with Photometry

As I mentioned, I have a built a 2msec photometer that I have used for several study areas and will describe these to help demonstrate some of what can be done by amateurs. I make no claim to originality in this work, and I am not an expert. But each of us sometime started with our first photocurve, so here goes.

5. Scintillation Studies

We all know that the atmosphere is not uniform, and that there are small regions called cells in the 6 inch size range, having non-uniform temperatures, some 2-10 miles up. The temperature variations cause variations in refractive index that affect seeing. We all know this, but few of us have connected the dots to understand scintillation. The basic mechanism is shown in Figure 2 and summarized below.

- Scintillation is an atmospheric phenomenon. Therefore, it must affect stars of all brightness equally. Bright stars scintillate as much

as faint ones. Of course, faint stars introduce additional noise sources including the shot noise from the sporadic arrival of small numbers of photons, and the risk of being submerged in other noise sources, whether in the detector element, electronics, or extraneous light sources.

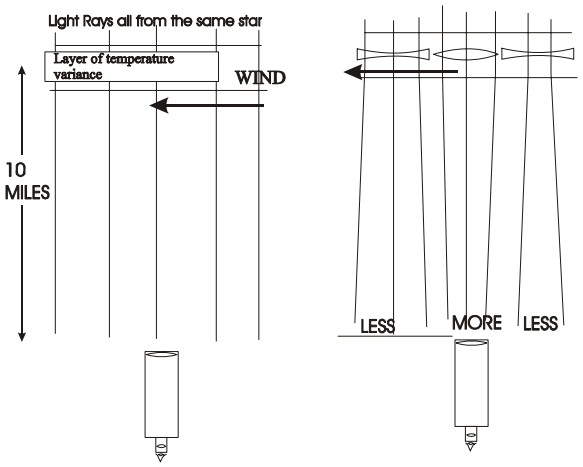

Figure 2. Cause of Scintillation

- The cells have an effective size of about 6 in., and move with the wind at perhaps 100 km/hr (100 ft/sec).
- The distortions in the wavefronts by the over and under focusing caused by the cells produces bright and dim patches of similar sizes at the objective of the scope. This patch of light is moving at 100ft/sec and crosses an amateur scope in about 10 ms.
- As the cell(s) cross the scope objective, more or less light is received and the apparent object brightness varies: this is scintillation
- One can average received brightness over time to measure the "true" average
- Or, one can average over space, i.e., have a bigger scope receiving a larger number of bright and faint cells that all merge at the focal point for a more accurate average intensity
- Or one can take several telescopes, each with photometers, and add the electrical signals together to produce the same improved average (one does not need adaptive optics)

How real is all this? Here are some data that show the effects.

Figure 3 shows three data sets using three apertures on a C11 to simulate different scope sizes. You can see that the bigger the scope, the more scintillation cells are averaged, the slower the time variation becomes, and the lower its amplitude. Using these data, one can see that detecting a 10% drop in five milliseconds is simply not feasible with a C11-no matter how bright the star!

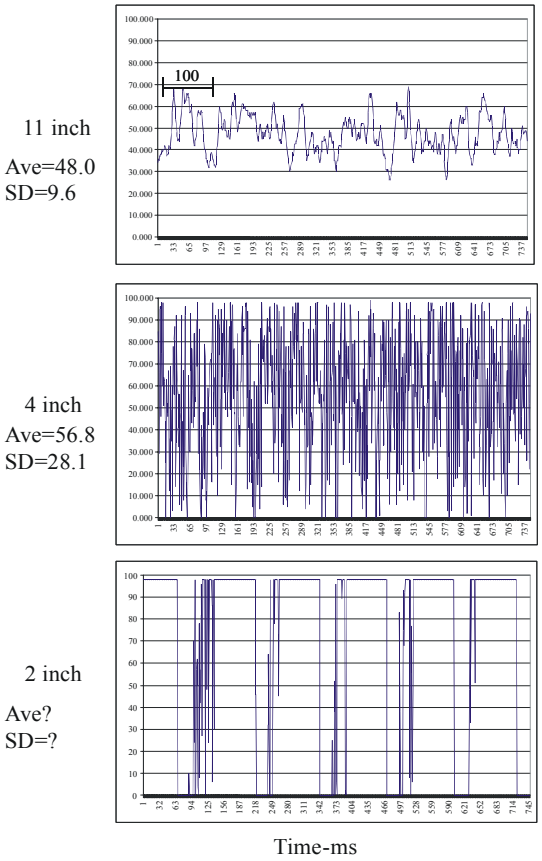

Figure 3. Scintillation with different Scope Sizes

As one examines the trace for the 11 inch scope, one can see that the time structure tends to occur in the 5-20 ms range. That is, there are few 1ms excursions, and there are few times when there is not a major change in 50 ms. One can even see suspicions of pieces of sine waves in the trace!

More quantitatively, one can do a Fourier transformation on the intensity time data to determine the amplitudes of the different frequencies of waves that make up the raw data. Excel will do this on up to 32,000 points, but 20 min of data at 1000 samples per second is a million points. Using Google, I found an inexpensive package that would do this called ScopeDSP (see References) that produced most of the graphs shown here.

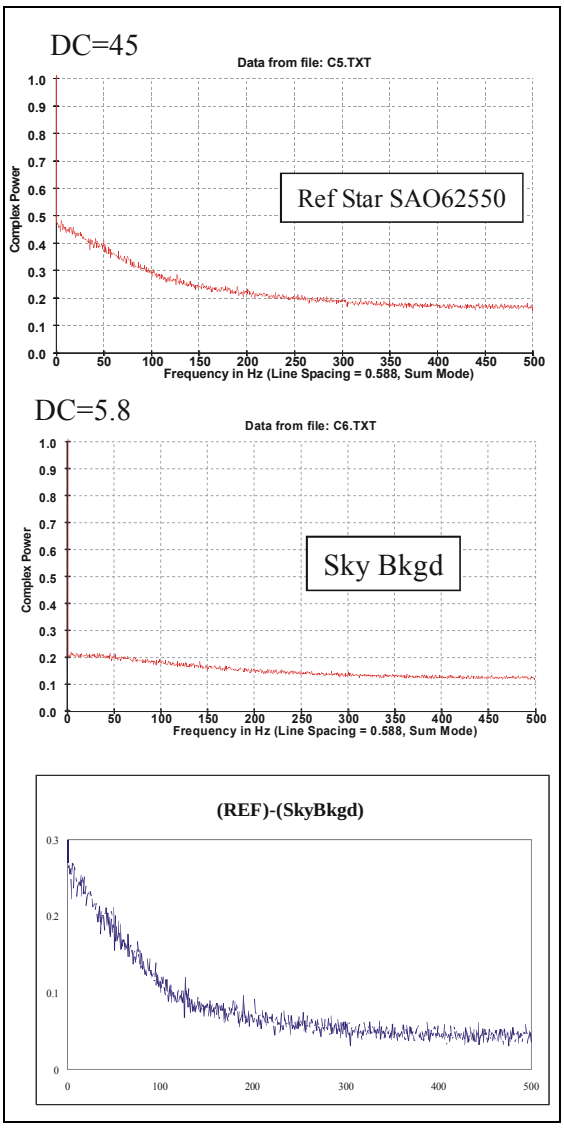

Figure 4. Scintillation Spectrum

In Figure 4, I show an example of Fourier spectra. The top graph shows the Fourier transformation of 20 min. of data similar to that shown in Figure 3(top). The frequencies run from close to zero to 500Hz. After this run, I then shifted the scope off the star, and obtained data leading to the middle spectrum of the background and instrumental noise--note that it is lower at all frequencies. The bottom graph shows the difference, which represents the star minus background, i.e., the spectrum of the scintillation noise. Most of the energy is below 100Hz, which is about how "fast" the cells move across the aperture, but there is substantial apparent energy in the higher frequency bands as well.

6. Eclipsing Binary Study

Years ago, one of our dome customers (my wife and I used to run Technical Innovations with HomeDome and ProDome) mentioned that he was searching for fast signals from stars. He was using a photometer and a tuned amplifier, slowly scanning the amplifier frequency while observing. I didn't have a photometer at that time, so I built a system that would use a video camera signal and measure the brightness of stars in the image in real time (reported as a poster at SAS2000). Thus, the data storage needed was only one digital value every 17ms, or less than 1 MB (not GB) per hour. With this, I could record hours of data, then do a Fourier analysis to calculate what frequency sine waves were buried in the signal. After much debate with the customer, he agreed that mine was the more efficient process.

Although I did some work with the video photometer several years ago, I decided to try again with my new fast photometer. I chose for my current target AW UMa, a close eclipsing binary (surely something must happen there!). Why did I pick this one? It is bright (6.9mag) so I have good signal, it is very high (75deg) in the sky (reduces scintillation), and it has an almost identical (brightness and spectrum) star only 30 a-min away for use as a reference.

At this writing, I have had three good nights (for Maryland) intermixing a total of 8 runs on AW and 4 on the Reference star. Most runs were about ten minutes long, with the mount easily keeping the star in the 1a-min diaphragm during the run. At 1000 samples/sec, there are about 0.5 million data points in each run. While doing these runs with the photometer, I also used a second scope and camera to measure the photocurve of AW, so that I could be sure to sample all the phases with the photometer. In the course of this measurement, I stumbled onto TU UMa, a 9mag RR Lyra type (pulsating star) that seems to show irregularities in the lightcurve – a worthy target, but a bit too faint until I get my 18inch scope into operation!

The resulting twelve Fourier spectra all look similar to Figure 4(top). There was no sign of any narrow (spike) or broad (hump) band frequency in the curves (except an occasional 60Hz spike). Although they appear similar, might there be more subtle systematic differences between AW and the Reference star spectra that show up in relatively narrow frequency bands?

To answer that question, I normalized each curve to its own average value over the range 45-450 Hz. For each curve, I then calculated the ratio of the average over a narrow frequency range (1-3Hz, 3-10Hz, etc) to that normalized value so that I could find the

relative strength of different frequency bands in each run, and then compare them. This result is in Figure 5. Each frequency band has a series of bars, and each bar is the relative strength of that frequency band, in the order I did the runs. The light bars are the AW, the dark are the Reference star.

One would hope to see in some frequency band that all the AW bars were higher (or lower) than the Reference bars: this would indicate some systematic difference between the stars. Alas, it is not so. In the lower three bands, we see that there were definite trends during the evenings in the effects of scintillation, i.e., slow variation in the energy in the scintillation bands 1-100Hz. In the higher frequency bands, there was less variation.

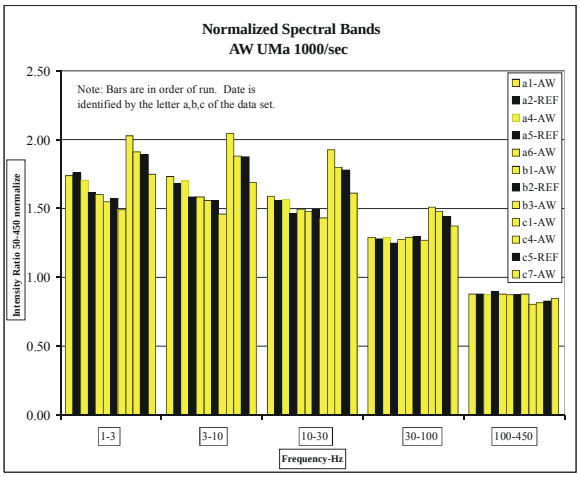

Figure 5. Spectral band strengths

Nowhere in the results are there systematic differences between the shapes of the AW and Reference star frequency spectra. Observing the low frequency bands, it is also clear that atmospheric scintillation changes can easily mask small signals unless there is a very nearby reference star that can be observed simultaneously with identical equipment (which I did not have).

Of course, using these measurements, we can only set a lower limit on a possible signal. From the variation in the data, and by injecting known signals into the data, we can estimate these limits. We could take more data using improved techniques to search for ever smaller effects. I believe there is at least one person in this room who regularly calls for "more data" whenever a question arises! But not for me this time: there are other things I want to do!

7. Conclusion and Future Options

It is clear from this initial effort that it is feasible for amateurs to use high speed photometry, and in some areas, make contributions to astronomical science. The equipment is reasonable in cost, and at least some of the techniques are well within our capability. Relatively little has been done in this area, so there is an open opportunity to identify and develop new avenues of investigation.

With scintillation being the limiting condition for a large class of interesting measurements, one thinks about bigger scopes! While my new 18in. will make some measurements more feasible, it is not really big enough. One thinks about 36 inch and bigger. Maybe we need to look again at stretching aluminized Mylar on a frame and sucking a vacuum. Hmm. That would take care of the spatial averaging, but can we correct the aberrations well enough to get the light into a reasonable size detector with a reasonable size (egg., 1 a-min) diaphragm? And then can we steer it well enough? We might think that flexure would be a tough problem so even a guide scope may not be enough, but we would have plenty of light so we should be able to pick off light from the central cone for a guidance system. Hey, if someone wants to build it, I'll offer my field!

8. Acknowledgements

I would like to acknowledge my debt to our former customer David Wright for his stimulation in starting this work many years ago. I am also thankful for the book *High Speed Astronomical Photometry* by another Brian Warner (i.e., not our own MPO Brian Warner) which so clearly lays out much of the science. And of course, to IAPPP-West and now SAS for the wonderful venue to share these ideas with other astronomers.

9. References

Warner, B. (1988) *High Speed Astronomical Photography.* Cambridge University Press.

ScopeDSP software for Fourier transformation. Iowegian International Corporation. www.iowegian.com

KIWI OSD. This device imprints GPS time onto video. Available from PFD Systems at http://www.pfdsystems.com/.

Go to www.Menkescientific.com for information on the photometer and other devices mentioned.

Differential CCD photometry Using Multiple Comparison Stars

David Boyd
BAAVSS and CBA Oxford
5 Silver Lane, West Challow, Wantage, OX12 9TX, UK
drsboyd@dsl.pipex.com

Abstract

This paper describes a method of performing differential CCD photometry using multiple comparison stars. The instrumental magnitudes of the comparison stars (obtained for example using AIP4WIN v2) are used to compute a weighted mean zero point for each image. The contributions of individual comparison stars are weighted according to their errors. The zero point and its error are then used to derive magnitudes and error estimates for a target object and for each of the comparison stars in the image. Variants of the method may be used for filtered and unfiltered data and for using whatever information is available about the comparison stars. Examples are given of the results of these analyses. Potential advantages of using multiple comparison stars include reduced errors on derived magnitudes compared with using a single comparison star, detection of inaccuracies in comparison star magnitudes, and recognition of variability in comparison stars.

1. Overview of the Method

The principle of the method is straightforward. We use multiple comparison stars to produce a weighted mean value for the zero point of each image. This zero point is then used to calculate a derived magnitude for the target object and for each comparison star in the image. We will assume in what follows that the target object is a variable star although it need not be.

We make the following assumptions: that there is a comparison star sequence available for the field which provides magnitudes and errors for each comparison star in one or more standard filter passbands; that each image has been measured using a program such as AIP4WIN v2 which provides instrumental magnitudes with error estimates for the variable and comparison stars; that transformation coefficients for the relevant filters and their errors have been measured in a calibration procedure; and that we are working with typical telescopic fields of less than 0.5º at altitudes above 30º.

2. Case 1

We will first consider the case where we have standard V- and I-band comparison star magnitudes and errors available in the sequence and we are able to make measurements through standard V- and I-band photometric filters. The conventional formula for the V magnitude for a star transformed to the standard photometric system (see for example [1]) is

$$V = v + T_{VI} * (V-I) + K^1_V * X + K^2_{VI} * X * (V-I) + Z^0_{VI}$$

where

- V is the standard V magnitude of the star (from the comparison star sequence)
- I is the standard I magnitude of the star (from the comparison star sequence)
- v is the observed instrumental magnitude in the V-band (from AIP4WIN v2)
- T_{VI} is a transformation coefficient defined as the gradient of V-v vs V-I
- X is the airmass of the star
- K^1_V is the 1st order atmospheric extinction coefficient in the V-band
- K^2_{VI} is the 2nd order atmospheric extinction coefficient for the (V-I) colour index
- Z^0_{VI} is the V-band exo-atmospheric zero point with respect to the (V-I) colour index

Because we are using differential photometry in small telescopic fields at an airmass below 2, we will make the approximation that the 1st and 2nd order atmospheric extinction terms are the same for all stars in the image and we will absorb them into a single endo-atmospheric zero point term for the image. The inaccuracy in doing this under these conditions is normally less than 0.5% but rises towards the blue end of the spectrum, so this approximation should be reviewed for validity when

observing with larger fields or at a larger airmass, particularly with a B filter.

The above formula for the transformed V magnitude can then be written as

$$V = v + T_{VI} * (V-I) + Z_{VI}$$

where

Z_{VI} is the V-band endo-atmospheric zero point with respect to the (V-I) colour index

A similar formula gives the standard I magnitude

$$I = i + T_{IV} * (V-I) + Z_{IV}$$

where

i is the observed instrumental magnitude in the I-band (from AIP4WIN v2)
T_{IV} is a transformation coefficient defined as the gradient of I-i vs V-I
Z_{IV} is the I-band endo-atmospheric zero point with respect to the (V-I) colour index

Suppose we have n comparison stars for each of which V and I are known from the comparison star sequence. For the j^{th} comparison star we have

$$V_j = v_j + T_{VI} * (V-I)_j + Z_{VI_j}$$

Hence

$$Z_{VI_j} = V_j - v_j - T_{VI} * (V-I)_j$$

$$\sigma Z_{VI_j}^2 = \sigma V_j^2 + \sigma v_j^2 + T_{VI}^2 * (\sigma V_j^2 + \sigma I_j^2) + \sigma T_{VI}^2 * (V-I)_j^2$$

where

σZ_{VI_j} is the standard deviation of Z_{VI_j}
σV_j is the standard deviation of V_j (from the comparison star sequence)
σI_j is the standard deviation of I_j (from the comparison star sequence)
σv_j is the standard deviation of v_j (from AIP4WIN v2)
σT_{VI} is the standard deviation of T_{VI} (from the calibration procedure)

We calculate weights according to the generic formula

$$w_j = 1 / \sigma_j^2$$

so we take the weight of Z_{VI_j} as

$$wZ_{VI_j} = 1 / \sigma Z_{VI_j}^2$$

Thus comparison stars with larger standard deviations contribute with less weight to the analysis. If we represent the weighted mean and weighted standard deviation in the mean (standard error) of Z_{VI} for the image as $\langle Z_{VI} \rangle$ and $\sigma\langle Z_{VI} \rangle$ respectively, we can calculate these as

$$\langle Z_{VI} \rangle = \Sigma_j (wZ_{VI_j} * Z_{VI_j}) / \Sigma_j wZ_{VI_j}$$

$$\sigma\langle Z_{VI} \rangle^2 = \Sigma_j (wZ_{VI_j} * (Z_{VI_j} - \langle Z_{VI} \rangle)^2) / ((n-1) * \Sigma_j wZ_{VI_j})$$

We can then use the weighted mean and weighted standard error of Z_{VI} for the image to derive a transformed V magnitude and its error for any object in the image, including the variable and each of the comparison stars, using

$$V_j = v_j + T_{VI} * (V-I)_j + \langle Z_{VI} \rangle$$

$$\sigma V_j^2 = \sigma v_j^2 + T_{VI}^2 * (\sigma V_j^2 + \sigma I_j^2) + \sigma T_{VI}^2 * (V-I)_j^2 + \sigma\langle Z_{VI} \rangle^2$$

The same procedure is used to derive transformed I magnitudes and errors

$$I_j = i_j + T_{IV} * (V-I)_j + \langle Z_{IV} \rangle$$

$$\sigma I_j^2 = \sigma i_j^2 + T_{IV}^2 * (\sigma V_j^2 + \sigma I_j^2) + \sigma T_{IV}^2 * (V-I)_j^2 + \sigma\langle Z_{IV} \rangle^2$$

where

σi_j is the standard deviation of i_j (from AIP4WIN v2)
σT_{IV} is the standard deviation of T_{IV} (from the calibration procedure)
$\langle Z_{IV} \rangle$ is the weighted mean of Z_{IV} (calculated as for Z_{VI} above)
$\sigma\langle Z_{IV} \rangle$ is the weighted standard error of Z_{IV} (calculated as for Z_{VI} above)

This is clearly an iterative process as V and I appear on both sides of the equation but it is straightforward to implement such an iterative process in a spreadsheet. Experience shows it usually converges after a small number of iterations.

3. Case 2

This is similar to Case 1 in that the same standard V and I magnitudes and filters are available. However we rewrite the formulae for the transformed V and I magnitudes in terms of (v-i) rather than (V-I) as follows.

$$V = v + T'_{VI} * (v-i) + Z'_{VI}$$

$$I = i + T'_{IV} * (v-i) + Z'_{IV}$$

where

T'_{VI} is a transformation coefficient defined as the gradient of V-v vs v-i
Z'_{VI} is the V-band endo-atmospheric zero point with respect to the (v-i) colour index
T'_{IV} is a transformation coefficient defined as the gradient of I-i vs v-i
Z'_{IV} is the I-band endo-atmospheric zero point with respect to the (v-i) colour index

Some manipulation will show that

$$T'_{VI} = T_{VI} / (1 - T_{VI} + T_{IV})$$
$$Z'_{VI} = Z_{VI} + (T_{VI} * (Z_{VI} - Z_{IV}) / (1 - T_{VI} + T_{IV}))$$
$$T'_{IV} = T_{IV} / (1 - T_{VI} + T_{IV})$$
$$Z'_{IV} = Z_{IV} + (T_{IV} * (Z_{VI} - Z_{IV}) / (1 - T_{VI} + T_{IV}))$$

The formulae for Z'_{VI_j} and its standard deviation $\sigma Z'_{VI_j}$ are

$$Z'_{VI_j} = V_j - v_j - T'_{VI} * (v-i)_j$$

$$\sigma Z'^2_{VI_j} = \sigma V_j^2 + \sigma v_j^2 + T'^2_{VI} * (\sigma v_j^2 + \sigma i_j^2) + \sigma T'^2_{VI} * (v-i)_j^2$$

As before, we can then derive transformed V magnitudes and errors

$$V_j = v_j + T'_{VI} * (v-i)_j + \langle Z'_{VI} \rangle$$

$$\sigma V_j^2 = \sigma v_j^2 + T'^2_{VI} * (\sigma v_j^2 + \sigma i_j^2) + \sigma T'^2_{VI} * (v-i)_j^2 + \sigma \langle Z'_{VI} \rangle^2$$

where the weighted mean and weighted standard error for Z'_{VI} are given by

$$\langle Z'_{VI} \rangle = \Sigma_j (wZ'_{VI_j} * Z'_{VI_j}) / \Sigma_j wZ'_{VI_j}$$

$$\sigma \langle Z'_{VI} \rangle^2 = \Sigma_j (wZ'_{VI_j} * (Z'_{VI_j} - \langle Z'_{VI} \rangle)^2) / ((n-1) * \Sigma_j wZ'_{VI_j})$$

The corresponding formulae for the transformed I magnitudes and errors are

$$I_j = i_j + T'_{IV} * (v-i)_j + \langle Z'_{IV} \rangle$$

$$\sigma I_j^2 = \sigma i_j^2 + T'^2_{IV} * (\sigma v_j^2 + \sigma i_j^2) + \sigma T'^2_{IV} * (v-i)_j^2 + \sigma \langle Z'_{IV} \rangle^2$$

This solution does not require iteration as the results are obtained directly in terms of measured and calculated quantities.

4. Case 3

In this case we have standard V magnitudes and (V-I) colour indices and their errors available in the sequence and we can measure using V- and I-band filters. The transformed V magnitude and its error are derived in the same way as in Case 2. We can manipulate the equations for V and I given in Case 2 to get the following formula which will enable us to calculate the transformed (V-I) colour index directly.

$$(V-I) = T'_{V-I} * (v-i) + Z'_{V-I}$$

where

T'_{V-I} is a transformation coefficient defined as the gradient of V-I vs v-i
Z'_{V-I} is the endo-atmospheric zero point for the (v-i) colour index

and it can be shown that

$$T'_{V-I} = 1 / (1 - T_{VI} + T_{IV})$$
$$Z'_{V-I} = (Z_{VI} - Z_{IV}) / (1 - T_{VI} + T_{IV}))$$

The formulae for Z'_{V-I_j} and its standard deviation $\sigma Z'_{V-I_j}$ are

$$Z'_{V-I_j} = (V - I)_j - T'_{V-I} * (v-i)_j$$

$$\sigma Z'^2_{V-I_j} = \sigma (V - I)_j^2 + T'^2_{V-I} * (\sigma v_j^2 + \sigma i_j^2) + \sigma T'^2_{V-I} * (v-i)_j^2$$

We then calculate the transformed (V-I) colour indices and their errors as

$$(V-I)_j = T'_{V-I} * (v-i)_j + \langle Z'_{V-I} \rangle$$

$$\sigma (V-I)_j^2 = T'^2_{V-I} * (\sigma v_j^2 + \sigma i_j^2) + \sigma T'^2_{V-I} * (v-i)_j^2 + \sigma \langle Z'_{V-I} \rangle^2$$

where the weighted mean and weighted standard error for Z'_{V-I} are given by

$$\langle Z'_{V-I}\rangle = \Sigma_j (wZ'_{V-I_j} * Z'_{V-I_j}) / \Sigma_j wZ'_{V-I_j}$$

$$\sigma\langle Z'_{V-I}\rangle^2 = \Sigma_j (wZ'_{V-I_j} * (Z'_{V-I_j} - \langle Z'_{V-I}\rangle)^2) / ((n-1) * \Sigma_j wZ'_{V-I_j})$$

5. Case 4

Here we have V magnitudes and errors but no colour information available in the comparison star sequence and we are able to make measurements through V- and I-band filters. We can derive the transformed V magnitude and its error as in Case 2.

6. Case 5

In this case we only have V magnitudes and errors available for stars in the sequence and we are only able to measure with a V-band filter so we are not able to transform our magnitude to the standard system. We can express the untransformed V magnitude as

$$V = v + Z_V$$

where

Z_V is the V-band endo-atmospheric zero point

so

$$Z_{V_j} = V_j - v_j$$

$$\sigma Z_{V_j}^2 = \sigma V_j^2 + \sigma v_j^2$$

The untransformed V magnitudes and errors are then

$$V_j = v_j + \langle Z_V\rangle$$

$$\sigma V_j^2 = \sigma v_j^2 + \sigma\langle Z_V\rangle^2$$

where

$$\langle Z_V\rangle = \Sigma_j (wZ_{V_j} * Z_{V_j}) / \Sigma_j wZ_{V_j}$$

$$\sigma\langle Z_V\rangle^2 = \Sigma_j (wZ_{V_j} * (Z_{V_j} - \langle Z_V\rangle)^2) / ((n-1) * \Sigma_j wZ_{V_j})$$

7. Case 6

In this case we have V magnitudes and errors from the sequence but we make our measurements without a filter or with a clear (C) filter. We can then only derive an untransformed C magnitude which is not in the standard system. Similarly to Case 5, we use the formula

$$V = c + Z_C$$

where

V is the standard V magnitude (from the sequence)

c is the unfiltered instrumental magnitude (from AIP4WIN v2)

Z_C is the unfiltered endo-atmospheric zero point

As before, we have

$$Z_{C_j} = V_j - c_j$$

$$\sigma Z_{C_j}^2 = \sigma V_j^2 + \sigma c_j^2$$

where

σc_j is the standard deviation of c_j (from AIP4WIN v2)

The untransformed C magnitudes and errors are then

$$C_j = c_j + \langle Z_C\rangle$$

$$\sigma C_j^2 = \sigma c_j^2 + \sigma\langle Z_C\rangle^2$$

where

$$\langle Z_C\rangle = \Sigma_j (wZ_{C_j} * Z_{C_j}) / \Sigma_j wZ_{C_j}$$

$$\sigma\langle Z_C\rangle^2 = \Sigma_j (wZ_{C_j} * (Z_{C_j} - \langle Z_C\rangle)^2) / ((n-1) * \Sigma_j wZ_{C_j}).$$

8. Transformation Coefficients and Filters

Note that only two independent transformation coefficients are required in all of the above cases. The others can be computed from these two, although they could of course be measured directly. This would be a good check for consistency.

The descriptions have been given in terms of V and I filters. We leave it as an exercise for the reader to develop analogous formulae for other filters.

9. Errors

The errors calculated using the above formulae take account of the following sources of uncertainty:

a) errors in the measured instrumental magnitudes due to statistical uncertainty in the ADU counts plus various noise and background sources inherent in the imaging, readout and

measurement processes (these are incorporated in the error provided by AIP4WIN v2);

b) errors in the standard magnitudes of the comparison stars which are usually also given in the sequence, otherwise they have to be estimated;

c) errors in the transformation coefficients which should be known from the calibration process.

10. Advantages of Using Multiple Comparison Stars

Using multiple comparison stars has several potential advantages over using a single comparison star. The random variations which occur in measurements of a single comparison star tend to be smoothed out when measurements of several stars are combined giving smaller errors in the derived magnitudes. Variability in comparison stars can easily be recognised and they can be omitted from the zero point calculation. Inaccuracies in the magnitudes of comparison stars given in the sequence can be identified as these usually lead to a large mean standard error in the zero point over the run. A small zero point error, on the other hand, is a good indication of internal consistency between the comparison star magnitudes.

A large standard error on the zero point for a single image usually indicates there was something wrong with that image, caused for example by an aircraft trail or a cosmic ray. Variation in the zero point during a run is a good indication of changing atmospheric conditions since deteriorating conditions will tend to reduce the zero point. As a rule of thumb, images are usually discarded where the zero point is more than about one magnitude lower than the average highest level.

11. Implementation

These formulae have been programmed into a series of spreadsheets. These take the output from the multiple image ensemble photometry routine in AIP4WIN v2 which contains instrumental magnitudes and errors for each measured star and they calculate derived magnitudes with error estimates. They produce plots which show the variation of the derived magnitudes and errors and the mean image zero point and its error over the run. They also calculate the airmass for each image and generate results in the format required to report to the BAAVSS, AAVSO and the CBA. The BAAVSS now archives measured instrumental magnitudes and errors of the variable and all comparison stars used in the analysis to enable reanalysis at a future date.

The following examples use data obtained with a 0.35m SCT operating at f/5.2 and an SXV-H9 CCD camera.

12. Example 1

Figures 1 and 2 show the transformed V and I magnitudes respectively for the variable and 5 comparison stars in a 4hr run of 15sec exposures using V and I filters on VY Aqr on 7 October 2006. Figure 3 shows the variation in the mean V and I image zero points during the run as the conditions changed with occasional breaks due to clouds. Table 1 lists the V and I magnitudes and errors given in the sequence for the 5 comparison stars and their mean derived V and I magnitudes and errors over the run. These results are calculated using the formulae in Case 1. It also shows the standard deviation of the derived magnitudes over the run labelled "V (or I) mag std dev" as a comparison with the calculated error. The comparison stars used in the zero point analysis are indicated. Given the larger error for star 138, this was not included in the analysis but its magnitude was calculated using the derived zero point. Table 2 shows the same data analysed according to Case 2.

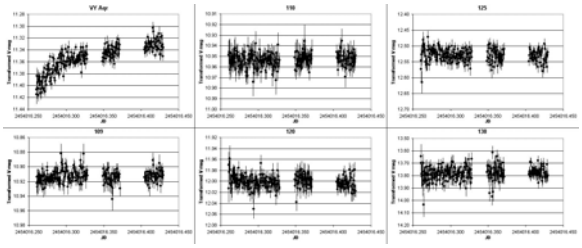

Figure 1: Transformed variable and comparison star V magnitudes

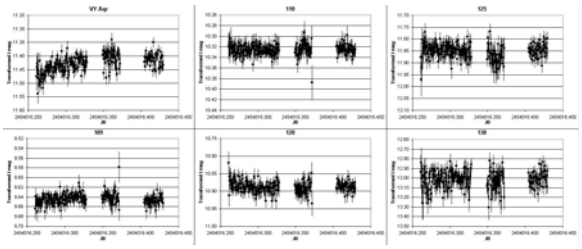

Figure 2: Transformed variable and comparison star I magnitudes

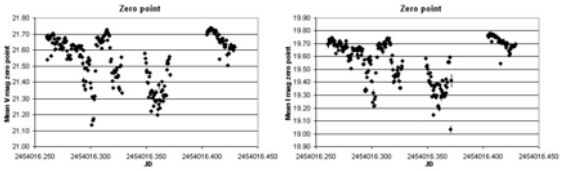

Figure 3: Mean V and I image zero points during a run

ID	V mag sequence	V error sequence	V mag derived	V error derived	V mag std dev	Used in analysis?
109	10.910	0.010	10.913	0.008	0.008	Y
110	10.957	0.010	10.953	0.008	0.007	Y
120	12.001	0.012	12.001	0.013	0.012	Y
125	12.526	0.015	12.530	0.019	0.020	Y
138	13.767	0.020	13.781	0.052	0.055	N
ID	I mag sequence	I error sequence	I mag derived	I error derived	I mag std dev	Used in analysis?
109	9.638	0.010	9.644	0.012	0.010	Y
110	10.336	0.010	10.326	0.013	0.010	Y
120	10.884	0.010	10.888	0.018	0.016	Y
125	11.843	0.010	11.852	0.033	0.031	Y
138	12.972	0.015	13.019	0.088	0.090	N

Table 1: Comparison star sequence and derived V and I magnitudes from Case 1

ID	V mag sequence	V error sequence	V mag derived	V error derived	V mag std dev	Used in analysis?
109	10.910	0.010	10.913	0.008	0.008	Y
110	10.957	0.010	10.953	0.009	0.007	Y
120	12.001	0.012	12.001	0.013	0.012	Y
125	12.526	0.015	12.529	0.019	0.019	Y
138	13.767	0.020	13.781	0.052	0.054	N
ID	I mag sequence	I error sequence	I mag derived	I error derived	I mag std dev	Used in analysis?
109	9.638	0.010	9.643	0.011	0.010	Y
110	10.336	0.010	10.325	0.015	0.011	Y
120	10.884	0.010	10.887	0.018	0.017	Y
125	11.843	0.010	11.851	0.034	0.033	Y
138	12.972	0.015	13.018	0.089	0.094	N

Table 2: Comparison star sequence and derived V and I magnitudes from Case 2

13. Example 2

Figures 4 and 5 show the transformed V and V-I magnitudes respectively for the variable and 5 comparison stars in a 5hr run of 60sec exposures using V and I filters on the variable 1RXS J224342.3+305526 (aka Bernhard 02) on 25 November 2005. Figure 6 shows the mean V and V-I image zero points. Table 3 lists the V magnitudes and errors given in the sequence for the 5 comparison stars together with estimated V-I values obtained from the quoted B-V values using a transformation based on Landolt stars. It also shows the mean derived V and V-I magnitudes and errors over the run for the comparison stars calculated using the formulae in Case 3, together with the standard deviation of the derived magnitudes over the run labelled "V (or V-I) mag std dev" as a comparison with the calculated error. The comparison stars used in the zero point analysis are indicated. Given the possible variability of star 153 and the larger errors on star 161, these were not included in the analysis.

It can be seen that, in this particular example, the calculated errors are considerably larger than the standard deviations of the derived magnitudes. This is because the standard V magnitudes given in the sequence were based on a single night of observation and therefore have larger scatter about their true values, and the V-I magnitudes were estimated. In consequence, the zero point errors are larger and this feeds through into the calculated errors. This correctly reflects the fact that the actual errors are somewhat larger than the standard deviations of the magnitudes might suggest due to the larger uncertainty in the sequence magnitudes.

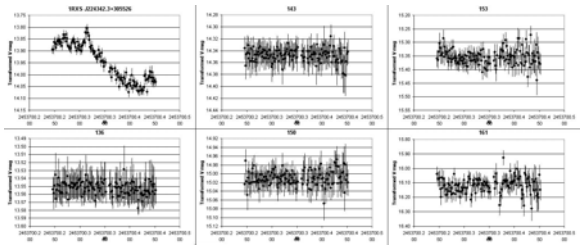

Figure 4: Transformed variable and comparison star V magnitudes

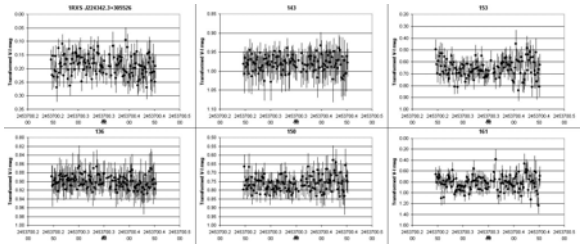

Figure 5: Transformed variable and comparison star V-I magnitudes

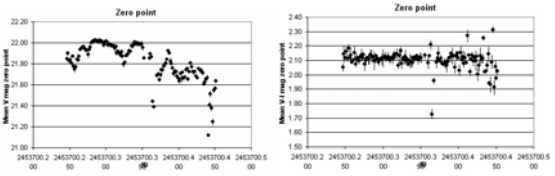

Figure 6: Mean V and V-I image zero points during a run

ID	V mag sequence	V error sequence	V mag derived	V error derived	V mag std dev	Used in analysis?
136	13.576	0.020	13.552	0.018	0.008	Y
143	14.329	0.020	14.348	0.021	0.011	Y
150	14.993	0.020	15.010	0.028	0.017	Y
153	15.325	0.030	15.355	0.034	0.028	N
161	16.070	0.040	16.118	0.059	0.053	N
ID	V-I mag sequence	V-I error sequence	V-I mag derived	V-I error derived	V-I mag std dev	Used in analysis?
136	0.917	0.050	0.901	0.030	0.017	Y
143	0.944	0.050	0.981	0.038	0.020	Y
150	0.793	0.050	0.761	0.062	0.041	Y
153	0.708	0.050	0.655	0.085	0.075	N
161	0.805	0.050	0.820	0.144	0.137	N

Table 3: Comparison star sequence and derived V and V-I magnitudes from Case 3

14. Example 3

Figures 7 and 8 show the untransformed V magnitudes and mean V zero point from a 6hr run of 15sec exposures using a V filter on V2362 Cyg on 1 November 2006. Table 4 lists similar V magnitude information to that given in Table 3. For information, it also includes V-I magnitudes from the sequence which were not used in the analysis. Given the variability of star D and the significantly different colours of stars F and G, these were not included in the analysis. These results are an example of Case 5.

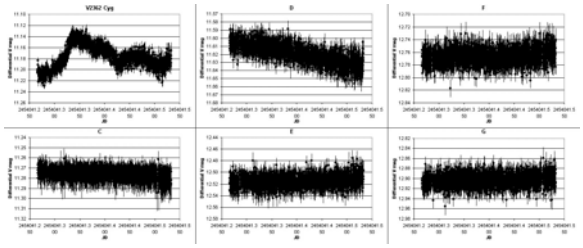

Figure 7: Untransformed variable and comparison star V magnitudes

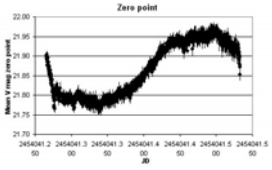

Figure 8: Mean V image zero point during a run

ID	V mag sequence	V error sequence	V-I sequence	V mag derived	V error derived	V mag std dev	Used in analysis?
C	11.270	0.010	0.340	11.270	0.007	0.003	Y
D	11.630	0.010	0.450	11.614	0.007	0.012	N
E	12.510	0.020	0.650	12.510	0.011	0.010	Y
F	12.790	0.020	1.580	12.761	0.013	0.014	N
G	12.910	0.020	1.750	12.898	0.014	0.014	N

Table 4: Comparison star sequence and derived V magnitudes from Case 5

15. Example 4

Figures 9 and 10 and Table 5 show untransformed results for a 6hr unfiltered (Clear) run of 20sec exposures on DW Cnc on 6 February 2007. For information, Table 5 also includes B-V magnitudes from the sequence which were not used in the analysis. Star 145 and 149 were not used in the analysis because of their different colours. This is an example of Case 6.

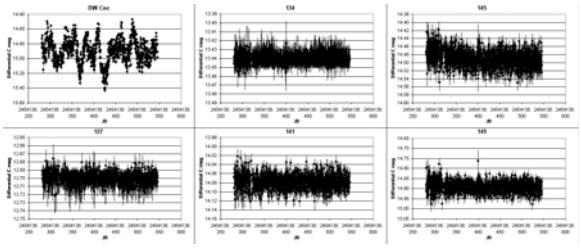

Figure 9: Untransformed variable and comparison star C magnitudes

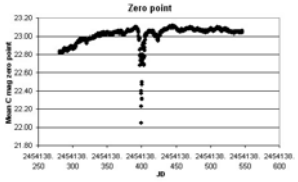

Figure 10: Mean C image zero point during a run

ID	V mag sequence	V error sequence	B-V sequence	C mag derived	C error derived	C mag std dev	Used in analysis?
127	12.695	0.014	0.464	12.700	0.007	0.007	Y
134	13.443	0.008	0.525	13.441	0.010	0.006	Y
141	14.080	0.011	0.529	14.079	0.014	0.012	Y
145	14.546	0.013	0.916	14.490	0.019	0.020	N
149	14.912	0.009	0.737	14.892	0.026	0.026	N

Table 5: Comparison star sequence and derived C magnitudes from Case 6

16. Acknowledgements

I would like to thank all my colleagues in the variable star community worldwide for their willingness to freely share information, experience and advice. This has made climbing the learning curve much less onerous than it might otherwise have been.

I am also grateful to the Royal Astronomical Society for an RAS Grant which has supported my participation in the Symposium and to the British Astronomical Association for a Ridley Grant which assisted development of my observing equipment.

17. References

[1] Massey P., Garmany C., Silkey M., Degioia-Eastwood K., Astron. J., 97, 107-130 (1989)

Galileo's Legacy

Small Telescope Science—1609 and 2009

Russell M. Genet
Orion Observatory
russmgenet@aol.com

* International conference 31 December 2008 – 5 January 2009
  See www.GalileosLegacy.org for conference details

* Conference will be held at the Makaha Resort, Waianae, Oahu, Hawaii
  See www.MakahaResort.net for resort details

Special Focus Sessions
Galileo and his telescopes and discoveries
SCTs and other commercial telescopes
Design and construction of small telescopes
Telescope control systems
Remotely accessed/robotic observatories
CCD cameras today
Spectrographs and aperture photometers
Surveys producing new objects to study
Data mining for amateurs and students
Undergraduate (and high school) astronomical research
Pro-am cooperation in astronomy
Intrinsically variable stars
Eclipsing binaries
Cataclysmic variables
Supernova searches
Asteroid astrometry
Asteroid photometry
Planetary transits
Microlensing

Tutorial sessions
Introduction to CCD cameras
Photometry essentials
Intrinsically variable stars
Eclipsing binary primer

Galileo's Legacy

Today's small telescope science is Galileo's Legacy. Not able to purchase a telescope or even a how-to book, Galileo designed and built his own 1.5-inch aperture telescope, thereby launching the honorable tradition of do-it-yourself telescope-making. In 1609, Galileo turned his newly-made telescope toward the heavens and, in rapid succession, discovered

the mountains on the Moon, a multitude of previously invisible stars, and four moons orbiting Jupiter. Not wishing to be scooped, Galileo wasted no time in describing his discoveries in *Sidereus Nuncius*. Many of Galileo's observations were made from his backyard—his only observatory while under house arrest.

Four centuries after Galileo's 1609 observations—thanks to the revolutionary trio of affordable CCD cameras, small go-to Schmidt-Cassegrain and home-brew telescopes, and personal computers—thousands of backyard Galileos around the planet are now probing cosmic mysteries every clear night. They conduct scientific research across a broad spectrum: tumbling asteroids, pulsating stars, eclipsing binaries, transiting planets, and sputtering matter as it spirals onto white dwarfs and neutron stars.

To commemorate Galileo and celebrate his legacy, 2009 has been designated the International Year of Astronomy (IYA). As midnight on New Year's Eve approaches, fireworks will light up the night sky at the Makaha Resort in Hawaii, launching the IYA with a five-day celebratory conference that will not only honor Galileo and his telescope, but also the many current builders and researchers—amateurs, students, and professionals—who are successfully using small telescopes, CCD cameras, and even spectrographs to advance astronomical science.

How do small telescopes in 2009 compare with Galileo's 1609 telescope? Today's backyard and campus telescopes have apertures around 15 inches (and beyond). With, typically, 10 times the aperture of Galileo's telescope, they have 100 times the light gathering power. Equipped with CCD cameras, they can accumulate photons for an hour, compared with $1/10^{th}$ of a second (or less) for Galileo's eye—some 36,000 times longer. Considering both photon gathering area and integration time, today's small telescopes and CCD cameras can accumulate an amazing 3,600,000 times more photons than Galileo's telescope and eye—not to mention the advantages inherent in today's greater resolution, computerized go-to, and image processing capabilities. No wonder these small telescopes with their CCD "eyes" are such powerful scientific research tools!

We invite you to join an eclectic gathering of amateur, student, and professional small-telescope researchers—not to mention home builders and commercial manufacturers—as, together, we celebrate Galileo's telescope and discoveries and, four centuries later, Galileo's legacy: the remarkable resurgence of small telescope science.

Time-Series Astronomical Photometry Conference

Equipment, Techniques, and Research Opportunities for Smaller Observatories

Russell M. Genet
California Polytechnic State University
rgenet@calpoly.edu

Conference will be held 22-24 June 2007
California Polytechnic State University
San Luis Obispo, California

INTRODUCTION

Thanks to the revolutionary trio of affordable CCD cameras, compact Schmidt-Cassegrain and other go-to telescopes, and highly capable personal computers, smaller observatories have become powerful scientific research facilities. Located in backyards and on college campuses, these observatories are making precise scientific measurements across a broad spectrum: tumbling asteroids, pulsating stars, eclipsing binaries, transiting planets, and sputtering matter as it spirals onto white dwarfs and neutron stars. The amateurs, students, and professors who utilize these observatories have produced a steady stream of high-quality papers, and regularly speak about their results at astronomical conferences.

Although some smaller observatories make astrometric and spectroscopic observations, the bulk of the measurements reported in the scientific literature are photometric time series—changes in the brightness and color of astronomical objects over time. Broad-band photometric measurements, as opposed to highly spread-out "narrow band" spectrographic measurements are well-suited to the meager photons available to smaller telescopes. Time series photometric observations, where one object, such as a star or asteroid, is observed continuously for many hours or even night after night, require considerable telescope time—a precious commodity rationed out in small portions to researchers at larger mountaintop observatories but readily available at smaller observatories.

Astronomical surveys, such as the Sloan Digital Sky Survey (SDSS) and the GNAT-MOTESS Survey, have produced a large number new objects whose light varies over time—pulsating stars, eclipsing binaries, asteroids, possible transits of planets across distant stars, etc. The problem with many of the objects these surveys turn up is they have only been observed a few times—"snapshots" caught now and then during the course of a survey. Understanding these objects requires a "movie," i.e. a series of closely-spaced, essentially continuous photometric observations, and this is exactly where appropriately equipped and operated smaller observatories shine.

CONFERENCE

Establishing, maintaining, and operating a modern smaller observatory equipped with computerized go-to telescopes, CCD cameras, and high-end PCs is no mean feat. To allow efficient operation, many smaller observatories are at least partially automated. Startup is manual, but once the object is acquired, it is automatically tracked and the data automatically recorded. CCD photometry produces large volumes of data—typically about a gigabyte per night. Data reduction and analysis is a somewhat complex process utilizing sophisticated software. The bottom line is that while modern, well-equipped smaller observatories can produce a high volume of cutting-edge science at surprisingly low cost, they are high-tech facilities/operations that require considerable practical knowledge. That is where the Time Series Astronomical Photometry Conference comes in. Its objectives are twofold: (1) to provide practical guidance with respect to photometric equipment and techniques for smaller observatories, and (2) to highlight the many research opportunities available to these observatories.

TALKS, TUTORIALS, AND WORKING SESSIONS

Talks, tutorials, and working sessions are invited in the following areas:

Overview Topics
** Pro-am Cooperation in astronomy
** Undergraduate astronomical research
** Surveys producing new objects to study

Telescopes and Observatories
** SCTs and other commercial telescopes
** Design and construction of small telescopes
** Telescope control systems
** Telescope control software
** Automating (or semi-automating) observatories
** Remotely accessed and robotic observatories

CCD Cameras (and other photometers)
** Introduction to CCD cameras
** CCD cameras today
** Aperture (IR) photometers

Photometry
** Photometry essentials
** Photometry reduction software
** Analysis software

Specific Observing Programs
** Asteroid photometry
** Short-period intrinsically variable stars
** Long-period intrinsically variable stars
** Eclipsing binaries
** Cataclysmic variables
** Planetary transits
** Microlensing

An Amateur Astronomer's Initial Asteroid Lightcurves

Charles Green
Elm Meadows Observatory
12463 Elm Meadows, Riverton, UT 84065
email cgreenx2@msn.com

Abstract

At the 2005 Society for Astronomical Sciences Symposium in Big Bear I set a goal to use my equipment and "hobby" time to generate useful asteroid lightcurves. My efforts continue to achieve this goal. Asteroids 916 America, 607 Jenny, 1297 Sonja and 77 Frigga have journeyed by Earth. I will share with you a brief summary of the experience and knowledge I gained from their visit.

1. Introduction

My interest in amateur astronomy goes back many years. A dark sky and ideal observation conditions were my main objectives. Then, with the onset of CCD cameras I realized that a compromise could be made in my hobby to work around light pollution, enjoy astronomy and maintain employment to pay the bills. With a CCD camera and a goto telescope it was even possible to sleep at night and take astronomical images.

Determining the period and amplitude of asteroid lightcurves is a goal I started after my interest was aroused at the 2005 Society for Astronomical Sciences Symposium in Big Bear. At the SAS conference I found affordable software to relieve much of the pain associated with data reduction. Using these programs I decided this endeavor would be the best use of my modest equipment and time.

At first my effort was toward seeking good telescope alignment in my backyard observatory. Then I started learning the basics of how to take darks and flats used for CCD camera calibration. I found that good, reliable data taken from images, even with good software, does not come easy. Finally, I succeeded in taking several series of images that could be used to practice data reduction.

I'm on the path to accomplish by goal, but I still have more work to do. Friends from my local astronomy group are very helpful and always available to offer their suggestions and support.

2. Observatory

A 10" Meade LX200 6.3 with a 6.3 focal reducer is placed on a pier in a 10'dome. The dome is mounted on a trailer. It was purchased at a local military surplus auction. A nearby work shed is used as a control/warm room. The CCD Camera is a SBIG ST-7E. MPO Connections software by Brian Warner, Bdw Publishing is used to control the telescope and the camera.

Future plans include a roll of roof near the shed to house more equipment.

Figure 1. Observatory

3. Observations and Data Reduction

All exposures are 120 seconds with a 600 seconds delay in light/new dark mode at CCD operating temperature –10 degrees C, unfiltered, differential photometry only. At the end of each night 0.5 second dome flats, and 0.5 second flat darks are obtained and respectively median combined for dark and flat correction. Data reduction is performed using MPO Canopus software, Brian Warner, Bdw Publishing.

My first attempt was asteroid 607 Jenny, chosen from the list of potential targets in Vol. 33 no. 2, Minor Planet Bulletin. Only one session 07/16/2006, 26 exposures were taken. Calibration exposures were not taken. No data points were obtained. From the im-

ages I was able to see results for a four hour unguided session and check focus variation.

The second asteroid attempt was 1293 Sonja, chosen from the list of potential targets in Vol. 33 no. 3, Minor Planet Bulletin. A total of 57 exposures were obtained on three nights, 2006 July 30, Aug. 27, 28; however, dark and flat images proved to be problematic and data reduction is still in process.

Up to this stage of my development I had been using a light box to generate my light flats. Images for calibration were improved by taking dome flats.

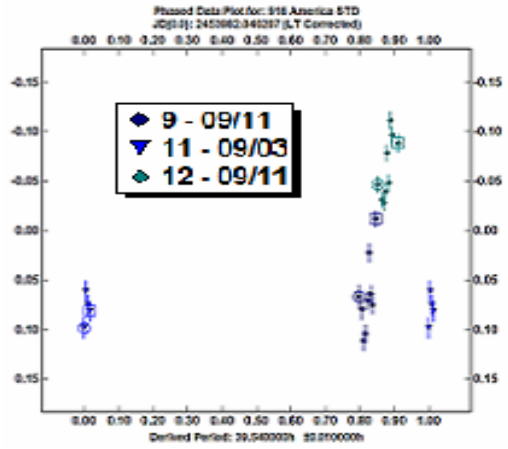

Figure 2. Asteroid 916 America

Asteroid 916 America was my third attempt. It was chosen from the list of potential targets in Volume 33 no. 3, Minor Planet Bulletin. A total of 33 data points from 74 exposures were obtained on three nights, 2006 Sept. 3, 4, 10. After viewing results from three sessions, I realized this was probably a poor choice. The long lightcurve period of 38 hrs would require more observations from different observers in different time zones. The data generated is shown in the phase plot figure 2.

The next asteroid attempt was 77 Frigga, chosen from the list of potential targets in Vol. 33 no. 4, Minor Planet Bulletin. A total of 58 data points from 285 exposures were obtained on four nights, 2006 Sept. 24, 25, 28, 29. A lightcurve was generated which is shown in Figure 3. The phase period 9.012 hours matches published results in Minor Planet Bulletin.

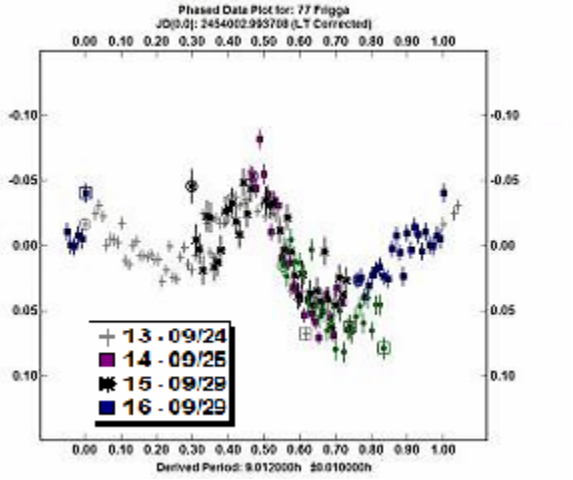

Figure 3. Asteroid 77 Frigga

4. Conclusions

Capturing an asteroid lightcurve period from a backyard observatory is very exciting. Good observing nights at my location are limited, and there are a lot of asteroid opportunities. I plan expansion to two telescopes. Future targets will include asteroids without known lightcurve periods. Determining the period and amplitude of an asteroid is the ultimate goal.

I learned a lot and gained much experience from working with the four asteroids. I plan to continue by efforts and publish useful data for others to use.

5. Acknowledgements

I would like to thank Kurt Fisher, member of the Salt Lake Astronomical Society MPO Study Group, for the help he gave me in understanding MPO Canopus data reduction software.

Thanks to Jerry and Cindy Foote, Vermillion Cliffs Observatory, Kanab, UT. They are always available as a mentor.

A special thanks goes to SAS member Robert Stephens, the guy who sold me the SBIG ST-7E CCD camera with the condition that it was to be use to generate photometry data.

6. References

Kurt Fisher , "A Canopus/PhotoRed Tip Sheet". http://members.csolutions.net/fisherka/astronote/ Photometry/PhotoRedStudy/pdf/ CanopusPhotoRedProcessStepsTips.pdf

Warner, B.D., Kaasalainen, M., Harris, A.W., Pravec, P. (2006). "Lightcurve Photometry Opportunities: April-June, " *Minor Planet Bull.* **33**, 46-47.

Warner, B.D., Kaasalainen, M., Harris, A.W., Pravec, P. (2006). "Lightcurve Photometry Opportunities: July-September, " *Minor Planet Bull.* **33**, 73-75.

Warner, B.D., Kaasalainen, M., Harris, A.W., Pravec, P., Benner, L.A.M. (2006). "Lightcurve Photometry Opportunities: October-December," *Minor Planet Bull.* **33**, 24-25.

Follow-Up Observations of GNAT MG1 Survey Stars: A Summer Community College Student Research Project

Noll Roberts
Dept. of Physical Science, Cuesta College
San Luis Obispo, CA 93403

1. Introduction

Along with two other community college students, Casey Milne and Neelie Jaggi, I used a 10-inch telescope at the Orion Observatory in the fall of 2006 to observe nine GNAT MG1 survey stars whose periods, due to heavy aliasing, were unknown. Two were found to be continuously variable. Lightcurves for these two stars, each with over a thousand data points, were obtained and the variable's periods were determined. This summer (2007), I will be using multiple telescopes to observe a considerably larger number of MG1 stars. I will, again, obtain extensive observations of those stars found to be continuously variable and will attempt to determine their periods.

2. Equipment

The scale of my observational program is determined by the availability of telescopes and CCD cameras. Two Meade LX-200 telescopes, one 10- and one 12-inch, on equatorial wedges and permanent piers at the Orion Observatory, will be my primary instruments. I may be able to set up, on tripods, two 8-inch Meade LX-200R telescopes from Cuesta College, although they are currently lacking equatorial wedges and guidescopes. One SBIG ST-8 camera and five SBIG ST-402 cameras are available. Observations with this equipment will be supplemented by observations made with two Meade 14-inch telescopes (and SBIG cameras), one located at the Dark Ridge Observatory in New Mexico, and the other at the Hill House Observatory in nearby Atascadero, California.

3. Data Reduction and Analysis

MPO Canopus/Photometry Reduction software will be used for data reduction and period analysis. Every effort will be made to reduce the data within a day or two of the observations so the results can be reviewed by the summer program's advisors and appropriate stars can be selected for the next round of observations.

4. TDI (Drift Scan)

I may attempt to utilize the two 8-inch Meade LX-200R Cuesta College telescopes (which lack equatorial wedges) as alt-az, non-tracking systems operating in a time-delayed-integration (TDI) drift scan mode to determine which of the GNAT candidates are continuously variable. The GNAT candidates are all located on a narrow strip of sky near the celestial equator, so repeated TDI scans of approximately a half-hour's duration may provide sufficient data to identify, simultaneously, a number of continuous variables. These would then be observed individually with the equatorial tracking telescopes.

Eclipsing Binary System CU Sagittae

Lee F. Snyder
Kings Canyon Observatory
257 Coventry Drive
Carson City, NV 89703
snyderlf@charter.net

John Lapham
Paradise View Observatory
3722 Paradise View
Carson City, NV 89703
j.lapham@sbcglobal.net

Abstract

A complete lightcurve and six new times of minima (Tmin) of CU Sge are presented. This is a system displaying characteristics similar by physical properties to W Ursae Majoris type contact systems but is not in contact. The lightcurve and computed parameters are presented identifying this binary system as detached with both stars smaller than their limiting Roche lobes and the secondary minimum displaying a total eclipse. The system has been ignored since its discovery and only sixty-eight timings have been published and no spectroscopic values have been derived.

1. Introduction

CU Sge is listed in the General Catalogue of Variable Stars (1949) as an Eclipsing Binary, DW, which are systems with similar properties to W UMa type contact systems but not in contact. It has been ignored but in 1935 and again in 1949 two papers were published in Germany on the orbital times of the system. Since that time, 68 times-of-minimum have been recorded. The lightcurve acquired is symmetrical and out of eclipse indicates the stars have spherical shapes. Modeling of the system by Binary Maker 3, Bradstreet (2004), obtained a fillout = -22% which makes the system detached. The derived temperatures indicate both stars are of spectral type F or G. No spectroscopic velocity curves have been obtained or found in the literature. The orbital period of the system appears to be stable with a slight indication of an increase in the 71 years of observed data.

2. Observations

CU Sge was observed at two observatories during the 2006 session. The Paradise View Observatory utilizes a Meade 14" LX200GPS with an STL-1301 SBIG camera maintaining 2007mm (79") focal length and field of view of 1.49 arcsec/pixel. The Kings Canyon Observatory uses a Meade 12" LX200 Classic with an SBIG ST=9XE yielding a 1920mm (75.6") focal length and FOV of 2.18 arcsec/pixel. All data were obtained in the V and R color system approximating the standard Johnson UBVRI photometric system. Since the comparison stars are on the same CCD images as the variable, extinction corrections for the data were not made.

Data were obtained at the telescope using the MPO Connections Software and reduced using the MPO Canopus software.

3. Photometric Solutions

The lightcurves obtained of CU Sge, Figure 3 in the V and R bands were modeled assuming both stars to be spectral type of F or G and main sequence type. The primary star was set at T = 6600 K and the secondary T was adjusted for modeling. Since the lightcurves indicated this to be a detached system, the radii inputs were used. Since no spectroscopic data is available different mass ratios were attempted until the eclipses were properly fitted. The secondary eclipse, see Figure 5, displays a total eclipse which made determining the mass ratio through trial and error modeling much easier. The best photometric mass ratio, q = 0.30, was determined by measuring the lightcurve residuals until a mass ratio produced the smallest sum of the squares. A fillout for the primary = -0.225 and for the secondary = -0.095 was obtained. Figure 4 displays the geometrical relationships of the surfaces of CU Sge at phase 0.24.

4. Orbital Period Variations

The O-C diagram in Figure 1 includes all the available CCD, photoelectric and visual eclipse times of minimum and were calculated with the linear ephemeris,

Min.I= 2,442,633.473 +0.7916749 E days **(1)**

These times of minimum display a large scatter of up to ± 0.06 days. A polynomial fit indicates a small periodic cyclic sinusoidal change, Figure 2. A least-squares solution yields the following quadratic ephemeris:

Min. I = 2,442,633.472855 ± 0.0078
+ (0.70167216 ± 2.735 x 10^{-6}) E
+ (1.2059 ± 9.169 x10^{-11}) x10^{-10} E^2 days **(2)**

This quadratic term in this equation reveals a continuous period decrease at a rate of dP/dt = +0.0096 sec yr^{-1} which corresponds to a period increase of 0.96 sec $century^{-1}$.

5. Conclusion and Discussion

From the photometric solutions and the light-curves it would be more appropriate to classify the binary system as semi-detached like Algol. I is also possible that the less massive secondary star is more evolved than the primary and mass is being transferred within the system. More data over time will determine is this is an Algol or W UMa type of system.

This research has made use of the SIMBAD database, operated at CDS, Strasbourg, France.

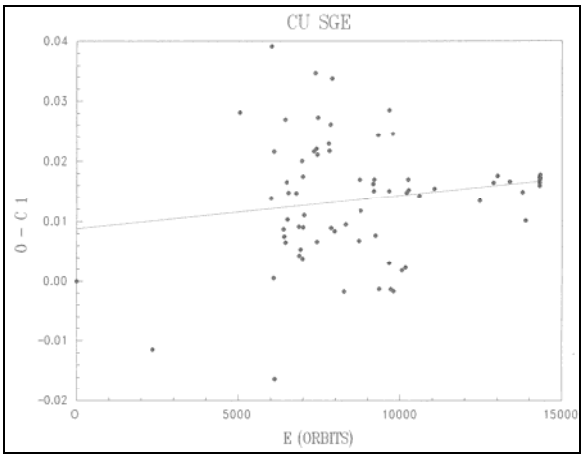

Figure 1. CU SGE O-C1 linear fit.

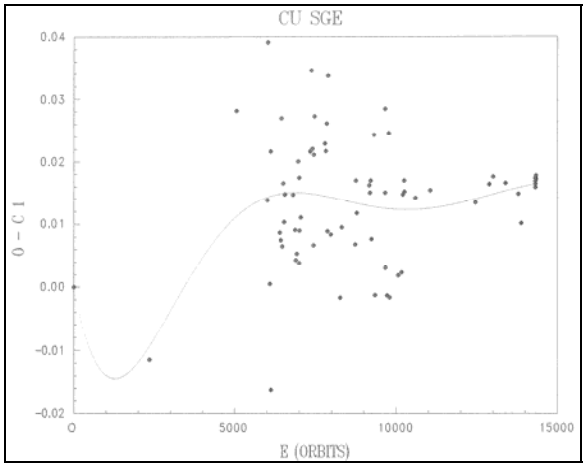

Figure 2. CU SGE O-C1 polynomial fit.

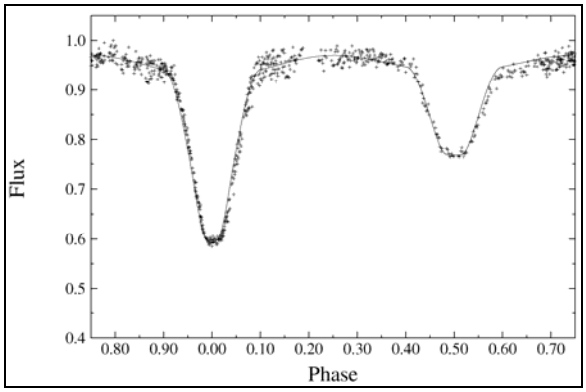

Figure 3. CU SGE modeled with lightcurve data.

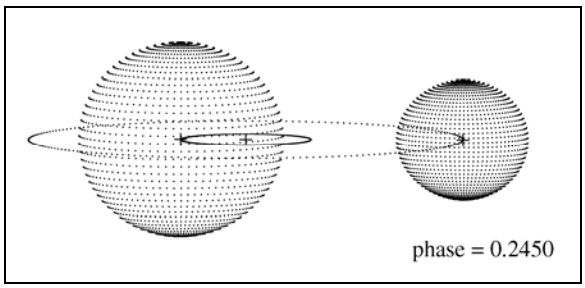

Figure 4. CU SGE 3-D modeling.

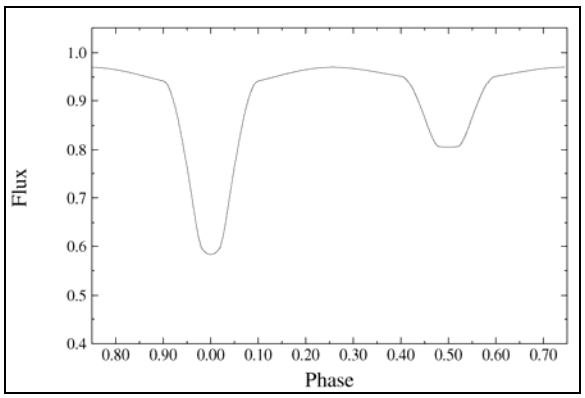

Figure 5. CU SGE modeled without lightcurve data.

Eclipsing Binary Systems
AN TAU, V506 OPH, V609 AQL, and RV TRI

John Lapham
Paradise View Observatory
3722 Paradise View
Carson City, NV 89703
j.Lapham@sbcglobal.net

Lee F. Snyder
Kings Canyon Observatory
257 Coventry Drive
Carson City, NV 89703
snyderlf@charter.net

Abstract

Almost complete light curves for AN TAU, V506 OPH, V609 AQL, and RV TRI, six new times of minimum (Tmin) for AN TAU, an EB/DW system, 14 new Tmin for V506 OPH, an EB/DW system, 4 new Tmin for V609 AQL, an EB/DW system, and 9 new Tmin for RV TRI, an EA/SD system are included. O-C1 and O-C2 values, linear and polynomial curves are displayed.

1. Introduction

During the last half of 2006, four (4) eclipsing binary systems were chosen for observation designed to optimize for long sessions with the target rising at an early evening hour, at a declination convenient to the mechanical limitations of the optical train. Selected systems were V506 OPH, an EB/DM type, V609 AQL, an EB/DW type, AN TAU, an EB/DM type and RV TRI, an EA/SD type (VizieR). Additional selection criteria beyond positioning included 7-13 magnitude range, and a period of 2 to .2 days. Beyond these basic criteria there was no specific agenda. There was a goal to attempt collecting enough data to create a complete light curve and resulting times of minima (Tmin) determined.
Each star was worked as many nights as possible, resulting in enough data points to create a light curve on each star system. Tmin were determined as were O-C calculations.

2. Observations

The Paradise View Observatory utilizes a Meade 14" LX200GPS with attached STL-1301 SBIG camera with a resulting 2007mm (79") focal length and an effective field of view of 1.49 arcsec/pixel (Figure 1). The Kings Canyon Observatory uses a Meade 12" LX200 classic with attached SBIG ST-9XE yielding a 1920mm (75.6") focal length and an effective field of view of 2.18 arcsec/pixel (Figure 2).

Star systems surveyed with associated information (VizieR) are displayed in Table 1. Table 2 lists database websites accessed in determining suitable star systems to observe and also provided additional information for various calculations. Times of minimum were obtained in the VR color system approximating the standard Johnson photometric system. Software used for reductions, charting and computations are listed in Table 3. Thirty-three (33) times of minimum were determined and are listed in Table 4.

A typical session starts days or weeks prior to the actual observation with a target selection. Using the AAVSO VSX query engine found at the AAVSO website (AAVSO VSX), potential candidates are selected and reviewed. TheSky6 software gives a visual feel for the candidates so local star densities can be seen, close neighbor systems that might make the target more challenging and actual rising, setting and air-mass 2.0 times. Once a star system is selected an observing and data collection script is created to coordinate the telescope and camera system for imaging through the night ending with a system shutdown and parking. Both observatories have standardized on the MPO software program "Connections" for scripting.

These observatories are not automated beyond the telescope and camera, so each night protective covers need to be removed and each morning replaced. Power and initiation procedures for the telescope and camera are manual as is the focus proce-

dure. Since an automated script is used, weather or the potential for foul weather, clouds, adverse winds and certain periods of the moon are factored into whether an observing session is prudent.

The following morning the equipment is secured and usually data reduction begins. The Software Bisque program "CCDSoft5" and MPO's "Canopus" are used to combine the images with flats, darks and bias which are collected most nights. The images are then run through Canopus to reduce the images for the data points and to graph the portion of the light curve for the night. These light curves are combined in Canopus to yield the corresponding more complete light curve for that system. The data is further analyzed using "PSI-Plot", "Peranso" and "Excel" at a later date.

Figure 1. Paradise View Observatory

Figure 2. Kings Canyon Observatory

System	Type	Spectral Type	Mag V	AML sec/year Observed
V506 OPH	EB/DM	A/F	11.20	+0.00579
V609 AQL	EB/DW	F8/-	11.70	-0.00990
AN TAU	EB/DM	A3/-	10.30	-0.04239
RV TRI	EA/SD	F9/K2	11.40	+0.01667

Table 1. List of Eclipsing Binary Systems Observed. AML=Angular Momentum Loss

Bob Nelson's O-C files	http://www.aavso.org/observing/programs/eclipser/omc/nelson_omc.shtml
SIMBAD	http://simbad.u-strasbg.fr/simbad/
VizieR	http://vizier.u-strasbg.fr/viz-bin/VizieR
AAVSO VSX	http://www.aavso.org/vsx/

Table 2. Database Websites Accessed

Software Bisque – CCDSoft5	Image Processing and CCD Camera Control
Software Bisque – TheSky6	Planetarium
Microsoft – Excel	Spreadsheet
MPO Software – Canopus/PhotoRed	Data Processing
MPO Software – Connections	Telescope and Camera Control
PERANSO	Period Analysis
PSI-Plot	Technical Plotting and Data Processing

Table 3. Software Used in Observation and Data Reduction

OBJECT	HJD +2,400,000	Sd	Filter	Type		OBJECT	HJD +2,400,000	Sd	Filter	Type
V506 OPH	53886.760500	0.00002	V	II		AN TAU	54035.737200	0.00003	V	I
V506 OPH	53886.763320	0.00006	R	II		AN TAU	54035.737000	0.00003	R	I
V506 OPH	53887.817538	0.00007	V	II		AN TAU	54038.964255	0.00001	V	I
V506 OPH	53887.822400	0.00006	R	II		AN TAU	54038.963245	0.00004	R	I
V506 OPH	53948.794500	0.00004	V	I		AN TAU	54039.775000	0.00007	V	II
V506 OPH	53948.793310	0.00005	R	I		AN TAU	54039.800846	0.00005	R	II
V506 OPH	53956.748960	0.00003	V	I		RV TRI	54077.919194	0.0003	R	I
V506 OPH	53956.748400	0.00005	R	I		RV TRI	54077.920690	0.0001	V	I
V506 OPH	53957.808500	0.00008	V	II		RV TRI	54076.785953	0.0003	R	II
V506 OPH	53957.799667	0.00007	R	II		RV TRI	54087.717593	0.0001	R	I
V506 OPH	53964.702818	0.00002	V	I		RV TRI	54088.857158	0.0002	R	II
V506 OPH	53964.704480	0.00005	R	I		RV TRI	54076.793463	0.0006	V	II
V506 OPH	53965.763161	0.00002	V	I		RV TRI	54087.718074	0.00004	V	I
V506 OPH	53965.762308	0.00004	R	I		RV TRI	54089.606204	0.0004	V	II
V609 AQL	53966.801237	0.00002	V	I		RV TRI	54088.850000	0.0002	V	II
V609 AQL	53966.800236	0.00004	R	I						
V609 AQL	53968.793472	0.00003	V	II						
V609 AQL	53968.761756	0.02000	R	II						

Table 4. Target Stars with New Times of Minima. Type I = Primary Type II = Secondary

3. Systems

3. 1. V506 OPH

V506 OPH, located at RA 17 41 04.2 hours, Dec +07 47 04 degrees is considered to be an EB/DM variable ranging in brightness from 11.2 to 12 magnitude and a period of 1.0604, Epoch of 2428543.603. VizieR describes an EB/DM as EB are "Beta Lyrae-type eclipsing systems. These are eclipsing systems having ellipsoidal components and light curves for which it is impossible to specify the exact times of onset and end of eclipses because of a continuous change of a system's apparent combined brightness between eclipses; secondary minimum is observed in all cases, its depth usually being considerably smaller than that of the primary minimum; periods are mainly longer than 1 day. The components generally belong to early spectral types (B-A). Light amplitudes are usually <2 mag in V. DM - Detached main-sequence systems. Both components are main-sequence stars and do not fill their inner Roche lobes." (SIMBAD, VizieR)

Bob Nelson's O-C chart contains 50 times of min between 1974 and 2004 (Nelson). Further searching of the literature revealed 12 more in 2005 (IBVSa). We were able to determine 14 more times of minimum in 2006 from our own imaging sessions.

O-C1 calculations were done on the times of minimum to determine what changes have been occurring since discovery. Further O-C2 calculations were accomplished using the PSI-Plot software to determine if there were any regular patterns of change. See Figures 3 and 4 for O-C curves and Figure 5 for the light curve created from 2006 sessions.

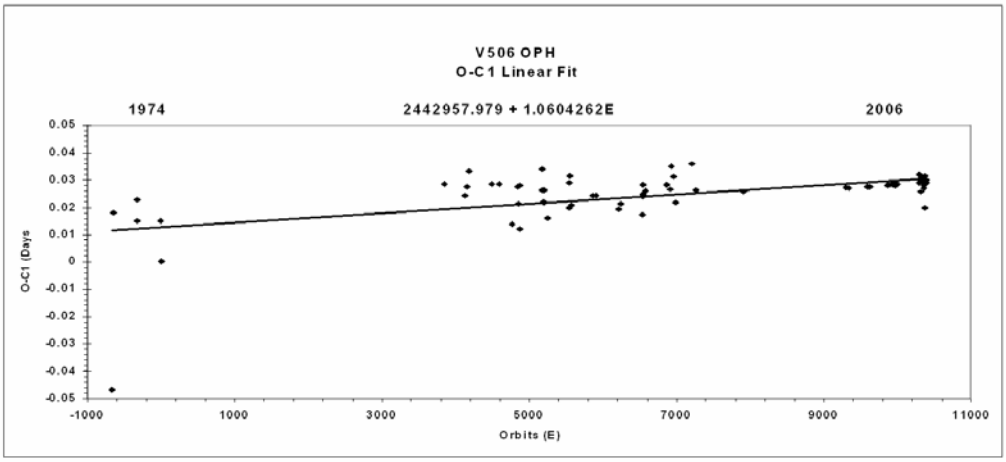

Figure 3. V506 OPH O-C1

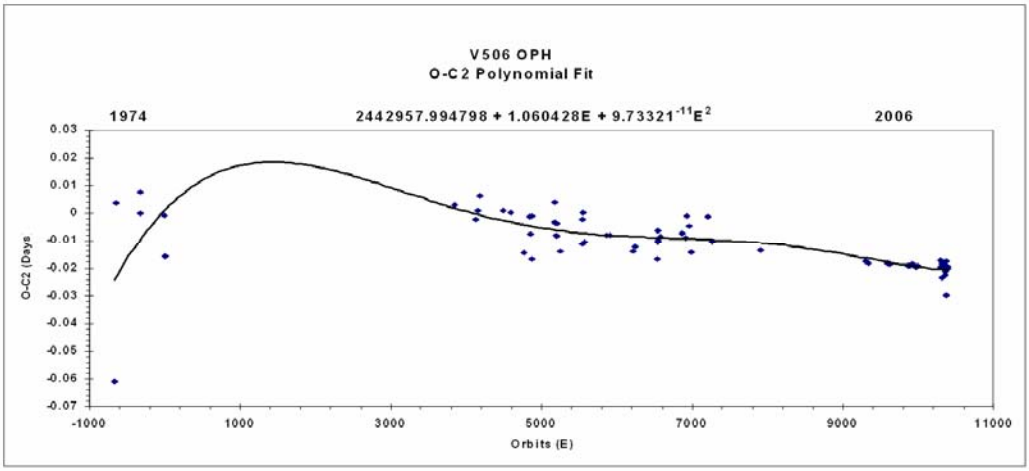

Figure 4. V506 OPH O-C2

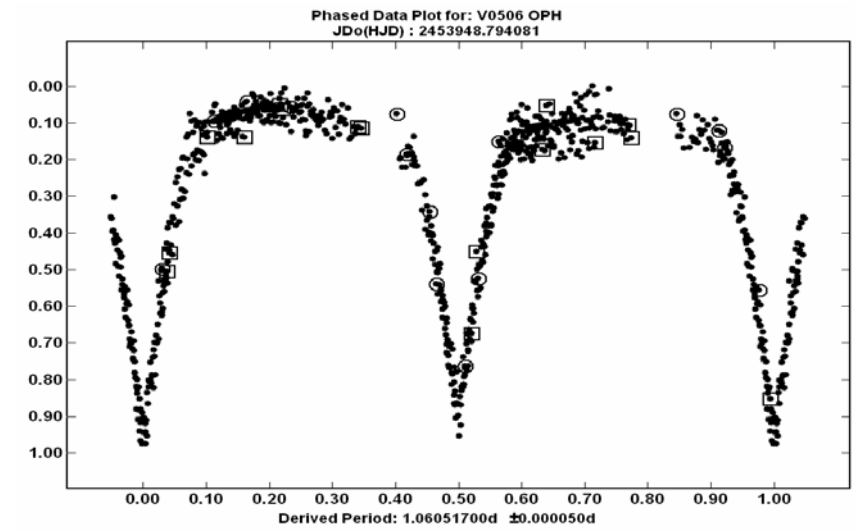

Figure 5. V506 OPH Light Curve

3. 2. V609 OPH

V506 OPH, located at RA 17 41 04.2 hours, Dec +07 47 04 degrees is considered to be an EB/DM variable ranging in brightness from 11.2 to 12 magnitude and a period of 1.0604, Epoch of 2428543.603. VizieR describes an EB/DM as EB are "Beta Lyrae-type eclipsing systems. These are eclipsing systems having ellipsoidal components and light curves for which it is impossible to specify the exact times of onset and end of eclipses because of a continuous change of a system's apparent combined brightness between eclipses; secondary minimum is observed in all cases, its depth usually being considerably smaller than that of the primary minimum; periods are mainly longer than 1 day. The components generally belong to early spectral types (B-A). Light amplitudes are usually <2 mag in V. DM - Detached main-sequence systems. Both components are main-sequence stars and do not fill their inner Roche lobes." (SIMBAD, VizieR).

Bob Nelson's O-C chart contains 50 times of min between 1974 and 2004 (Nelson). Further searching of the literature revealed 12 more in 2005 (IBVSa). We were able to determine 14 more times of minimum in 2006 from our own imaging sessions.

O-C1 calculations were done on the times of minimum to determine what changes have been occurring since discovery. Further O-C2 calculations were accomplished using the PSI-Plot software to determine if there were any regular patterns of change. See Figures 3 and 4 for O-C curves and Figure 5 for the light curve created from 2006 sessions.

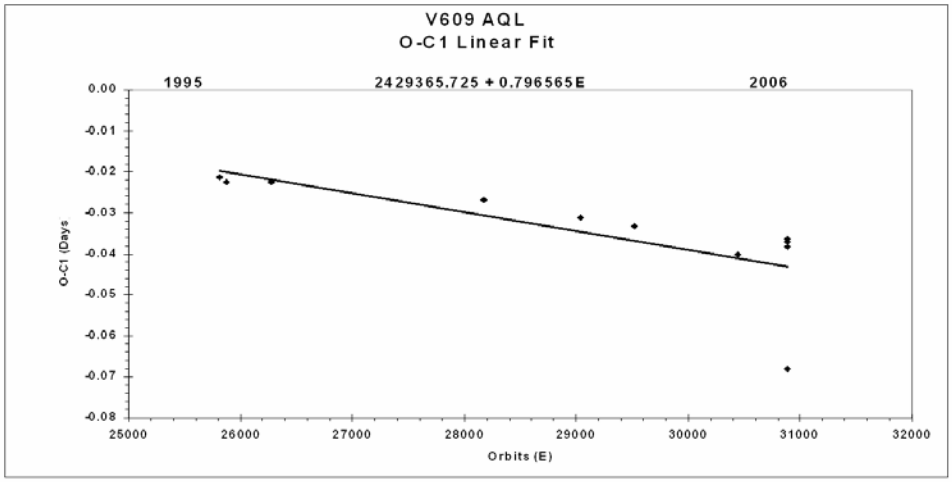

Figure 6. V609 AQL O-C1

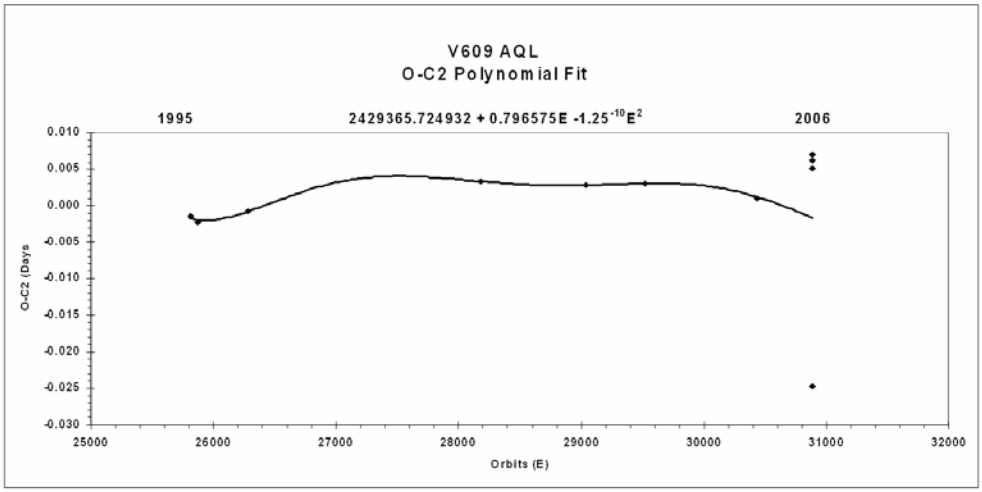

Figure 7. V609 AQL O-C2

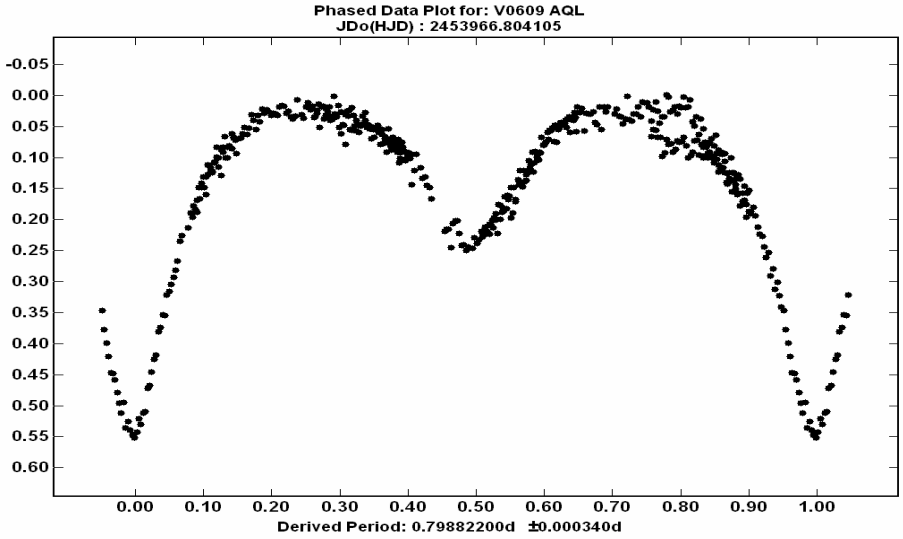

Figure 8. V609 AQL Light Curve

3. 3. AN TAU

AN TAU, located at RA 03 56 11.4 hours, Dec +29 31 23 degrees is considered to be an EB/DM like V 506 OPH described in section 3.1. The system ranges in brightness from 10.3 to 11.15 mag and has a period of 1.614640, Epoch of 2428181.3880 (SIMBAD, VizieR).

Bob Nelson's O-C charts contain 14 times of minimum (Nelson) and a reference search turned up 2 more times of minimum (IBVSd). Our observations produced another 6 times of minimum. Nelson describes the O-C relationship as "Very Uncertain". As such we haven't added any curves to the charted O-C1 data as seen in Figure 9.

O-C1 calculations were done on the times of minimum to determine what changes have been occurring since discovery. Further O-C2 calculations were accomplished using the PSI-Plot software to determine if there were any regular patterns of change. Figure 10 displays the polynomial fit for the O-C2 data. Figure 11 is the light curve from this year's observations.

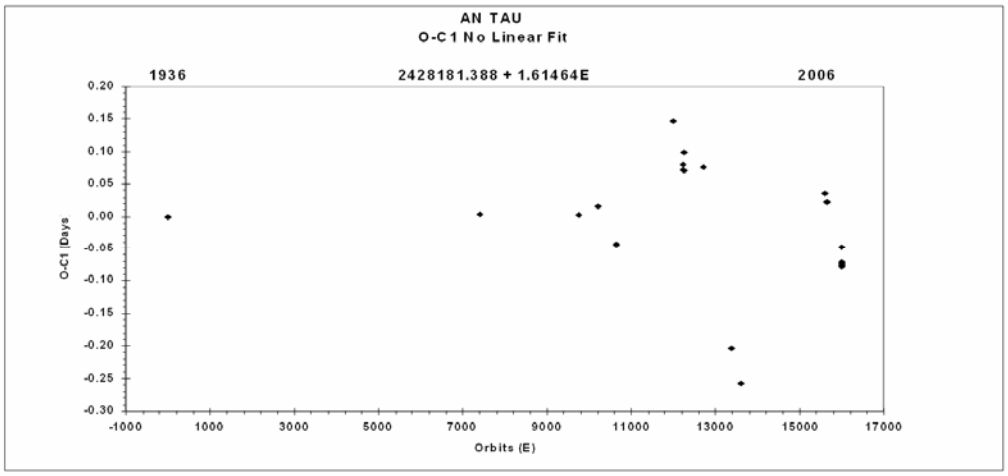

Figure 9. AN TAU O-C1

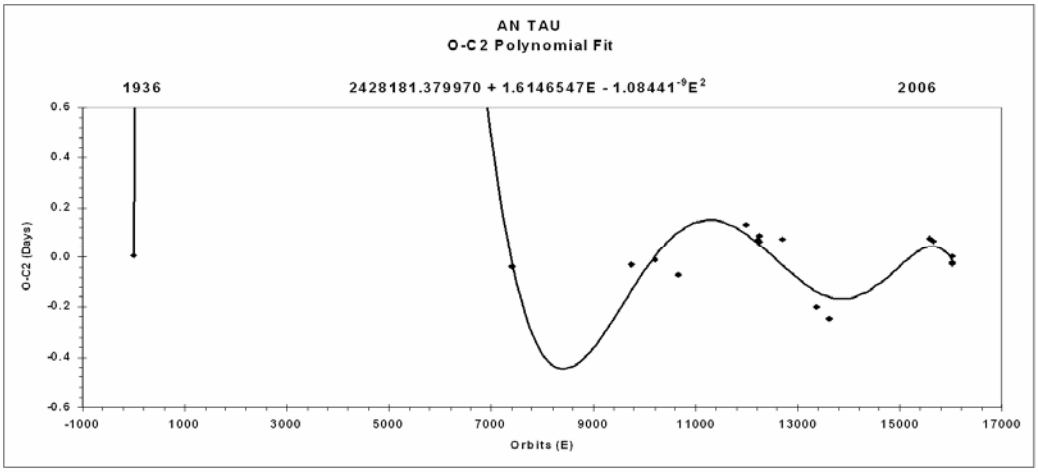

Figure 10. AN TAU O-C2

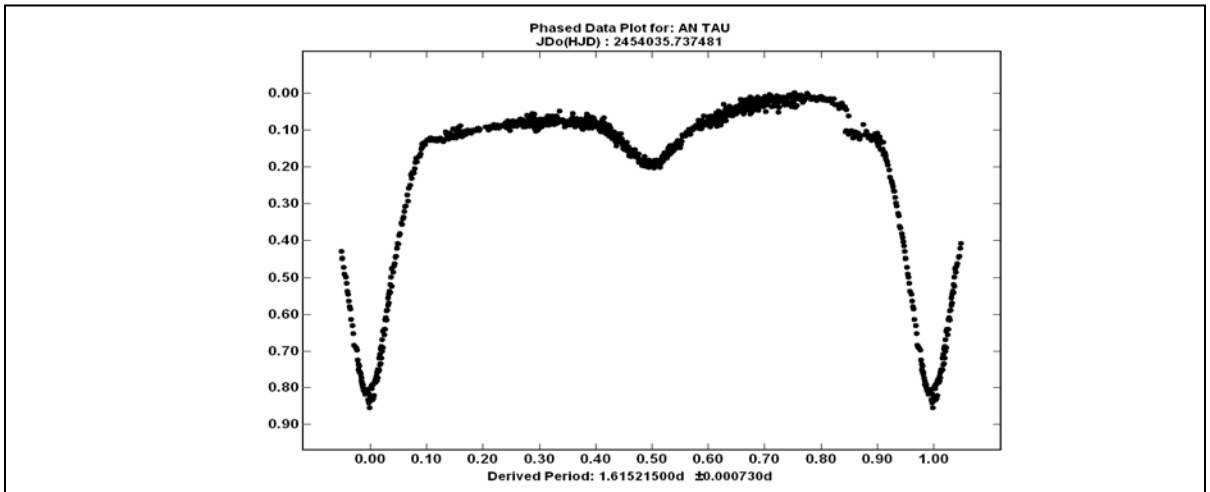

Figure 11. AN TAU Light Curve

3. 4. RV TRI

RV TRI, located at RA02 13 18.2 hours, Dec +37 01 01 degrees is listed as an EA/SD variable. This system ranges in brightness from 11.5 to 13.3, has a period of 0.753666480 and Epoch of 2446033.3080. VizieR describes the EA component as "Algol (beta Persei)-type eclipsing systems. Binaries with spherical or slightly ellipsoidal components. It is possible to specify, for their light curves, the moments of the beginning and end of the eclipses. Between eclipses the light remains almost constant or varies insignificantly because of reflection effects, slight ellipsoidality of components, or physical variations. Secondary minima may be absent. An extremely wide range of periods is observed, from 0.2 to >= 10000 days. Light amplitudes are also quite different and may reach several magnitudes." and SD as "Semidetached systems in which the surface of the less massive component is close to its inner Roche lobe." (SIMBAD, VizieR)

Bob Nelson's O-C file for RV TRI contains 198 times of minimum (Nelson), reference review discovered another 3 times of minimum (IBVSe, f) and for this paper we derived 9 more times of minimum.

O-C1 calculations were done on the times of minimum to determine what changes have been occurring since discovery. Further O-C2 calculations were accomplished using the PSI-Plot software to determine if there were any regular patterns of change. Figures 12 and 13 are the charts derived from the O-C1 and O-C2 calculation. Figure 14 is the light curve from this year's observations.

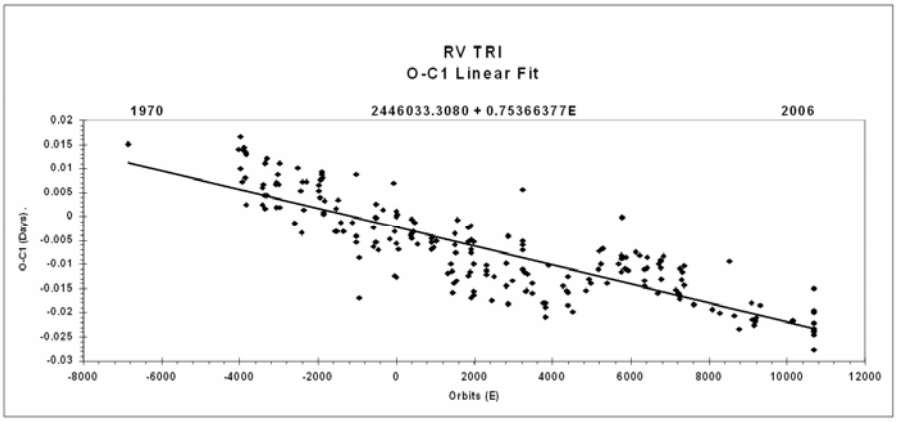

Figure 12. RV TRI O-C1

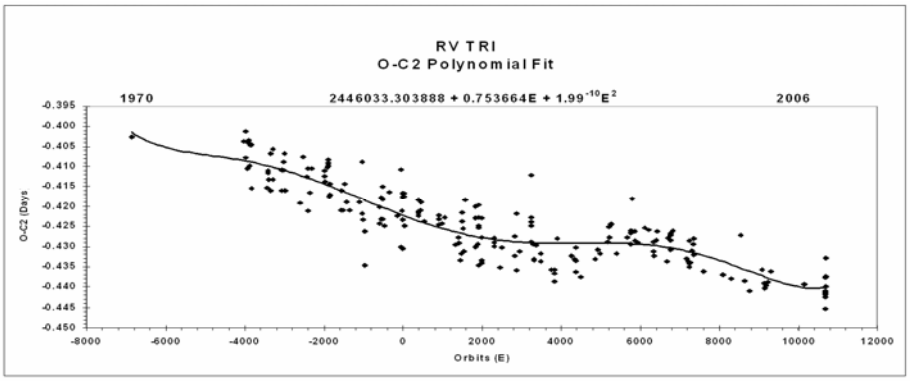

Figure 13. RV TRI O-C2

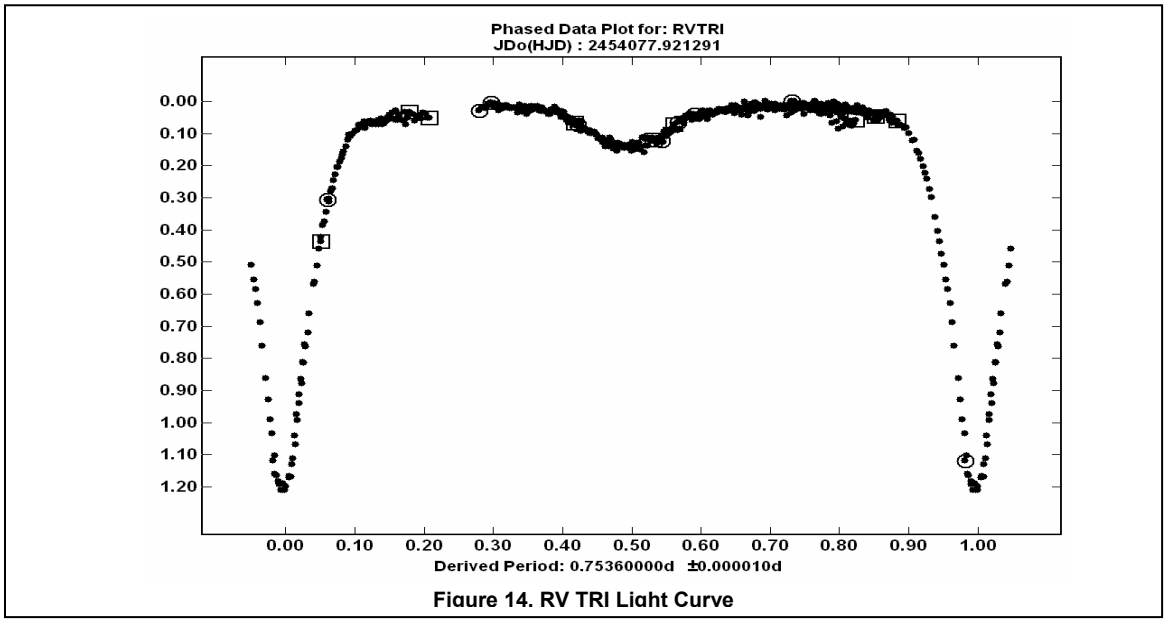

Figure 14. RV TRI Light Curve

4. Conclusion

Four eclipsing binary systems were observed in 42 sessions during the last half of 2006 with the intention of collecting enough data to provide a complete light curve for each system. As demonstrated we were able to produce high quality, almost complete light curves on each system, capturing enough primary and secondary eclipses to determine 33 new times of minimum. It was also shown that the new data fit nicely with O-C data and curves created in previous work.

The whole procedure has been a stimulating learning process that involved learning how to work with the hardware, integrating the software into the process, and doing on-line research to aid in selecting appropriate targets. This was all done with off the shelf equipment and relatively inexpensive software to produce high quality data comparable to previous research.

5. References

2003IBVS.5438....1D (2003 *IAU Inform. Bull. Var. Stars* **5438**, 1.

2006IBVS.5670....1L (2006). *IAU Inform. Bull. Var. Stars* **5670,** 1.

2006IBVS.5672....1N (2006) *IAU Inform. Bull. Var. Stars* **5672**, 1.

2006IBVS.5676....1K (2006). *IAU Inform. Bull. Var. Stars* **5676**, 1.

2006IBVS.5694....1K (2006) *IAU Inform. Bull. Var. Stars* **5694**, 1.

2006IBVS.5731....1H (2006). *IAU Inform. Bull. Var. Stars* **5731**, 1.

2007IBVS.5745....1S (2007) *IAU Inform. Bull. Var. Stars* **5745**, 1.

AAVSO VSX Web Site: http://www.aavso.org/vsx/

Bob Nelson's O-C Tables, AAVSO Site:
http://www.aavso.org/observing/programs/eclipser/omc/nelson_omc.shtml

SIMBAD Web Site:
http://simbad.u-strasbg.fr/simbad/

VizieR Web Site:
http://vizier.u-strasbg.fr/viz-bin/VizieR

A Pellicle Autoguider for the DSS-7 Spectrograph

Gary M. Cole
Starphysics Observatory
14280 W. Windriver Ln, Reno, NV 89511
garycole@mac.com

Abstract

A pellicle beamsplitter has been developed to guide long exposures for a SBIG DSS-7 spectrograph on a C-14 telescope. The motivation for this work was to get good quality classification spectra for variable stars in the 12+ magnitude range. The poster will discuss design tradeoffs, physical implementation, and include sample results.

1. Introduction

The SBIG DSS-7™ Spectrograph provides a combination of useful resolution (R~400) and unusually high efficiency nearing 40% (Holmes 2005).

This combination significantly extends the magnitude limit of spectroscopic observations that can be made with 20-40cm class telescopes. The resolution is more than sufficient for high quality stellar classification work and is particularly well suited for red variable stars.

2. Background

Stellar classification was the major focus of observational astronomy in the period from 1870 to 1920, culminating with the remarkable work of Annie Jump Cannon in the Henry Draper survey.

These spectra stop at about 9th magnitude, and have limited red coverage due the limitations of the instrumentation and photographic plates.

Despite the passage of newly 100 years, a quick check of the SIMBAD system showed only some 560K objects with spectral classifications.

In particular, many red objects that are routinely monitored by AAVSO observers do not have published classifications.

Until the introduction of the DSS7 there were limited opportunities to explore the spectra of objects below 8th magnitude.

On one side was the SBIG SGS instrument, which provided excellent resolution, but is limited to about 9th magnitude at 1-hour exposure.

On the other side was the use of a grism, objective prism, or simple diffraction grating. These have limited resolution (typically R~80).

The DSS-7, in contrast, can reach 9th magnitude in about 30 seconds at R~400 and allows much better background subtraction than a simple grating. And it is matched with a highly red sensitive camera.

3. Instrumentation

The DSS-7 presents a slit onto which the star image must be maintained during the exposure. On a C-14 telescope, this slit subtends approximately 2.2 arc seconds at F13.

The instrument provides a imaging mode for initial positioning, but has no provision for guiding during the exposure.

While I have no doubt that some amateurs have systems that are drift free for long periods of time, I don't. Hence the challenge was to find a way to exploit the efficiency inherent in the device by enabling long guided exposures.

Note that while the DSS-7 guiding problem is very similar to that found in normal imaging, it is not exactly the same. The difference is that the star position is absolutely fixed, you cannot slide the image back and forth to get a guide star on the guide chip.

The second point is a corollary of the first, there will always be a guide star at a fixed position i.e., the star on the slit.

There are several standard ways of guiding long duration images: Independent guide scope, off-axis guide camera, a coplanar guider and on-axis guiders.

In my case I found that differential flexure limited exposures to 5 minutes using my co-mounted C-8/ST7 as independent auto-guider.

The use of a coplanar guide chip (the SBIG self guiding design) does apply because the entire image space is illuminated by the dispersed spectrum.

In a meeting with Dr. Russ Genet, Tom Smith, Dr. Dale Mais, Dr. Eric Crane, John Pye, Dr. Alan Holmes of SBIG and myself held at Orion Observatory in August of 2006, we considered a number of alternatives for guiding the DSS-7.

These concepts included off-axis, near-axis and on-axis alternatives. The near-axis idea, proposed by Tom Smith, was to use a hole in the middle of a flip

mirror. The on-axis concept, which I pursued after the meeting, was to make use of a simple optical element called a "pellicle". In retrospect, I am not sure who introduced this idea, but Alan Holmes made some comment about it, so I will give him credit.

Pellicles are thin films of Nitrocellulose, which can be used as optical windows and as beamsplitters.

According to the information provided by the Edmund Optics catalog, they have a flat spectral transmission over the 400-800nm range of the spectrograph.

Using a pellicle as a beamsplitter, one can guide on the same star that illuminates the spectrograph slit. Essentially this becomes an on-axis guider.

4. Design considerations

Using a beamsplitter reduces the amount of light reaching the spectrograph. Since my objective was to image dim stars, I wanted the least light loss consistent with guiding requirements.

The practical limit for using the DSS-7 is reached when the star image obtained using the imaging mode is too dim to allow convenient positioning onto the slit using short exposures (1-5 seconds).

The imaging mode of the DSS uses a zero order reflection from the grating as its mirror. This grating reflects about 15% in zero order. Hence the DSS image is about two magnitudes fainter than an equivalent direct image.

As a practical matter, I have found that 14th Magnitude is about the limit for star positioning. In this case, a 14th magnitude star has the apparent brightness of a 16th magnitude star in the DSS imaging mode. This is about the limit of a 5 second integration.

My goal was to provide the auto-guider with an image of similar brightness. Using the rule of thumb that 10th magnitude = 0.1 seconds for guiding, an effective 16th magnitude requires a guide time of about 25 seconds.

The choice of beamsplitter ratios, however, is rather limited. You can get an uncoated pellicle that reflects 8% or a coated one that reflects 33%, 40% or 50%.

What I wanted was 15% to match the grating. I choose the 8% pellicle figuring I would rather have more transmission and a longer guide cycle.

5. Construction

A TECHSPEC™ Pellicle Beamsplitter (NT39-478) was obtained from Edmund Industrial Optics. The pellicle is mounted on an aluminum ring 35-mm in diameter and 4.7 mm thick.

Figure 1. The 8% pellicle on its mounting assembly.

An older Celestron® off-axis guider body was recycled to hold the assembly. The pickoff mirror and field stop were easily removed leaving a 1.5 inch main body with a 1.25 inch side tube.

To mount the pellicle, I used a section of 1.25 PVC plumbing pipe. The outside diameter of this provided a close fit to the inside of the guider body.

A 45-degree cut was made using a miter box. The pellicle ring was attached to a metal plate and then to the finished face with superglue. The glue provides an adequate bond between the aluminum ring and PVC plastic, but it can be broken when needed.

Figure 2. Looking through the pellicle.

Note that while the clear aperture of the pellicle is 25mm, it is reduced to an ellipse of about 17 by 25 mm when mounted at 45 degrees. The mounting ring itself is about 4 mm high, which also slightly vignettes the beam.

In my system, the pellicle sees an f/13 beam. The 17 millimeter light cone allows a maximum back distance of about 220mm to fully illuminate an on-axis star.

Collimating this simple assembly with the spectrograph proved more difficult than I had envisioned. A series of thumbscrews were threaded into the housing to push the inner tube for collimation.

Final alignment was done on a C-5 telescope. A crosshair eyepiece was mounted in the pellicle tube and another mounted in a collimated diagonal mounted behind the assembly. Tweaking the thumbscrews brought the alignment to within 5 arc minutes, within the field of the guide camera.

6. Telescope Installation

First Light was achieved on October 26, 2007 using the assembly shown in Figure 3 mounted on the C-14. A piggybacked C-8 provides photometry.

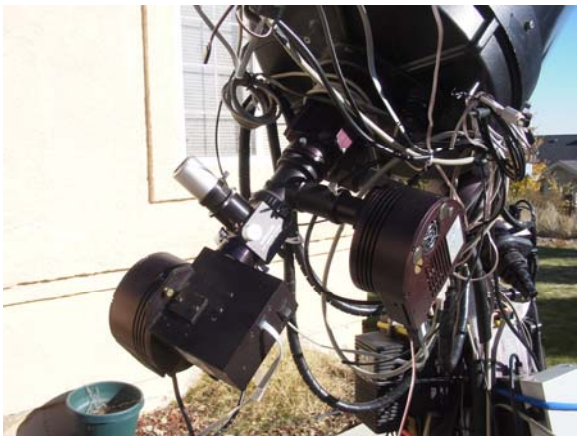

Figure 3. The pellicle is at the top with a ST-7E camera mounted on the long arm to the right. It is followed by a flip mirror and the DSS-7 assembly with its ST7-ME.

The initial test used the ST-7E guide camera at prime focus, but this was later changed to about f6 with the inclusion of a focal reducer. This also allowed the guide camera to move closer to the axis.

7. Observations

The image quality at the guide camera was not quite as good as I expected. I attribute some of this to unwanted reflections in my mounting hardware, but some loss in quality may be due to the pellicle. Significant distortions and reflections can be seen in Figure 4.

The pellicle surface is rated at 1 wave per inch. My FWHM at the spectrograph is about 5 arc seconds, and about 8 at the guider.

There was no visible degradation in the transmitted image, either though the spectrograph or in the eyepiece at high magnification.

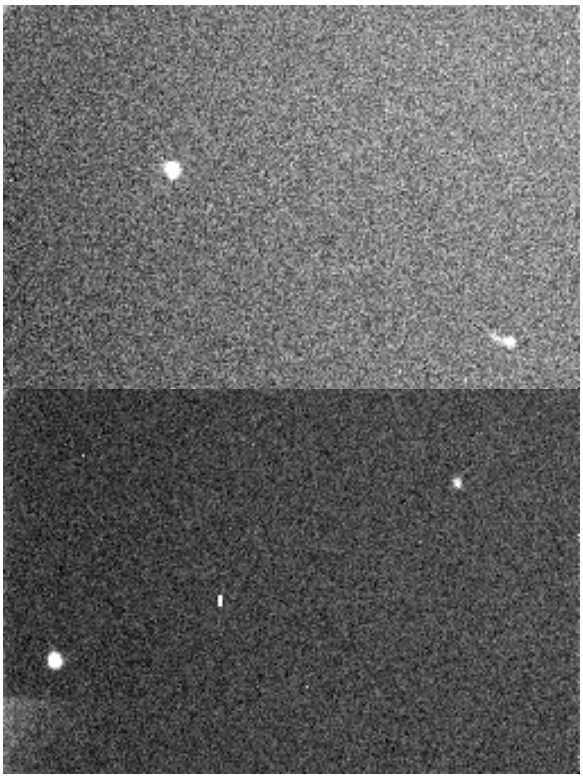

Figure 4. Peliicle guider image above and DSS image below. Vertical axis is flipped.

I have done guiding up to 1 hour and the star remains in the slit at the end of the exposure, proving that any remaining local flexure is negligible. Figures 5 and 6 illustrate this.

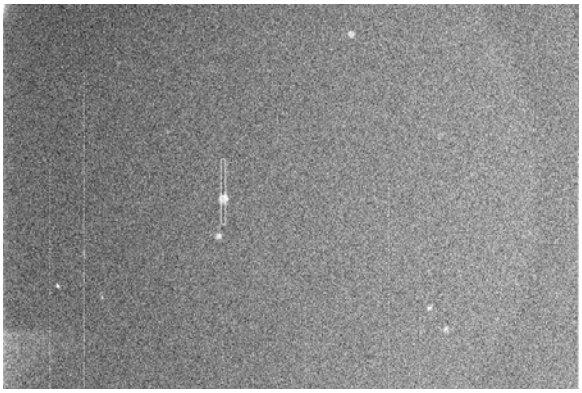

Figure 5. After 60 minutes of guiding, star UV Tau is still centered on the slit.

The image brightness was measured several times and was consistent with my expectations. The guider star images are about ½ as bright as the spectrograph stars images at equivalent focal lengths.

This combination of effects has meant that guiding on stars at the limit of the spectrograph has proved more difficult than I had anticipated. I have had to use exposures beyond 10 seconds with deep binning to track on the target star at Magnitude 13. On my G-11 mount this can lead to quite a bit of image wander.

For slightly brighter objects, the guider has worked very well, allowing convenient long duration spectrometry of stars at Magnitude 12 and guiding on galaxy cores such as M66. It also appears well suited for polarimetric and time series spectrometry where maintaining the exact pixel position is necessary. (Figure 7)

Figure 6. 2400-second pellicle guided DSS spectrum of UV TAU. Strong undulating TiO bands at middle right show ~M6 type. Skyglow accounts for all other lines. Simultaneous photometry showed the V magnitude was below 15, and I-band magnitude near 12.

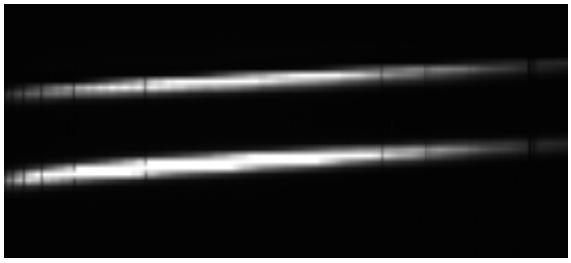

Figure 7. Direct addition of two spectra of Alpha And. A Savart calcite plate before the slit creates parallel spectra of opposite polarizations. Note that spectra are on precisely the same pixels in both exposures as indicated by the narrow central bands. This also illustrates potential for precision time series spectroscopy.

8. Future Plans

I am in the process of replacing the ST-7E as a guide camera with a much lighter weight SBIG remote guide head and shortening the entire assembly to about 6 inches. This in turn necessitates shortening the arm of the guider body to allow the camera to reach focus. With this I am intending to continue my work on classification of AAVSO variable stars and development of a spectro-polarimetric capability for the DSS7.

9. Conclusions

A pellicle beamsplitter works very well with the DSS7 spectrograph to allow long duration spectroscopy with an average quality mount.

Guiding on the target star makes this process no more difficult to set up than using separate guide scope.

The independent guider allows long duration time series spectroscopy below 10th magnitude.

The choice of an 8% pellicle is probably not the optimal one. I intend to try a 33% one in the future to create a better balance between the guide star brightness and the spectrometer. The faster guiding may well make up for a 25% reduction in slit illumination.

Using one of the available 2-inch pellicles would provide an easy way to guide imaging without the usual problems of finding a guide star. This could be mounted in a modified Meade flip mirror assembly as done by Smith (2006).

10. Acknowledgements

I would like to acknowledge the help of Eric Crane, Russ Genet, Alan Holmes, Dale Mais, John Pye and Tom Smith for their design suggestions and encouragement in this project.

11. Acknowledgments

This research has made use of the SIMBAD database, operated at CDS, Strasbourg, France.

This research made use of NASA's Astrophysics Data System.

12. References

Cole, G. (2001). "A Spectropolarimeter Based On The SBIG Spectrometer." *International Amateur-Professional Photoelectric Photometry Communication* **84**, 13.

The Edmund Industrial Optics Catalog 2006, 70.

Holmes, A. (2005). "Operating Instructions for the Santa Barbara Instrument Group Deep Space Spectrograph (DSS-7)." Santa Barbara Instrument Group, Santa Barbara, CA. http://www.sbig.com.

Smith, T., Genet, R., Heather, C. (2006). "A Compact, Off the Shelf, Low Cost Dual Channel Photometer." *Proceedings for the 25th Annual Conference of the Society for Astronomical Sciences*, ed. Warner et al., 87-90.